UNIVERSITY OF SHEFFIELD

DEPARTMENT OF CIVIL AND STRUCTURAL ENGINEERING

T H E A N A L Y S I S A N D D E S I G N O F

I N F L A T A B L E D A M S

by

Adil Dawood Alwan
(B.Sc., M.Sc.)

A thesis submitted to the University
of Sheffield for the Degree of
Doctor of Philosophy

November 1979

NOTATION

A	=	cross-sectional area of a channel.
A'	=	cross-sectional area of the membrane material.
a	=	upstream portion of base length.
a_1	=	numerical exponent.
a'	=	acceleration.
B	=	base length of the dam.
b	=	breadth of sharp-crested rectangular weir.
b_d	=	total length of downstream profile.
b_u	=	total length of upstream profile.
b_1	=	numerical exponent.
C	=	radius of upstream profile of the dam with downstream head equal to zero.
C'	=	radius of upstream profile of dam with downstream head = DH.
C_1	=	coefficient of discharge over the sharp-crested rectangular weir.
C_D	=	coefficient of discharge over the inflatable dam.
C_1, C_2, C_3, C_4	=	polynomial coefficients.
C'_2	=	a constant of integration.
DH	=	downstream head.
E	=	normal elliptic integral of the second kind.
$\hat{E}$	=	complete elliptic normal integral of the second kind.
F	=	normal elliptic integral of the first kind.
$\hat{F}$	=	complete elliptic normal integral of the first kind.
F_G	=	gravity force.
F_1	=	upstream hydrostatic force on the element.
F_2	=	internal air force on the element.

To my parents

ACKNOWLEDGEMENTS

The author wishes to express thanks to his supervisor, Dr. F.A. Johnson, for his most helpful advice and encouragement throughout the project and for his help during the preparation of this thesis.

Grateful thanks are also due to the Department Technical Staff, in particular Mr. G. Brawn, for their invaluable assistance.

The operators and staff of the University of Sheffield Computing Service are thanked for their helpfulness and advice.

The author also wishes to thank Miss G.E. Probert for her assistance in checking the final manuscript.

Acknowledgements are due to the Faculty of Engineering, University of Basrah for providing the financial support for this work.

The author particularly thanks Mrs. J. Czerny for typing this thesis.

SUMMARY

An alternative method to overcome the high cost and time required for the design, analysis, construction and operating of a conventional water control structure is an inflatable dam. The basic aim of this project is to study both theoretically and experimentally the behaviour and performance of inflatable dams under hydrostatic and hydrodynamic conditions and to develop a design method.

A finite element approach is developed in order to analyse air, water and a combination of air and water inflated dams to determine the shape and tension of the membrane of the dam under hydrostatic and hydrodynamic conditions.

A series of models of inflatable dams were constructed and tested under hydrostatic and hydrodynamic conditions. The shapes of these models were compared with the theoretical shapes obtained from the theoretical analysis. The comparison shows there was a good relationship between the experimental and theoretical shapes.

A new formula was derived for calculating the rate of flow over the air, water and air/water inflated dams theoretically. This develops the potential for applying an inflatable dam as a device for measuring discharge.

A design technique for a dam was developed to design air, water and air/water inflated dams under hydrostatic conditions. This technique can be used for the design of dams with different geometry of base length.

Computer programs were written for the analysis and design of the dams based on the finite element approach and considerable efforts were undertaken to simplify the input data and the output results. A sub-program was developed to provide the results in graphical form, if required.

CONTENTS

		Page
	Acknowledgements.	i.
	Summary.	ii.
	Contents.	iv.
	List of figures.	ix.
	List of tables.	xvii.
	Notation.	xx.
CHAPTER 1.	INTRODUCTION.	
1.1	General.	1.
1.2	Uses of Inflatable Dams.	3.
1.2.1	Increasing the Output of a Hydro-Electric Power Station.	3.
1.2.2	Flood Control.	3.
1.2.3	Increasing Capacity of Existing Dams.	4.
1.2.4	Controlling the Water Table.	4.
1.2.5	Emergency Check Valves.	4.
1.2.6	Further Uses of Inflatable Dams.	4.
1.3	Advantages and Disadvantages of an Inflatable Dam.	6.
1.4	Limitations of Analysis and Design.	6.
1.4.1	Limitations of Existing Techniques.	6.
1.4.2	Development of a New Technique.	7.
CHAPTER 2.	REVIEW OF PREVIOUS WORK.	
2.1	History of the Inflatable Dam.	9.
2.2	Prototype Construction of Dams.	9.
2.3	Model Construction of Dams.	10.
2.4	Theoretical Method of Analysis.	16.
2.4.1	Theoretical Method of Anwar.	18.
2.4.1.1	Analysis of a Dam under Hydrostatic Conditions.	18.
2.4.1.1.1	Air Inflated Dam.	18.
2.4.1.1.2	Water Inflated Dam.	21.
2.4.1.2	Air Inflated Dam under Hydrodynamic Conditions.	23.
2.4.2	Theoretical Method of Harrison.	24.
2.4.3	Theoretical Method of Clare.	25.

		Page
2.4.3.1	Analysis of a Dam with Downstream Head Zero.	27.
2.4.3.2	Analysis of a Dam with a Downstream Head.	30.
2.4.4	Theoretical Method of Binnie.	30.
2.4.5	Theoretical Method of Parbery.	31.
2.5	Comparison Between the Various Theoretical Methods of Analysis.	34.
2.6	Discussion of the Limitations of the Theoretical Methods of Analysis.	36.
CHAPTER 3.	MODEL TESTS UNDER HYDROSTATIC CONDITIONS.	
3.1	Introduction.	40.
3.2	Laboratory Apparatus.	41.
3.2.1	Test Tank.	41.
3.2.2	Air Pressure Inflation Equipment.	41.
3.2.3	Water Pressure Inflation Equipment.	44.
3.2.4	Profile Gauge.	46.
3.3	Model Material.	46.
3.3.1	Properties of N.T. Fabric.	49.
3.4	Model Design.	52.
3.5	Model Construction.	53.
3.5.1	Bag Construction.	53.
3.5.2	Base Plate of the Model.	56.
3.5.3	Anchoring System of the Bag to the Base Plate.	56.
3.5.4	Inflation Technique.	57.
3.5.5	End Fixing.	57.
3.6	Testing of the Models.	59.
3.6.1	Profile Measuring Technique.	60.
3.6.2	Air Inflated Models.	62.
3.6.3	Water Inflated Models.	64.
3.6.4	Air/Water Inflated Models.	67.
CHAPTER 4.	THEORETICAL ANALYSIS OF A DAM UNDER HYDROSTATIC CONDITIONS.	
4.1	Introduction.	71.
4.2	Method of Analysis.	72.
4.2.1	Stress Analysis of the Profile.	74.

		Page
4.2.2	Initial Trial Values of Tension and Slope.	78.
4.2.3	Co-ordinate Positions of Points on the Profile.	79.
4.2.4	Adjusting Initial Values of Tension and Slope.	82.
4.3	Computer Programs.	85.
4.3.1	Computer Program (AID)	85.
4.3.2	Computer Program (AID1)	87.
4.3.2.1	Input/Output Data for Program (AID1).	89.
4.3.2.2	Range of Application of Program (AID1)	89.
4.3.3	Stability of the Analytical Technique.	92.
4.4	Comparison Between Experimental and Theoretical Cross-Sectional Profiles.	93.
4.5	Effect of Operational Parameters.	104.
4.5.1	Effect of Variation of Upstream Head and Internal Pressure with a Constant Downstream Head.	104.
4.5.1.1	Tension.	108.
4.5.1.2	Elongation.	112.
4.5.1.3	Upstream Slope.	116.
4.5.1.4	Downstream Slope.	121.
4.5.1.5	Maximum Dam Height.	125.
4.5.2	Effect of Variation of Downstream Head and Internal Pressure for a Constant Upstream Head.	131.
4.5.2.1	Tension.	131.
4.5.2.2	Elongation.	135.
4.5.2.3	Upstream Slope.	135.
4.5.2.4	Downstream Slope.	142.
4.5.2.5	Maximum Dam Height.	142.
4.5.3	Effect of Variation of the Internal Pressure on the Dam for Constant Upstream and Downstream Heads.	153.
4.6	Comparison Between Air, Water and Air/Water Dams.	162.

		Page
CHAPTER 5.	THE ANALYSIS OF DAMS UNDER HYDRODYNAMIC CONDITIONS.	
5.1	Introduction.	169.
5.2	Design and Construction of the Model.	170.
5.3	Experimental Test.	172.
5.3.1	Shape of the Dam.	172.
5.3.1.1	Profile Measuring Technique.	172.
5.3.1.2	Measurement of Shape of the Dams.	173.
5.3.2	Behaviour of the Dams.	176.
5.3.2.1	Air Inflated Dam.	176.
5.3.2.2	Water Inflated Dam.	179.
5.3.2.3	Air/Water Inflated Dam.	181.
5.4	Theoretical Method of Dam's Analysis.	184.
5.5	Comparison Between Experimental and Theoretical Shapes of the Dam.	187.
5.6	Effects of Operational Parameters on the Tension and the Shape of Membrane.	190.
5.6.1	Effects of Operational Parameters on the Tension in the membrane.	193.
5.6.2	Effects of Operational Parameter on the Shape of the Dams.	193.
5.7	Measuring Tension in the Membrane.	200.
CHAPTER 6.	DISCHARGE COEFFICIENT FOR INFLATABLE DAMS.	
6.1	Introduction.	212.
6.2	Discharge Measurement.	214.
6.2.1	Volumetric Calibration of the Weir Plate.	214.
6.3	Model Tests.	218.
6.4	Flow Characteristics over Dams.	218.
6.5	Calculation of the Coefficient of Discharge.	222.
6.6	Computer Program (AID3)	238.
6.7	Comparison of Methods of Determining Discharge.	240.
6.8	Factors Effecting the Coefficient of Discharge.	244.
6.9	Effects of Downstream Head of Upstream Head.	250.

		Page
CHAPTER 7.	DESIGN OF AN INFLATABLE DAM.	
7.1	Introduction.	255.
7.2	Theoretical Method of Design.	257.
7.2.1	Base Length and Internal Pressure.	257.
7.2.2	Membrane Length.	258.
7.2.3	Design Procedure.	259.
7.3	Computer Programs.	260.
7.3.1	Computer Program (DID)	260.
7.3.2	Computer Program (DID1)	263.
7.3.2.1	Base and Membrane Lengths.	264.
7.3.2.2	Calculating Internal Pressure.	264.
7.3.2.3	Procedure of Design.	267.
7.3.2.4	Input/Output Data.	267.
7.4	Examples of Design of an Inflatable Dam.	271.
7.5	Recommendations for the Design of a Model Inflatable Dam.	276.
7.5.1	Model Design to Test Under Hydrostatic conditions.	278.
7.5.2	Model Design to Test Under Hydrodynamic conditions.	279.
CHAPTER 8.	CONCLUSION AND RECOMMENDATIONS FOR FUTURE WORK.	
8.1	Conclusion.	281.
8.2	Recommendations for Future Work.	284.
APPENDIX A.		286.
APPENDIX B.		288.
APPENDIX C.		291.
REFERENCES.		294.

LIST OF FIGURES

		Page
	CHAPTER 1.	
Fig.1.1	Inflatable dam preserves Bournemouth water supply.	5.
	CHAPTER 2.	
Fig.2.1	Construction of water inflated dam.	11.
2.2	Water inflated technique.	14.
2.3	Anwar's analysis of an inflatable dam.	20.
2.4	Harrison's Analysis of a dam under hydrostatic conditions.	26.
2.5	Clare's analysis of water inflated dam.	28.
2.6	Parbery's analysis of a dam under hydrostatic conditions.	32.
	CHAPTER 3.	
Fig.3.1	Plan of test tank.	42.
3.2	Laboratory apparatus.	43.
3.3	Inflation apparatus.	45.
3.4	Profile gauge and base anchoring system.	47.
3.5	Stress-strain relationship of N.T. fabric.	50.
3.6	Stress-strain relationship of N.T. fabric (polynomial degree 3).	51.
3.7	Typical dam profile under static conditions, designed using computer program (DID).	54.
3.8	Single sheet bag construction.	55.
3.9	Typical experimental profiles of air inflated dams.	63.
3.10	Behaviour of air inflated dam when deflated (hydrostatic).	65.
3.11	Typical experimental profiles of water inflated dams.	66.
3.12	Behaviour of water inflated dam when deflated (hydrostatic).	68.
3.13	Typical experimental profiles of air/water inflated dams.	69.
	CHAPTER 4.	
Fig.4.1 (A)	Pressures acting on the dam.	75.
(B)	Forces acting on an individual element.	75.

		Page
Fig.4.2	Method of calculating co-ordinates of points on the profile.	81.
4.3	Effect of adjusting T and θ to minimise mis-close.	83.
4.4	Example of output of analysis program (AID)	88.
4.5	Example of output of analysis program (AID1)	90.
4.6	Flow chart of program (AID1)	91.
4.7	Comparison between experimental and theoretical profiles of a typical air dam.	96.
4.8	Comparison between experimental and theoretical profiles of a typical water dam.	97.
4.9	Comparison between experimental and theoretical profiles of a typical air/water dam.	98.
4.10	End effects on the cross-sectional profiles.	103.
4.11	Variation of tension in membrane with upstream head for various air pressures.	109.
4.12	Variation of tension in membrane with upstream head for various water pressures.	110.
4.13	Variation of tension in membrane with upstream head for various air/water pressures.	111.
4.14	Variation of elongation in membrane with upstream head for various air pressures.	113.
4.15	Variation of elongation in membrane with upstream head for various water pressures.	114.
4.16	Variation of elongation in membrane with upstream head for various air/water pressures.	115.
4.17	Variation of upstream slope of membrane with upstream head for various air pressures.	117.
4.18	Variation of upstream slope of membrane with upstream head for various water pressures.	118.
4.19	Variation of upstream slope of membrane with upstream head for various air/water pressures.	119.
4.20	Variation of downstream slope of membrane with upstream head for various air pressures.	122.
4.21	Variation of downstream slope of membrane with upstream head for various water pressures.	123.
4.22	Variation of downstream slope of membrane with upstream head for various air/water pressures.	124.

Page

Fig. 4.23 Variation of maximum dam height with upstream head for various air pressures. 126.

4.24 Variation of maximum dam height with upstream head for various water pressures. 129.

4.25 Variation of maximum dam height with upstream head for various air/water pressures. 130.

4.26 Variation of tension in membrane with downstream head for various air pressures. 132.

4.27 Variation of tension in membrane with downstream head for various water pressures. 133.

4.28 Variation of tension in membrane with downstream head for various air/water pressures. 134.

4.29 Variation of elongation in membrane with downstream head for various air pressures. 136.

4.30 Variation of elongation in membrane with downstream head for various water pressures. 137.

4.31 Variation of elongation in membrane with downstream head for various air/water pressures. 138.

4.32 Variation of upstream slope of membrane with downstream head for various air pressures. 139.

4.33 Variation of upstream slope of membrane with downstream head for various water pressures. 140.

4.34 Variation of upstream slope of membrane with downstream head for various air/water pressures. 141.

4.35 Variation of downstream slope of membrane with downstream head for various air pressures. 143.

4.36 Variation of downstream slope of membrane with downstream head for various water pressures. 144.

4.37 Variation of downstream slope of membrane with upstream head for various air/water pressures. 145.

4.38 Variation of maximum dam height with downstream head for various air pressures. 146.

4.39 Variation of maximum dam height with downstream head for various water pressures. 147.

4.40 Variation of maximum dam height with downstream head for various air/water pressures. 148.

Page

Fig. 4.41 Variation of maximum upstream head with downstream head for various air pressures. 149.

4.42 Variation of maximum upstream head with downstream head for various water pressures. 151.

4.43 Variation of maximum upstream head with downstream head for various air/water pressures. 152.

4.44 Variation of maximum dam height with air pressure for constant upstream and downstream heads. 155.

4.45 Variation of maximum dam height with water pressure for constant upstream and downstream heads. 156.

4.46 Variation of maximum dam height with air/water pressures for constant upstream and downstream heads. 157.

4.47 Typical behaviour of the cross-sectional profile of air dams under hydrostatic conditions for various internal air pressures. 159

4.48 Typical behaviour of the cross-sectional profile of water dams under hydrostatic conditions for various internal water pressures. 160.

4.49 Typical behaviour of the cross-sectional profile of air/water dams under hydrostatic conditions for various internal air/water pressures. 161.

4.50 Variation of maximum upstream head with air pressure. 165.

4.51 Variation of maximum upstream head with water pressure. 166.

4.52 Variation of maximum upstream head with air/water pressures. 167.

CHAPTER 5.

Fig. 5.1 Typical profile of an air inflated model dam subjected to hydrodynamic conditions using program 'DID'. 171.

5.2 Profile gauge. 174.

5.3 Typical experimental profile of inflatable dams for various air and water pressures. 177.

5.4 Variation of maximum dam height with overflow head for various air pressures. 178.

5.5 Behaviour of air inflated dam when deflated (hydrodynamic). 180.

		Page
Fig. 5.6	Variation of maximum dam height with overflow head for various water pressures.	182.
5.7	Behaviour of water inflated dam when deflated (hydrodynamic).	183.
5.8	Variation of maximum dam height with overflow head for various air/water pressures.	185.
5.9	Behaviour of air/water inflated dam when deflated (hydrodynamic).	186.
5.10	Example of output from program (AID2) for analysing dams under hydrodynamic conditions.	189.
5.11	Typical example of the comparison between experimental shape and theoretical (40 elements & 180 elements) shape of dams.	191.
5.12	Variation of tension in membrane with overflow head for various air, water and air/water pressures.	194.
5.13	Variation of elongation in membrane with overflow head for various air, water and air/water pressures.	195.
5.14	Variation of tension in membrane with overflow head for various downstream heads.	196.
5.15	Variation of upstream slope of membrane with overflow head for various air, water and air/water pressures.	198.
5.16	Variation of downstream slope of membrane with overflow head for various air, water and air/water pressures.	201.
5.17	Variation of upstream slope of membrane with overflow head for various downstream heads.	202.
5.18	Variation of downstream slope of membrane with overflow head for various downstream heads.	203.
5.19	Typical behaviour of the cross-sectional profiles of air inflated dams under hydrodynamic conditions for various internal air pressures.	204.
5.20	Typical behaviour of the cross-sectional profiles of water inflated dams under hydrodynamic conditions for various internal water pressures.	205.
5.21	Typical behaviour of the cross-sectional profiles of air/water inflated dams under hydrodynamic conditions for various internal air pressures.	206.

Page

Fig. 5.22 Apparatus for the experimental measurement of tension in the membrane. 208.

5.23 Calibration curve for the strain gauges. 209.

CHAPTER 6.

Fig. 6.1 Rectangular channel. 215.

6.2 Rectangular-crested weir. 215.

6.3 Calibration curve for the rectangular sharp-crested weir. 217.

6.4 Behaviour of a low flow over a dam. 220.

6.5 Behaviour of an intermediate flow over a dam. 221.

6.6 Natural ventilation of the underside of the nappe. 223.

6.7 Variation of the coefficient of discharge with flow rate for various air pressures. 225.

6.8 Variation of the coefficient of discharge with flow rate for various water pressures. 226.

6.9 Variation of the coefficient of discharge with flow rate for various air/water pressures. 227.

6.10 Effect of downstream head on the coefficient of discharge for an air inflated dam. 228.

6.11 Effect of downstream head on the coefficient of discharge for a water inflated dam. 229.

6.12 Effect of downstream head on the coefficient of discharge for an air/water inflated dam. 230.

6.13 Variation of overflow head, H, with depth of water above the crest level, h, for various air, water and air/water pressures. 235.

6.14 Variation of S with H/R for various air pressures. 236.

6.15 Variation of S with H/R for various water pressures. 237.

6.16 Typical examples of analysis of inflatable dams under hydrodynamic conditions by using program (AID3) and 40 elements. 240.

6.17 Variation of the radius of curvature of dam crest with overflow head for various air, water and air/water inflated dams. 246.

6.18 Variation of the coefficient of discharge with overflow head for various air, water and air/water pressures. 247.

Page

Fig. 6.19 Variation of the radius of curvature of the dam crest with overflow head for various downstream heads. 248.

6.20 Variation of the coefficient of discharge with overflow head for various downstream heads. 249.

CHAPTER 7.

Fig. 7.1(A) An inflatable dam under the design condition. 256.

(B) Calculation of the initial length of the membrane. 256.

7.2 Flow chart for computer program (DID). 261.

7.3 Variation of dam height with ratio of base length/dam height. 265.

7.4 Variation of allowable tension in membrane with internal pressure. 268.

7.5 Variation of allowable tension in membrane with membrane length. 269.

7.6 The design of an air inflated dam. 272.

7.7 The design of a water inflated dam. 273.

7.8 The design of an air/water inflated dam. 274.

7.9 The design of inflatable dams with inclined bases in the upward direction. 275.

7.10 The design of inflatable dams with inclined bases in the downward direction. 277.

LIST OF TABLES

Page

CHAPTER 2.

Table 2.1 Properties of materials (Clare Ref. 8). 12.

2.2 Properties of model materials. 17.

2.3 Qualitative comparison of theoretical methods of analysis. 35.

2.4 Effect of membrane weight on tension and shape of an inflatable dam. 37.

2.5 Effect of different extensibility on tension and shape of an inflatable dam (Harrison Ref. 26). 38.

CHAPTER 3.

Table 3.1 Properties of membrane materials. 48.

3.2 Tests of air inflated models. 62.

3.3 Tests of water inflated models. 64.

3.4 Tests of air/water inflated models. 70.

CHAPTER 4.

Table 4.1 Description of input data of program (AID) 86.

4.2 Description of output data of program (AID) 86.

4.3 Analysis of a dam using different numbers of elements. 95.

4.4 Comparison between experimental and theoretical cross-sectional profile of air inflated dams. 100.

4.5 Comparison between experimental and theoretical cross-sectional profile of water inflated dams. 101.

4.6 Comparison between experimental and theoretical cross-sectional profile of air/water inflated dams. 102.

4.7 Hydrostatic conditions for analysis of air inflated dams with the downstream head constant and equal to zero. 105.

4.8 Hydrostatic conditions for analysis of air inflated dams with the upstream head constant and equal to 270 mm. 105.

		Page
Table 4.9	Hydrostatic conditions for analysis of water inflated dams with the downstream head constant and equal to zero.	106.
4.10	Hydrostatic conditions for analysis of water inflated dams with the upstream head constant and equal to 220 mm.	106.
4.11	Hydrostatic conditions for analysis of air/water inflated dams with downstream head constant and equal to zero.	107.
4.12	Hydrostatic conditions for analysis of air/water inflated dams with upstream head constant and equal to 250 mm.	107.
4.13	Analysis of three types of inflation under various internal pressure for constant upstream and downstream heads.	154.
4.14	Comparison between air, water and air/water dams.	164.

CHAPTER 5.

Table 5.1	Hydrodynamic conditions when measuring the cross-sectional profile of the dams.	175.
5.2	Description of input data of program (AID2).	188.
5.3	Percentage differences between experimental and theoretical crest height and shape of dams.	192.
5.4	Effects of overflow head and internal pressures on the upstream slope.	199.
5.5	Effects of overflow head and internal pressures on the downstream slope.	199.
5.6	Comparison between experimental and theoretical tensions in the fabric.	210.

CHAPTER 6.

Table 6.1	Range of heads and pressures parameters for model tests under hydrodynamic conditions.	219.
6.2	Comparison between Clare and Alwan methods of calculating discharge (water inflated dam).	241.
6.3	Comparison between Baker and Alwan methods of calculating discharge (water inflated dam).	242.
6.4	Effects of weight and extensibility of membrane on discharge.	243.

Page

Table 6.5 Effect of downstream head on upstream and overflow heads for air inflated dam. 251.

6.6 Effect of downstream head on upstream and overflow heads for water inflated dam. 252.

6.7 Effect of downstream head on upstream and overflow heads for air/water inflated dam. 253.

CHAPTER 7.

Table 7.1 Design ratios of B/H_1 and H_1/H_2. 258.

7.2 Description of input data of program (DID) 262.

7.3 Description of output data of program (DID) 262.

7.4 Description of input data or program (DID1) 270.

7.5 Description of output data of program (DID1) 270.

NOTATION

A	=	cross-sectional area of a channel.
A'	=	cross-sectional area of the membrane material.
a	=	upstream portion of base length.
a_1	=	numerical exponent.
a'	=	acceleration.
B	=	base length of the dam.
b	=	breadth of sharp-crested rectangular weir.
b_d	=	total length of downstream profile.
b_u	=	total length of upstream profile.
b_1	=	numerical exponent.
C	=	radius of upstream profile of the dam with downstream head equal to zero.
C'	=	radius of upstream profile of dam with downstream head = DH.
C_d	=	coefficient of discharge over the sharp-crested rectangular weir.
C_D	=	coefficient of discharge over the inflatable dam.
C_1, C_2, C_3, C_4	=	polynomial coefficients.
C'_2	=	a constant of integration.
DH	=	downstream head.
E	=	normal elliptic integral of the second kind.
$\hat{E}$	=	complete elliptic normal integral of the second kind.
F	=	normal elliptic integral of the first kind.
$\hat{F}$	=	complete elliptic normal integral of the first kind.
F_G	=	gravity force.
F_1	=	upstream hydrostatic force on the element.
F_2	=	internal air force on the element.

F_3 = internal water force on the element.

F_4 = weight of membrane force.

F_5 = downstream hydrostatic force on the element.

f = extension ratio of the membrane under load.

g = acceleration due to gravity.

H = overflow head.

H_p = horizontal hydrostatic component.

H_1 = maximum upstream head.

h = depth of water at the crest section (critical depth).

h_{c_1} = depth of centre of the upstream hydrostatic force below the upstream free water surface.

h_{c_2} = depth of centre of the internal water force below the internal free water surface.

h_{c_3} = depth of centre of the downstream hydrostatic force below the downstream free water surface.

L = length of the element.

LT = total length of the membrane.

L_r = scale ratio.

M = mass of water.

m' = ratio of internal water depth to upstream depth.

P = resultant of internal pressure.

P' = resultant pressure at arbitrary point of the membrane at downstream section.

P_1 = resultant pressure of hydrostatic forces on the dam.

p = internal air pressure of the dam.

p_1 = internal water pressure of the dam.

Q = discharge over the dam.

Q' = maximum design discharge.

q = discharge over the dam per unit width.

R = radius of curvature of crest of the dam.

R' = initial radius of curvature of the dam.

R_1 = resultant of hydrostatic forces acting on the first element.

R_2 = resultant of hydrostatic forces acting on the second element.

S = a constant.

S' = length along unstretched perimeter.

S_1 = ultimate stress of the membrane material.

T = tension in the membrane.

T' = ultimate tension of the membrane material.

T_o = initial tension in the membrane at the upstream fixture.

T_A = tension in the node A.

T_B = tension in the node B.

TL = initial length of the membrane.

UH = upstream head.

V = velocity approach of the flow in the channel.

V_p = Vertical hydrostatic component at point p on the membrane.

W = horizontal component of internal water pressure.

w = weight of the membrane per unit area.

x,y = co-ordinates.

Y_{max} = maximum height of the dam (crest height).

α = proportional factor.

β = angle of tangent to the dam at any point on upstream profile.

γ = specific weight of water.

ΔL = elongation in the element.

ε = strain in the fabric = $\frac{\Delta L}{L}$

θ = initial upstream slope of the dam at the upstream fixture.

θ_A = slope of element at node A.

θ_B = slope of element at node B.

θ_i = slope of element at node i.

θ_1 = upstream slope of the dam at upstream fixture.

θ_2 = downstream slope of the dam at downstream fixture.

ρ = density of water.

μ = fluid viscosity.

σ = stress in the fabric.

ϕ = inclination of the tangent in S' direction to the horizontal.

CHAPTER 1.

INTRODUCTION.

1.1 General.

The ever increasing demands placed on the water resources of the earth necessitate more and more control by man. The simpler and more economical these control systems can be the easier they can be designed, constructed and operated. Typical examples are dams for the storage of water, weirs and flumes for water level control and flow measurement and various types of control gate for flow diversion or control. All of these types of structure require considerable detailed structural and hydraulic design and are usually of a permanent nature requiring in some instances complex and expensive installation.

Inflatable dams have been considered as a suitable alternative form of control overcoming many of the design, construction and operational difficulties of conventional structures. The simplest and most common type of inflatable dam consists of a single sheet of rubberised fabric folded into a tubular shaped bag which is then sealed into place during installation. The bag is fixed at the base and normally would be inflated by air, water or a combination of air and water, although other fluids could be used.

In the past most prototype inflatable dams were designed and analysed by constructing models of varying scale ratios[1,2], and the results obtained from the model tests were used to calculate the design parameters (membrane length, base length

and inflation pressure) of the prototype. Because of the limitation of this design approach many inflatable dam failures[3,4,5] during operation have occurred due to a lack of information about the performance and behaviour under a variety of hydrostatic and hydrodynamic conditions in particular upstream head, downstream head and type and magnitude of inflation fluid.

The first theoretical method dealing with the analysis of an inflatable dam was published by Anwar (1967)[6] and this was followed by Harrison[7], Clare[8], Binnie[9] and the latest paper was published by Parbery[10] in 1976. The methods of analysis in these approaches are described in detail in Chapter 2.

All previous theoretical methods have limits to the range of operational parameters of upstream head, downstream head and type of inflation fluid and also base geometry and material properties that can be accommodated.

The work is concerned with the development of a theoretical analysis using a finite element approach with a computer solution in order to analyse and design an inflatable dam covering the whole range of operational parameters and incorporating material properties and any base shape likely to be encountered in practice. This analysis was applied to dams inflated by air, water and a combination of both air and water under hydrostatic and hydrodynamic conditions. However the technique can also be used for other inflation fluids.

A computer program was written to use the finite element approach for both the analysis and design of an inflatable dam

under hydrostatic conditions. The program of analysis was later extended to use for the analysis of a dam under hydrodynamic conditions and in particular to calculate the rate of flow passing over the dam as it acts as a weir.

Experimental investigations of the behaviour of the dams under hydrostatic and hydrodynamic conditions were studied and comparisons made between the profiles of the dams obtained from experimental work and theoretical analysis.

Two previous workers, Clare[8] and Stodulka[11], dealt with the design of an inflatable dam and both used graphical solutions for their designs. However, many limitations apply to these techniques as described in Chapter 7.

A technique was developed to design a dam to cover a wide range of parameters.

1.2 Uses of Inflatable Dams.

The inflatable dam has a wide range of possible applications and some of the more important uses so far attempted are described below:

1.2.1 Increasing the Output of a Hydro-Electric Power Station.

The installation of an inflatable dam on the crest of a conventional dam (Koombooloomba Dam, Australia[2]) increased the depth of water on the upstream side and from the additional head the electrical output of the system was increased.

1.2.2 Flood Control.

The installation of an inflatable dam across a river enables the control of a flood by allowing an inflow flood diversion to a reservoir before the river reaches levée height. This type of application of inflatable dams are being used in Australia[4].

1.2.3 Increasing the Capacity of Existing Dams.

The capacity of the existing dams at U.S.A.[12] was increased by the installation on the dam crest of an inflatable dam. Thus allowing additional water to be stored during the rainy season for irrigation use in the dry season.

1.2.4 Controlling the Water Table.

Inflatable dams are being used in Holland[13] to keep the water table high enough to prevent ground water falling down too far with resulting drying out of agricultural land.

1.2.5 Emergency Check Valves.

Inflatable dams were installed at intervals along the length of a drainage canal in Holland[14] to conserve the water in the canal should either side of the canal banks be breached.

1.2.6 Further uses of Inflatable Dams.

In all of the above mentioned schemes the inflatable dam formed a major part of the scheme. However, many minor uses have also been made.

An inflatable dam has been used as a weir to control the tail-water level at the outlet of a tunnel[3], for river diversion[4] and to regulate river level[15]. Such dams have also been used for irrigation schemes[16,17] and to maintain water supplies[18] as shown in Fig.1.1.

A further use was the replacement of a concrete dam up to 7.5 m[8,12] high and also use as a lock system, a sluice gate, salinity barriers and for flashboard[19] replacement.

In this report additional possible applications of inflatable dams are described later, in particular the use for flow measurement (see Chapter 6).

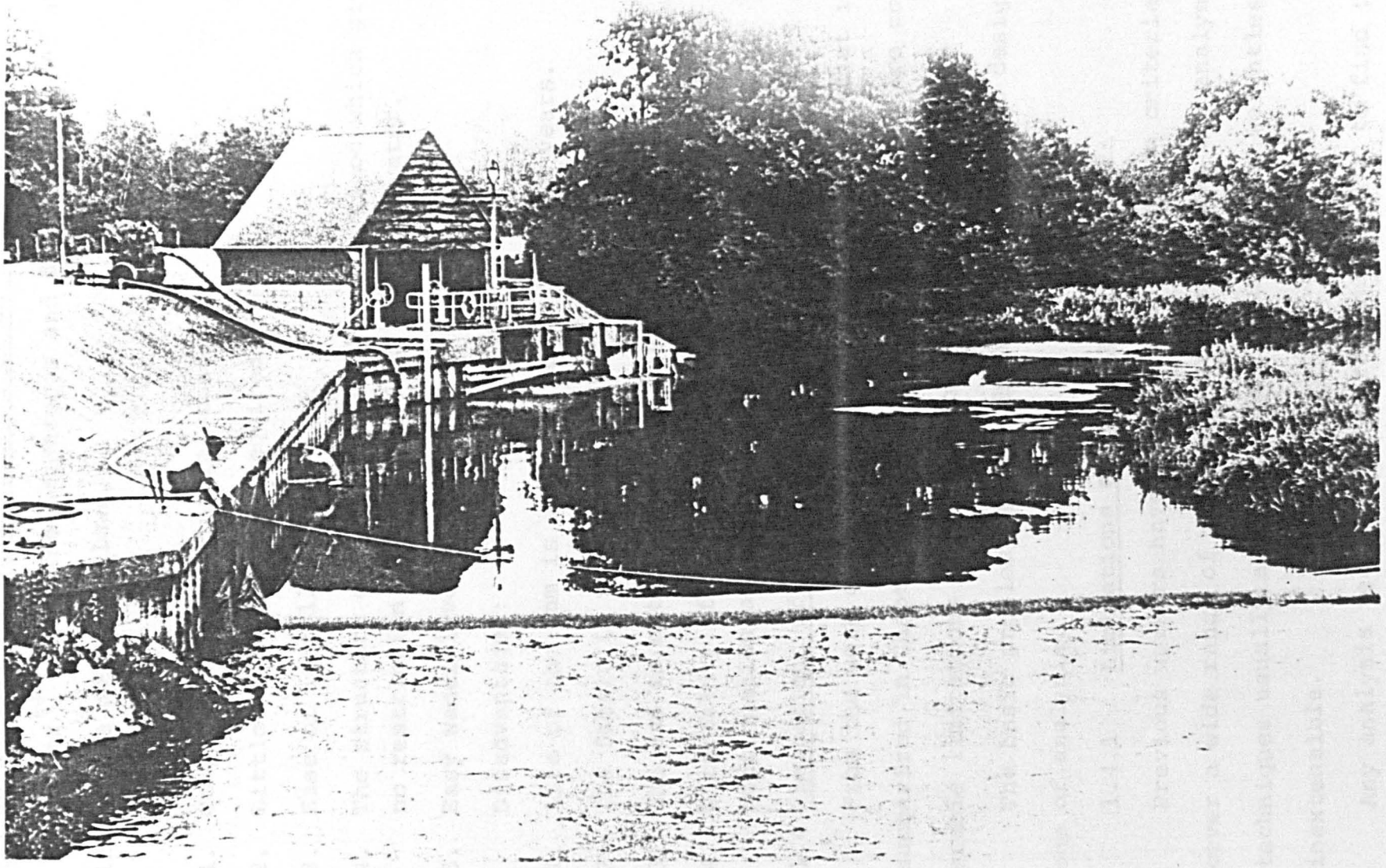

FIG. (1-1) INFLATABLE DAM PRESERVES
BOURNMOUTH WATER SUPPLIES

1.3 Advantages and Disadvantages of an Inflatable Dam.

Conner[4] lists the advantages and disadvantages of an inflatable dam as follows.

Advantages:

1. Comparatively low initial cost.
2. Little maintenance is required.
3. Ease of installation.
4. The structure can be deflated during a flood which gives no restriction to the free flow of flood-water.
5. Easy water level control.

Disadvantages:

1. Life of the dam is expected to be about 20 years.
2. The fabric is vulnerable to vandalism.
3. The dam is not suitable for high overflow.
4. Uncertainty of fabric behaviour with age and under a continuation of dynamic loads.

1.4 Limitations of Analysis and Design.

From the work carried out by early researchers that is summarized in Chapter 2, it can be seen that there are considerable limitations to their approach.

The basic problem can be subdivided into one of design and one of analysis.

1.4.1 Limitations of Existing Techniques.

Previous workers have not established design criteria that cover a wide range of practical structures and the analysis techniques usually assume the fabric used to be weightless and inextensible.

Any analysis technique requires the ability to find the shape and tension of the membrane of the dam for a given range

of heads and inflation pressures for a particular fabric. These are achieved with varying degrees of success as detailed in Chapter 2.

1.4.2 Development of a New Technique.

The analysis problem is to find the shape and tension of the membrane of the dam for a given upstream and downstream head, base length, membrane length, internal pressure and properties of the membrane. The design problem is to find the membrane length, base length, inflation pressure and shape of the dam for a given upstream and downstream design head and material properties and also to predict the dam behaviour under operational conditions that may be different from the design conditions.

The shape of the dam is a function of external forces due to upstream head and downstream head and internal forces due to the inflation pressures and weight of the membrane. A technique to calculate the shape and tension in the membrane was the first stage of this project.

The shape and tension of the membrane was calculated using a finite element approach under various hydrostatic conditions (see Chapter 4) and this calculated shape compared with the shape of the dam obtained from experimental work.

The shape and tension was also calculated under various hydrodynamic conditions and was compared with experimental work (see Chapter 5).

A number of formulae were derived to determine the overflow rate for a given head passing over the dam, as described

in Chapter 6. Such that a theoretical stage-discharge relationship can be produced if a dam is used for flow measurement.

The technique developed for the design of an inflatable dam is based on the minimum length of material required as described in Chapter 7.

The material used for all the dams in this project was N.T fabric (see Chapter 3) and the fluids chosen for inflation were air, water and a combination of both air and water as these fluids are not only readily available and inexpensive but have insignificant variations in their properties with variations of temperature between 0^{o} C - 25^{o} C [20] (see Appendix A). These fluids are also those most likely to be used in practice mainly due to their availability.

CHAPTER 2.

REVIEW OF PREVIOUS WORK.

2.1 History of the Inflatable Dam.

The concept of an inflatable dam was first conceived in 1956 by Iberston[19] under the trade name of Fabridam when a structure was required to replace the flashboards after each flood period of the Los Angeles River in the U.S.A. A suitable material was developed and the first dam was completed and installed in 1957.

Since 1957 many dams have been constructed in various parts of the world[1,2,4,12,13,14,15,21] and have been used for many purposes (see section 1.2).

Dams have been constructed with heights varying from 0.5 m to 5 m[12] and it has been suggested that a dam could be constructed to a maximum height of 7.5 m[8]. Although there have not been restrictions on the lengths of dams it has been suggested[12] that the length should not exceed 150 m for economic purposes in terms of shipping and handling during installation.

2.2 Prototype Construction of Dams.

The inflatable dam is usually constructed from a sheet of rubberised fabric folded in a tubular shape forming the bag of the dam which is sealed in place during installation. The bag has to be anchored to the base of the channel or attached to an existing structure. This can be achieved by a single upstream anchoring or a double anchor system one upstream and

one downstream. A typical fastening is attached to a reinforced concrete slab with structural steel members or clamps and anchor bolts, although alternative methods may be used. The bag may be inflated by air or water or a mixture of both to the required height and deflated when not required. An example of the construction of an inflatable dam suggested by Firestone Tire & Rubber Company[12] is illustrated in Fig. 2.1.

The choice of fabric for an inflatable dam depends upon the working environment of the material and the loads to which it will be subjected during its working life. The physical and mechanical properties of commercially available fabric was reviewed by Clare[8] and these are summarized in table 2.1.

From the material listed in table 2.1, Butyle Rubber, Neoprene, Hypalon, Polythene and P.V.C. have all been used successfully in marine environments. Neoprene compounds have proved to be the best type of coating, their weathering characteristics are excellent and their life expectancy has been determined to be in the region of 20 years. Hypalon can be used as an outer coating on the Neoprene since it has very good resistance to abrasion.

2.3 Model Construction of Dams.

Because of the problem of the realistic design of dams, in many instances it has been necessary to resort to the construction and testing of a model dam. The geometry of an inflatable dam being based on the broad design criteria developed by other workers. However in some instances the geometry of the dam is fixed by an existing structure which dictates the size of the inflatable dam.

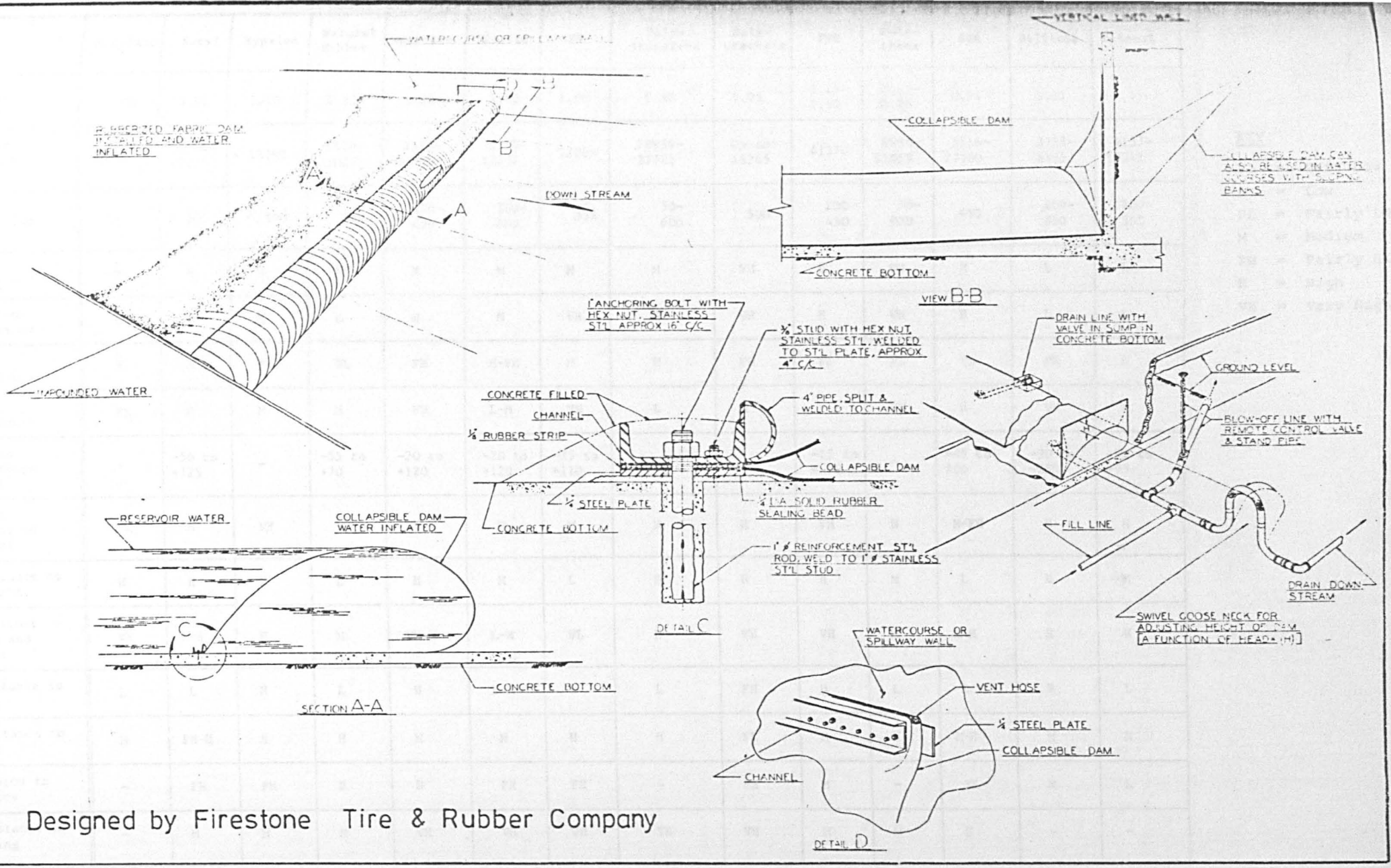

FIG. (2 – 1) CONSTRUCTION OF WATER INFLATED DAM

	Nefylate	Butyl	Hypalon	Natural Rubber	Neoprene	Nitrite	ER	Poly-propylene	Poly-urethane	PVC	Poly-thene	SBR	Silicone	Thiorol
Specific gravity	1.09	0.92	1.10	0.93	1.23	1.00	1.00	0.90	1.05	1.25-1.50	0.92-0.96	0.94	1.25	1.35
Tensile strength (kN/m^2)	10342	5516-17237	> 13790	5516-31027	5516-20685	5516-17237	22064	28959-37922	Up to 48265	41370	6895-15858	5516-27580	2758-6895	4137-10342
Tensile elongation (%)	-	< 800	< 500	500	650-850	200-600	335	50-600	500	200-450	50-800	450	200-350	200-350
Tear strength	M	M	M	FH	H	M	M	M	VH	H	VH	M	L	L
Abrasion resistance	M	M	H	H	H	M	VH	H	VH	H	VH	H	L	L
Heat resistance	H	M	FH	FL	FH	M-FH	M	H	FH	FL	FL	FL	VH	L
Cold resistance	FL	H	M	H	FH	L-M	VH	L	M	VL	VH	H	VH	H
Working temp.range (°C)	-	-50 to +125	-	-55 to +70	-20 to +120	-20 to +120	-75 to +110	- to +150	-	-15 to + 78	-	-45 to 100	-90 to +250	-50 to +95
Ageing resistance general	VH	H	VH	M	H	H	M	H	H	VH	H	M-FH	H	H
Resistance to sunlight	H	H	H	L	H	M	L	H	H	H	M	L	H	M
Resistance to ozone and corona	VH	M-H	H	M	FH-H	L-M	VL	H	VH	VH	M	L-M	H	H
Resistance to flame	L	L	H	L	H	L-M	L	L	FH	H	L	L	H	L
Resistance to water	M	FH-H	H	H	M	M	H	H	FL	M	H	M-H	M	M
Adhesion to fabrics	-	FH	FH	H	H	FH	FH	-	FH	M	-	FH	M	L
Resistance to flexing	-	M	M	M	VH	VH	VH	VH	VH	M	M	H	-	-

KEY

VL = Very Low
L = Low
FL = Fairly Low
M = Medium
FH = Fairly High
H = High
VH = Very High

TABLE 2.1 PROPERTIES OF MATERIALS (CLARE REF. 8).

The following models were constructed both for studying the behaviour and performance of a prototype dam and for the comparison of the profile obtained from theoretical and experimental work under hydrostatic and hydrodynamic conditions.

All previous models were constructed by the double anchor system, the bag of the model being anchored from the upstream and downstream side to the base and the ends of the bag sealed (see Figs. 2.3A and 2.5). [12,15,16] However, some of the prototypes were constructed by the single anchor system, the bag being anchored on the upstream side only as illustrated in Fig.2.1, section A.A. This latter technique is used for water inflated dams which due to the internal water produce high pressures on the base which cause the base to lay on the bed. The dam is usually inflated by low water pressure (slightly higher than the upstream head) and used under zero downstream head in order to overcome the uplift pressure which occurs under the bag when inflated by high pressure or when exposed to a downstream head. If this single anchor technique is applied to an air inflated dam then the problem of uplift due to upstream head becomes major.

An alternative technique of inflation[22] used only for water inflated dams is to fold the open ends up the bank above the height of the internal head of water as illustrated in Fig.2.2. The height of the bank should be higher than the crest height of the dam in order to contain the internal water. One problem with this technique of inflation is the resulting variable internal pressure during operation when the upstream and downstream heads change.

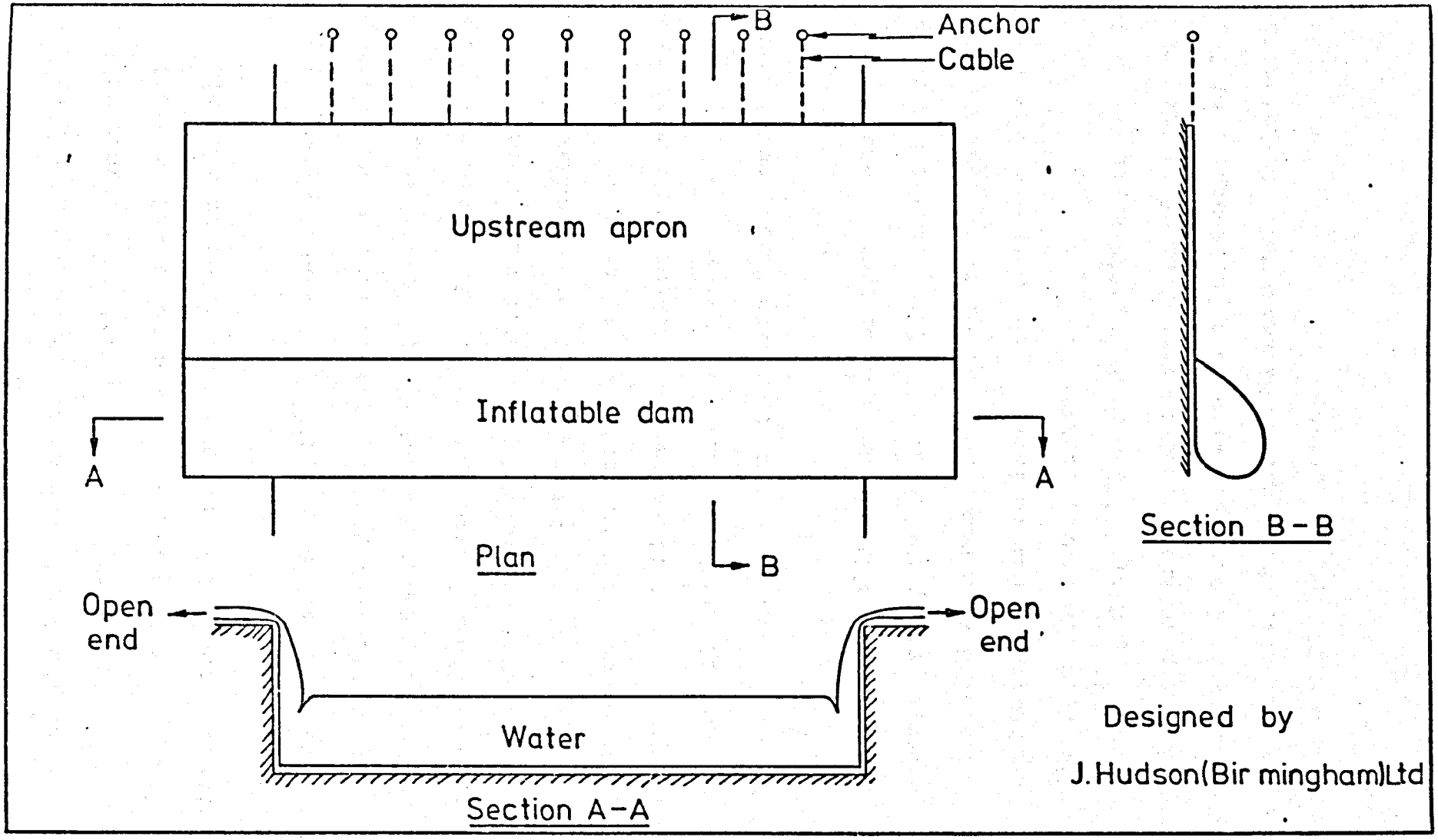

FIG. (2-2) WATER INFLATED TECHNIQUE

All the theoretical analysis described later is based on the double anchor system as one of the previous model tests. As the object of this work is to overcome the limitation of the techniques of other works and to develop design criteria, then all further work relates to a double anchor system.

Baker[1] and Shepherd[2] constructed models to study the behaviour of prototype dams particularly under hydrodynamic conditions. Baker's model consisted of a membrane length of 0.70 m and base length of 0.22 m. The model was inflated by water pressure and tested under different combinations of overflow head, internal water pressure and downstream head. The purpose of building the model was to study the behaviour of the prototype of an inflatable dam which was suggested as a possible means of regulating the tail water level at the outlets of a tunnel used for river diversion during construction of Mangla Dam.

Shepherd, built a model dam of approximate height 0.3 m in order to study the behaviour of the inflatable dam which was suggested as a possible means of attachment to the crest of Koombooloomba dam to increase the output of the power station from the increased head.

Anwar[6], Clare[8] and Stodulka[11] built models in order to compare the theoretical profile of the dam obtained from theoretical analysis with an experimental profile. Anwar made two models, the first model was 0.305m in height and the second was 0.226 m in height.

Clare made different sizes of models from various types of fabrics. The length of membrane of the models varied from 0.27 m to 1.75 m and the base length varied from 0.05 m to 0.45 m and the approximate height of the models varied from 0.1 m to 0.34 m.

Stodulka constructed a model having membrane length 0.96 m and base length 0.3m and the approximate height was 0.3 m.

The properties of the fabrics used to construct these models are illustrated in table 2.2.

2.4 Theoretical Methods of Analysis.

The object of any theoretical analysis is to calculate the tension in the membrane and the shape of the profile (including the maximum dam height) for given upstream and downstream heads applied to a particular length of membrane of known physical properties under a known inflation pressure and base length.

The first published theoretical study of the analysis of an inflatable dam to determine the tension and shape of the membrane was by Anwar[6] in 1967. The analysis dealt with air or water inflated dams under hydrostatic conditions and an air inflated dam under hydrodynamic conditions.

In 1970 Harrison[7] developed a finite element method for analysis of a dam under hydrostatic conditions. This method was used for the analysis of a dam inflated by air, water and a combination of air and water.

However, Clare[8] (1972) and Binnie[9] (1973) developed the theoretical method of Anwar for the analysis of a dam inflated by water and exposed to hydrostatic conditions only.

No.	Model Investigator	Material	Thick-ness (mm)	Weight (kg/m^2)	Tensile Strength (kN/m)
1.	Baker	Rubberized cloth	1.58	-	-
2.	Shepherd	1) Uncoated nylon	-	0.081	-
		2) Neoprene coated nylon	-	0.221	-
3.	Anwar	Polythene	0.254	0.237	1.92-4.20
4.	Clare	1) Polythene	0.254	0.254	3.85
		2) Rubber	0.792	1.010	6.00
		3) Rubber insert	0.698	1.133	6.74
		4) Combination of rubber and rubber insert	1.501	2.230	15.00
		5) Rubber backed canvas	0.381	1.021	3.68
5.	Stodulka	Neolon fabric	-	0.221	-

TABLE 2.2 PROPERTIES OF MODEL MATERIALS.

The latest theoretical method was published by Parbery[10] (1976). This method was used to analyse a dam under hydrostatic conditions and dealt with dams inflated by air, water and air/water pressures.

These methods are described in detail in sections 2.4.1, 2.4.2, 2.4.3, 2.4.5 and 2.4.6.

2.4.1 Theoretical Method of Anwar.

Anwar derived a set of mathematical equations to determine the shape of air or water inflated dams under hydrostatic conditions. These equations were dependent upon the following assumptions:

1. The membrane of the dam is weightless and inextensible.
2. The upstream head is always the same as the dam height.
3. The dam is constructed on a horizontal slab.
4. The downstream side of the membrane is laid tangential to the base at the downstream anchor.
5. The downstream head is equal to zero.
6. The membrane length and base length are ignored.
7. In the case of water inflated dams, the end of the downstream membrane is fixed above a horizontal base (see Fig.2.3B).

These assumptions were also applied to the analysis of an air inflated dam under hydrodynamic conditions.

2.4.1.1 Analysis of a Dam under Hydrostatic Conditions.

2.4.1.1.1 Air Inflated Dam.

i) Tension in the Membrane.

The tension in the membrane cannot be found by this technique until the shape has been theoretically or experimenally

obtained. The tension is assumed constant around the membrane and its magnitude is taken as that occurring at the crest of the dam

$$T = \frac{1}{2} \alpha \rho g (Y_{max})^2 \quad \ldots\ldots \quad (2.1)$$

where

T = tension in the membrane.

α = factor of proportionality for internal pressure.

ρ = density of water.

g = acceleration due to gravity.

Y_{max} = height of the dam.

ii) Profile of the Dam.

The profile of the dam is obtained from considering the upstream and downstream sections of the dam separately. The upstream and downstream sections are defined as being the portions of the dam which are upstream and downstream respectively of the perpendicular line through the foundation from the crest of the dam as shown in Fig.2.3A.

(a) Upstream Profile.

The differential equation of the shape of the upstream profile is its tangent equation as follows:

$$\tan \beta = \frac{V_p}{H_p}$$

where

β = angle of tangent to the dam at any point on the upstream profile.

V_p = vertical component of the hydrostatic force.

H_p = horizontal component of the hydrostatic force.

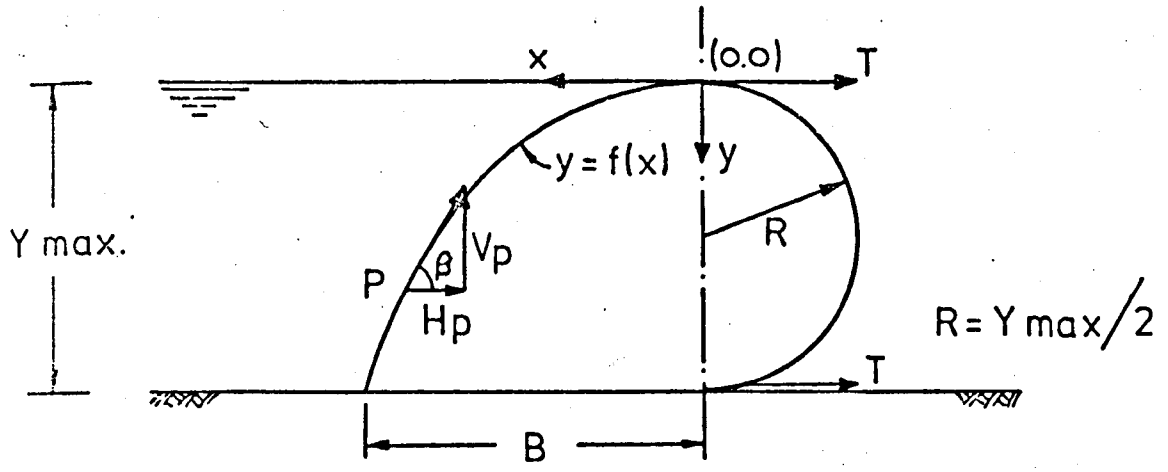

(A) AIR INFLATED DAM UNDER HYDROSTATIC CONDITIONS

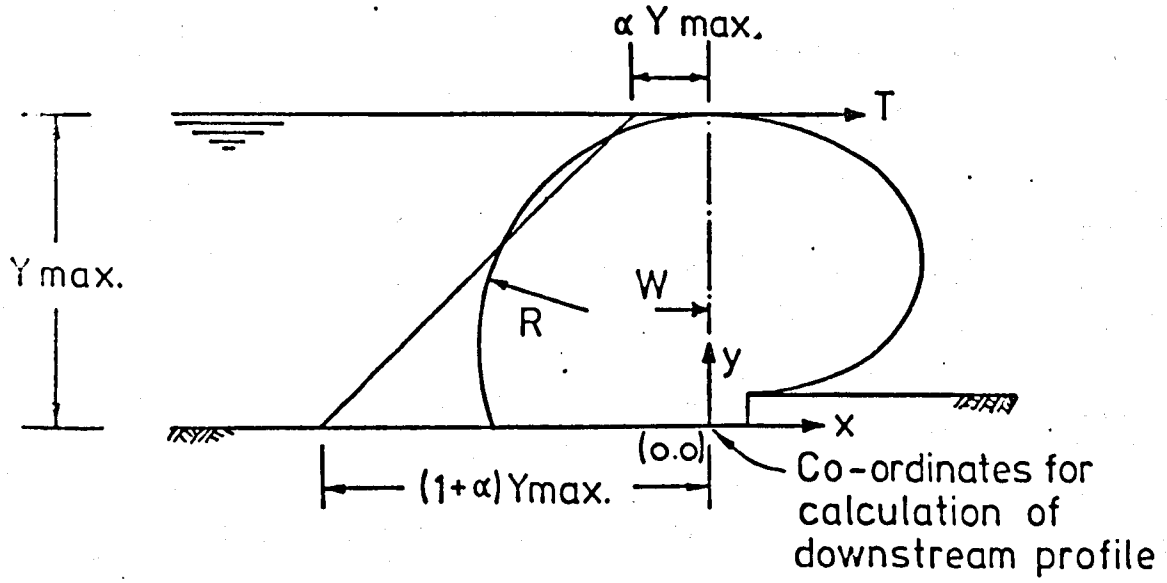

(B) WATER INFLATED DAM UNDER HYDROSTATIC CONDITIONS

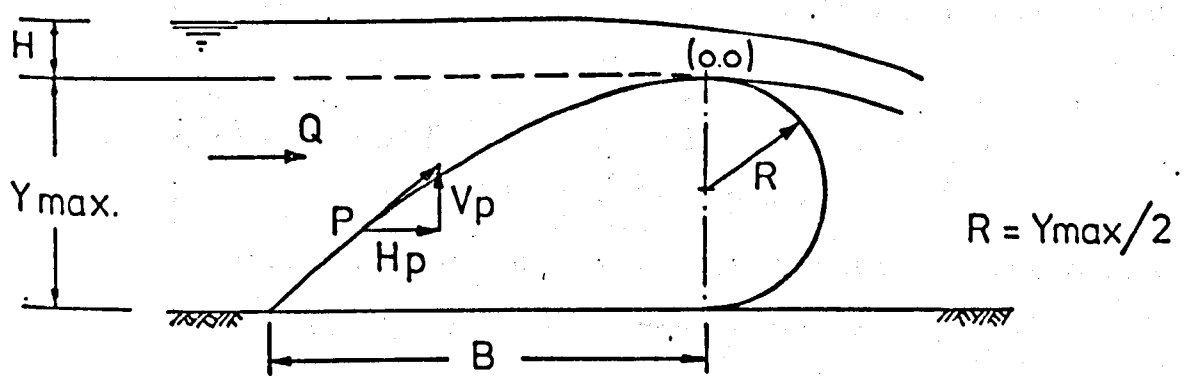

(C) AIR INFLATED DAM UNDER HYDRODYNAMIC CONDITIONS

FIG. (2-3) ANWAR'S ANALYSIS OF AN INFLATABLE DAM

The magnitude of H_p and V_p at an arbitrary point p per unit length are:

$$H_p = \frac{1}{2} \alpha \rho g (Y_{max})^2 + \frac{1}{2} \rho g y^2 - \alpha \rho g (Y_{max}) \cdot y \quad .. \quad (2.3)$$

and

$$V_p = \alpha g \int f(x)\, dx - \alpha \rho g (Y_{max}).x \quad ..... \quad (2.4)$$

in which x and y are the co-ordinates of the point p and f(x) is an analytical function describing the shape of the dam.

Substituting equations 2.3 and 2.4 in equation 2.2 to obtain the profile of the upstream section:

$$\frac{X}{Y_{max}} = \sqrt{2\alpha} \left\{ 2 \hat{E} \sqrt{\frac{\alpha}{2}} - \hat{F} \sqrt{\frac{\alpha}{2}} = E \left[\text{arc cos } \left(\frac{Y}{\alpha (Y_{max})} \right) \sqrt{\frac{\alpha}{2}} \right] \right.$$

$$\left. + 0.5\ F \left[\text{arc cos } \left(\frac{Y}{\alpha (Y_{max})} - 1 \right) \sqrt{\frac{\alpha}{2}} \right] \right\} \quad ..... \quad (2.5)$$

where E and F are the elliptic integrals of second and first kind respectively, and the circumflexion denotes that the integrals are complete.

(b) Downstream Profile.

The downstream profile is assumed to be a semi-circular curve of diameter Y_{max} (see Fig.2.3A).

2.4.1.1.2 Water Inflated Dam.

i) Tension in the Membrane.

The horizontal component of the internal water pressure (W) per unit length acting on the membrane is:

$$W = \frac{1+2\alpha}{2} \rho g (Y_{max})^2 \quad \ldots\ldots \quad (2.6)$$

and the line of action of this component is $(\frac{1+3\alpha}{1+2\alpha}) \frac{Y_{max}}{3}$ above O as shown in Fig.2.3B.

By taking the moment of forces about O, then the tension at the crest is:

$$T = \frac{1+3\alpha}{6} \rho g (Y_{max})^2 \quad \ldots\ldots \quad (2.7)$$

ii) Profile of the Dam.

The profile of the dam is considered to be made up of an upstream and downstream section as previously defined.

(a) Upstream Profile.

The differential equation for the upstream membrane profile is obtained using the same principles as used in the air inflated dam. The horizontal and vertical components of the hydrostatic force acting on an arbitrary point p per unit length are given by:

$$H_p = \frac{1+3\alpha}{6} \rho g (Y_{max})^2 - \alpha \rho g (Y_{max}) \cdot y \quad \ldots\ldots \quad (2.8)$$

and

$$V_p = - \alpha \rho g (Y_{max}) \cdot x \quad \ldots\ldots \quad (2.9)$$

The tangent β at the point p of the dam can be written as:

$$\tan \beta = \frac{- \alpha \rho g (Y_{max}) \cdot x}{\frac{1+3\alpha}{6} \rho g (Y_{max})^2 - \alpha \rho g (Y_{max}) \cdot y} \quad \ldots \quad (2.10)$$

Operating on this equation the shape of the upstream profile is given by:

$$\left[\frac{x}{(Y_{max})}\right]^2 + \left[\frac{y}{(Y_{max})}\right]^2 = \frac{1+3\alpha}{3\alpha} \left[\frac{y}{(Y_{max})}\right] \quad \ldots\ldots \quad (2.11)$$

Equation 2.11 represents the equation of a circle with radius $[(1+3\alpha)/6\alpha]$ and is a tangent to the x-axis at the crest.

(b) Downstream Profile.

The downstream profile is obtained from

$$T = P' R \quad \ldots\ldots \quad (2.12)$$

where T (the tension in the membrane) was given by equation 2.7, P' is the pressure at an arbitrary point of the membrane on the downstream section and is given by

$$P' = \rho g [(1+\alpha) Y_{max} - y] \quad \ldots\ldots \quad (2.13)$$

where R is the radius of curvature at that point and is given by:

$$R = \left[\frac{1 + (\frac{dy}{dx})^2}{\frac{d^2y}{dx^2}} \right]^{3/2} \quad \ldots\ldots \quad (2.14)$$

Substituting equations 2.13 and 2.14 into equation 2.12 yields

$$\frac{x}{(Y_{max})} + C'_2 = \alpha E (K_1, \phi) - (\alpha - 1 - \frac{1}{3\alpha}) F (K_1, \phi) \quad \ldots \quad (2.15)$$

in which C'_2 is a constant of integration and E and F are the elliptic integral of the second and first kind.

2.4.1.2 Air Inflated Dam under Hydrodynamic Conditions.

The tension and cross-sectional profile of the dam was studied for an air inflated dam under hydrodynamic conditions by assuming the flow over the crest being similar to jet flow,

as shown in Fig.2.3c. The theoretical approach of calculating the tension and the shape of the dam is similar to the approach which was used for analysis of an air inflated dam under hydrostatic conditions (section 2.4.1.1) except that allowances were made in the analysis of the upstream profile for an approach velocity and static pressure due to an increased head.

2.4.2 Theoretical Method of Harrison.

In 1970 Harrison[7] developed a finite element method (which was used previously for the analysis of a suspension cable [22,24]) for analysis of an inflatable dam. This method was used to analyse a dam inflated by air, water and air/water pressure and to determine the tension and the shape of the membrane of the dam. However, this analysis of the membrane was dependent on three basic assumptions:-

(1) The behaviour of the three-dimensional structure was represented by a two-dimensional transverse of unit width.

(2) The perimeter of the dam was composed of a finite number of small straight elements and loads acting on the nodes of the elements.

(3) The behaviour of the fabric used for constructing the dam had a linear stress-strain relationship.

The weight and extensibility of the membrane was included throughout the analysis. The method was also used for the analysis of a dam with different base geometry to a flat base.

The method could analyse a dam under different combinations of upstream head, downstream head and internal air, water and

air/water pressure. However, when the dam was exposed under conditions of upstream head = dam height, this method was not applicable due to the unknown maximum height and distribution of the hydrostatic forces on the membrane.

The hydrostatic pressures acting on the dam were due to the upstream head, downstream head, internal pressure and weight of membrane as shown in Fig.2.4A. The actual tension and the cross-sectional profile of the dam were determined by dividing the membrane into n elements and n+1 nodes and assuming initial values of tension and slope of the first upstream element. The loads acting on each node due to the hydrostatic pressures were calculated in order to find the tension in the element and the co-ordinates of the nodes as shown in Fig.2.4B. This procedure was carried out around the whole membrane to locate its shape.

If the co-ordinate at the last node did not coincide with the known co-ordinate of the downstream anchor point, the procedure for determining the co-ordinate of the nodes on the profile needs to be repeated with adjusted values of initial tension and slope of the first element (see section 4.2 of Chapter 4).

The equations for applying this technique are detailed in Chapter 4 as the work of the author is based on an extension of Harrison's method.

2.4.3 Theoretical Method of Clare.

Clare[8] used a mathematical analysis to determine the shape of the profile for a water inflated dam under hydrostatic conditions. This analysis was dependent upon the following assumptions:-

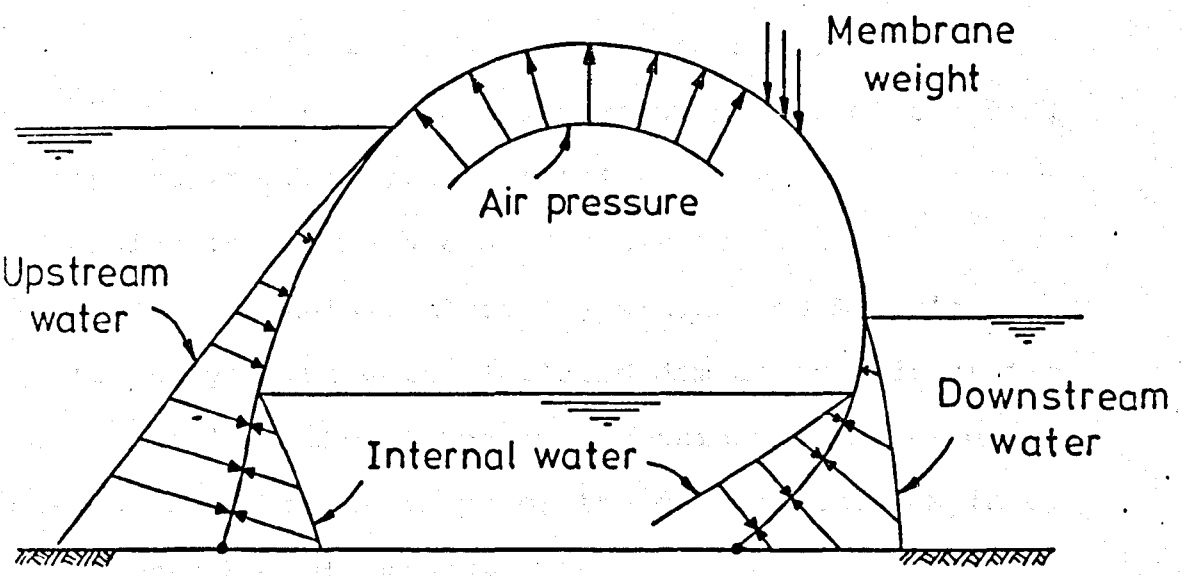

(A) FORCES ACTING ON THE MEMBRANE OF A DAM

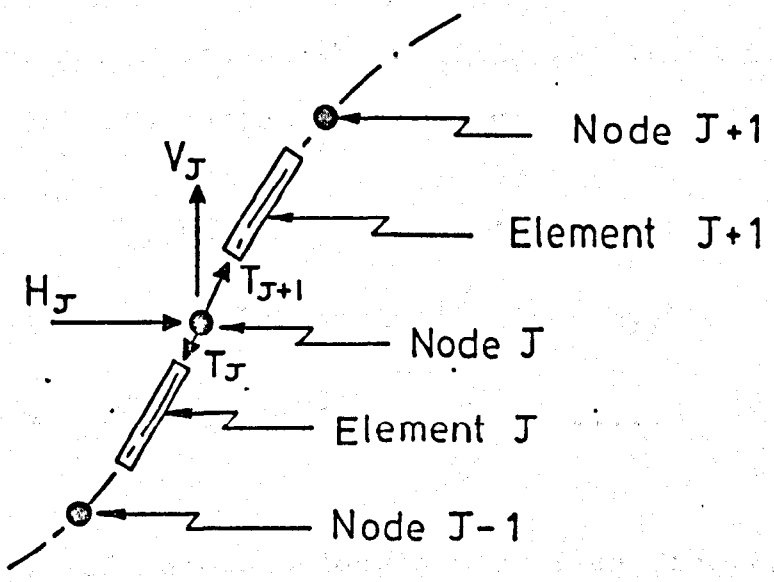

(B) FORCES ACTING ON NODES

FIG.(2-4) HARRISON'S ANALYSIS OF A DAM
UNDER HYDROSTATIC CONDITIONS

(1) The membrane is weightless and inextensible.

(2) The dam is laid flat at the downstream side.

(3) Upstream head is equal to the maximum height of the dam.

(4) The base of the dam is horizontal.

(5) The tension in the membrane is constant.

His approach to this analysis is similar to Anwar's approach to analyse the water inflated dam under hydrostatic conditions. This method takes into consideration the effects of downstream head on the shape of the dam and the length of the membrane can be determined.

The analysis of the profile was considered by analysis of the upstream section and downstream section of the profile separately as shown in Fig.2.5.

2.4.3.1 Analysis of a Dam with Downstream Head Zero.

(a) Upstream Profile.

The upstream section of the profile was found to be an arc of a circle with radius C given by

$$C = \frac{T}{\rho g \alpha (Y_{max})} \quad \ldots\ldots \quad (2.16)$$

The total upstream profile length is given by:

$$bu = \frac{\pi C}{2} + C \sin^{-1}\left(\frac{a}{C}\right) + a \quad \ldots\ldots \quad (2.17)$$

where

bu = total membrane length RAPQ (see Fig. 2.5).

a = upstream portion of basic length and is given by

$$a = \sqrt{\frac{2T}{\rho g \alpha} - (Y_{max})} \quad \ldots\ldots \quad (2.18)$$

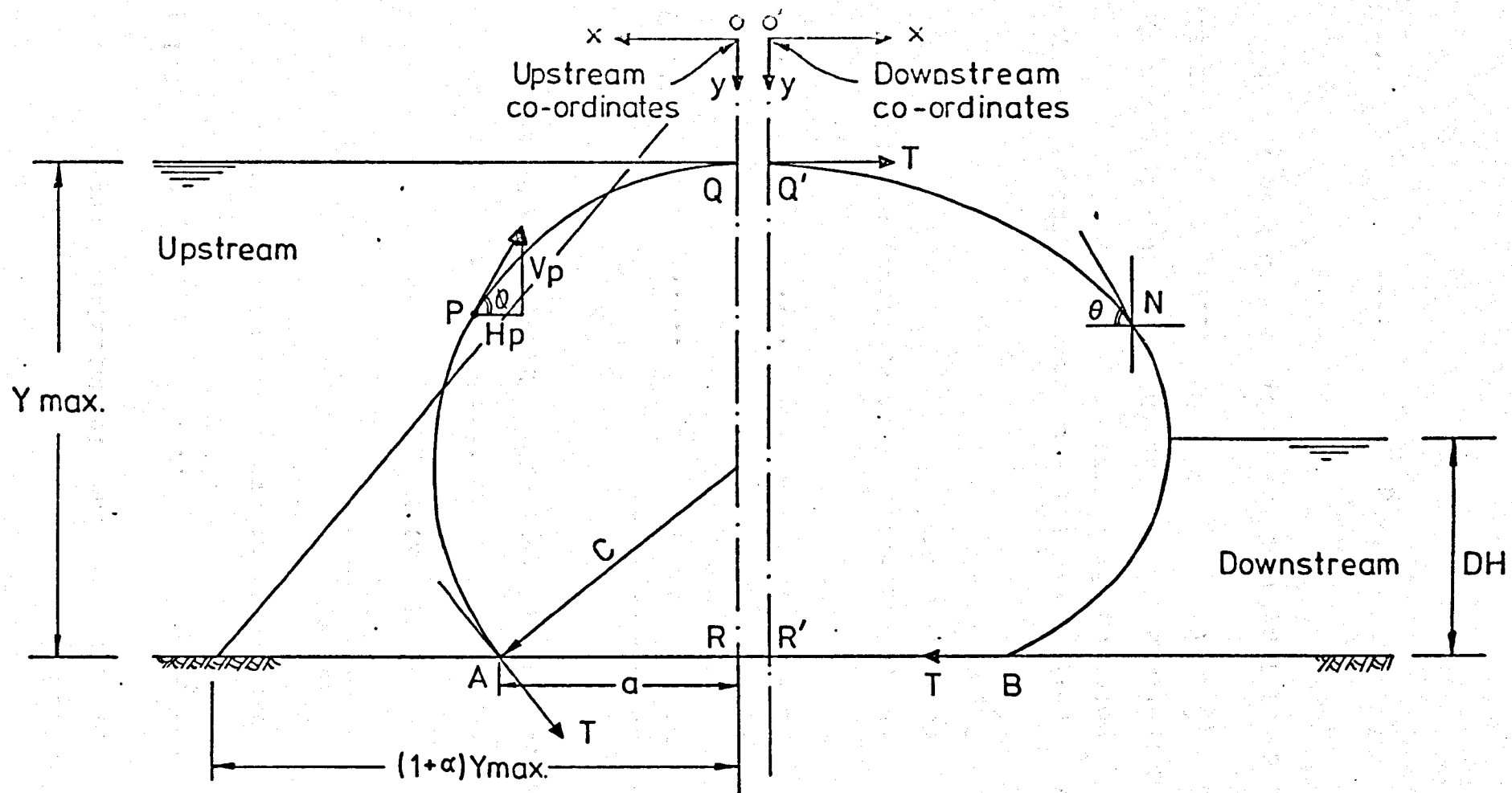

FIG. (2-5) CLARE'S ANALYSIS OF WATER INFLATED DAM

(b) Downstream Profile.

The tension in the membrane is calculated from

$$T = \frac{\Delta^2 K^2 \rho g}{4} \quad \ldots\ldots \quad (2.19)$$

and is assumed constant around the membrane and

$$K^2 = 1 - \frac{(\alpha . y_{max})^2}{\Delta^2}$$

in which $\Delta = (1 + \alpha) Y_{max}$

The downstream profile was found to be the arc of an elliptic curve and the shape of arc being given by the expression

$$\frac{y}{\Delta} = \sqrt{1 - K^2 \sin^2 \phi} \quad \ldots\ldots \quad (2.20)$$

$$\frac{x}{\Delta} = (1 - \tfrac{1}{2} K^2) \hat{F} - \hat{E} \quad \ldots\ldots \quad (2.21)$$

where

x,y = the co-ordinates of an arbitrary point N on the downstream profile.

$\phi = \frac{\pi - \theta}{2}$

where θ = angle formed between tangent to the arbitrary point on the downstream profile.

Then, the downstream profile length R'BNQ' (b_d) is given by

$$b_d = (\hat{F} - \hat{E}) \quad \ldots\ldots \quad (2.22)$$

Hence, the total length of the membrane with base length (LT) is

$$LT = b_u + b_d \quad \ldots\ldots \quad (2.23)$$

2.4.3.2 Analysis of a Dam with a Downstream Head.

(a) Upstream Profile.

When the dam supports a downstream head equal to DH, the upstream profile was found to be the arc of a circle with radius C and was calculated from equation 2.16.

(b) Downstream Profile.

The tension in the membrane was calculated by:

$$\frac{T\ (1-\cos\theta)}{\delta\ \rho\ g} = \frac{K'^2}{2} \quad \ldots\ldots \quad (2.24)$$

where

$$\delta = [((1+\alpha).\ Y_{max}) - DH]^2$$

$$K'^2 = 1 - \frac{(\alpha.Y_{max})^2}{\delta}$$

DH = downstream head.

The shape of the profile of the downstream side was found as a cross-section of a circle with radius C'

$$C' = \frac{T}{\rho\ f\ \delta} \quad \ldots\ldots \quad (2.25)$$

for the section below the downstream level. However, the section above the downstream level was determined by a similar approach to that used for the downstream profile for a dam with zero downstream head.

2.4.4 Theoretical Method of Binnie.

Binnie[9] used a similar approach to Clare for analysis of a water inflated dam (with similar limitations of analysis) in order to calculate the shape of the upstream and downstream profiles. This analysis was used for a dam with a downstream head equal to zero.

2.4.5 Theoretical Method of Parbery.

The latest theoretical analysis of an inflatable dam was published by Parbery[10] in 1976. This method deals with the analysis of air, water and air/water inflated dams under hydrostatic conditions. The method consists of a set of differential equations of equilibrium to determine the tension and the shape of the profile.

The analysis is carried out on a membrane divided into n straight elements and n+1 nodes. The resultant of forces acting on each element due to internal pressure are determined in order to calculate the tension and slope of the first element, as shown in Fig.2.6.

The tension is found from:-

$$T = T_o + wy \quad \ldots\ldots \quad (2.25)$$

where

T = tension in the element per unit width.

T_o = T(o) initial tension of the membrane at the origin (upstream anchor) of profile co-ordinates per unit width.

w = weight of membrane per unit area.

y = co-ordinate.

The initial tension and slope of the first element is calculated from a set of differential equations and by assuming the behaviour of the stress-strain relationship of the membrane material to be linear.

The differential equations of equilibrium are:

$$\frac{d\phi}{dS'} = \frac{f}{T_o + wy} (P - w \cos \phi) \quad \ldots\ldots \quad (2.26)$$

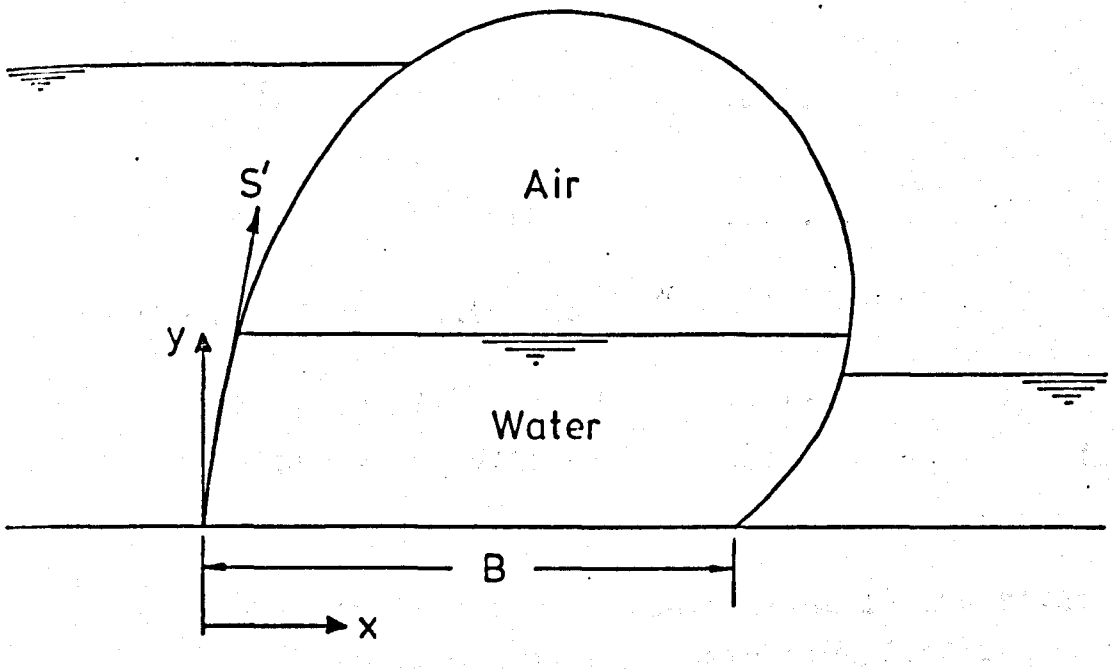

(A) Parbery's inflatable dam

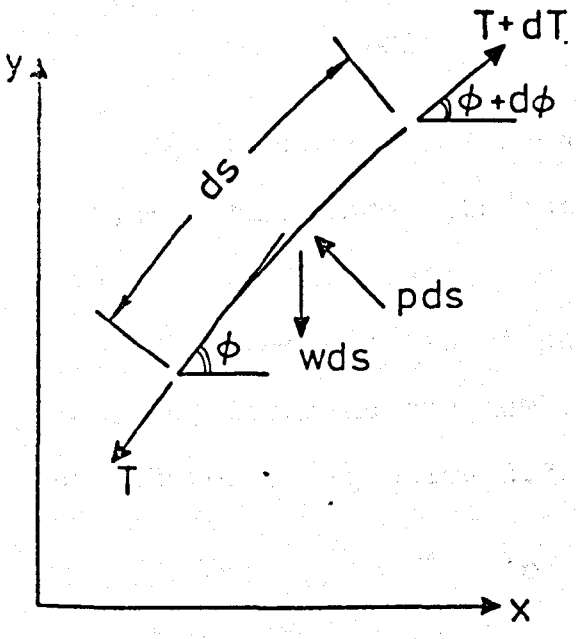

(B) Load on an element

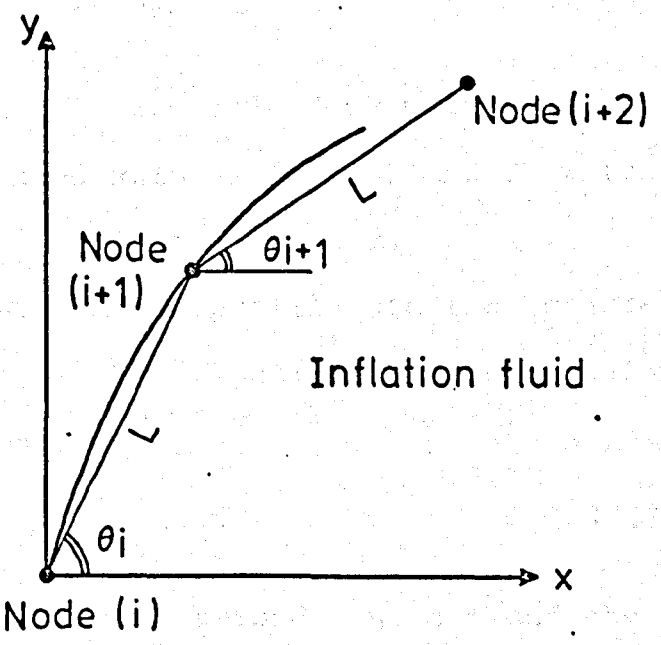

(C) Analysis of a dam

FIG.(2-6) PARBERY'S ANALYSIS OF A DAM UNDER HYDROSTATIC CONDITIONS

$$\frac{dx}{dS'} = f \cos \phi \quad \ldots\ldots \quad (2.27)$$

$$\frac{dy}{dx} = f \sin \phi \quad \ldots\ldots \quad (2.28)$$

With the boundary conditions

$$x(0) = y(0) = 0 \quad \ldots\ldots \quad (2.29)$$

$$x(L) = B,\ y(L) = 0 \quad \ldots\ldots \quad (2.30)$$

Where

ϕ = inclination of the tangent in the S' direction to the horizontal (see fig. 2.6A).

S' = the length along unstretched perimeter.

f = extension ratio of the membrane under load.

P = resultant of the internal pressure.

x,y = co-ordinates of an arbitrary point on the profile.

Equations 2.26, 2.27 and 2.28 are solved by using the Runge-Kutta method with estimated values of $\phi(0)$ and T_o which are then refined using the Newton-Raphson method.

The co-ordinates of points on the profile are then calculated and by assuming the membrane to be weightless and inextensible, and therefore equation 2.25 becomes:

$$T = T_o \quad \ldots\ldots \quad (2.31)$$

and the tension round the membrane is around constant and the co-ordinates of the point on the profile are given by

$$x = L \left\{ \cos \theta_i \left[2 - \frac{7}{12} \left(\frac{PL}{T} \right)^2 \right] + \frac{PL}{T} \sin \theta_i \right\} \quad \ldots \quad (2.32)$$

$$y = L \left\{ \sin \theta_i \left[2 - \frac{7}{12} \left(\frac{PL}{T}\right)^2 \right] - \frac{PL}{T} \cos \theta_i \right\} \quad \ldots \quad (2.33)$$

where

θ_i = slope of element i.

L = length of element.

2.5 Comparison Between the Various Theoretical Methods of Analysis.

A qualitative comparison was carried out on the conditions of membrane analysis, dam construction and operational procedure (upstream head, downstream head and internal pressure) by considering the analysis of a dam by Anwar, Harrison, Clare, Binnie and Parbery methods.

Table 2.3 illustrates the comparison between these theoretical methods under hydrostatic conditions.

From the table it can be seen that in all the methods except Harrison's it is assumed that weightless and inextensible membranes are used when deriving the equations for determining the shape of the dam and the tension in the membrane. Harrison's method assumed the behaviour of the stress-strain relationship in the membrane to be linear.

The tension in the membrane by the methods of Anwar, Clare, Binnie and Parbery must be constant around the membrane due to the assumptions made, whereas Harrison's method allows for a variable tension.

Clare and Binnie analysed dams inflated by water only, Anwar used dams inflated either by air or water but Harrison and Parbery included dams inflated by a mixture of air and water in their analysis. An allowance for a different

Conditions of Analysis	Anwar	Harrison	Clare	Binnie	Parbery
a) Membrane					
1. Including weight and extensibility of membrane.	No	Yes	No	No	No
2. Behaviour of stress-strain relationship of membrane is non-linear.	No	No	No	No	No
b) Construction					
1. Horizontal flat base is not necessary.	No	Yes	No	No	No
2. Inflation by air.	Yes	Yes	No	No	Yes
3. Inflation by water.	Yes	Yes	Yes	Yes	Yes
4. Inflation by air and water.	No	Yes	No	No	Yes
c) Hydrostatic					
1. Downstream head equal to zero.	Yes	Yes	Yes	Yes	Yes
2. Downstream head greater than zero.	No	Yes	Yes	No	Yes
3. Upstream head less than dam height.	No	Yes	No	No	Yes
4. Upstream head equal to dam height.	Yes	No	Yes	Yes	Yes
5. Downstream profile laid flat on the base (downstream slope = 0).	Yes	No	Yes	Yes	Yes
6. Downstream profile is not laid flat at downstream side.	No	Yes	No	No	Yes

TABLE 2.3 QUALITATIVE COMPARISON OF THEORETICAL METHODS OF ANALYSIS.

geometry of the base to a flat base for the dam is included in Harrison's analysis only and the other analyses used a horizontal base throughout.

The main problem with Harrison's method is that it cannot be used for the analysis of a dam when the upstream head equal to the height of the dam or when the dam is laid flat at the downstream fixture (see section 4.5.1.4).

Consequently none of the aforementioned methods can be used to analyse satisfactorily a dam under overflow conditions when the dam is inflated by air, water and air/water pressure, although Anwar analysed air inflated dams under overflow conditions with the severe limitations described in section 2.4.1.

2.6 Discussion of the Limitation of the Theoretical Methods of Analysis.

The significance of the limitations of the various methods is highlighted by the results of tables 2.4 and 2.5 which show the significance of considering the weight and extensibility of the membrane in calculating the tension and shape under different internal pressures.

Parbery[25] states that the membrane weight has minor effects on the tension and shape of the dam. From analysis carried out by the author using equations detailed in chapter 4, the results given in table 2.4 show that this statement by Parbery is true when the dam is inflated by high internal pressures, but as the pressure is decreased the weight of the membrane becomes more significant in calculation of the shape and tension.

The extensibility has significant effects on the tension and the shape of the membrane as demonstrated by Harrison[26] and illustrated in table 2.5.

Fluid	No.	Weight of Membrane (Kg/m^2)	Upstream		Maximum Dam Height (mm)	Downstream	
			Tension (kN/m)	Slope (deg.)		Tension (kN/m)	Slope (deg.)
Air pressure = 5.886 kN/m^2	1	0.0	0.825	124.8	299.87	1.059	49.2
	2	0.391	0.825	124.9	299.81	1.058	49.1
	3	0.50	0.824	124.9	299.80	1.058	49.1
	4	1.00	0.822	125.0	299.72	1.056	49.1
	5	1.50	0.820	125.0	299.64	1.054	49.0
	6	2.0	0.819	125.1	299.57	1.053	48.9
	7	3.0	0.816	125.2	299.37	1.050	48.8
Air pressure = 1.962 kN/m^2	1	0.0	0.250	80.8	300.50	0.318	36.6
	2	0.391	0.248	80.8	300.28	0.317	36.4
	3	0.50	0.248	80.7	300.22	0.316	36.3
	4	1.00	0.246	80.5	299.86	0.315	36.0
	5	1.50	0.245	80.4	299.65	0.313	35.7
	6	2.0	0.243	80.3	299.26	0.312	35.4
	7	3.0	0.240	80.0	298.65	0.308	34.7

TABLE 2.4 EFFECT OF MEMBRANE WEIGHT ON TENSION AND SHAPE OF AN INFLATABLE DAM.

Conditions of Analysis

Upstream head = 270 mm
Downstream head = 100 mm
Membrane length = 787 mm
Material = N.T. Fabric (see section 3.3.1)
Base length = 225 mm
Number of elements= 40
Number of nodes = 41

No.	Elastic Modulus (kN/m^2)	Upstream		Maximum Dam Height (m)	Downstream	
		Tension (kN/m)	Slope (deg.)		Tension (kN/m)	Slope (deg.)
1	206.85×10^3	229.67	107.06	6.457	230.57	0.0
2	206.85×10^4	219.36	105.42	5.990	219.57	4.51
3	206.85×10^5	218.28	105.21	5.942	218.47	6.09
4	206.85×10^6	218.16	105.19	5.939	218.35	6.25

TABLE 2.5 EFFECT OF DIFFERENT EXTENSIBILITY ON TENSION AND SHAPE OF AN INFLATABLE DAM (HARRISON REF. 26).

Conditions of analysis

Upstream head	=	5.79 m
Downstream head	=	1.52 m
Membrane length	=	18.24 m
Membrane weight	=	7.33 Kg/m^2
Membrane thickness	=	7.62 mm
Base length	=	6.08 m
Number of elements	=	50
Number of nodes	=	51

These two parameters (weight and extensibility) of the membrane are included only in the Harrison analysis. A further advantage of his analysis is the allowance for different geometry base of the dams and different combinations of hydrostatic conditions.

Finally, the Harrison method is most suitable to use for analysis because it contains two static equilibrium equations at the node.

In view of the advantages of the Harrison method over all the other forms of analysis his technique was taken as the most suitable for use in this work and as a result of this investigation has been modified to a minimum even further the assumptions in applying his technique.

Modifications have been made to the position where the hydrostatic forces are considered to act on the membrane and on the behaviour of stress-strain relationship of membrane material which can be considered as non-linear if necessary. This new method can be used for the solution of a wide range of problems which are described in detail in Chapters 4, 5, 6 and 7.

CHAPTER 3.

MODEL TESTS UNDER HYDROSTATIC CONDITIONS.

3.1 Introduction.

To check the theoretical design procedure for hydrostatic conditions of an inflatable dam, it was decided to construct a series of models designed by the theoretical technique detailed in Chapter 7. These were tested and the experimental results compared with those determined from the theoretical analysis developed in this study.

Although designed for inflation by air the model was also tested to study its behaviour when inflated by water and an air/water mixture.

A computer program detailed in Chapter 7 was used to design a model dam to maintain a 300.0 mm upstream head and an assumed 100.0 mm downstream head, as the design conditions. Section 3.4 describes the design criteria for this particular dam.

The construction of the model and its associated air and water inflation devices together with test tank are all described in this chapter.

A description of the techniques for measuring the cross-sectional profile of the dam across its width when exposed to hydrostatic conditions is given in section 3.2.4.

The cross-sectional profile was measured under different combinations of upstream and downstream head and a range of internal air, water and air/water pressures as described in section 3.7.

A comparison between the experimental profile obtained from these measurements and the profile obtained from the theoretical analysis is discussed in chapter 4.

3.2 Laboratory Apparatus.

3.2.1 Test Tank.

All experimental work was carried out in a rectangular tank 4.267 m long x 1.03 m wide x 0.387 m deep constructed in 10 mm thick clear perspex and illustrated in Fig.3.1 and Fig.3.2A.

A centrifugal pump, with 30 ℓ/s maximum flow rate, supplied the tank through a 100 mm diameter delivery pipe, which divided into two 50 mm diameter flexible pipes feeding one end of the tank, each pipe incorporating a control valve.

A movable 12.5 mm thick perspex gate was fixed at the downstream end of the tank to control the downstream depth of flow below the model dam as shown in Fig.3.2A.

It was possible to divert the outflow from the test tank to a volumetric tank (a concrete rectangular tank measuring 3.040 m in length x 1.219 m in width x 0.711 m in depth) by a galvanised steel rectangular channel, 220.0 mm wide and 250.0 mm deep, connected to the outlet of the tank. The water from the measuring tank could be diverted back to the main laboratory sump through a vertical drain pipe with a control valve. This facility was not required for the hydrostatic tests but was used for flow measurement in the hydrodynamic tests described in Chapters 5 and 6.

Two single point depth gauges were positioned in the test tank to enable the measurement of water depth upstream and downstream of the dam as illustrated in Fig.3.1 and Fig.3.2A.

3.2.2 Air Pressure Inflation Equipment.

An inlet air line was connected to the base of the model by an 8 mm diameter nylon tube from the laboratory compressed air

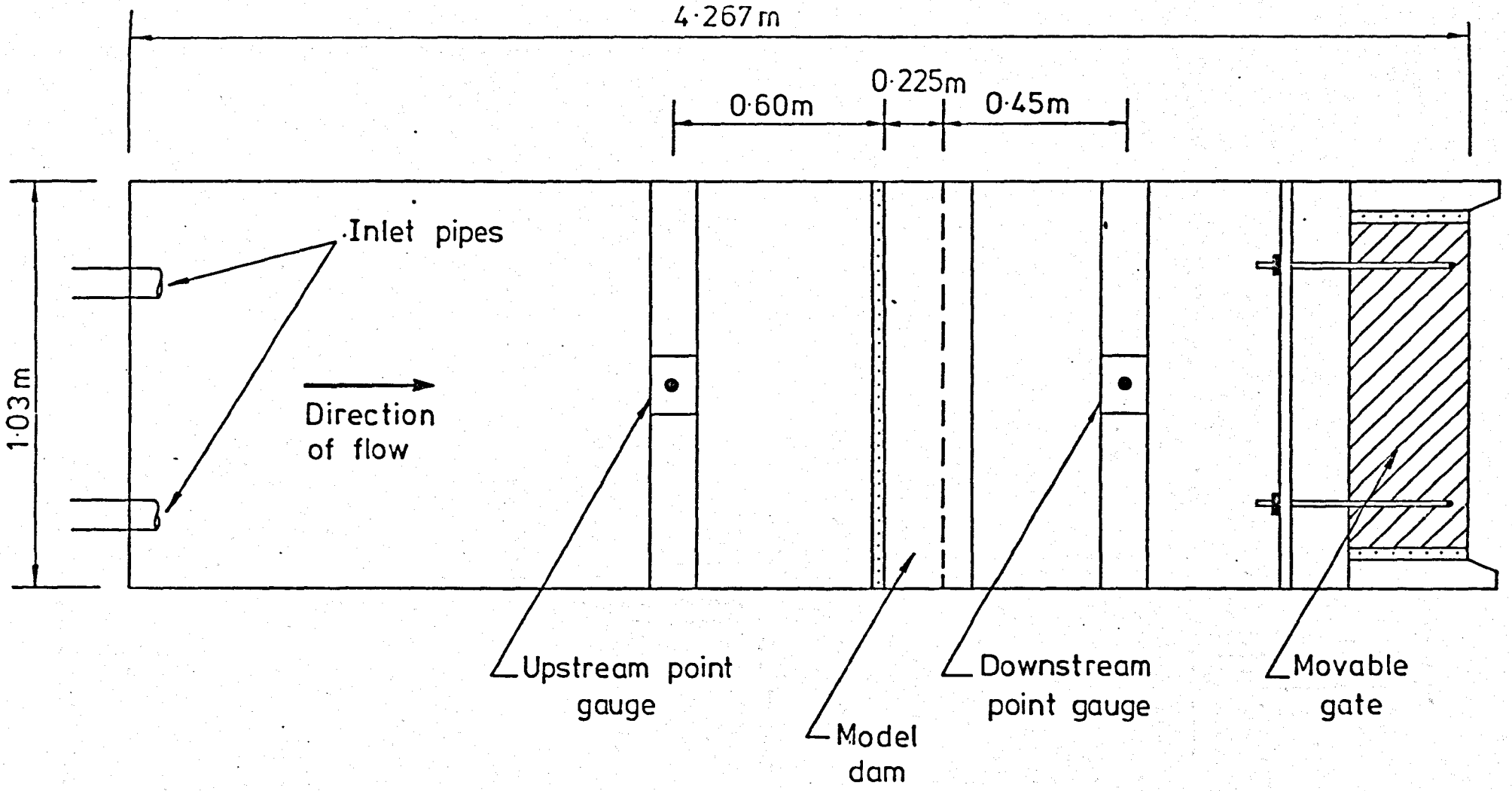

FIG. (3-1) PLAN OF TEST TANK

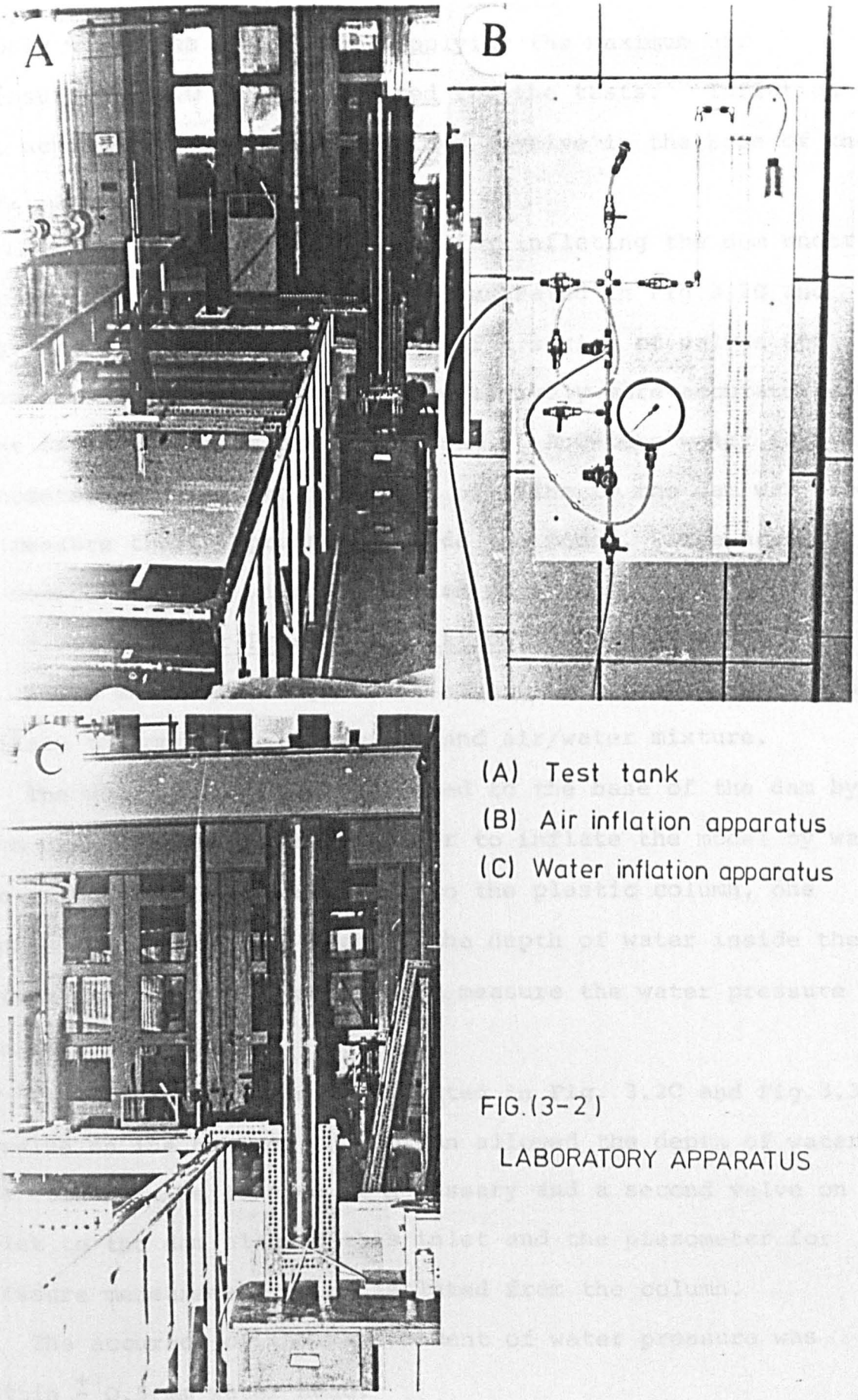

(A) Test tank

(B) Air inflation apparatus

(C) Water inflation apparatus

FIG.(3-2)

LABORATORY APPARATUS

supply which was capable of supplying the maximum air pressure of 10.0 kN/m^2 required for the tests. Inflation was achieved by releasing air from a valve in the base of the dam.

The air pressure device used for inflating the dam under air and air/water inflation is illustrated in Fig.3.2B and Fig.3.3A. This device consists of a series of valves and pressure gauges to allow the progressively more accurate adjustment of the air pressure in the dam. A U-tube water filled manometer connected to the inlet air line to the dam was used to measure the air pressure inside the model. The accuracy of measurement was within $\pm$ 0.5 mm water head.

3.2.3 Water Pressure Inflation Equipment.

A 200 mm diameter by 1.50 m high plastic column was used to inflate the model by both water and air/water mixture.

The water column was connected to the base of the dam by an 8 mm diameter nylon tube in order to inflate the model by water. Two piezometers were connected to the plastic column, one piezometer was used to measure the depth of water inside the column and the other was used to measure the water pressure inside the model.

The water column is illustrated in Fig. 3.2C and Fig.3.3B. A valve on the base of the column allowed the depth of water in the column to be lowered if necessary and a second valve on the inlet to the dam allowed this inlet and the piezometer for pressure measurement to be isolated from the column.

The accuracy of the measurement of water pressure was within $\pm$ 0.5 mm water head.

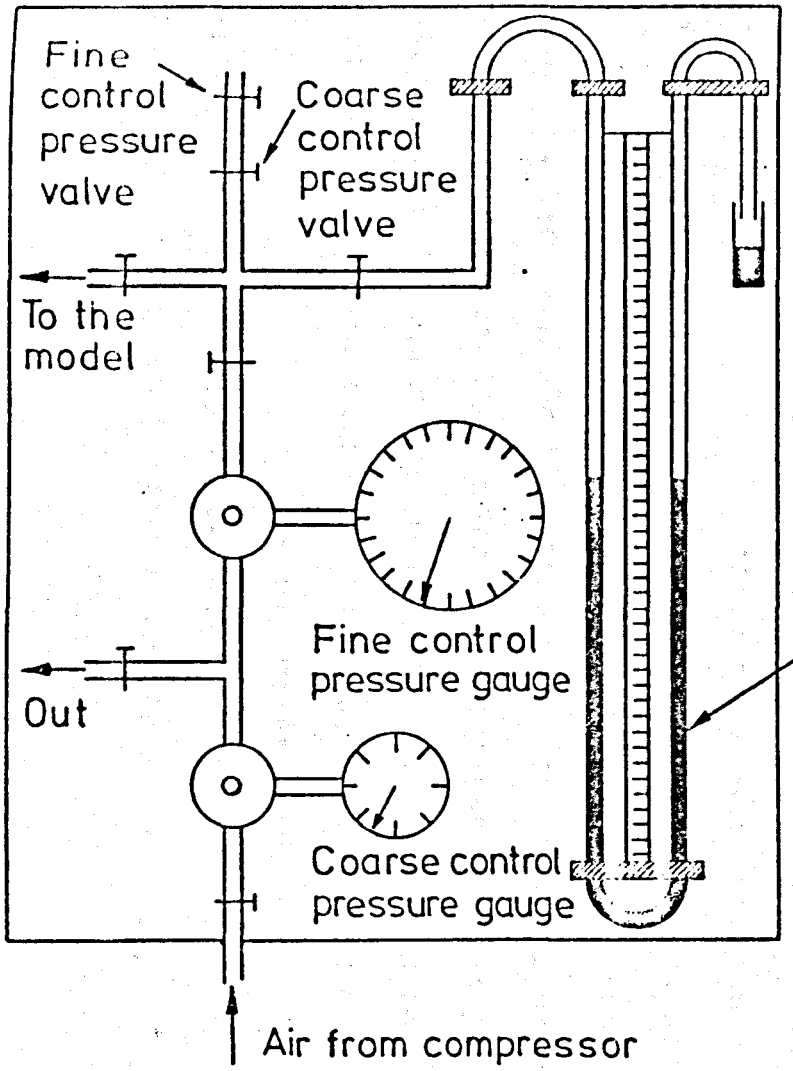

(A) Air inflation apparatus

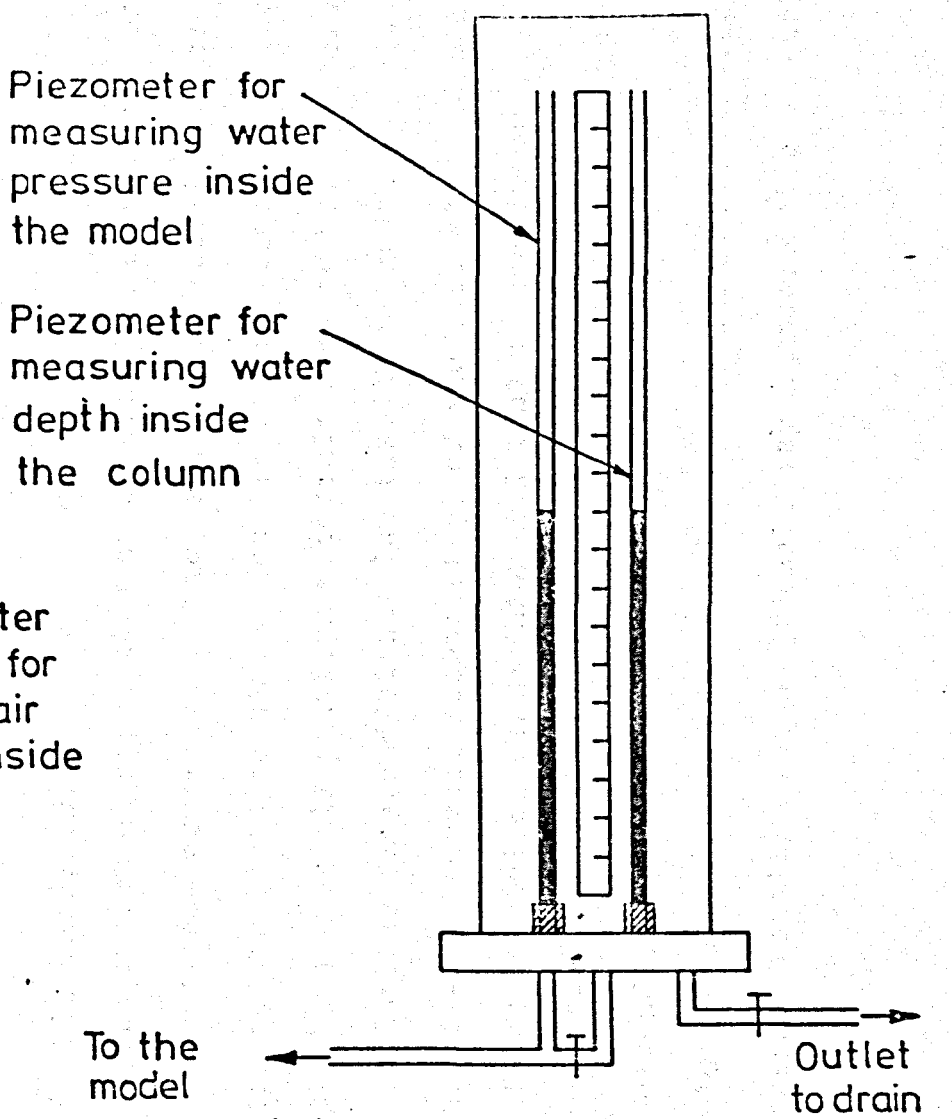

(B) Water inflation apparatus

FIG.(3-3) INFLATION APPARATUS

3.2.4 Profile Gauge.

A point depth gauge was modified to measure the vertical and horizontal displacement of the inflatable dam and this is shown diagrammatically in Fig.3.4.

Two horizontal pins were connected to the gauge; one was used for measuring the profile of the membrane on the upstream face of the dam and the other used for measuring the profile on the downstream face. The profile gauge was able to move in a horizontal plane perpendicular to the line of the dam in order to measure any horizontal deformation of the profile under different inflation conditions.

The profile gauge was also capable of movement in the line of the dam in order to measure the cross-sectional profile at any section.

The technique used to measure the profile is detailed in section 3.6.1.

3.3 Model Material.

The important properties of a suitable material for an inflatable dam are weight, thickness, stress-strain relationship and tensile strength. The literature survey (see table 2.2) shows that all previous materials used to build models of inflatable dams had either low tensile strengths or high densities. However, irrespective of the size of the dam by building a model of a 0.30m high and 1.03 m long dam using low tensile material, the tension in the membrane of the model under the anticipated loads may be high and could cause damage to the dam. Because high density materials usually have low flexibility a model built of such

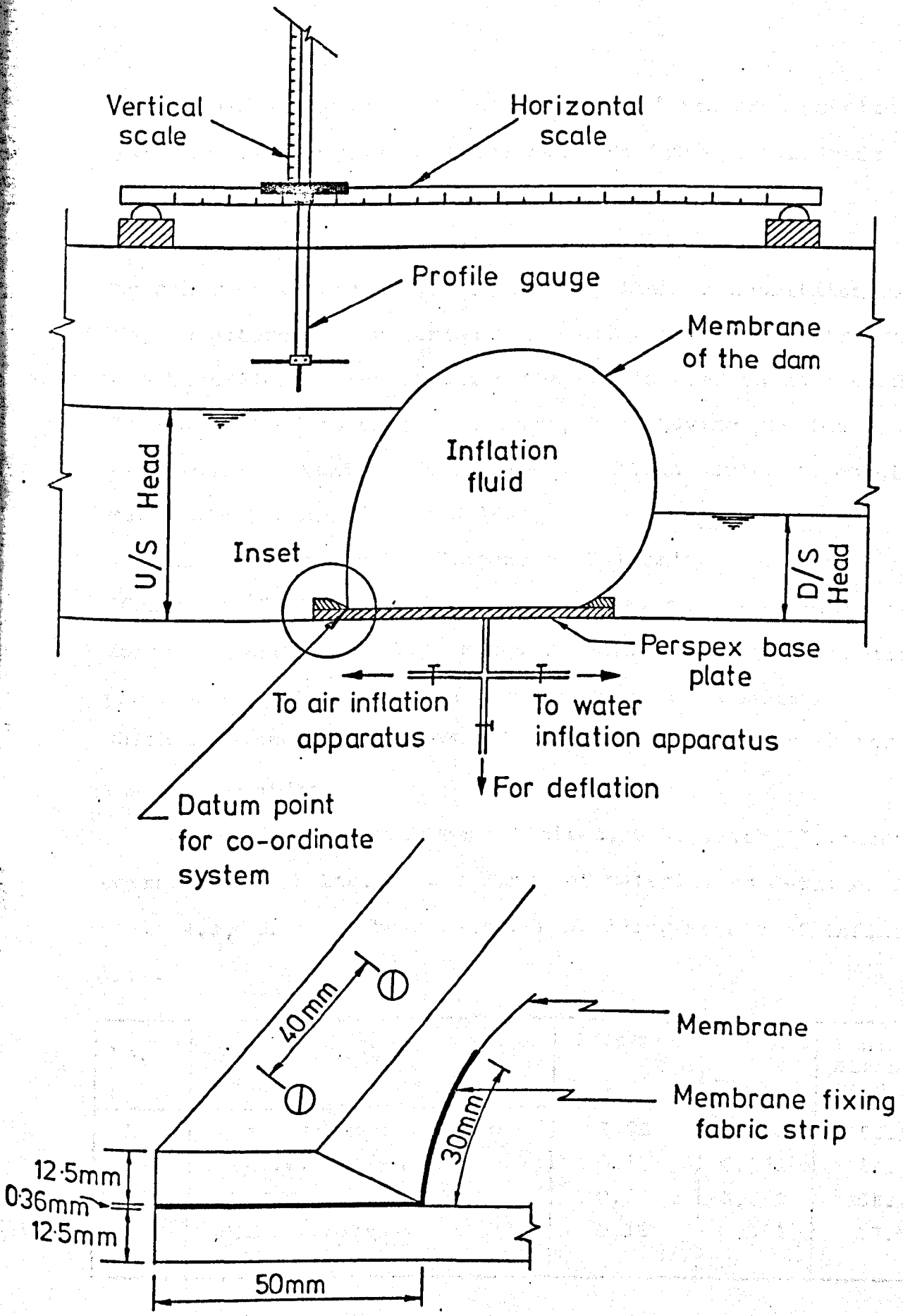

FIG. (3-4) PROFILE GAUGE AND BASE ANCHORING SYSTEM

a material would have low deformation of its cross-sectional profile when subjected to the range of hydrostatic loads during the tests at this scale.

These difficulties with the materials of the models used by other workers (and yet ignored by them) necessitated seeking an alternative material which had high tensile strength and high flexibility to build the models used in this study. It was decided to contact the Companies having previous experience of building such dams to obtain advice on possible materials for building models.

The Public Service Company of Colorado, U.S.A. (Gunnerson[27], personal correspondence) suggested using reinforced rubber material. However, this material had similar properties of high tensile strength and high density which resulted in low flexibility material and this therefore was not considered.

John Hudson (Birmingham) Limited, U.K. (Fish[22], personal correspondence) listed four kinds of material as detailed in table 4.1, that had been used for building models of inflatable dams.

No.	Material	Thickness (mm)	Weight (Kg/m^2)	Tensile Strength (kN/m)
1	Neopren coated nylon	1.93	2.100	156.96
2	P.V.C. coated	0.83	0.852	84.36
3	P.V.C. coated	0.53	0.680	58.87
4	N.T. fabric	0.36	0.391	27.56

TABLE 3.1 PROPERTIES OF MEMBRANE MATERIAL.

He recommended using N.T. fabric to build such a model, as this relatively new material had the necessary properties of low density and high tensile strength giving the degree of flexibility required.

It was therefore decided to use N.T. fabric for all models.

3.3.1 Properties of N.T. Fabric.

The weight and thickness of N.T. fabric were measured in the laboratory and found to be 0.391 Kg/m^2 and 0.36 mm respectively.

The stress-strain relationship of the fabric was determined from a strip, 200 mm long by 25.4 mm in width. The strip was fixed on a tensile testing machine and the elongation measured for a range of load increments up to failure of the strip. This was repeated on a second strip to check the consistency of the material. The maximum tensile strength of the material was found to be 27.56 kN/m in both cases.

Fig.3.5 shows the relationship between the stress and the strain of the N.T. fabric from which it can be seen that the relationship is non-linear. The equation of the curve in Fig.3.5 was determined by a polynomial curve fitting technique available as a standard computer program from the Library of the Computer Centre of the University of Sheffield.

The best fitting curve was obtained for a polynomial of degree 3 as shown in Fig.3.6, and the equation of this curve takes the form:

$$\varepsilon = C_1 + C_2 \sigma + C_2 \sigma^2 + C_4 \sigma^3$$

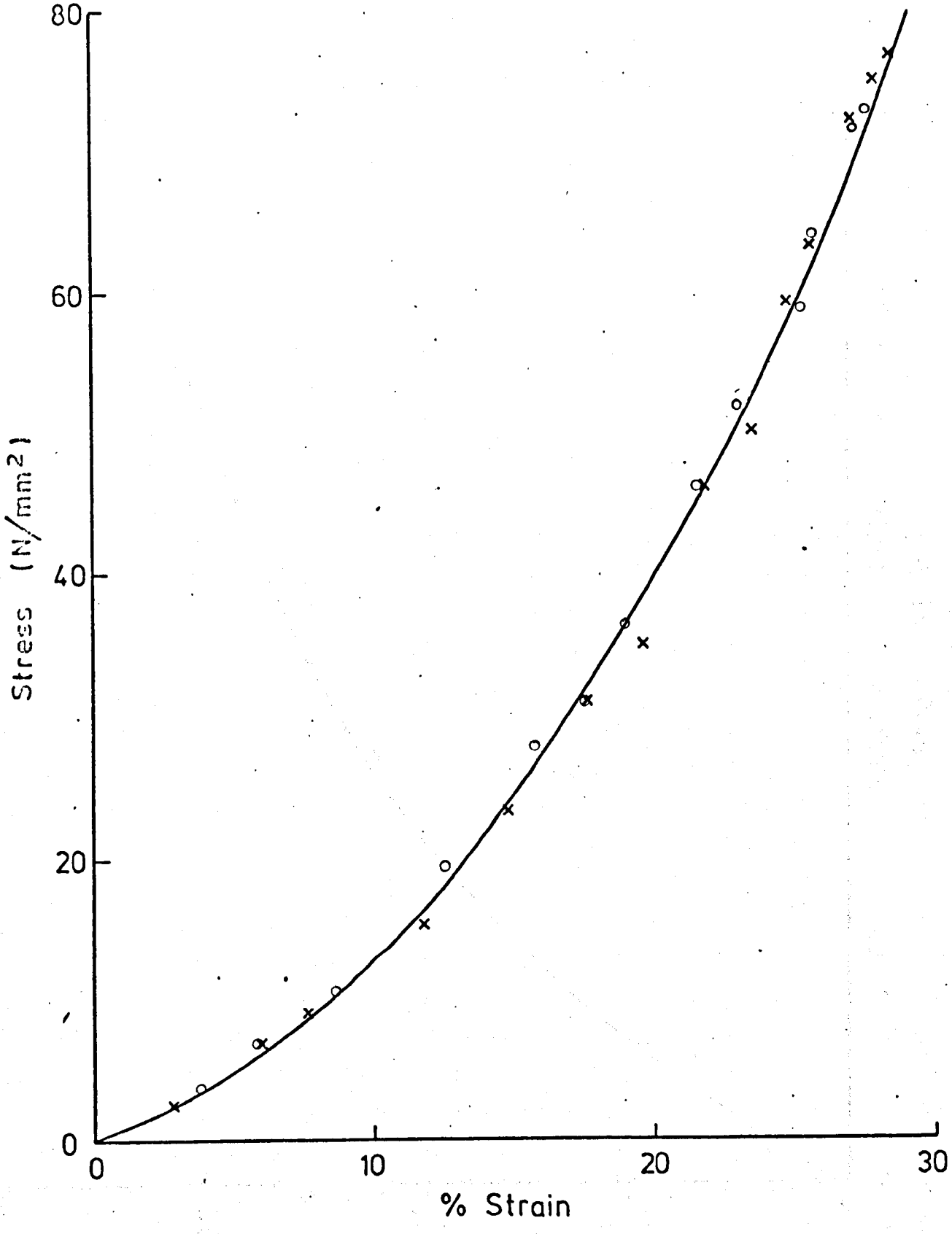

FIG. (3-5) STRESS – STRAIN RELATIONSHIP OF N.T. FABRIC

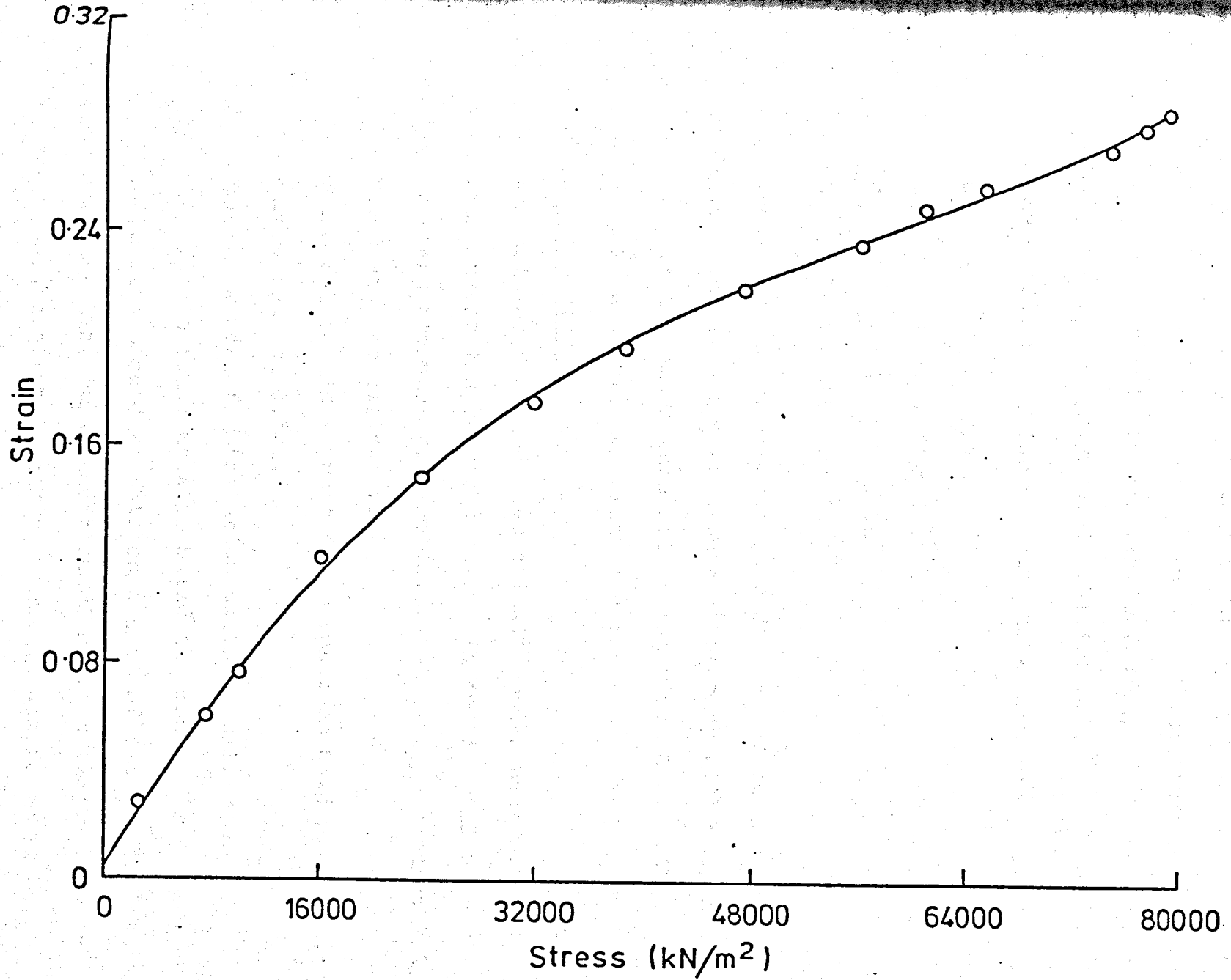

FIG. (3-6) STRESS-STRAIN RELATIONSHIP OF N.T. FABRIC (POLYNOMIAL DEGREE 3)

where

ε = strain in the fabric = $\frac{\Delta L}{L}$

ΔL = elongation in the fabric (m)

L = original length of the fabric (m)

σ = stress in the fabric (kN/m^2)

C_1, C_2, C_3 and C_4 = polynomial coefficients.

The coefficients for the N.T. fabric were:

C_1 = 0.4063378×10^{-2}

C_2 = 0.8544707×10^{-5}

C_3 = $-0.1148294 \times 10^{-9}$

C_4 = $0.6611830 \times 10^{-15}$

These results were obtained under normal room temperature conditions and it has been assumed that they will not change with respect to temperature within the range 0° to 25° C likely to be encountered during the tests.

3.4 Model Design.

A model was designed theoretically under hydrostatic conditions using the theory detailed in section 4.2 of chapter 4 and computer program (DID) detailed in section 7.3.1.

The design conditions were:

(1) The model should support 0.3 m upstream head with downstream head of 0.1 m.

(2) Air to be used for inflation of the model.

(3) N.T. fabric to be used to build the model.

The design procedure obtains a size of dam and inflation pressure to satisfy the condition of minimum length of membrane. This minimum length of membrane was found to be

0.787 m with an inflation air pressure of 5.886 kN/m^2 and dam base length of 0.225 m. The detailed design conditions are shown in Fig.3.7.

3.5 Model Construction.

The model consisted of five components:

(a) Bag.

(b) Base plate.

(c) Base fixing.

(d) Inflation.

(e) End fixing.

Each component is described in detail in section 3.5.1, 3.5.2, 3.5.3, 3.5.4 and 3.5.5 respectively.

3.5.1 Bag Construction.

It was decided to construct the bag of the model out of a single rectangular sheet of N.T. fabric and to seal this on three sides, using an adhesive, Dunlop 1310, recommended by the fabric manufacturer.

The bond strength of the sealed fabric was tested in the laboratory on a tensile testing machine for 10 mm, 20 mm and 30 mm overlaps, as shown in Fig.3.8 and was found equal to 2.5 kN/m, 3.0 kN/m and 3.5 kN/m respectively. Although the 10 mm and 20 mm overlap withstood tensile forces in excess of those anticipated in the tests, it was decided to use a 30 mm overlap capable of withstanding a 3.5 kN/m load as good adhesive contact over the whole area could not be guaranteed and also the large overlap would help to reduce the risk of leakage.

A 14 mm diameter hole to accommodate the inflation tube was cut in the sheet at the position shown in Fig.3.8. This

U/S HEAD	=	0.3000	METER
D/S HEAD	=	0.1000	METER
WATER PRESSURE	=	0.0000	METER
AIR PRESSURE	=	5.8860	KN/SQ.M
ORIGINAL LENGTH	=	0.7866	METER
NEW LENGTH	=	0.8064	METER
U/S TENSION	=	0.8112	KN/M
D/S TENSION	=	1.0391	KN/M
BASE LENGTH	=	0.2250	METER
MAX. HEGHTH	=	0.3002	METER

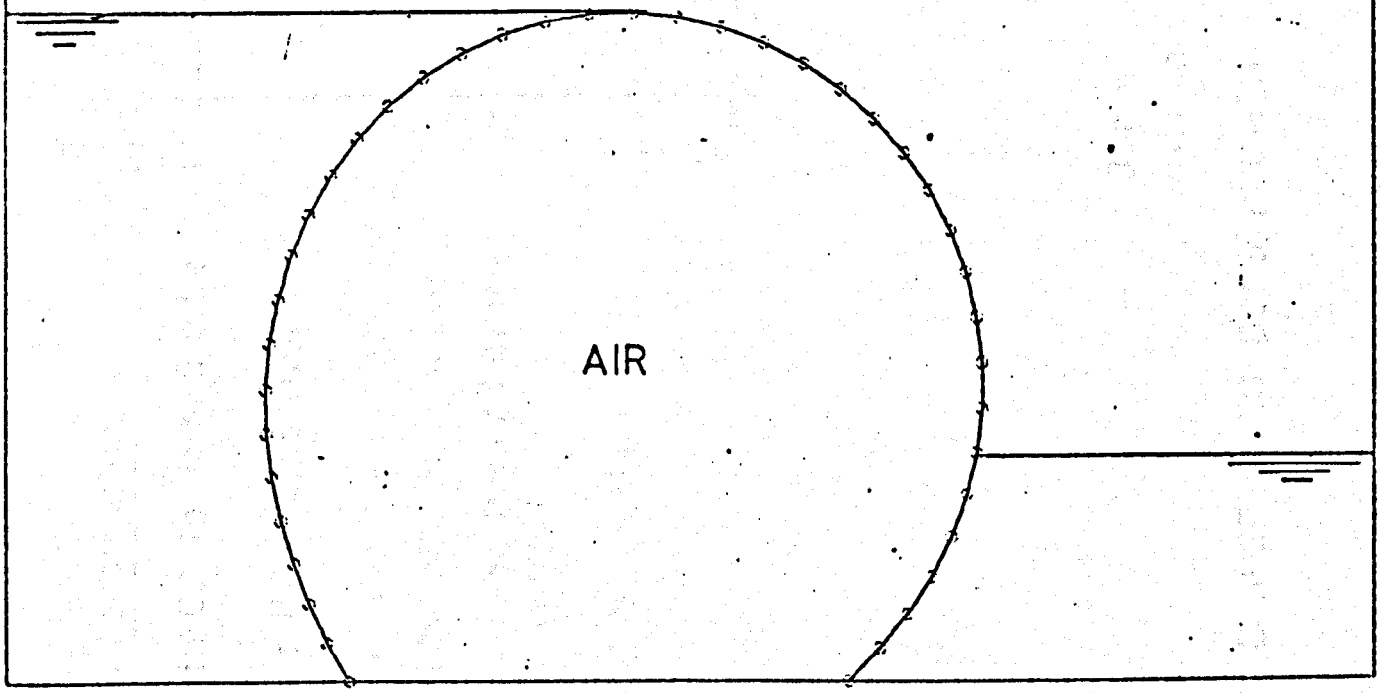

FIG.(3- 7) TYPICAL DAM PROFILE UNDER HYDROSTATIC CONDITIONS DESIGN USING COMPUTER PROGRAM (DID)

Procedure of bag construction

(1) Seal AB with CD to form a tube

(2) Seal the end BD of the tube

(3) Fit a valve on the crest if the model is to be inflated by water or air/water near the end of the of the tube AC

(4) Seal the end AC of the tube

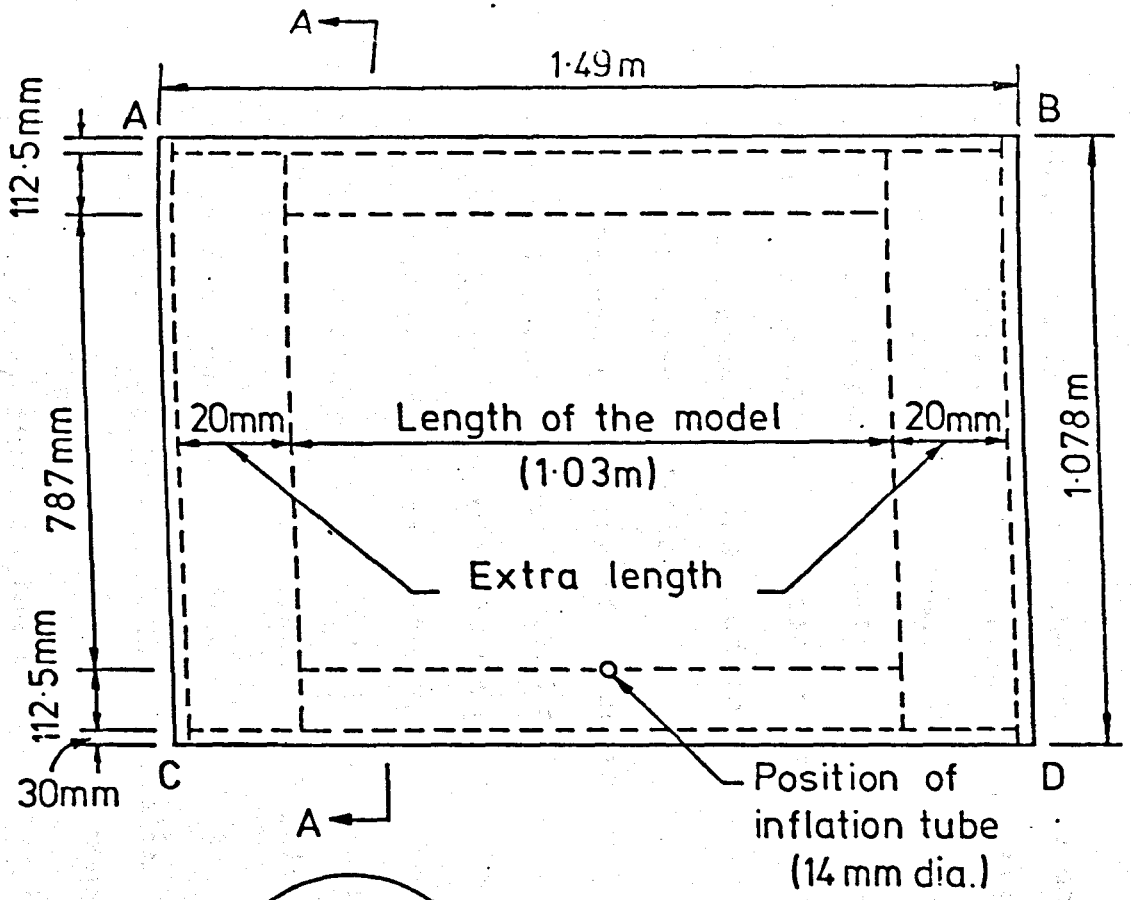

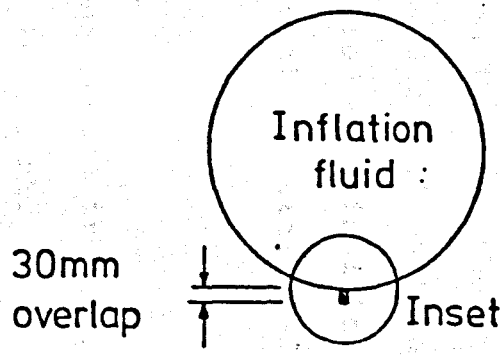

Section A-A

After construction

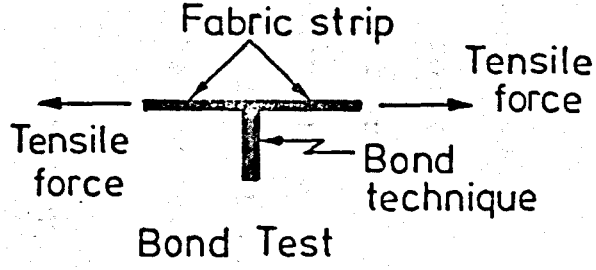

Bond Test

FIG. (3–8) SINGLE SHEET BAG CONSTRUCTION

figure also demonstrates the procedure used to make a bag from a single sheet indicating the position of the folds and the sequence of sealing. An internally threaded brass tube of 13 mm outside diameter was sealed with washers into this hole to allow connection of the inflation pipe to the bag. A similar technique was used to instal a valve in the bag for use with water inflation.

The sheet consists of a section 0.787 m long required by the design and a section 0.225 m long to allow for the base of the dam together with 30 mm pieces required for the overlaps.

Additional material is required round the sides to allow the sealed ends of the bag to be unstressed when inflated. This procedure for assessing the additional material needed is detailed in section 3.5.5.

3.5.2 Base Plate of the Model.

The base plate of the model was constructed from 12.5 mm thick perspex, fixed on the base of the test tank. The length of the plate was 325 mm (225 mm was the design length of the base of the dam, and 50 mm on both sides to be used to fix the bag to the base) as shown in Fig.3.4.

3.5.3 Anchoring System of the Bag to the Base Plate.

Two fabric strips, 80 mm in width and 1.03 m in length, were attached to the bag to form the flaps that were clamped between the base plate and two perspex strips, one on the upstream side and one on the downstream side to hold the dam in place (see Fig.3.4). The distance between the perspex strips was equal to the base length (225 mm) of the dam.

3.5.4 Inflation Technique.

Three kinds of inflation were used, air, water and a combination of the two. A nylon pipe, 8 mm external diameter, was attached to the brass tube of 13 mm external diameter, which passed through the bag and base plate to allow inflation to take place. The pipe was connected to three nylong pipes, each 8 mm in diameter, each with an isolating valve, as shown in Fig.3.4. One of these pipes was used for inflation by air and was connected directly to the air control device, one was used to inflate the bag by water and was connected directly to the water column and the third was used for deflation.

In the case of the water inflated models, a valve was fixed on the crest near to one end of the bag to allow release of the air during the inflation process. This same technique allowed control of the air pressure for air/water inflation.

It should be noted that once the required internal water pressure from the water column was achieved the isolating valve was closed so that the pressure remained constant irrespective of the height of the dam. If the valve was left open then the pressure changed due to changes in the height of the dam due to deformation.

3.5.5 End Fixing.

To control the leaks through the free ends of the model an extra length was added to the original length of the bag (original length equals the width of the test tank (1.03 m)). The extra length was folded inside the bag in order to make the cross-sectional profile at the end similar to the profile at the centre under load.

To study the effects of the extra length on the deformation of the cross-sectional profile, three models were built. The first model had one third of its height as extra length on each side, the second model had two thirds of its height as extra length and the third model had an extra length equal to its height.

The models were inflated by air and tested under upstream heads varying from 100 mm to 300 mm and a downstream head equal to zero and internal air pressure varying from 1.962 kN/m^2 to 5.886 kN/m^2. The cross-sectional profile at the centre of the model was measured using the technique described in section 3.5.4 and compared with the theoretical profile obtained from the theoretical analysis (see section 4.4).

The tests showed that the model with extra length equal to its height produced a high pressure on the perspex wall of the test tank. This eliminated leakage round the sides but the end effects restricted the deformation of the cross-sectional profile of the model at the centre.

The profile of the model with extra length equal to one third its height was distorted easily with different static conditions closely with the experimental profile in good agreement with the theoretical profiles. However, leakage at the ends was excessive, particularly when the model was inflated to low air pressures. Because of the unknown effect of leakage on the ends, no attempt was made to quantify the comparison between the profiles.

It was concluded therefore that the model with extra length equal to two thirds its height was the most suitable

because of the limited leakage at the ends which could be stopped by other means and minimum end effects on the deformation of the profile at the centre. The significance of possible end effects is discussed in section 4.4 of Chapter 4.

To further minimize the end effects on the deformation of the profile, oil was used to lubricate the contact area of the perspex wall of the test tank and the ends of the model. The leaks were eliminated at the ends and underneath the base by using flexible oil tape (Dinso tape) attached to the base and sides of the test tank and the model.

3.6 Testing of the Models.

The object of the tests was to ascertain the significance of the effect of different inflation fluids over a range of pressures and different range of upstream and downstream heads on a particular size of dam from experimental work and to compare these results with those predicted from the theoretical analysis.

The project was not concerned with the long term operation of a single dam. Because the fabric used was plastic and not elastic then long term operation of the same model would have resulted in an elongation of the material and hence a larger dam.

To overcome this problem a model when it had been inflated to a high pressure was discarded and a new model of the same dimensions used for further tests. This required the building of three sets of identical models to test under hydrostatic conditions. The first set consisted of three models tested under upstream and downstream heads both varying from 100 mm

to 300 mm and inflated by air pressures varying from 1.962 kN/m^2 to 5.886 kN/m^2 as detailed in table 3.2. The second set consisted of three models tested under upstream heads varying from 75 mm to 250 mm, downstream head varying from zero to 250 mm and inflated by water pressures varying from 400 mm to 1000 mm water heads above the base level of the dam as detailed in table 3.3. The third set consisted of two models tested under a constant upstream head of 250 mm, constant downstream head of 100 mm and inflated by air pressure varying from 1.962 kN/m^2 to 5.886 kN/m^2 and water pressure varying from 50 mm to 250 mm water head as detailed in table 3.4.

All models were constructed to the same dimensions (membrane length equal to 787 mm and base length equal to 225 mm).

The object of using three models inflated by air or water and two models inflated by air/water was to avoid the elongation in the membrane as discussed earlier.

A computer program was written to plot the experimental cross-sectional profile of the model on the computer graph plotter from the experimental profile co-ordinates.

3.6.1 Profile Measuring Technique.

The method of measuring the cross-sectional profile of the dam with the profile gauge described in section 3.2.4 was as follows:

1. Before inflation occured, the profile gauge was set on a fixed point on the dam which could be used as a datum point. This point was taken as the base of the dam on the upstream

side (see Fig.3.4) and the pointers were positioned so that they just came into contact with the membrane.

2. The co-ordinates of this datum point were found from the horizontal and vertical scales of the profile gauge. The vertical co-ordinate of this point was always zero but the horizontal co-ordinate depended on the position of the dam relative to the horizontal scale which could not be adjusted to zero.

3. The model was inflated to the required pressure and exposed to the required upstream and downstream depths of water.

4. The profile gauge was raised vertically in increments of 20 mm and at each increase the horizontal pointer was moved into contact with the membrane and the co-ordinates of this point read from the appropriate scales of the profile gauge.

5. The horizontal co-ordinate of this new point relative to the datum point was found by subtracting the new horizontal scale reading from the horizontal co-ordinate of the datum point. This was repeated for each 20 mm vertical increment until the crest of the dam was reached and the exercise was then carried out on the downstream face by decreasing the vertical co-ordinate in 20 mm increments. The accuracy for measuring vertical co-ordinate was within $\pm$ 0.1 mm but for the horizontal co-ordinates was within $\pm$ 0.5 mm, the difference being due to the types of scales.

This technique of measuring the co-ordinates of the membrane was only used for measuring the cross-sectional profile for hydrostatic conditions. The technique for the dynamic state is described in section 5.3.1.

3.6.2 Air Inflated Models.

Three models were made and tested under different combinations of upstream head, downstream head and internal pressure as illustrated in table 3.2.

In all tests the cross-sectional profile of the model was measured and an example of computer plot of the results for air pressure 1.962 kN/m^2 and 5.886 kN/m^2 under heads of 300 mm upstream and 100 mm downstream is shown in Fig.3.9.

The comparison between the theoretically and experimentally obtained profiles is discussed in chapter 4. However, it was observed that the higher the air pressure the more rigid the dam and the less the deformation of the profile under the

Model No.	Test No.	U/S Head (mm)	D/S Head (mm)	Air Pressure (kN/m^2)
1.	1	300.0	100.0	1.962
	2	300.0	100.0	2.943
	3	300.0	100.0	3.924
	4	300.0	100.0	4.905
	5	300.0	100.0	5.886
2.	1	100.0	100.0	5.886
	2	200.0	100.0	5.886
	3	270.0	100.0	5.886
3.	1	300.0	150.0	5.886
	2	300.0	240.0	5.886
	3	300.0	300.0	5.886

TABLE 3.2 TESTS OF AIR INFLATED MODELS.

SYMBOL	=	o	SYMBOL	=	⊠
U/S HEAD	=	300.0 MM	U/S HEAD	=	300.0 MM
D/S HEAD	=	100.0 MM	D/S HEAD	=	100.0 MM
AIR PRESSURE	=	5.886 KN/SQ.M	AIR PRESSURE	=	1.962 KN/SQ.M
WATER PRESSURE	=	0.0 MM	WATER PRESSURE	=	0.0 MM
MAX. HEIGHT	=	304.0 MM	MAX. HEIGHT	=	306.0 MM

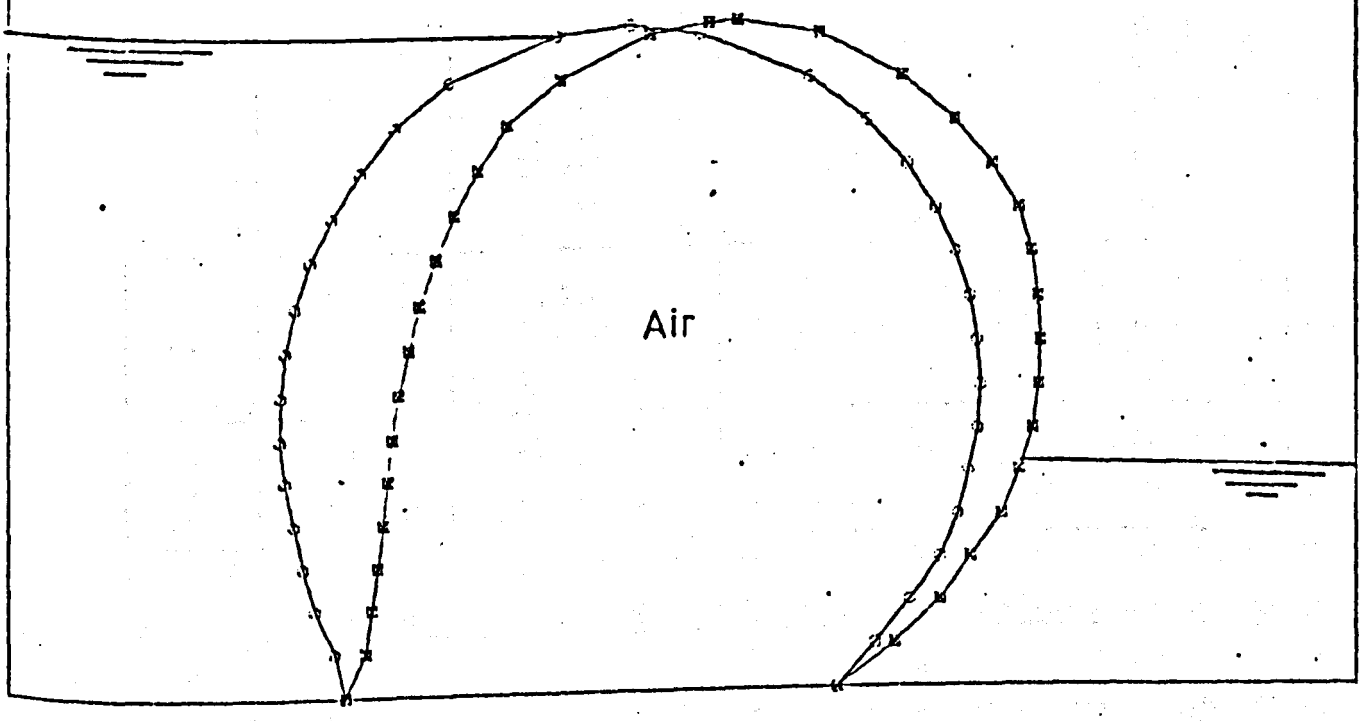

FIG. (3-9) TYPICAL EXPERIMENTAL PROFILES OF AIR INFLATED DAMS

maximum hydrostatic load. Although profiles were only measured under a maximum pressure of 5.886 kN/m^2, it was observed that when at the end of a test the air pressure was increased to 9.81 kN/m^2 then no distortion was possible under the maximum hydrostatic loads.

During the deflation of a model the V-notch effect first observed by Stodulka[11] was also observed as illustrated in the sequence of photographs in Fig.3.10.

3.6.3 Water Inflated Models.

Table 3.3 gives the heads and pressure for the three models inflated by water.

Model No.	Test No.	U/S Head (mm)	D/S Head (mm)	Water Head (mm)
1.	1	250.0	100.0	400.0
	2	250.0	100.0	450.0
	3	250.0	100.0	500.0
	4	250.0	100.0	600.0
	5	250.0	100.0	800.0
	6	250.0	100.0	1000.0
2.	1	75.0	0.0	600.0
	2	150.0	0.0	600.0
	3	250.0	0.0	600.0
3.	1	250.0	150.0	600.0
	2	250.0	250.0	600.0

TABLE 3.3 TESTS OF WATER INFLATED MODELS.

Profiles of the dams were measured for all tests and an example of the computer plot of the results for water pressures of 600 mm and 400 mm under heads of 250 mm upstream and 100 mm downstream are shown in Fig.3.11.

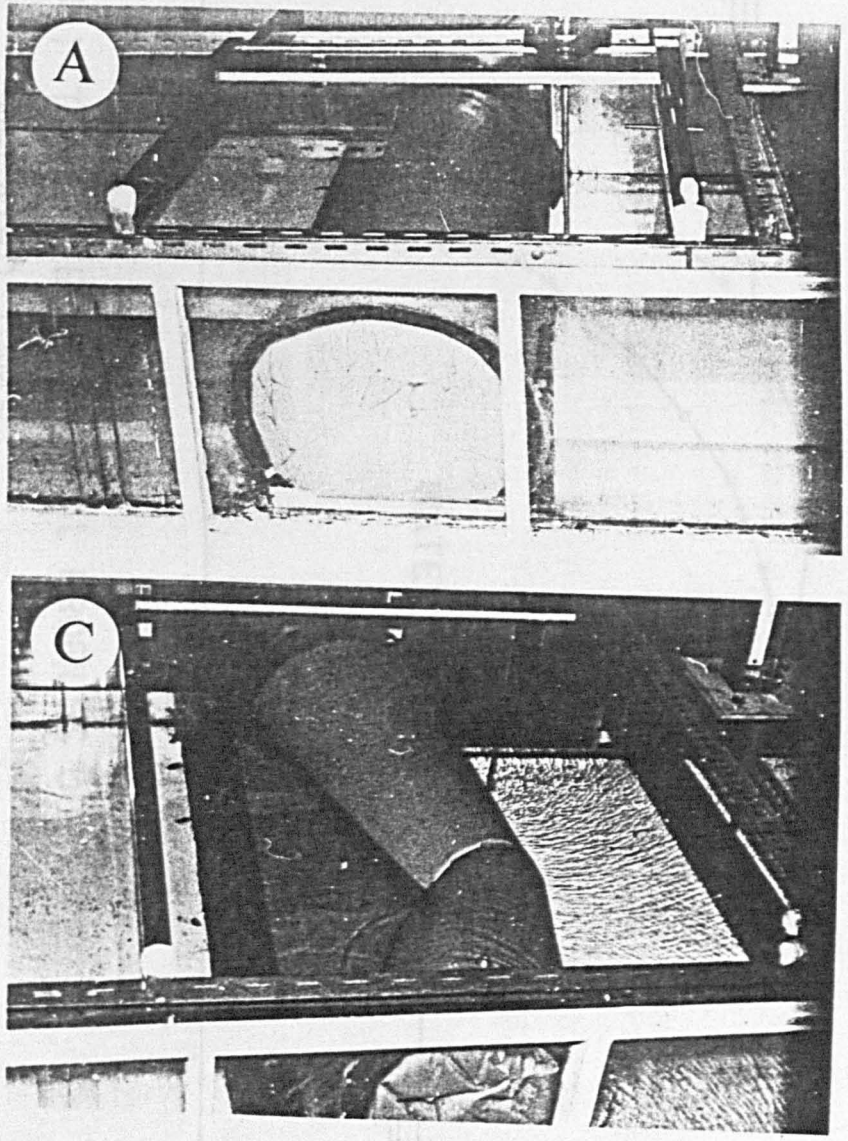

(A) Air pressure = 5·886 kN/m^2

(B) Air pressure = 1·962 kN/m^2

(C) Air pressure = 0·735 kN/m^2

FIG. (3–10) BEHAVIOUR OF AIR INFLATED DAM WHEN DEFLATED (HYDROSTATIC)

SYMBOL	=	o	SYMBOL	=	⊠
U/S HEAD	=	250.0 MM	U/S HEAD	=	250.0 MM
D/S HEAD	=	100.0 MM	D/S HEAD	=	100.0 MM
AIR PRESSURE	=	0.000 KN/SQ.M	AIR PRESSURE	=	0.000 KN/SQ.M
WATER PRESSURE	=	600.0 MM	WATER PRESSURE	=	400.0 MM
MAX. HEIGHT	=	277.5 MM	MAX. HEIGHT	=	261.0 MM

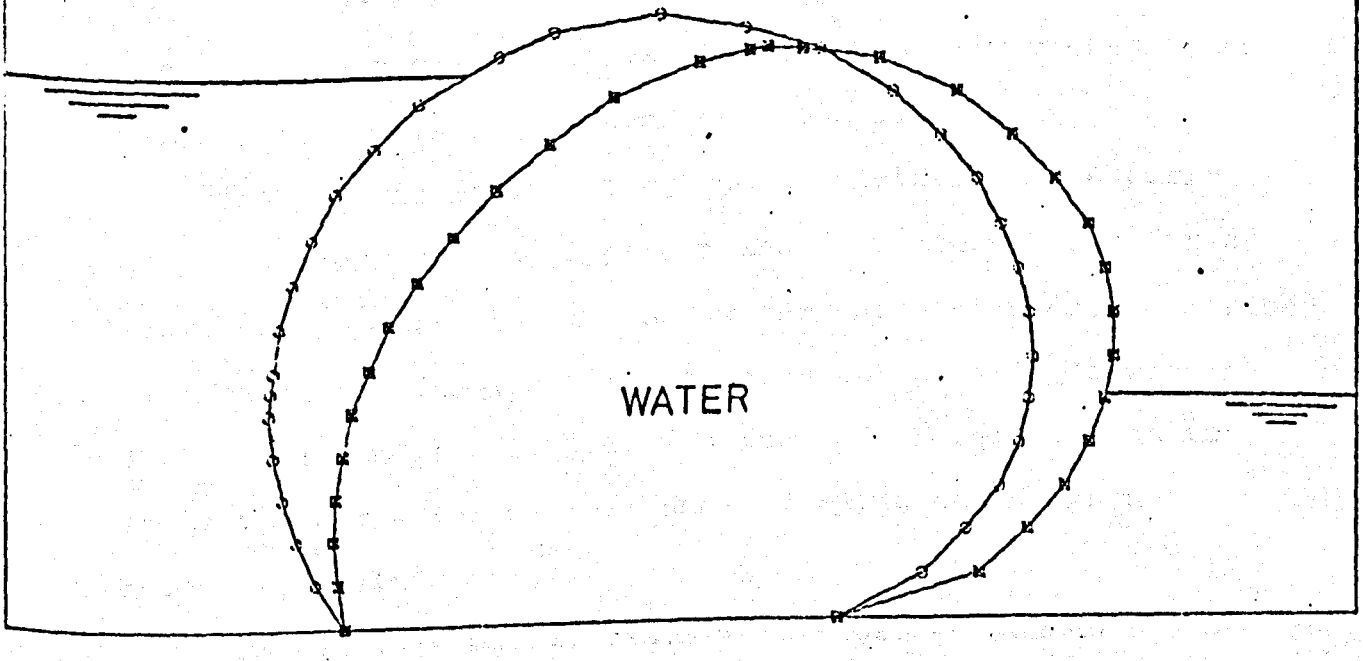

FIG. (3-11) TYPICAL EXPERIMENTAL PROFILES OF WATER INFLATED DAMS

The first model was tested under an internal water pressure equal to 300 mm water head, but the test failed because of the heavy leaks between the ends of the model and the sides of the test tank resulting from the excessive deformation of the model. It was found that a minimum internal water pressure of 400 mm was required to overcome this problem.

It was also found that the internal water pressure of 1000 mm resulted in a dam so rigid that no measurable deformation took place under the maximum hydrostatic loads.

Observations carried out when the dam was deflated showed that the V-notch of the air deflation did not occur but a gradual reduction in height and elongation in the width over the length of the dam occurred as shown in Fig.3.12.

3.6.4 Air/Water Inflated Models.

Two models were made and tested under constant upstream and downstream heads with varying internal air pressure and water pressure as illustrated in table 3.4.

The results of comparing the theoretical and experimental profiles under varying upstream and downstream heads for a given pressure for the air and water inflated models described in section 4.4 show that the theoretical profile is within 5% for all conditions. It was decided therefore that to study the air/water mixture under varying heads was not necessary at this stage.

The profiles of all tests were measured and an example is the computer print of these results shown in Fig.3.13.

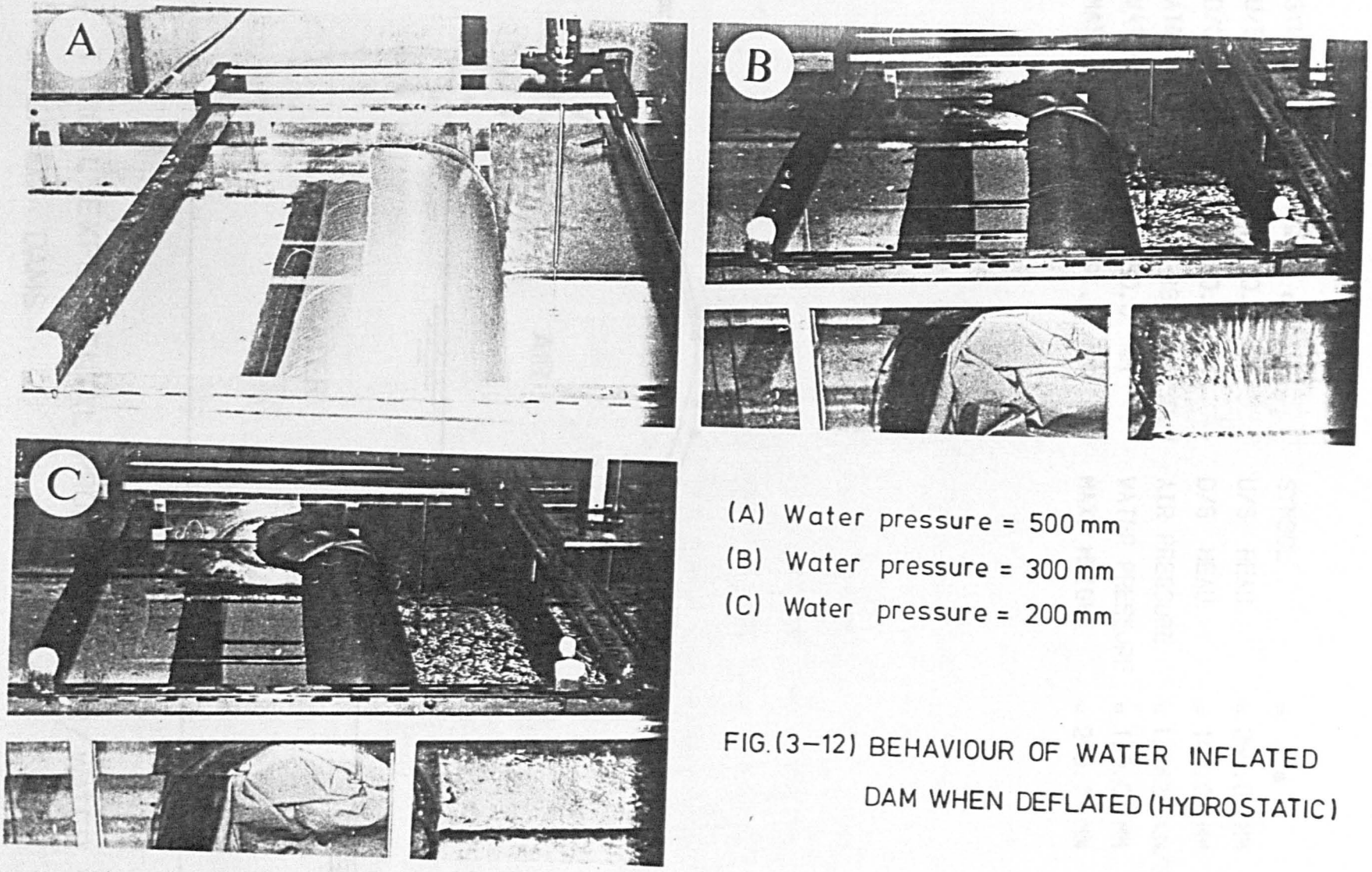

(A) Water pressure = 500 mm

(B) Water pressure = 300 mm

(C) Water pressure = 200 mm

FIG.(3–12) BEHAVIOUR OF WATER INFLATED DAM WHEN DEFLATED (HYDROSTATIC)

SYMBOL	=	o	SYMBOL	=	⊠
U/S HEAD	= 250.0	MM	U/S HEAD	= 250.0	MM
D/S HEAD	= 100.0	MM	D/S HEAD	= 100.0	MM
AIR PRESSURE	= 5.886	KN/SQ.M	AIR PRESSURE	= 1.962	KN/SQ.M
WATER PRESSURE	= 150.0	MM	WATER PRESSURE	= 150.0	MM
MAX. HEIGHT	= 291.0	MM	MAX. HEIGHT	= 290.7	MM

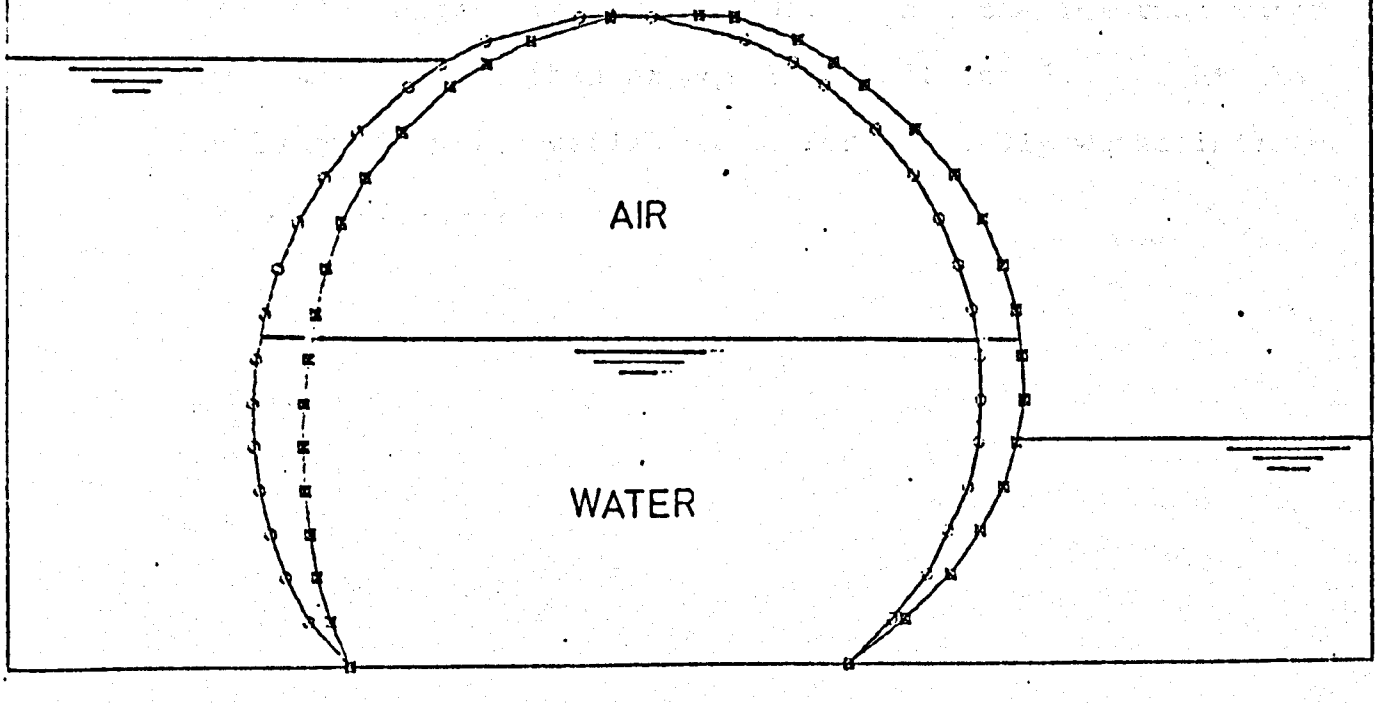

FIG. (3–13) TYPICAL EXPERIMENTAL PROFILES OF AIR/WATER INFLATED DAMS

Model No.	Test No.	U/S Head (mm)	D/S Head (mm)	Air P. (kN/m^2)	Water P. (mm)
1.	1	250.0	100.0	1.962	150.0
	2	250.0	100.0	2.943	150.0
	3	250.0	100.0	3.924	150.0
	4	250.0	100.0	4.905	150.0
2.	1	250.0	100.0	5.886	50.0
	2	250.0	100.0	5.886	150.0
	3	250.0	100.0	5.886	250.0

TABLE 3.4 TESTS OF AIR/WATER INFLATED MODELS.

When the dam was deflated by releasing internal water from the base of the dam the V-notch effect was observed for the dam inflated with internal water depth less than half of the dam's height, (see Fig.3.10). When the internal water depth was greater than or equal to half the dam height the dam behaved during deflation as for a totally water inflated dam (see Fig. 3.12).

CHAPTER 4.

THEORETICAL ANALYSIS OF A DAM UNDER HYDROSTATIC CONDITIONS.

4.1 Introduction.

The main characteristics of inflatable dams that it is necessary to be able to determine are the tensions in the fabric and the shape of the cross-sectional profile. The literature survey (Chapter 2) described the activities of five workers (Anwar, Harrison, Clare, Binnie, Pabery) who had previously published work on the theoretical analysis of inflatable dams under hydrostatic conditions.

All of these methods of analysis involve the solution of a number of long mathematical equations to calculate the profile, this requiring a number of assumptions to be made about the boundary conditions. In section 2.6 it was argued that further development of the approach of Harrison[7] to find a theoretical solution to the problem was justified.

This chapter details the modification of his finite element approach to analyse an inflatable dam under hydrostatic conditions. The method developed is applicable to the wide range of conditions of inflation fluid and base geometry likely to be met in a prototype design.

Computer programs were written for the analysis of the dams under a different combinations of upstream head, downstream head and internal air, water and air/water pressures to give the following parameters:

(a) Tension in the membrane.

(b) Stretch length of the membrane.

(c) Co-ordinates of each element.

A sub-program was connected to the main program in order to plot the cross-sectional profile of the dam obtained from this analysis.

A comparison was carried out between the theoretical cross-sectional profile and the experimental cross-sectional profile of the dam (see Chapter 3), and this is described in section 4.4. This comparison demonstrated a good relationship between the theoretical method and the results obtained from model tests.

4.2 Method of Analysis.

The Harrison-Newton method (1970) for the analysis of an inflatable dam under hydrostatic conditions was modified to obtain a more accurate shape and tension in the membrane of the dam. The method has also been modified to analyse a dam when overflow occurs (see chapter 5).

Harrison's method was dependent upon three basic assumptions for the analysis of the stresses in the membrane of the dam:-

(a) The behaviour of the three dimensional structure can be represented by the behaviour of a two dimensional transverse section of unit width.

(b) The perimeter of the cross-section of the dam is composed of a finite number of small straight elements, and the static loads are acting on the nodes.

(c) The material of the dam is elastic and that the stress-strain relationship of the material can be assumed to be linear.

Harrison's analysis technique has limitations for the analysis of dams under hydrostatic conditions, and cannot be applied when:-

(1) The dam has upstream head (UH) = dam height (Y_{max}), see Fig.4.1A).

(2) The dam is laid flat at the downstream anchor (downstream slope $\theta_2 = 0$, see Fig.4.2).

(3) The dam has overflow.

Modifications for the analysis were carried out on the assumption of Harrison about the stress analysis of the profile and the analysis technique itself as follows:-

(a) Modification of assumption of stresses in the profile.

(1) The static loads due to the upstream head, downstream head, internal air, water and air/water pressures, and weight of membrane are acting on the elements.

(2) If the material of the membrane is plastic, the behaviour therefore of the stress-strain relationship is non-linear

(b) Modification of the analysis technique.

The modification of the analysis technique was made to overcome the limitations of the Harrison's analysis technique. The present technique also included the analysis of a dam under different combinations of upstream and downstream heads and internal air, water and air/water pressures and different geometry of base shape.

The first modification produced a more accurate profile shape of a dam under both hydrostatic and hydrodynamic conditions but the second modification allows application of the analysis technique to a much wider range of practical field problems.

This analysis always considers the dam to be inflated initially by both air and water and for the condition where only one fluid is applicable the pressure due to the other fluid is specified as being equal to zero when the analysis is carried out. This enables all possibilities to be considered in the one set of equations.

It has been assumed in this study that the effect of temperature on air, water and material properties can be ignored over the range of temperature likely to be evaluated (of the order of 0^{o} to 25^{o} C). However, the likely significance of this is discussed in appendix A.

4.2.1 Stress Analysis of the Profile.

The forces acting on the profile of the dam are due to an upstream hydrostatic force, a downstream hydrostatic force, an inflated air pressure, an inflated water pressure and the weight of the membrane as shown in Fig.4.1A. In order to calculate the magnitude and direction of each force on the dam, the membrane of the dam is divided into n equal elements. The ends of each element are classified as nodes and hence for n elements, there are n+1 nodes. Each element is considered as either an upstream element or downstream element depending on whether it receives an upstream or downstream hydrostatic force.

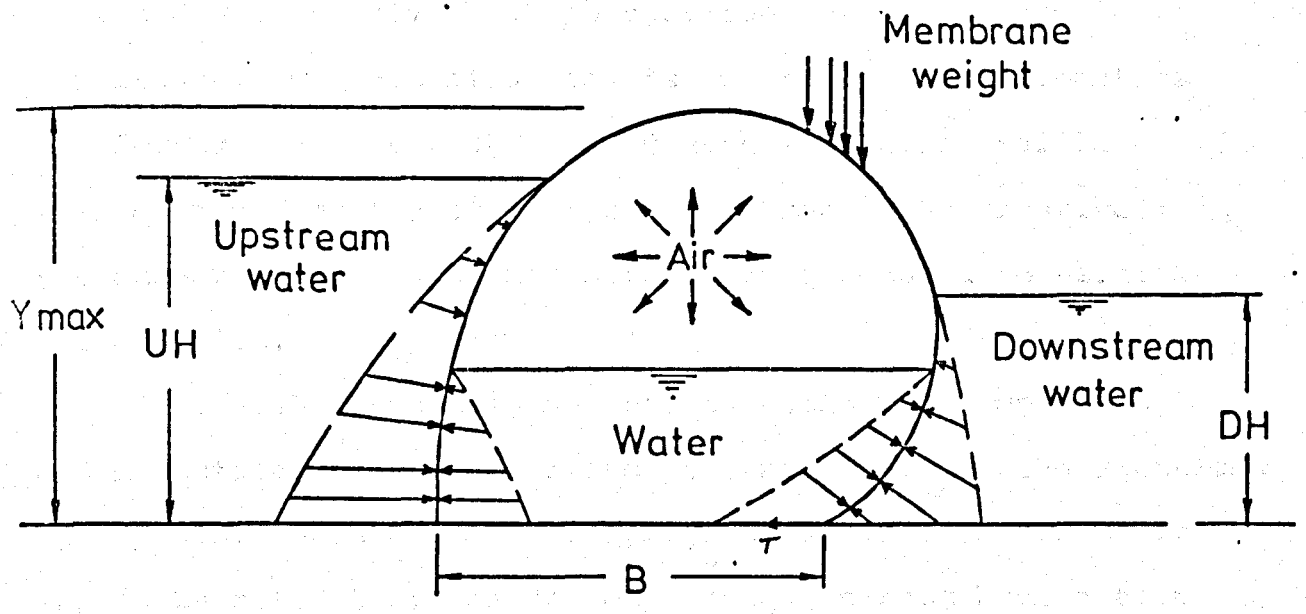

FIG. (4–1A) PRESSURES ACTING ON THE DAM

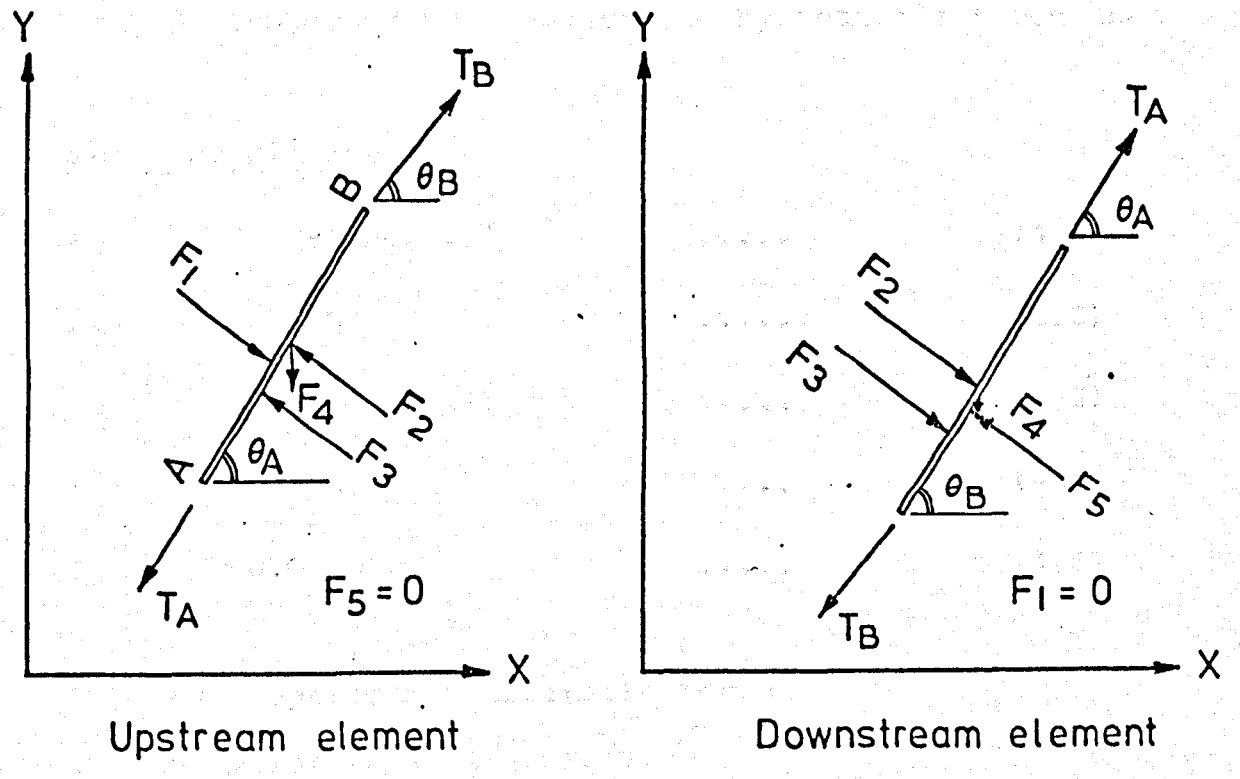

FIG. (4–1B) FORCES ACTING ON AN INDIVIDUAL ELEMENT

Although it is possible for the element at the crest of the dam to receive both an upstream and downstream force simultaneously, this situation is not taken into account as the forces would be very small due to the horizontal level of this element and therefore can be ignored. Alternatively, the number of elements chosen could be increased to eliminate this problem.

Fig. 4.1B shows all the forces acting on an upstream and downstream element of a dam per unit width. The equations to calculate each of these forces are as listed below. It should be noted that the forces F_1 and F_5 cannot both act on the same element at the same time and if the element is subjected to an upstream hydrostatic force then $F_5 = 0$ and similarly if subjected to a downstream hydrostatic force then $F_1 = 0$.

(i) Upstream Element.

$$F_1 = \gamma . hc_1 . L \quad ..... \quad (4.1)$$

$$F_2 = p . L \quad ..... \quad (4.2)$$

$$F_3 = \gamma . hc_2 . L \quad ..... \quad (4.3)$$

$$F_4 = w . L \quad ..... \quad (4.4)$$

$$F_5 = 0.0 \quad ..... \quad (4.5)$$

where

F_1 = upstream hydrostatic force.

F_2 = internal air force.

F_3 = internal water force.

F_4 = weight of membrane force.

F_5 = downsteam hydrostatic force.

γ = specific weight of water.

hc_1 = depth of centre of the upstream hydrostatic force below the upstream free water surface.

p = internal air pressure.

L = length of the element.

hc_2 = depth of centre of the internal water force below the internal free water surface.

w = weight of the element per unit area.

Knowing the properties of air, water and the material the forces can be calculated using these equations. Considering the horizontal equilibrium of these forces on element AB (see Fig. 4.1B)

$$T_B \text{ Cos } \theta_B = T_A \text{ Cos } \theta_A + (F_3 + F_2 - F_1) \text{ Sin } \theta_A \ldots \quad (4.6)$$

where

T_A = tension in node A.

θ_A = slope of element AB at A.

T_B = tension in node B.

θ_B = slope of element AB at B.

For vertical equilibrium

$$T_B \text{ Sin } \theta_B = (F_1 - F_2 - F_3) \text{ Cos } \theta_A + T_A \text{ Sin } \theta_A + F_4 \ldots (4.7)$$

To allow T_B and θ_B to be calculated from equations (4.6 and 4.7) it is necessary to know the values for T_A and θ_A.

For the first element in the series it is necessary to assume trial values for T_A and θ_A. Section 4.2.2 describes the technique for obtaining realistic trial values for these parameters. When T_B and θ_B have been found they form

the new T_A and θ_A values for the next element and the process can then be repeated for all elements.

An adjustment to the trial values of T_A and θ_A can be made based on the closing error of the known co-ordinates of the last node and this procedure is detailed in section 4.2.4.

(ii) Downstream Element.

A similar analysis can be carried out on a downstream element, but in this case equation (4.1) for F_1 becomes zero and F_5 is:

$$F_5 = \gamma \cdot hc_3 \cdot L \quad \ldots\ldots \quad (4.8)$$

where hc_3 = depth of centre of downstream hydrostatic force below the downstream free water surface.

4.2.2 Initial Trial Values of Tension and Slope.

In the early stages of the study arbitrary values were chosen for the initial values of tension and slope of the first element. When a number of dams had been analysed more realistic estimates of the initial values could be made to use in analysing new dams. However, a better approach adopted later is to consider obtaining initial values by assuming the shape of the membrane to be circular. With this shape the tension in the membrane (T) is

$$T = P_1 R' \quad \ldots\ldots \quad (4.9)$$

where

P_1 = resultant pressures of static loads.

R' = radius of the circle.

The equilibrium of static forces acting on the dam in the horizontal direction (Fig.4.1A) is

$$\frac{1}{2}\ \gamma\ (UH)^2 = T + T \cos\theta_1 + \frac{1}{2}\ \gamma\ (DH)^2 \qquad \ldots\ldots \qquad (4.10)$$

Therefore

$$\theta_1 = \cos^{-1}\left\{\left[\frac{\gamma}{2}\ (\ (UH)^2 - (DH)^2)\ /\ T\ \right] - 1.0\right\} \ldots\ (4.11)$$

where

UH = upstream head.

DH = downstream head.

θ_1 = upstream slope of the dam.

From equations (4.9) and (4.11), the initial trial values of upstream tension and slope at the first element can be calculated.

4.2.3 Co-ordinate Positions of Points on the Profile.

The analysis for the stresses in the profile gives results which calculate the angle to the horizontal of the tension force in each element. The tension force with zero angle has a direction that is horizontal and moves from the upstream to the downstream force and all other angles are considered to be assumed in an anti-clockwise direction from this line.

Knowing the co-ordinates of the first node it is possible to calculate the co-ordinates of the second node using the angle and new length of the element after elongation due to the tension. This exercise can be repeated for all elements to find the co-ordinates of each node and hence the cross-sectional profile.

The method to determine the cross-sectional profile is given below.

1. Divide the membrane length into n elements, as shown in Fig. 4.2.
2. Calculate an initial value of tension and slope at the first upstream element by assuming the profile to be circular (section 4.2.2), (Fig.4.2, step 2).
3. From the initial tension, the elongation ΔL of the first element can be calculated using the stress-strain relationship of the material. (Fig.4.2, step 3).
4. Using the initial slope angle of the first element and the new length $L + \Delta L$, the co-ordinates of the second node (x,y) can be found assuming the first node has co-ordinates $(0,0)$ (Fig.4.2, step 4).

   Therefore

   $$x = (L + \Delta L) \cos \theta$$

   $$y = (L + \Delta L) \sin \theta$$

5. From equations (4.1), (4.2), (4.3), (4.4) and (4.5) the forces acting on the first element can be calculated and the resultant of these forces (R_1) can be found. From equations (4.6) and (4.7) the horizontal and vertical components of the tension (T'_x and T'_y) at the second node are computed and the magnitude and direction of the combined tension at the second element is found. Steps 3 and 4 are then repeated to find the co-ordinates of the third node (Fig. 4.2, step 5).
6. To obtain more accurate co-ordinates of the second node, re-calculations are made of the static forces acting

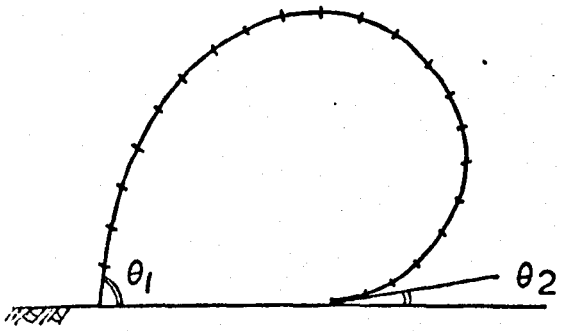

Step No.1

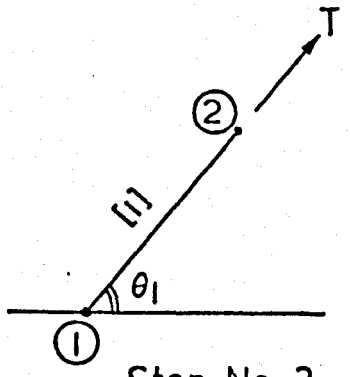

Step No. 2

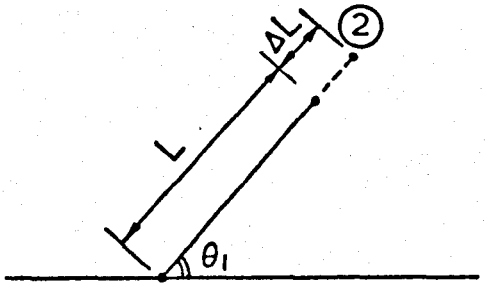

Step No.3

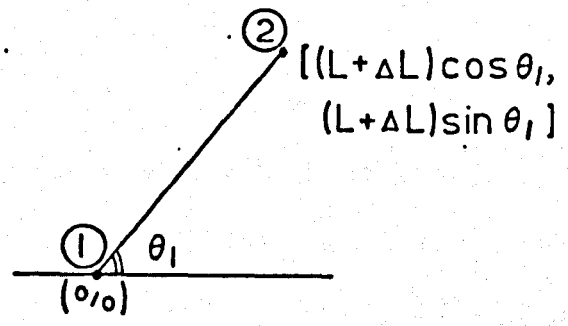

Step No.4

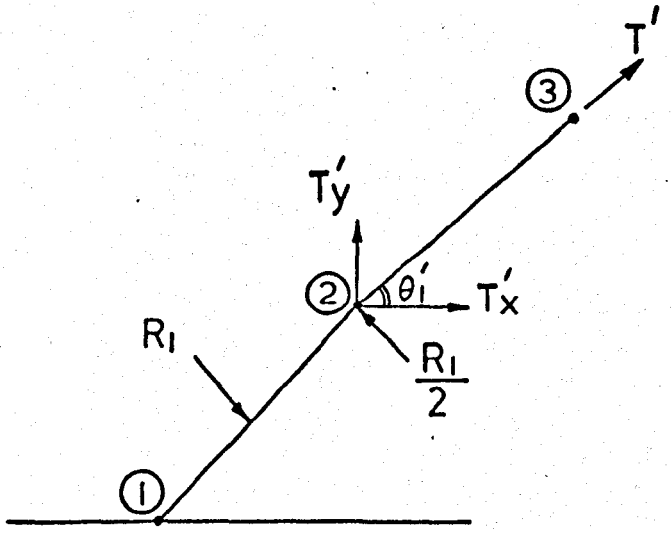

Step No.5

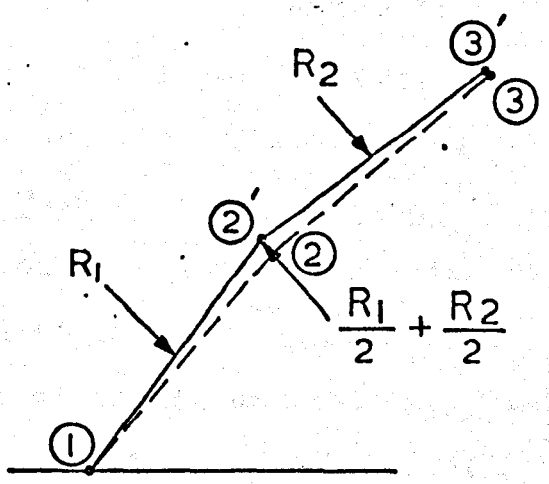

Step No.6

FIG. (4－2) METHOD OF CALCULATING CO-ORDINATES OF POINTS ON THE PROFILE

on this node due to the resultant of the static forces acting on the first element (R_1) and the second element (R_2), as shown in Fig. 4.2, step 6.

The new location of node 2 then becomes 2' and this gives a better estimate of 3' for the location of the third node.

This procedure continues around the membrane until the co-ordinates of the final node are computed. It will be found in general that there will not be agreement with the known co-ordinates of the last node. This closing error results from the initial trial values of tension and slope of the first element and an adjustment to these values can now be made and the procedure from step 3 repeated until the calculated position of the last node coincides with the known co-ordinates.

It should be noted that it is not necessary for the final node to be in the same horizontal plane as the first node (i.e. a horizontal base plate) provided, the co-ordinates of the final node are known this analysis can be carried out.

4.2.4 Adjusting Initial Values of Tension and Slope.

The Newton method of iteration of a pair of non-linear equations of two unknowns is used to improve the initial trial values of tension and slope of the first element. This method is described in detail by Whittaker and Robinson (1946)[28]. A diagrammatic representation of the adjustment of the tension and slope of the first element is illustrated in Fig.4.3.

The x-misclose and y-misclose are the results of the analysis of a dam under assumed values of initial tension (T)

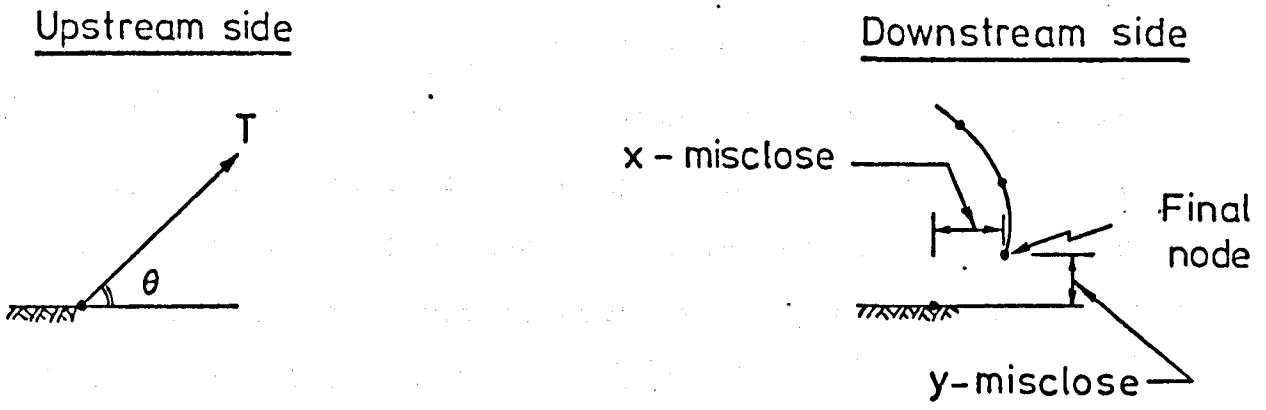

(a) Analysis assuming T, θ

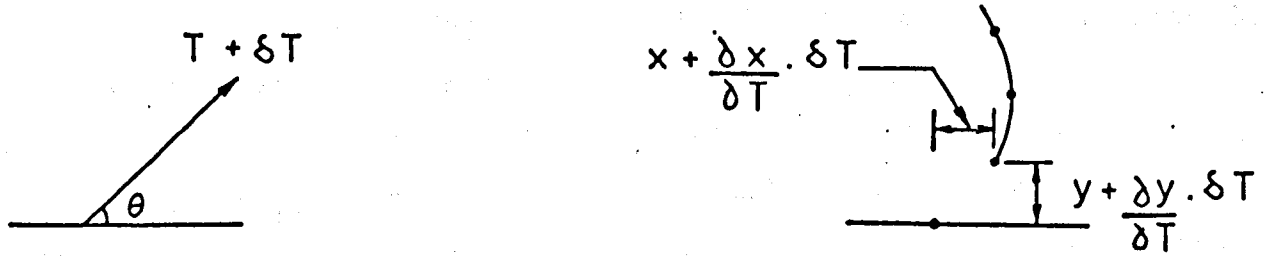

(b) Analysis assuming $T+\delta T$, θ

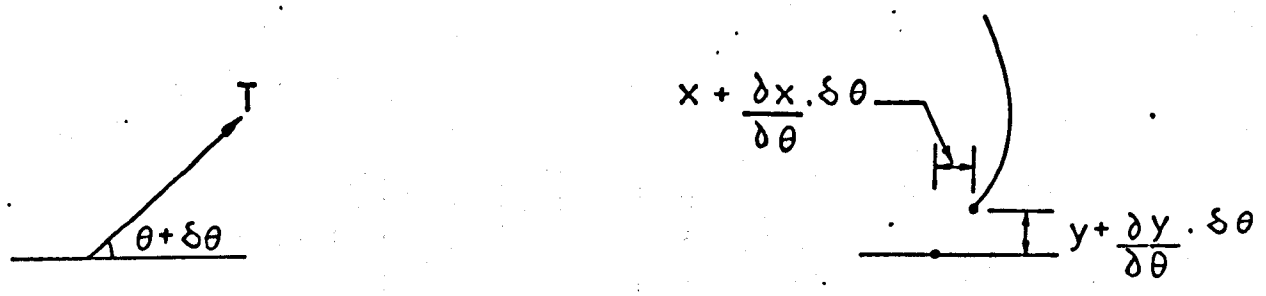

(c) Analysis assuming T, $\theta+\delta\theta$

FIG. (4-3) EFFECT OF ADJUSTING T AND θ TO MINIMISE MISCLOSE

and slope (θ) in the first element (Fig.4.3A). When the analysis is repeated with T increased by a small amount (δT), different misclose components will be calculated from which the rate of change of the x-misclose and y-misclose with respect to T may be approximately evaluated as illustrated in Fig.4.3B. The analysis can be repeated with θ increased by a small amount ($\delta\theta$) and the rate of change of the x and y misclose with respect to θ is calculated as shown in Fig.4.2C.

The adjusted values of T and θ are determined numerically from Newton's expression:

$$T_{(Adjust)} = T - \left[x \cdot \frac{\partial y}{\partial \theta} - y \cdot \frac{\partial x}{\partial \theta} \right] / Z$$

$$\theta_{(Adjust)} = \theta - \left[y \cdot \frac{\partial x}{\partial T} - x \cdot \frac{\partial y}{\partial T} \right] / Z$$

where

$$Z = \frac{\partial x}{\partial T} \cdot \frac{\partial y}{\partial \theta} - \frac{\partial y}{\partial T} \cdot \frac{\partial x}{\partial \theta}$$

But in general

$$\begin{bmatrix} T_{(Adjust)} \\ \theta_{(Adjust)} \end{bmatrix} = \begin{bmatrix} T \\ \theta \end{bmatrix} - \begin{bmatrix} \frac{\partial x}{\partial T} & \frac{\partial x}{\partial \theta} \\ \frac{\partial y}{\partial T} & \frac{\partial y}{\partial \theta} \end{bmatrix}^{-1} \cdot \begin{bmatrix} x \\ y \end{bmatrix}$$

This procedure of adjustment of T and θ continues until the x-misclose and y-misclose are reducted to a negligible value which is within predetermined limits.

4.3 Computer Programs.

All programs used either for analysis or design of inflatable dams are written in Fortran IV language for use on the University of Sheffield computer type ICL 1906S.

For this part of the study a program (AID), later modified to program (AID1) for the analysis of a dam under hydrostatic conditions was written. At a later stage this program was modified to program (AID2) (see section 5.4) used for the analysis of a dam under hydrodynamic conditions. The program (AID2) was expanded to program (AID3) to calculate the rate of flow over a dam. This program (AID3) can be used for the analysis of dams under either conditions.

A list of the program (AID3) and a guide to its use is kept in the Department of Civil and Structural Engineering of the University of Sheffield.

4.3.1 Computer Program (AID).

A computer program (AID) was written to analyze theoretically the performance of an inflatable dam under hydrostatic conditions. The program used the finite elements method of analysis (see section 4.2) to determine the cross-sectional profile of the dam and the variation of tension around the profile. The analysis was carried out for dams inflated by air, water and air/water pressures under different combinations of upstream and downstream heads.

The input data for the program was contained on eight cards as shown in table 4.1.

If a plot of the cross-sectional profile was not required, then this could be achieved by punching the numerical values on card No. 8 equal to zero.

Initially card No. 4 was not included but this limited the program to analyse a dam constructed of only one type of fabric, in order to generalize the program to analyse a dam built from any fabric, card No. 4 was inserted and contains the polynomial coefficients of the stress-strain relationship for the fabric to be used (see section 3.3.1).

Card No.	Information
1	number of dams to be analysed.
2	number of elements and nodes of the membrane.
3	thickness, length of membrane and weight of fabric per unit area.
4	polynomial coefficients of the stress-strain relationship for the fabric.
5.	initial value of tension in first element, initial value of slope in first element and x,y misclose allowable.
6	x-co-ordinate and y-co-ordinate of first and final nodes.
7	upstream head, downstream head, internal water pressure, and internal air pressure.
8	x-scale and y-scale.

TABLE 4.1 DESCRIPTION OF INPUT DATA OF PROGRAM (AID).

The output of the program is given in table 4.2

Item No.	Information
1	number of iterations.
2	values of x and y misclose.
3	original length of the membrane.
4	new length of the membrane (stretch length).
5	maximum height of the dam.
6	x-co-ordinate, y-co-ordinate of each node and tension and slope of each element.

TABLE 4.2 DESCRIPTION OF OUTPUT DATA OF PROGRAM (AID).

The program will enable a plot of the cross-sectional profile of the dam to be made.

Fig.4.4 shows an example of the plot of the profile where the tensions specified are those in the first (upstream) element and the last (downstream) element.

4.3.2 Computer Program (AID1).

It was found necessary to be able to determine the maximum upstream head that the dam could support under certain hydrostatic conditions and hence the program (AID) was modified to program (AID1) to solve this problem in addition to a modification to analyse the dam when the membrane on the downstream side is in contact with the base.

In a few cases of analysis of inflatable dams by program (AID) the adjustment of the misclose resulted in a divergence rather than a convergence after a few iterations especially when the dams were inflated under low internal pressures. This divergence occurred due to an inaccurate assumption of the initial values of tension and slope of the first upstream element.

To minimize the occurrence of divergence in subsequent work, the subroutine "TENSION" (described in section 4.2.2) was added to the main program (AID1). The task of this subroutine was to choose the most appropriate initial values of tension and slope for the first element. This choice was dependent on the static conditions of the dam (upstream head, downstream head, internal pressures and weight of membrane).

U/S HEAD	=	0.2500	METER
D/S HEAD	=	0.0000	METER
WATER INSIDE	=	0.5000	METER
AIR PRESSURE	=	0.0000	KN/SQ.M
ORIGINAL LENGTH	=	0.7870	METER
NEW LENGTH	=	0.7983	METER
U/S TENSION	=	0.3784	KN/M
D/S TENSION	=	0.5161	KN/M
MAX. HEIGHT	=	0.2705	METER

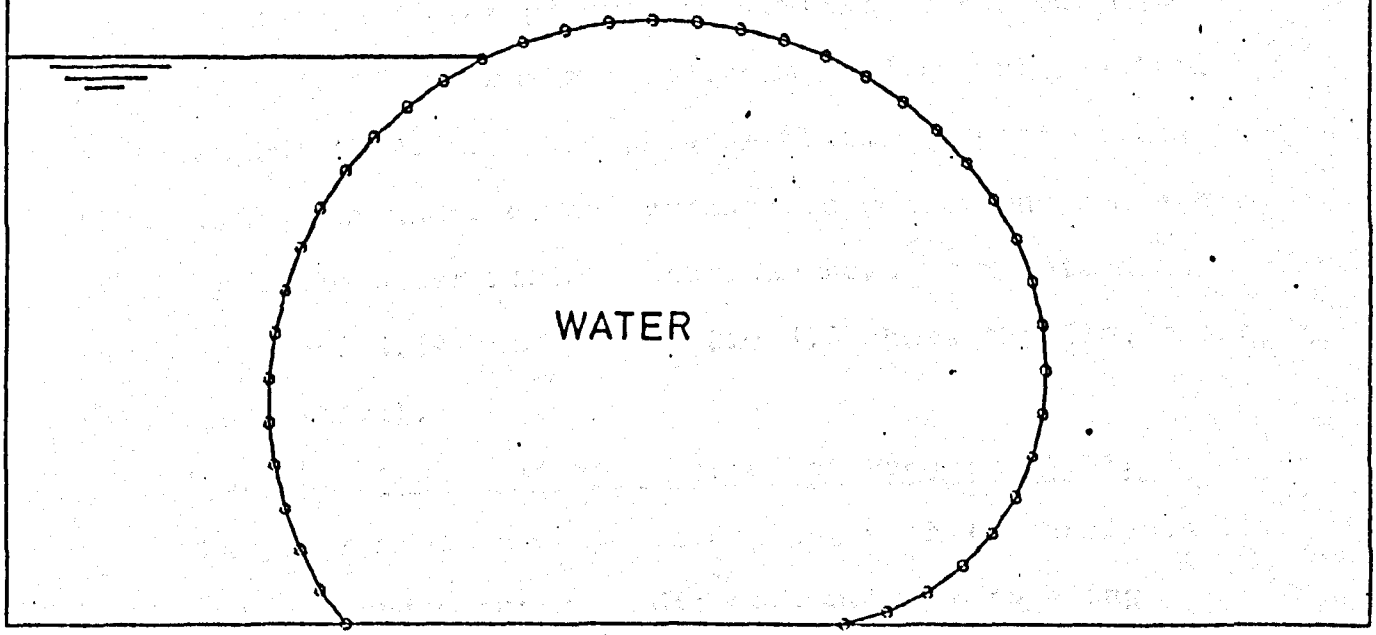

FIG. (4-4) EXAMPLE OF OUTPUT OF ANALYSIS PROGRAM (AID)

4.3.2.1 Input/Output Data for Program (AID1).

The input data of program (AID1) was the same as the input data of program (AID) (table 4.1) except for card No. 5 which contained the five parameters as follows:-

(1) Base length.

(2) Design height of the dam.

(3) Accuracy of misclose components.

(4) Maximum upstream head.

(5) Decision required for plotting the profile of maximum upstream head.

Parameter No. 4 is equal to numerical number 1 if a calculation of the maximum upstream head is required and equal to zero if it is not required. This method is also applied to parameter No. 5 if a plot of the profile at maximum upstream head is required or not.

The output of the program is similar to the output of program (AID) if the maximum upstream head is not required as shown in Fig.4.5A. The program allowed a plot of the profile of the dam under given hydrostatic conditions and a plot of the profile under maximum upstream head if required as shown in Figs. 4.5A and 4.5B. Fig.4.6 shows the flow chart of program (AID1).

4.3.2.2 Ranges of Application of Program (AID1).

The program was capable of dealing with the analysis of any dam under hydrostatic conditions, subject to being capable of design by the technique described in chapter 7. It was also possible to deal with:

(1) Different base shapes (horizontal, curved, inclined.... etc.) provided the co-ordinates of the final node are known.

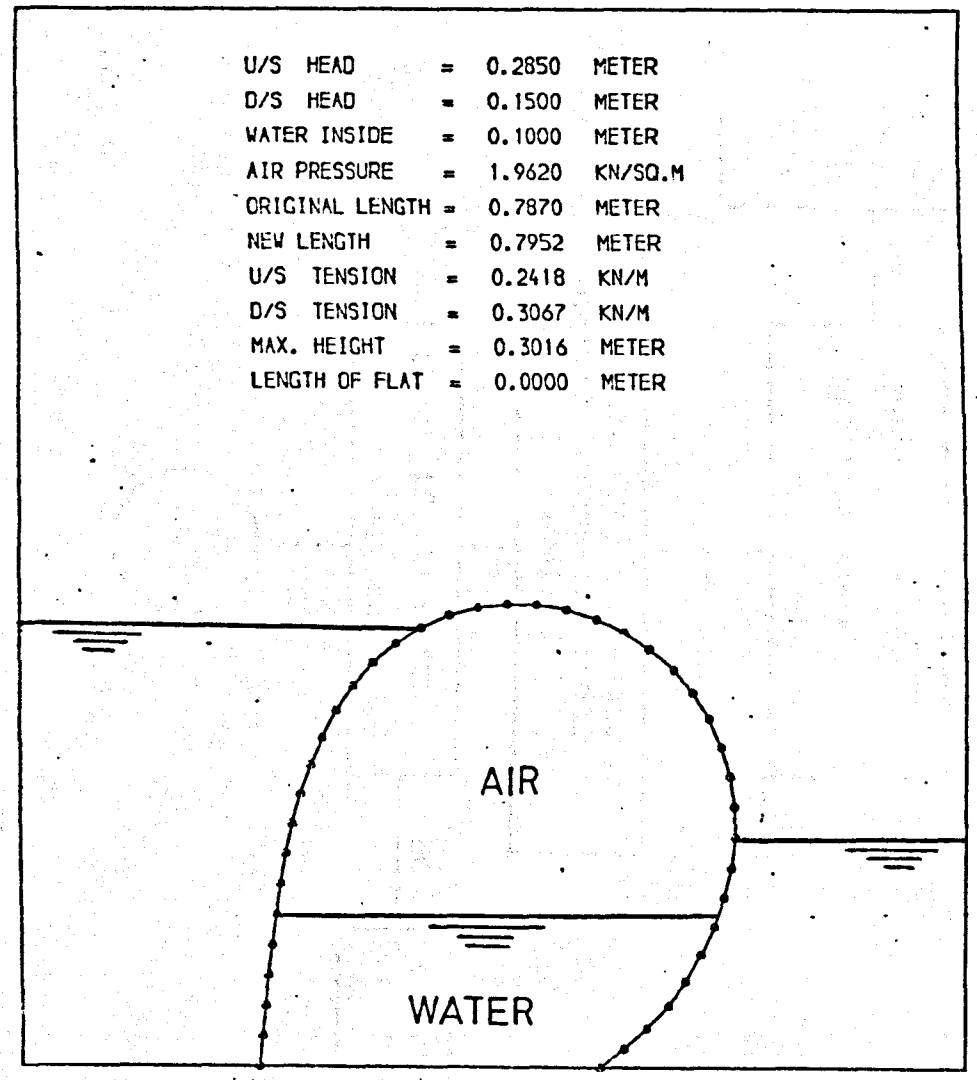

(A) Upstream head = 0·285 m

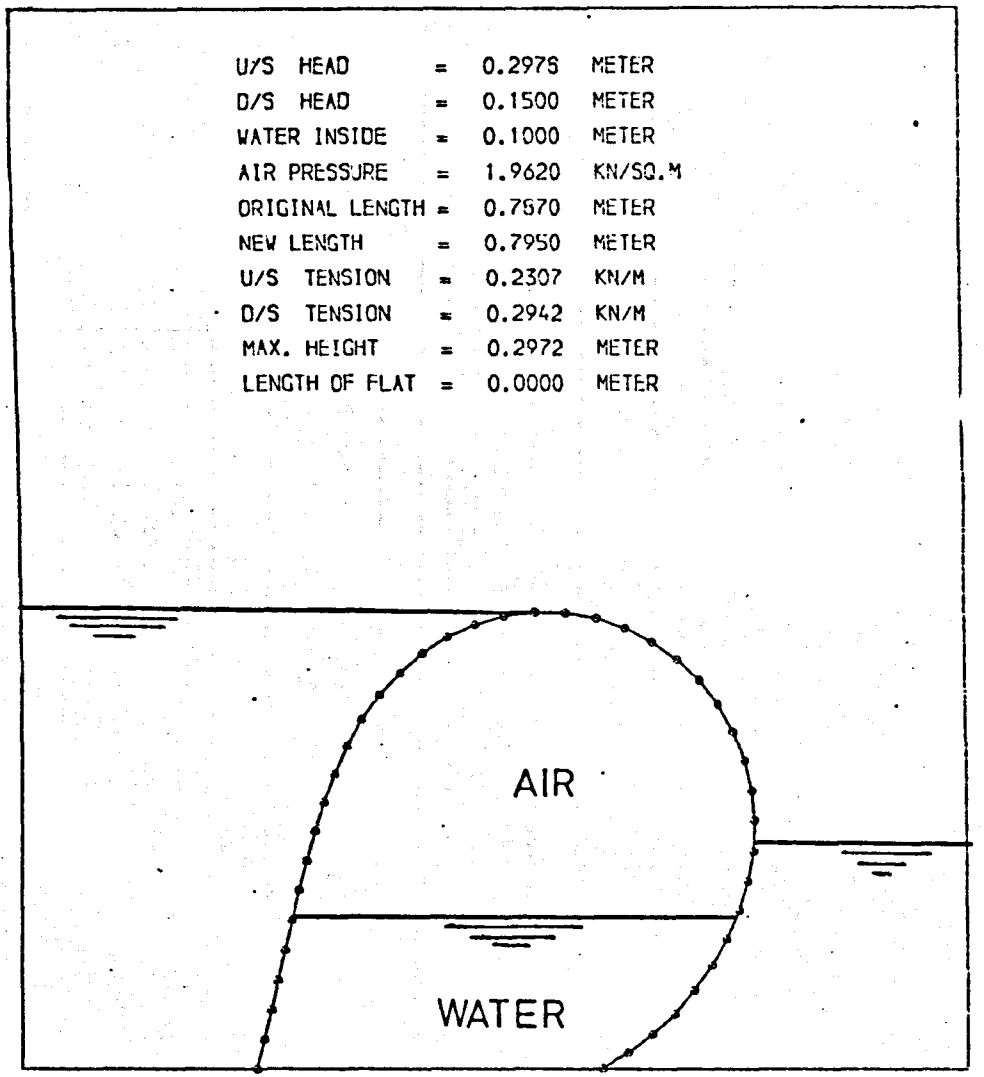

(B) Maximum upstream head

FIG. (4– 5) EXAMPLE OF OUTPUT OF ANALYSIS PROGRAM (AID 1)

Test No.	Air Press. (kN/m^2)	U/S Head (mm)	D/S Head (mm)	Max.Dam Height (mm)			% Abs.Diff. in Height		% Abs.Diff. in Shape	
				Exp.	40 El.	180 El.	40 El.	180 El.	40 El.	180 El.
1	1.962	300.0	100.0	306.0	289.3	275.9	5.45*	9.81*	7.61	7.72
2	2.943	300.0	100.0	307.5	299.6	292.8	2.56*	4.78*	7.21	7.83
3	3.924	300.0	100.0	308.0	300.1	295.7	2.56	4.00*	3.15	5.50
4	4.905	300.0	100.0	305.0	300.2	296.9	1.57	2.65*	3.52	5.96
5	5.886	300.0	100.0	304.0	300.0	297.6	1.31	2.10*	4.29	4.20
6	5.886	100.0	100.0	293.5	291.9	293.3	0.45	0.06	5.17	3.06
7	5.886	200.0	100.0	296.0	296.0	296.8	0.20	0.06	5.22	3.33
8	5.886	270.0	100.0	298.5	299.5	297.9	0.33	0.20	5.50	3.35
9	5.886	300.0	150.0	302.0	301.5	299.4	0.16	0.86*	6.32	3.25
10	5.886	300.0	240.0	306.0	304.3	304.0	0.55	0.65	6.60	2.08
11	5.886	300.0	300.0	308.5	305.8	306.7	0.87	0.58	6.47	3.55
						Mean	1.45	2.34	5.56	4.53

*Overflow occurred.

TABLE 4.4 COMPARISON BETWEEN EXPERIMENTAL AND THEORETICAL CROSS-SECTIONAL PROFILE OF AIR INFLATED DAMS.

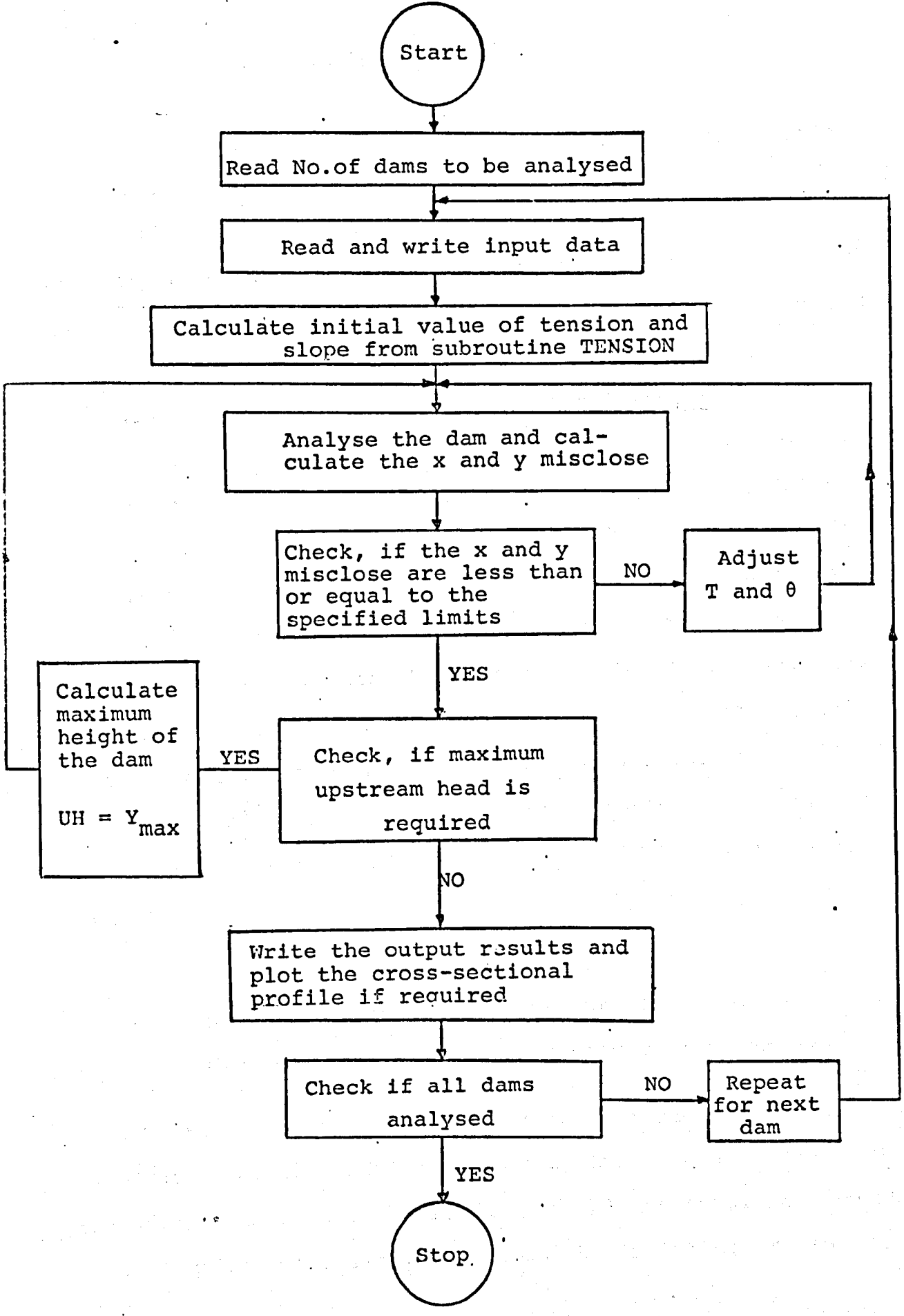

FIG. (4-6) FLOW CHART OF PROGRAM (AID1)

(2) The condition for the support of the maximum upstream head.

(3) The condition when the membrane on the downstream side is in contact with the bed.

(4) Inflated by air, water and air/water.

An analysis of problems using different inflation fluids could easily be accommodated by replacing the properties of the relevant fluid in place of those for air and water pressures.

4.3.3 Stability of the Analytical Technique.

The stability of the analytical technique is dependent upon the magnitude and type of inflation (air, water or air/water) and the maximum upstream head which can be held by a dam without overflow occurring. The theoretical analysis can only cope with the situation where the membrane is tensioned throughout its whole cross-sectional profile. Under low pressure this may not be the case. A dam where stability of the technique occurs is classified as a stable dam.

Stodulka[11] assumed the inflation ratio α for a stable air dam under hydrostatic conditions should be greater than 1.0.

$$\text{i.e.} \quad \alpha = p/H_1$$

where p = internal air pressure of the dam.

H_1 = maximum upstream head of the dam.

In the present analysis for a dam inflated by 1.962 kN/m^2 air pressure under a maximum upstream head at 295.4 mm and downstream head zero, it was possible to obtain a theoretical solution (Fig.4.44), for which the inflatable ratio

α = 0.677 and to compare this with the experimental results for these conditions.

However for the dam under the same upstream and downstream heads and air pressure of 1.864 kN/m^2 it was not possible to obtain a theoretical solution.

It is therefore possible to obtain theoretical solutions for $\alpha < 1.0$ using this technique with the limiting α value being of the order of 0.677.

For all water dams under hydrostatic conditions (downstream head = 0) tested by Clare[8] all were stable. In the study α = 1.50 was the lowest value of α for the range of inflation pressure and upstream head values used for the theoretical analysis of water inflated dams and a theoretical solution was obtained from the analysis technique. However values of $\alpha \geq 1.5$ were always found for the experimental dams, all of which were stable.

However, the stability of air/water dams is dependent upon the magnitude of water depth inside the dam. If a dam is inflated partially by water pressure head which is greater than or equal to half of the dam height, then it will behave similar to a water dam. If the depth of water inside is less than a half of the dam height, the dam will behave similar to an air dam (see section 3.6.4).

4.4 Comparison Between Experimental and Theoretical Cross-Sectional Profiles.

The shape and maximum height of the dams obtained from the experimental work (Chapter 3) were compared with the theoretical shape and maximum height of the dam obtained from the

theoretical analysis. The theoretical shape was obtained from the analysis of the membrane composed of both 40 and 180 elements. These two sizes were chosen from a study of a number of element groups detailed in table 4.3 which shows the results of the parameters for a dam using element groups ranging from 20 to 180 at 20 element intervals.

The 40 element analysis was used in subsequent analyses as this gave the dam a higher maximum height than any other number of elements. The difference in average tension, elongation and maximum height of the membrane for all element groups between 40 and 180 was less than 0.5%,and the difference in upstream slope was less than 5.0%. A further advantage of using 40 elements is that it is less time-consuming on the computer. It was therefore decided to use 40 elements for the analysis of dams except when the profile was required in which case 180 elements were used.

The program was limited to analyse a dam composed of a maximum of 199 elements and 200 nodes. However, the program could be extended to incorporate a greater number of elements if required, but this is not likely to significantly improve the analysis but would be very consuming in computer time.

Comparisons were carried out with a number of dams inflated by air, water and air/water and tested under different combinations of upstream head and downstream head (see tables 3.2, 3.3 and 3.4).

Figs. 4.7, 4.8 and 4.9 show examples of the comparison between the experimental shape and the theoretical shape using 40 and 180 elements for all three types of inflation.

Number of Elements	Maximum Dam Height (mm)	U/S Tension (kN/m)	D/S Tension (kN/m)	Average Tension (kN/m)	U/S Slope (degrees)	Elong-ation (mm)
20	298.90	0.6950	1.1337	0.9143	133.96	19.87
40	299.51	0.8242	1.0580	0.9411	124.81	20.12
60	299.09	0.8652	1.0244	0.9448	122.46	20.17
80	298.73	0.8852	1.0062	0.9457	121.35	20.19
100	298.50	0.8971	0.9946	0.9458	120.70	20.20
120	298.33	0.9051	0.9867	0.9459	120.27	20.21
140	298.19	0.9108	0.9810	0.9459	119.97	20.22
160	298.06	0.9150	0.9766	0.9458	119.74	20.22
180	297.97	0.9180	0.9732	0.9457	119.57	20.22

TABLE 4.3 ANALYSIS OF A DAM USING DIFFERENT NUMBERS OF ELEMENTS.

Analysis conditions.

Upstream head	=	270.0 mm
Downstream head	=	100.0 mm
Air pressure	=	5.886 kN/m^2
Water pressure	=	0.0
Membrane length	=	787.0 mm
Base length	=	225.0 mm

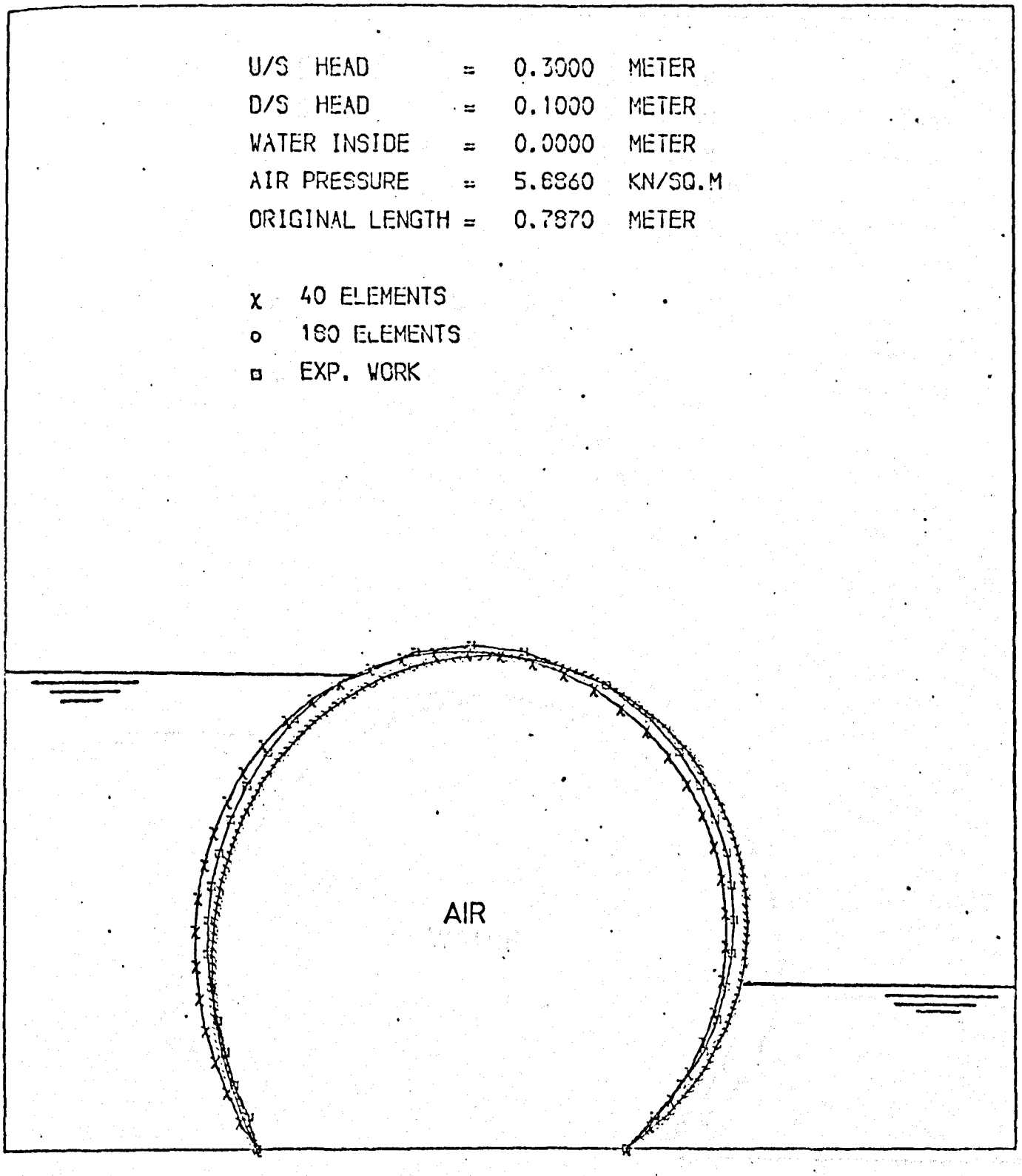

FIG. (4– 7) COMPARISON BETWEEN EXPERIMENTAL AND THEORETICAL PROFILES OF A TYPICAL AIR DAM

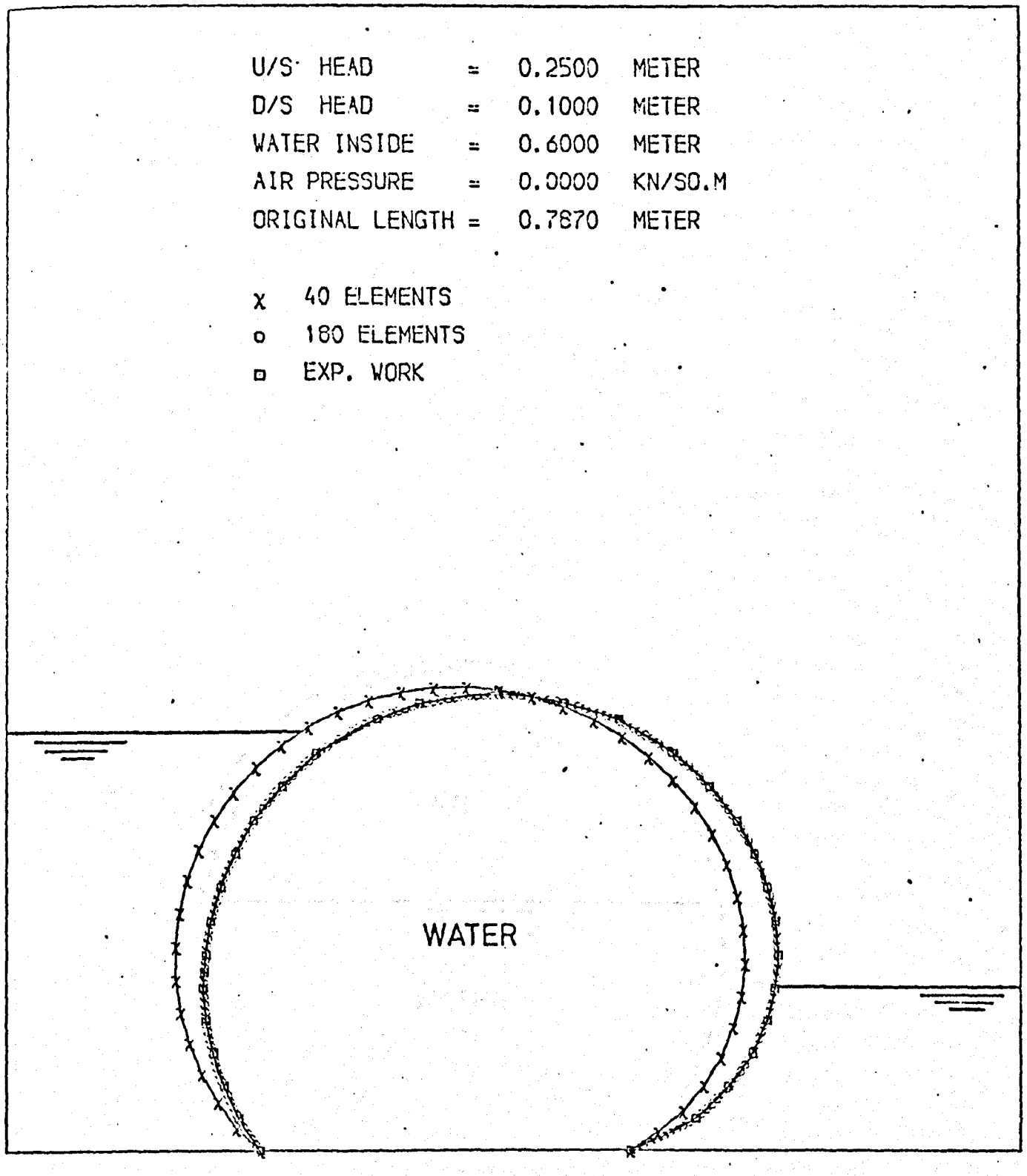

FIG. (4- 8) COMPARISON BETWEEN EXPERIMENTAL AND THEORETICAL PROFILES OF A TYPICAL WATER DAM

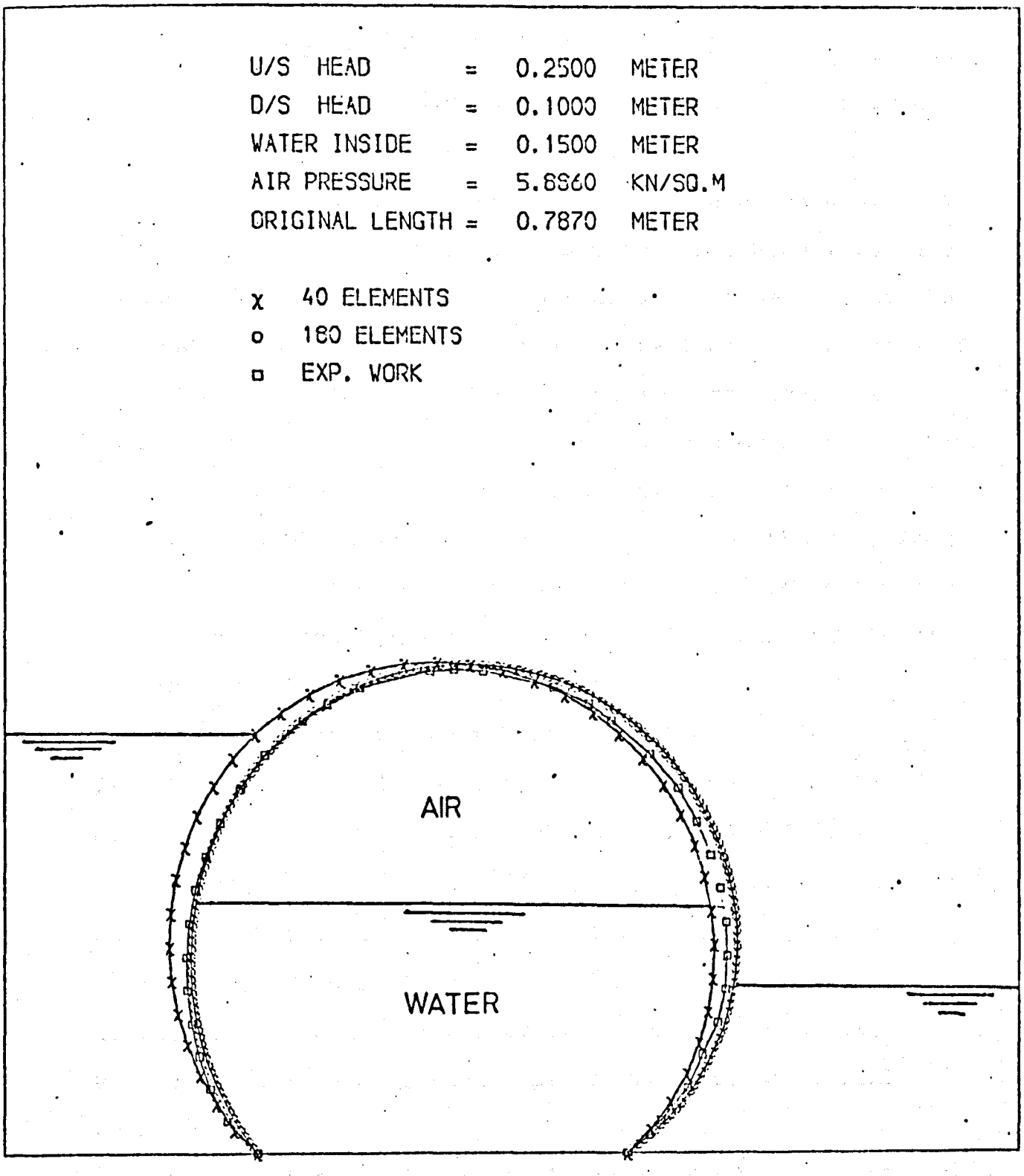

FIG. (4- 9) COMPARISON BETWEEN EXPERIMENTAL AND THEORETICAL PROFILE OF A TYPICAL AIR/WATER DAM

Tables 4.4, 4.5 and 4.6 show the difference in shape and maximum dam height for air, water and air/water inflated dams respectively. All differences are expressed as a percentage of the experimental height or shape.

The difference in shapes of the dams were calculated by comparing the experimental co-ordinates of four points on the upstream face and four points on the downstream face of the dam and the crest point with the theoretical co-ordinates of the equivalent points. The elevation of the four points on each side was 50 mm, 100 mm, 150 mm, 200 mm above the base level. The co-ordinates of all points were relative to the origin point which was taken as the centre of the base length of the dam. A general shape difference for each dam was calculated by averaging the absolute differences at the nine points.

The difference in the maximum height of the dam varied from 0.1% to 10% and the difference in shape varied from 0.1% to 8% for all dams (see tables 4.4, 4.5 and 4.6).

The highest percentage difference of 10% in maximum dam height was due to the overflow load acting on the membrane which resulted in an increase in the distortion of the dam and at the same time caused a decrease in the maximum height. Higher percentage differences are found with lower inflated pressures.

The significant difference in shape may be attributed to the effects of the ends on the cross-sectional profile at the centre as shown in Fig.4.10. The experimental cross-sectional profile (Chapter 3) which was used for comparison

No.	Water Press. (mm)	U/S Head (mm)	D/S Head (mm)	Max.Dam Height (mm)			% Abs.Diff. in Height		% Abs.Diff. in Shape	
				Exp	40 El.	180 El.	40 El.	180 El.	40 El.	180.E
1	400.0	250.0	100.0	261.0	256.7	243.4	1.65	6.74*	7.01	7.68
2	450.0	250.0	100.0	271.5	268.0	255.7	1.27	5.82	6.51	5.06
3	500.0	250.0	100.0	275.5	273.5	265.2	0.71	3.74	5.90	4.52
4	600.0	250.0	100.0	277.5	279.4	275.1	0.67	0.86	4.37	0.05
5	800.0	250.0	100.0	285.5	285.0	282.7	0.09	0.35	4.80	4.90
6	1000.0	250.0	100.0	288.5	288.2	287.5	1.21	1.23	7.32	2.97
7	600.0	75.0	0.0	270.5	264.2	268.9	2.31	0.56	6.79	3.67
8	600.0	150.0	0.0	273.7	271.1	271.1	0.93	0.71	5.48	1.82
9	600.0	250.0	0.0	277.0	278.2	270.8	0.43	2.21	3.46	4.53
10	600.0	250.0	150.0	279.5	281.1	278.3	0.58	0.42	5.02	4.17
11	600.0	250.0	250.0	286.5	283.7	285.3	0.96	0.41	5.99	4.94
						Mean	0.98	2.09	5.69	4.02

*Overflow occurred.

TABLE 4.5 COMPARISON BETWEEN EXPERIMENTAL AND THEORETICAL CROSS-SECTIONAL PROFILE OF WATER INFLATED DAMS.

No.	Air Press. (kN/m^2)	Water Press. (mm)	U/S Head (mm)	D/S Head (mm)	Max. Dam Height (mm)			% Abs.Diff. in Height		% Abs.Diff. in Shape	
					Exp	40 El.	180 El.	40 El.	180 El.	40 El.	180 El.
1	1.962	150.0	250.0	100.0	290.7	291.8	282.8	0.04	2.69	7.26	7.87
2	2.943	150.0	250.0	100.0	292.0	294.1	289.7	0.27	0.29	6.74	4.91
3	3.924	150.0	250.0	100.0	292.7	294.9	291.8	0.77	0.24	6.11	3.82
4	4.905	150.0	250.0	100.0	293.5	295.2	293.0	0.21	0.06	5.71	3.55
5	5.886	50.0	250.0	100.0	294.5	299.1	297.4	1.53	0.98	5.26	3.75
6	5.886	150.0	250.0	100.0	291.0	295.6	294.5	1.58	1.05	6.91	2.85
7	5.886	250.0	250.0	100.0	287.0	288.2	286.8	0.42	0.73	7.32	2.28
							Mean	0.69	0.87	6.47	4.14

TABLE 4.6 COMPARISON BETWEEN EXPERIMENTAL AND THEORETICAL CROSS-SECTIONAL PROFILE OF AIR/WATER INFLATED DAMS.

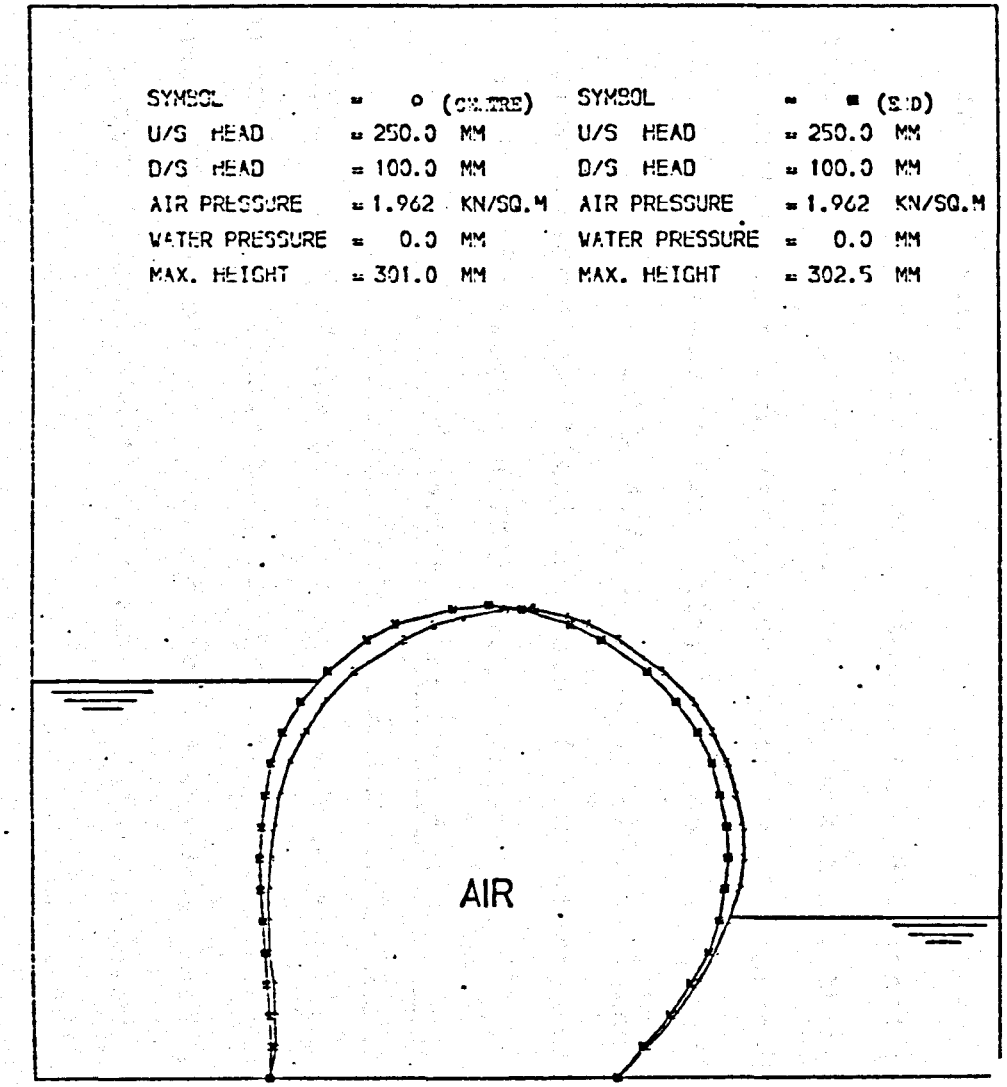

(A) Air inflated dam

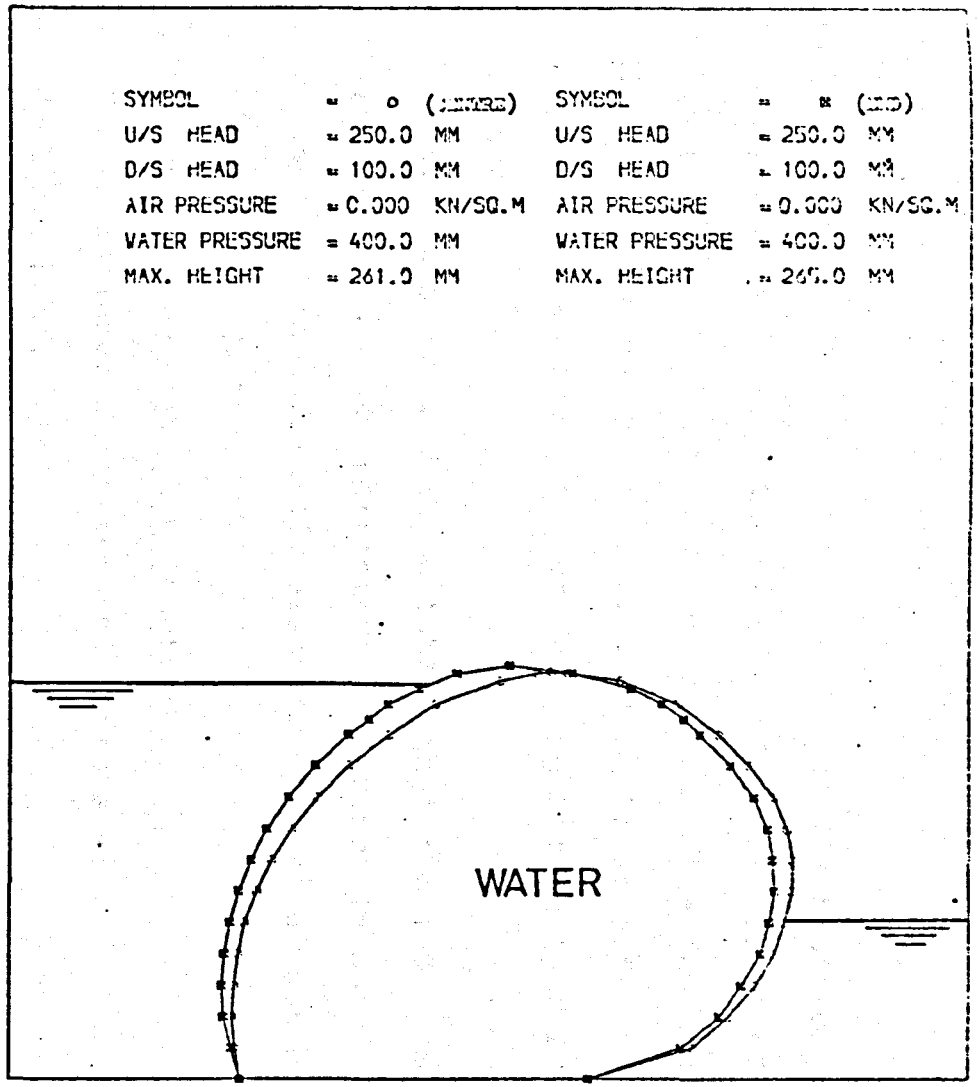

(B) Water inflated dam

FIG. (4-10) END EFFECTS ON THE CROSS-SECTIONAL PROFILES

was measured at the centre of the dam and it has been shown from experimental tests that the significant effect of ends on the profile of the centre appeared when the dam was inflated by low pressures (Fig.4.10). These effects can be minimized when the ratio of dam length to height is increased.

It can be seen from these tables that the 180 element analysis gives a lower percentage difference in shape for most cases and therefore 180 elements were used when shape profiles were required.

4.5 Effect of Operational Parameters.

The operational parameters of a dam are:-

1. Upstream head.
2. Downstream head.
3. Internal pressure.

To study the effects of variation of operational parameters on the shape and tension of the membrane, three dams were analysed under different combinations of upstream head, downstream head and internal air, water and air/water pressures as illustrated in table 4.7, 4.8, 4.9, 4.10, 4.11 and 4.12. The results of the theoretical analysis of the membrane were obtained using program (AID1) with 40 elements.

4.5.1 Effect of Variation of Upstream Head and Internal Pressure with a Constant Downstream Head.

The effect of variation of upstream head and internal pressure on the tension, elongation, upstream slope, downstream slope and maximum height of the membrane for a downstream head equal zero were investigated and the results are detailed below.

Test No.	Air Pressure (kN/m^2)	U/S Head (mm)	D/S Head (mm)
1	5.886	100.0	0.0
2	5.886	150.0	0.0
3	5.886	180.0	0.0
4	5.886	220.0	0.0
5	5.886	250.0	0.0
6	5.886	270.0	0.0
7	5.886	290.0	0.0
8	5.886	299.8	0.0
1	3.924	100.0	0.0
2	3.924	150.0	0.0
3	3.924	180.0	0.0
4	3.924	220.0	0.0
5	3.924	250.0	0.0
6	3.924	270.0	0.0
7	3.924	290.0	0.0
8	3.924	299.1	0.0
1	1.962	100.0	0.0
2	1.962	150.0	0.0
3	1.962	180.0	0.0
4	1.962	220.0	0.0
5	1.962	250.0	0.0
6	1.962	270.0	0.0
7	1.962	280.0	0.0
8	1.962	287.4	0.0

TABLE 4.7 HYDROSTATIC CONDITIONS FOR ANALYSIS OF AIR INFLATED DAMS WITH THE DOWNSTREAM HEAD CONSTANT ANE EQUAL TO ZERO.

Test No.	Air Pressure (kN/m^2)	U/S Head (mm)	D/S Head (mm)
1	5.886	270.0	50.0
2	5.886	270.0	100.0
3	5.886	270.0	150.0
4	5.886	270.0	200.0
5	5.886	270.0	250.0
1	3.924	270.0	50.0
2	3.924	270.0	100.0
3	3.924	270.0	150.0
4	3.924	270.0	200.0
5	3.924	270.0	250.0
1	1.962	270.0	50.0
2	1.962	270.0	100.0
3	1.962	270.0	150.0
4	1.962	270.0	200.0
5	1.962	270.0	250.0

TABLE 4.8 HYDROSTATIC CONDITIONS FOR ANALYSIS OF AIR INFLATED DAMS WITH THE UPSTREAM HEAD CONSTANT AND EQUAL TO 270 mm.

Test No.	Water Pressure (mm)	U/S Head (mm)	D/S Head (mm)
1	600.0	100.0	0.0
2	600.0	150.0	0.0
3	600.0	180.0	0.0
4	600.0	220.0	0.0
5	600.0	250.0	0.0
6	600.0	270.0	0.0
7	600.0	277.1	0.0
1	500.0	100.0	0.0
2	500.0	150.0	0.0
3	500.0	180.0	0.0
4	500.0	220.0	0.0
5	500.0	250.0	0.0
6	500.0	267.6	0.0
1	400.0	115.0	0.0
2	400.0	150.0	0.0
3	400.0	180.0	0.0
4	400.0	200.0	0.0
5	400.0	220.0	0.0
6	400.0	246.2	0.0

TABLE 4.9 HYDROSTATIC CONDITIONS FOR ANALYSIS OF WATER INFLATED DAMS WITH THE THE DOWNSTREAM HEAD CONSTANT AND EQUAL TO ZERO.

Test No.	Water Pressure (mm)	U/S Head (mm)	D/S Head (mm)
1	600.0	220.0	50.0
2	600.0	220.0	100.0
3	600.0	220.0	150.0
4	600.0	220.0	200.0
1	500.0	220.0	50.0
2	500.0	220.0	100.0
3	500.0	220.0	150.0
4	500.0	220.0	200.0
1	400.0	220.0	50.0
2	400.0	220.0	100.0
3	400.0	220.0	150.0
4	400.0	220.0	200.0

TABLE 4.10 HYDROSTATIC CONDITIONS FOR ANALYSIS OF WATER INFLATED DAMS WITH THE UPSTREAM HEAD CONSTANT AND EQUAL TO 220 mm.

Test No.	Air Pressure (kN/m^2)	Water Pressure (mm)	U/S Head (mm)	D/S Head (mm)
1	3.924	200.0	100.0	0.0
2	3.924	200.0	150.0	0.0
3	3.924	200.0	180.0	0.0
4	3.924	200.0	220.0	0.0
5	3.924	200.0	250.0	0.0
6	3.924	200.0	270.0	0.0
7	3.924	200.0	288.3	0.0
1	3.924	100.0	100.0	0.0
2	3.924	100.0	150.0	0.0
3	3.924	100.0	180.0	0.0
4	3.924	100.0	220.0	0.0
5	3.924	100.0	250.0	0.0
6	3.924	100.0	270.0	0.0
7	3.924	100.0	296.7	0.0
1	1.962	200.0	100.0	0.0
2	1.962	200.0	150.0	0.0
3	1.962	200.0	180.0	0.0
4	1.962	200.0	220.0	0.0
5	1.962	200.0	250.0	0.0
6	1.962	200.0	260.0	0.0
7	1.962	200.0	262.9	0.0
1	1.962	100.0	100.0	0.0
2	1.962	100.0	150.0	0.0
3	1.962	100.0	180.0	0.0
4	1.962	100.0	220.0	0.0
5	1.962	100.0	250.0	0.0
6	1.962	100.0	270.0	0.0
7	1.962	100.0	281.5	0.0

TABLE 4.11 HYDROSTATIC CONDITIONS FOR ANALYSIS OF AIR/WATER INFLATED DAMS WITH DOWNSTREAM HEAD CONSTANT AND EQUAL TO ZERO.

Test No.	Air Pressure (kN/m^2)	Water Pressure (mm)	U/S Head (mm)	D/S Head (mm)
1	3.924	200.0	250.0	50.0
2	3.924	200.0	250.0	100.0
3	3.924	200.0	250.0	150.0
4	3.924	200.0	250.0	200.0
1	3.924	100.0	250.0	50.0
2	3.924	100.0	250.0	100.0
3	3.924	100.0	250.0	150.0
4	3.924	100.0	250.0	200.0
1	1.962	200.0	250.0	50.0
2	1.962	200.0	250.0	100.0
3	1.962	200.0	250.0	150.0
4	1.962	200.0	250.0	200.0
1	1.962	100.0	250.0	50.0
2	1.962	100.0	250.0	100.0
3	1.962	100.0	250.0	150.0
4	1.962	100.0	250.0	200.0

TABLE 4.12 HYDROSTATIC CONDITIONS FOR ANALYSIS OF AIR/WATER INFLATED DAMS WITH UPSTREAM HEAD CONSTANT AND EQUAL TO 250 mm.

4.5.1.1 Tension.

The tension in the membrane was determined by calculating the average tension between the first (upstream fixture) and the final element (downstream fixture). The tension in the membrane decreases as the upstream head increases for all dams as shown in Figs. 4.11, 4.12 and 4.13 respectively. These graphs also show that the tension in the membrane is lower the lower the internal pressure. When the dam is inflated by high air pressure (5.886 kN/m^2), the decrease in tension with the rising upstream head is fairly steady until the upstream head is equal to 220 mm (Fig.4.11). However, when the upstream head increases above this level the tension decreases at an increasing rate. This phenomenon also occurs for the other two inflation pressures tested but the point where the decrease becomes more rapid changes, this tending to happen at a lower upstream head the lower the inflation pressure.

In the case of water inflated dams, the curve of decreasing tension with rising upstream head behaved differently from the air dams as can be seen from Fig.4.12. This difference is probably due to the distribution of the internal water pressure which is acting on the membrane from within being different from the effect of an air pressure. Again lower tensions are associated with lower inflation pressures.

The behaviour of the tension of the air/water dams (Fig.4.13) appears to be similar to the air dam. From this figure it can be seen that the tension decreases when the depth of water inside the dam decreases for a constant air pressure and that lower tensions are associated with lower inflation pressures.

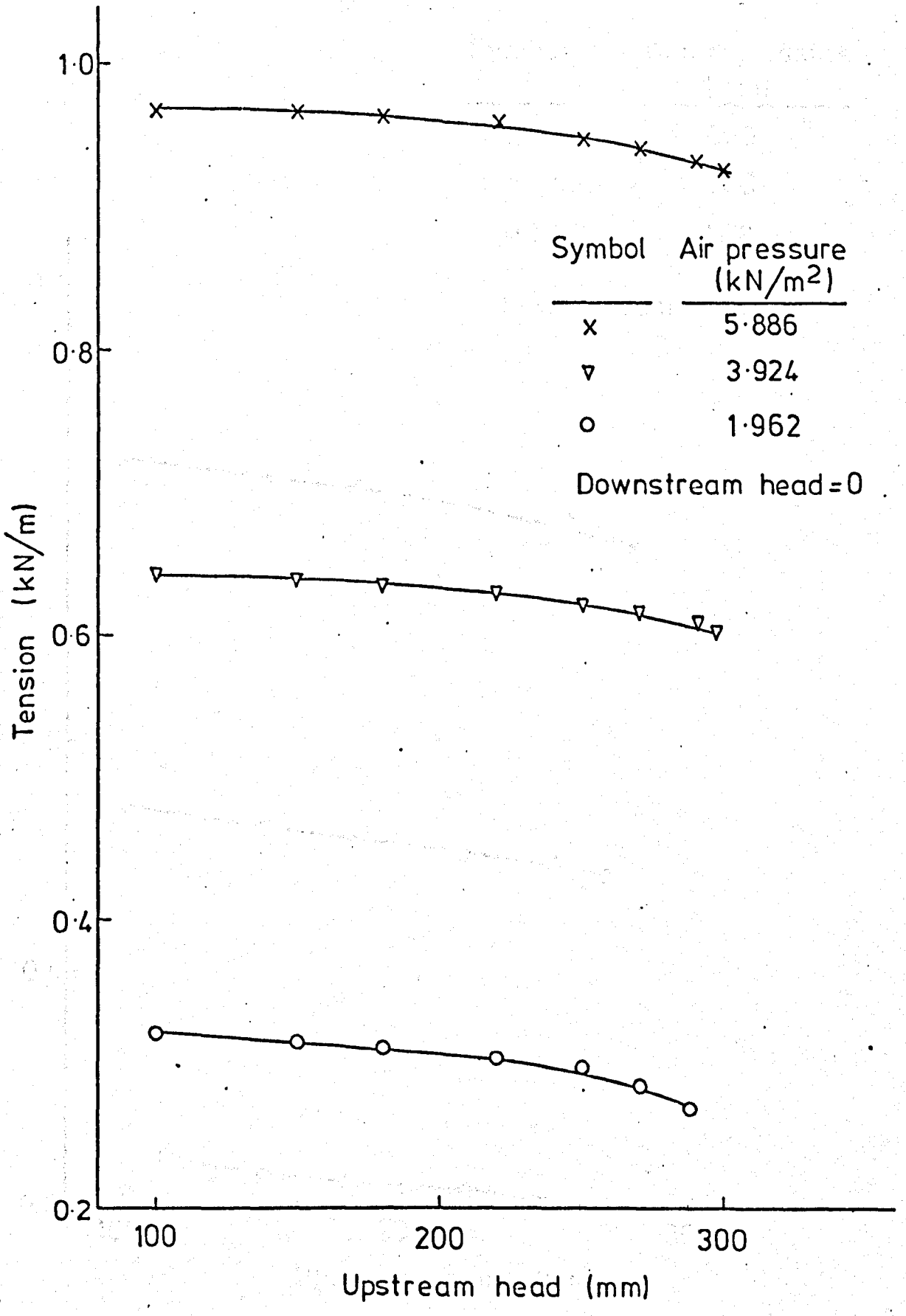

FIG. (4–11) VARIATION OF TENSION IN MEMBRANE WITH UPSTREAM HEAD FOR VARIOUS AIR PRESSURES

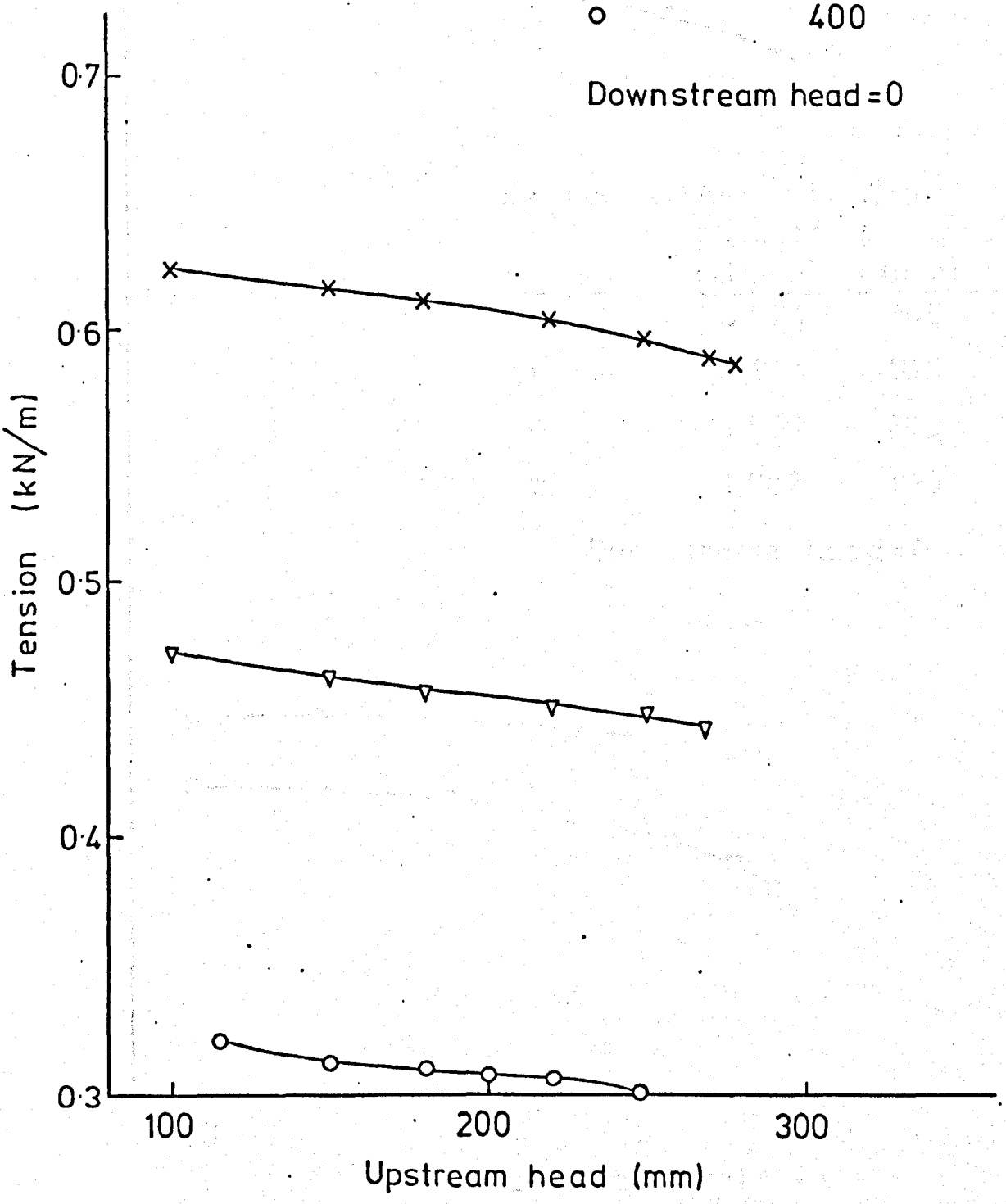

FIG. (4-12) VARIATION OF TENSION IN MEMBRANE WITH UPSTREAM HEAD FOR VARIOUS WATER PRESSURES

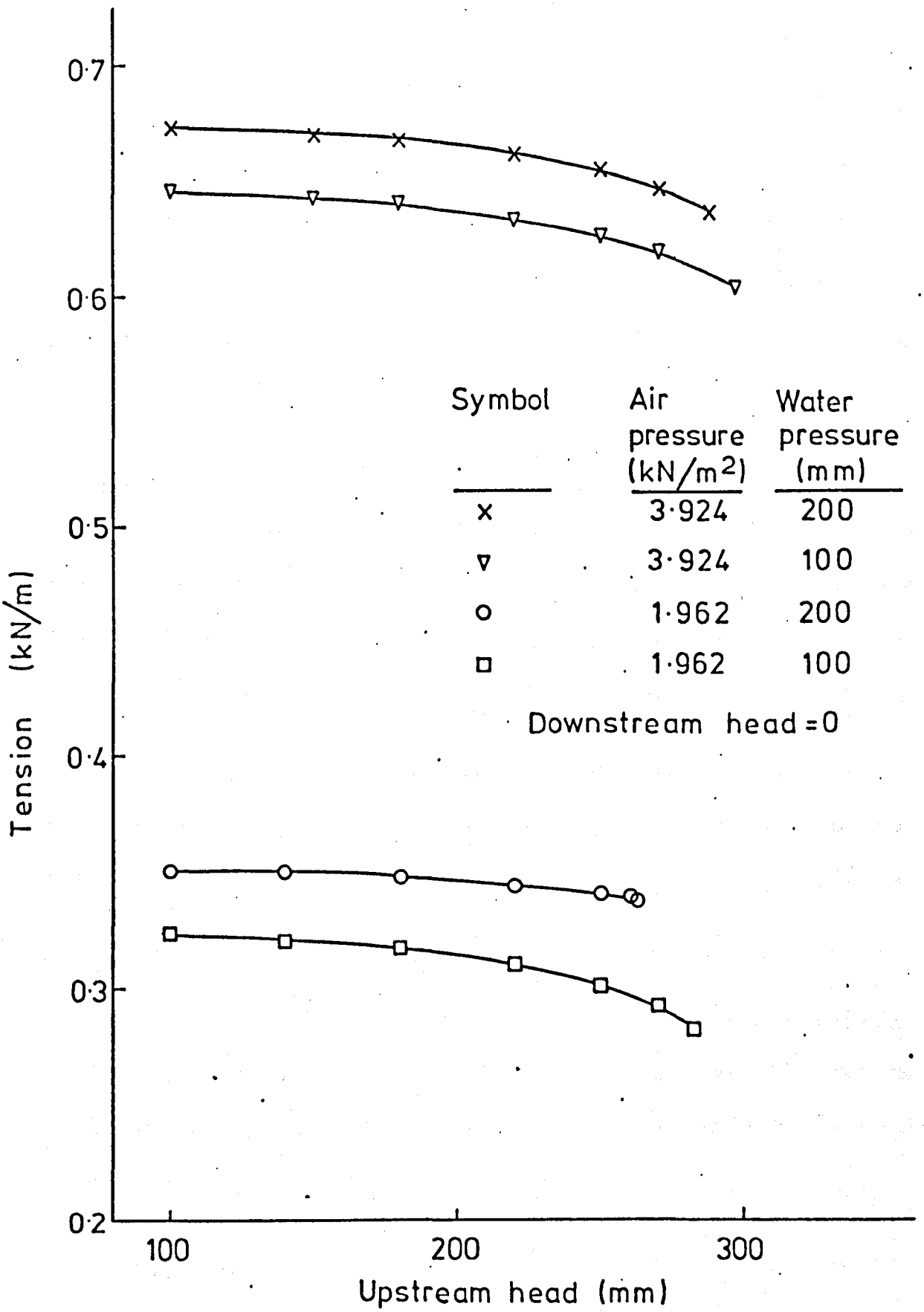

FIG.(4–13) VARIATION OF TENSION IN MEMBRANE WITH UPSTREAM HEAD FOR VARIOUS AIR/WATER PRESSURES

The decrease in tension of air, water and air/water membranes when the upstream head rises may be attributed to the decrease in the resultant pressure exerted on each element due to a combination of upstream load, downstream load, internal pressure and weight of the membrane. Considering the various pressures (see Fig. 4.1B) the horizontal component of the force F_1 is increased when the upstream head rises. This increase in F_1 produces a decrease in the horizontal component of the forces acting on the element AB (equation 4.6), and therefore the tension in the membrane decreases. Also when the internal pressure falls, the resultants of the horizontal and vertical forces (F_2 and F_3) are decreased. This reduction in the internal forces also results in a reduction in the tension in the membrane.

The tension depends on the density and strength of the material although one would expect similar relationships to exist for other materials. These graphs are only applicable to the N·T fabric used in this study.

4.5.1.2 Elongation.

The elongation of the membrane was calculated by subtracting the new length of the membrane (determined by the theoretical analysis) from the original length. Figs. 4.14, 4.15 and 4.16 illustrate the relationships between the elongation of the membrane with a rising upstream head for air, water and air/water inflated dams respectively.

It can be seen from these graphs that elongation curves behave in a similar manner to the tension curves (see section

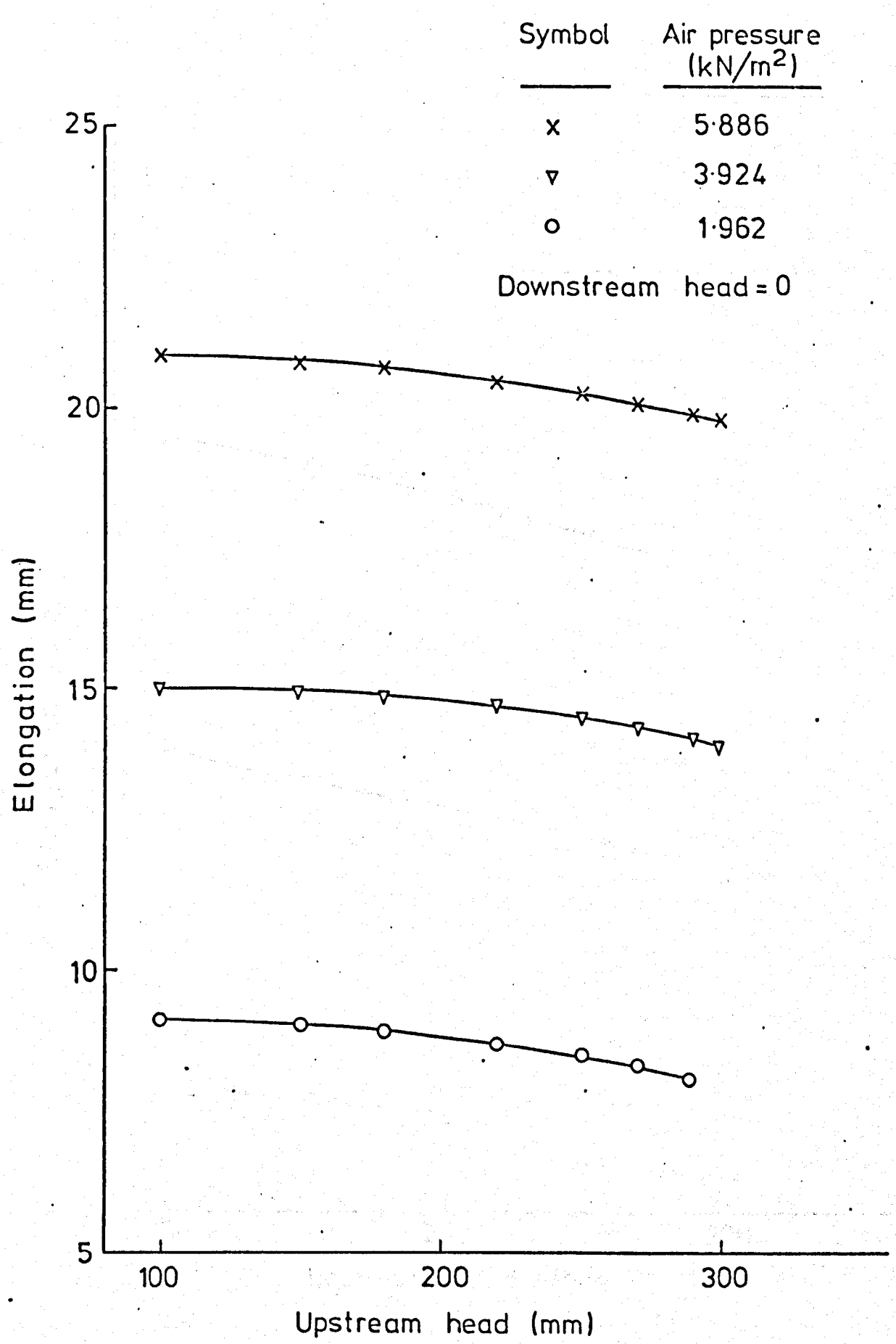

FIG. (4–14) VARIATION OF ELONGATION IN MEMBRANE WITH UPSTREAM HEAD FOR VARIOUS AIR PRESSURES

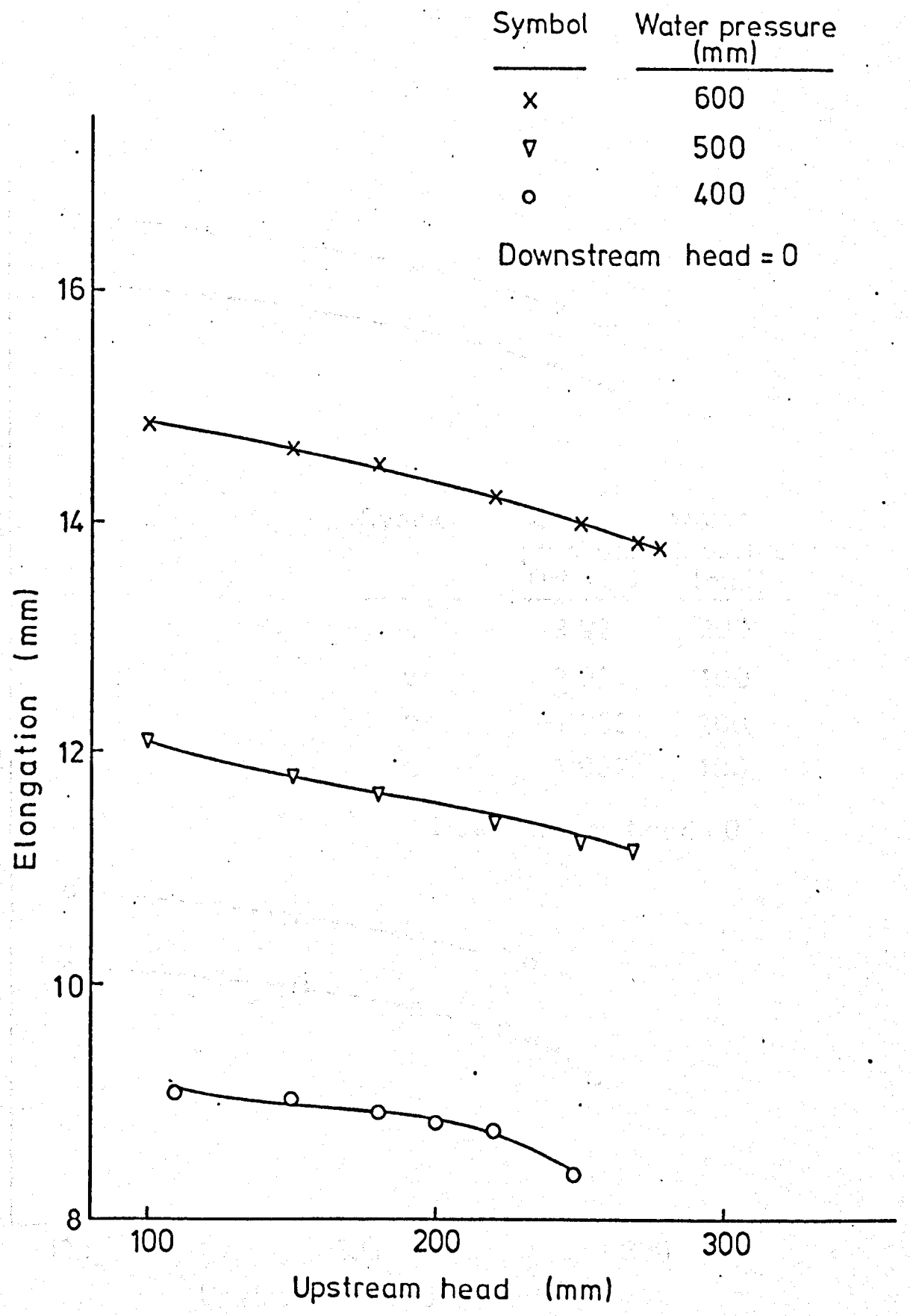

FIG. (4-15) VARIATION OF ELONGATION IN MEMBRANE WITH UPSTREAM HEAD FOR VARIOUS WATER PRESSURES

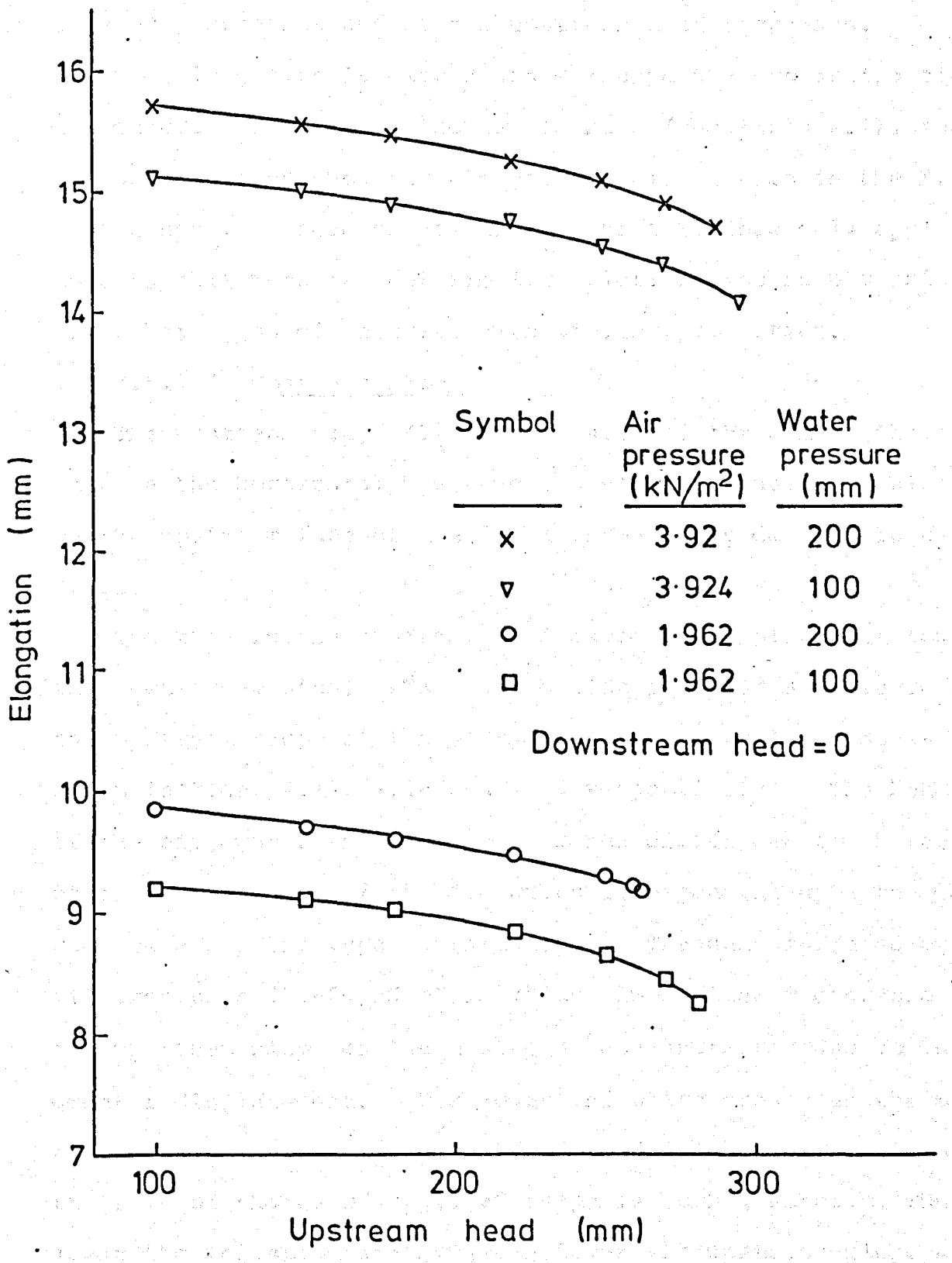

FIG. (4–16) VARIATION OF ELONGATION IN MEMBRANE WITH UPSTREAM HEAD FOR VARIOUS AIR/WATER PRESSURES

4.5.1.1), and that elongation decreases when the internal pressure decreases and as the upstream head increases.

The elongation is also dependent upon the properties of the material from which the dam is made (see table 2.1), and the above graphs show the elongation which occurs in the N.T. fabric used. These relationships are therefore only applicable to this material but similar relationships should exist for other types of material with similar properties.

4.5.1.3 Upstream slope.

The upstream slope (θ_1 in Fig. 4.2) of the dam is the angle between the horizontal base and the slope of the first element on the upstream face of the dam as previously defined in section 4.2.3.

The rise in the upstream head caused a displacement towards the downstream side. This distortion produced a decrease in the upstream slope of the air, water and air/water dams as shown in Figs. 4.17, 4.18 and 4.19 respectively. The behaviour of the air, water and air/water graphs differ due to the deformation in the shape of the dam which is dependent upon the magnitude and the type of inflation. The dams inflated by high air pressures (5.886 kN/m^2) have an almost linear decrease in the upstream slope as the upstream head increases due to the greater displacement. For lower inflation pressures the displacement with increasing upstream head is much greater and the rate of change of upstream shape is much greater. The lower the inflation pressure the lower the upstream slope as displacement becomes easier.

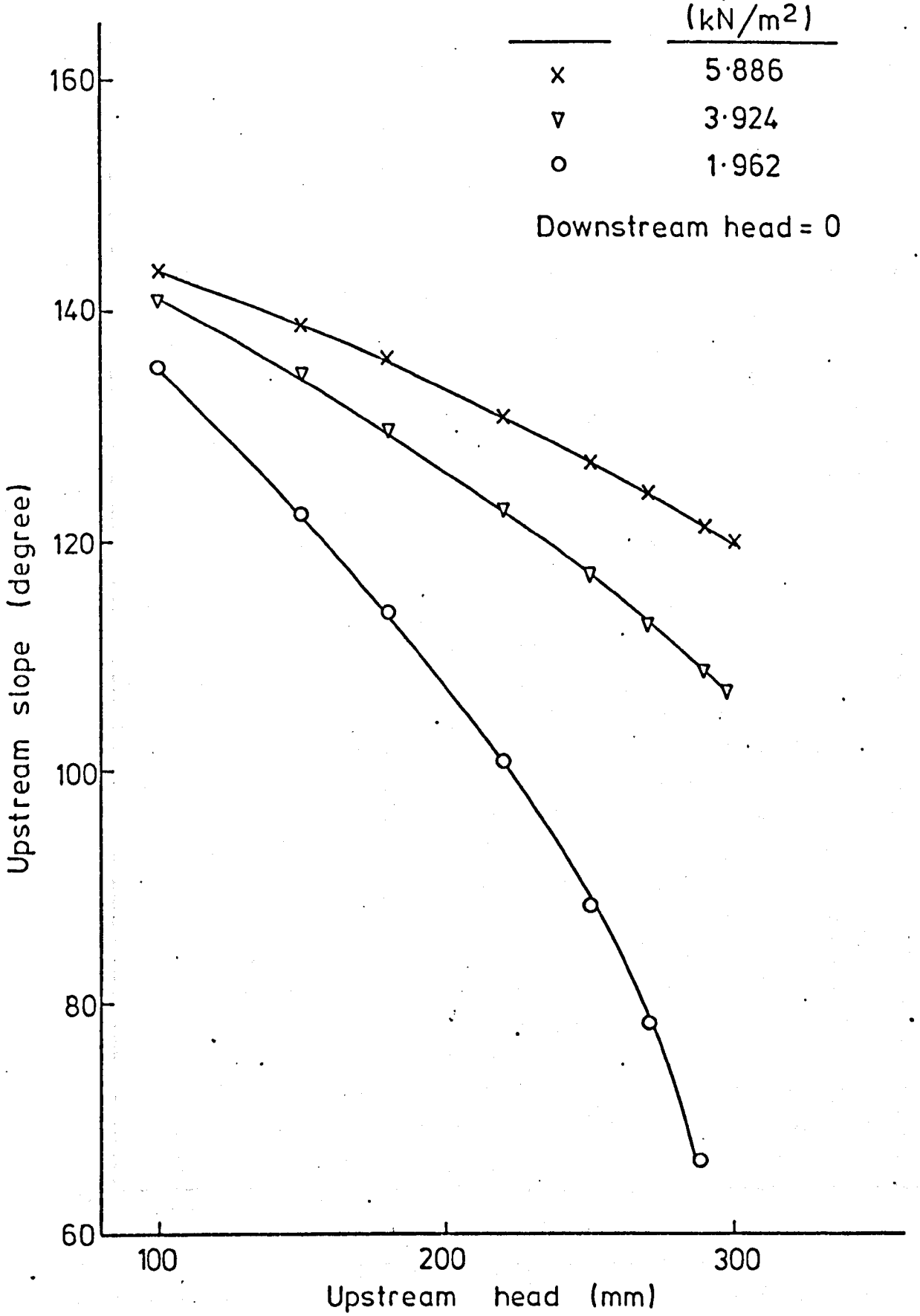

FIG.(4—17) VARIATION OF UPSTREAM SLOPE OF MEMBRANE WITH UPSTREAM HEAD FOR VARIOUS AIR PRESSURES

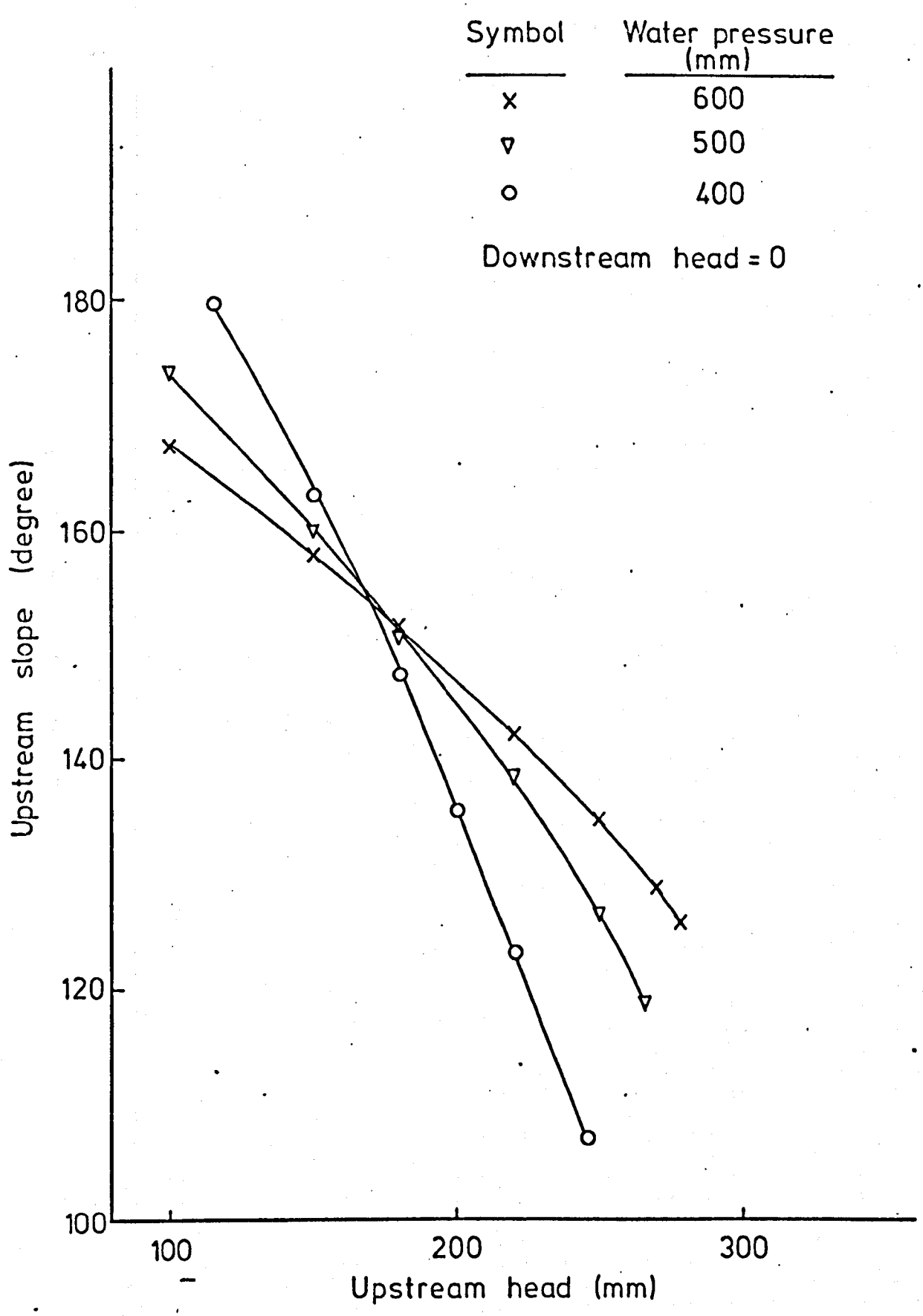

FIG. (4-18) VARIATION OF UPSTREAM SLOPE OF MEMBRANE WITH UPSTREAM HEAD FOR VARIOUS WATER PRESSURES

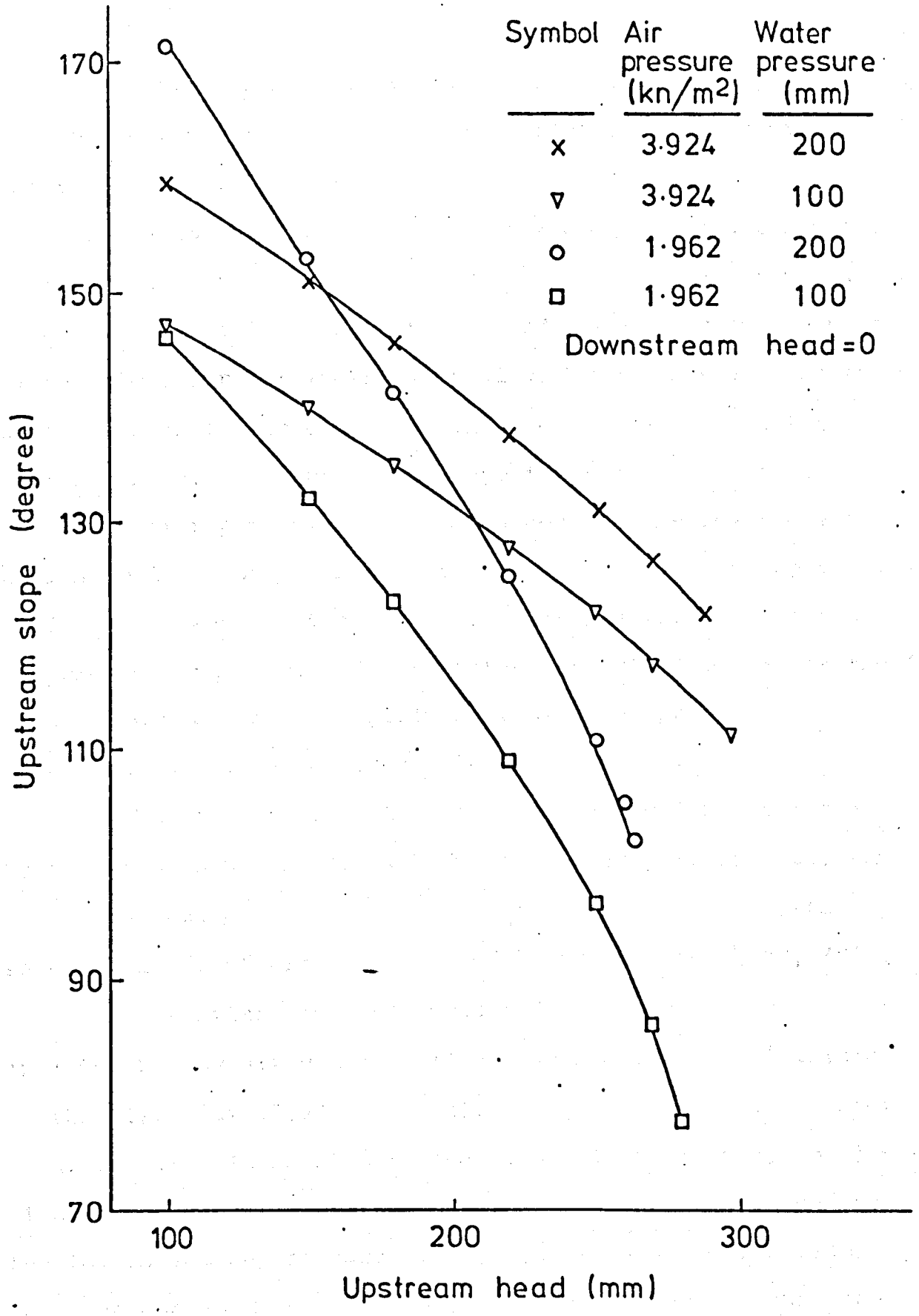

FIG. (4—19) VARIATION OF UPSTREAM SLOPE OF MEMBRANE WITH UPSTREAM HEAD FOR VARIOUS AIR/WATER PRESSURES

However, this behaviour only occurs with air inflated dams and does not occur when the dam is inflated by water or air/water pressures.

Fig. 4.18 shows the results for a dam analysed for water inflated pressures of 600 mm, 500 mm and 400 mm water head. The graphs show that for low upstream heads below 160 mm the upstream slope is greater for lower internal water pressures. As the upstream head is increased the lines converge until after 160 mm upstream head. The upstream slope is greater for greater internal water pressures. This is because the low pressure dam begins to lie flat at the upstream fixture under low upstream heads and because of the internal water pressure decrease at the crest of the dam. The resistance to displacement of the low pressure dam decreases rapidly above 160 mm upstream head resulting in a lower upstream slope of the dam.

In the case of air/water dams, the dam which was inflated by an air pressure of 3.924 kN/m^2 and water pressure 200.0 mm water head was distorted less than the dam inflated by the same magnitude of air pressure and 100.0 mm water head, (Fig. 4.19). A similar behaviour occurred when the dam was inflated by low air pressure (1.962 kN/m^2) but the distortion of the first dam (3.924 kN/m^2 air with 200 mm or 100 mm water head) resulted in an almost linear reduction in upstream slope with an increase in upstream head. The change in shape for the low inflation pressure is much greater as the upstream head increases. This phenomena caused the low pressure dam to distort less than the high pressure dam when both dams were

analysed under upstream heads varying from 100 mm to 154 mm and downstream head equal zero. Above this level of upstream head (154 mm), the low pressure dam started to distort more than the high pressure dam.

In the case of water depth inside the dam being low (100 mm) the dam behaved in a similar way to air inflated dam.

4.5.1.4 Downstream Slope.

The downstream slope (θ_2 in Fig.4.2) of the dam is the angle between the horizontal base and the slope of the last element.

The behaviour of the downstream slope of air dams is similar to the behaviour of the upstream slope of the dam under various upstream heads and internal air pressures as shown in Fig.4.20. Thus downstream slope decreases with rising upstream head and decreases when internal air pressure decreases. However, the behaviour of the variation of downstream slope with upstream head and internal pressure of water for air/water inflated dams differs from that for air inflated dams as shown in Fig.4.21 and 4.22 respectively.

A different relationship between downstream slope and upstream head for water inflated dams exists compared with that for the upstream slope (Fig.4.18). In this curve (Fig.4.21) as the upstream head increases then the downstream slope decreases without any convergence of the graphs for each water pressure. Fig.4.21 also shows that the downstream slope decreases with increasing internal water pressure, as the dam

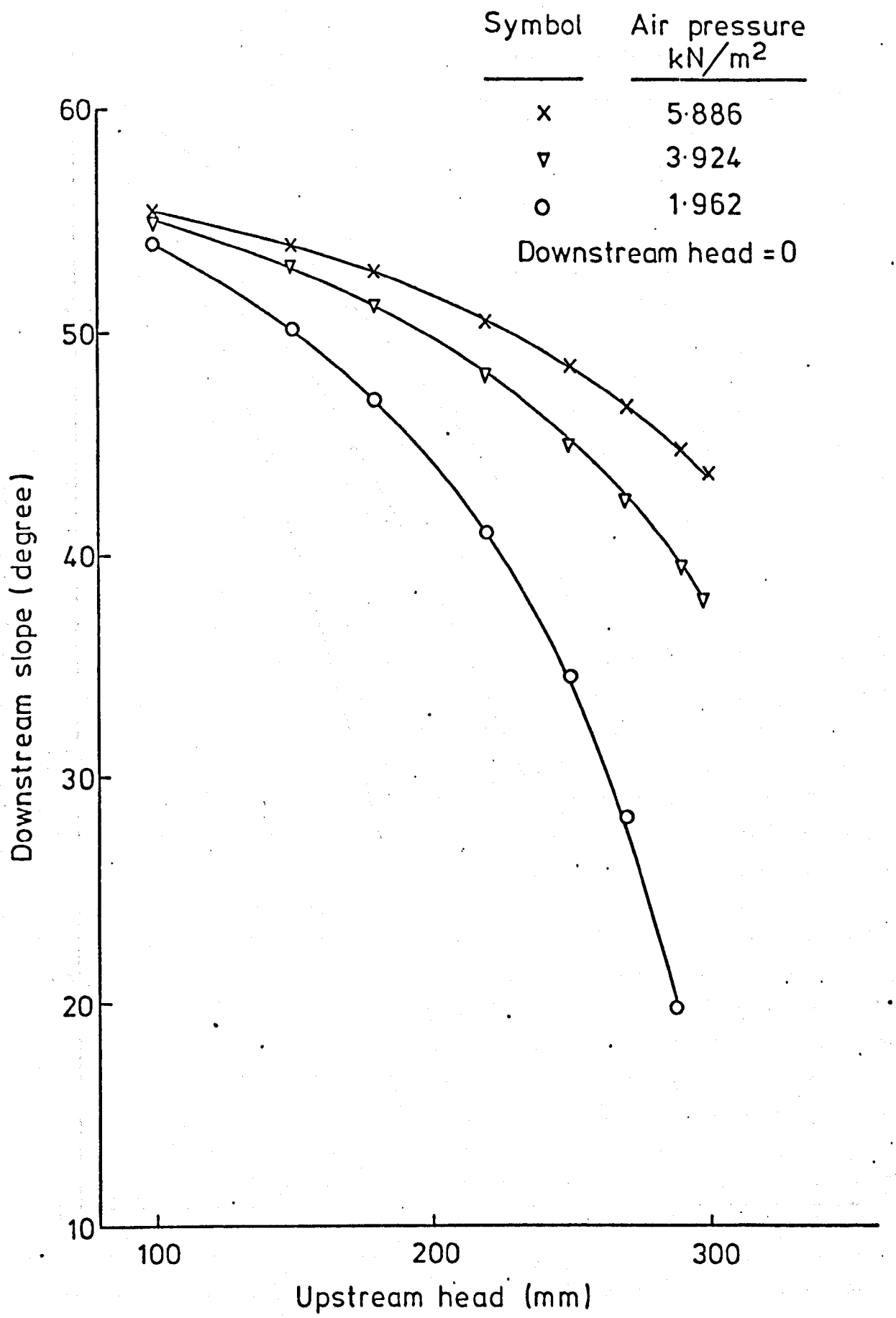

FIG. (4–20) VARIATION OF DOWNSTREAM SLOPE OF MEMBRANE WITH UPSTREAM HEAD FOR VARIOUS AIR PRESSURES

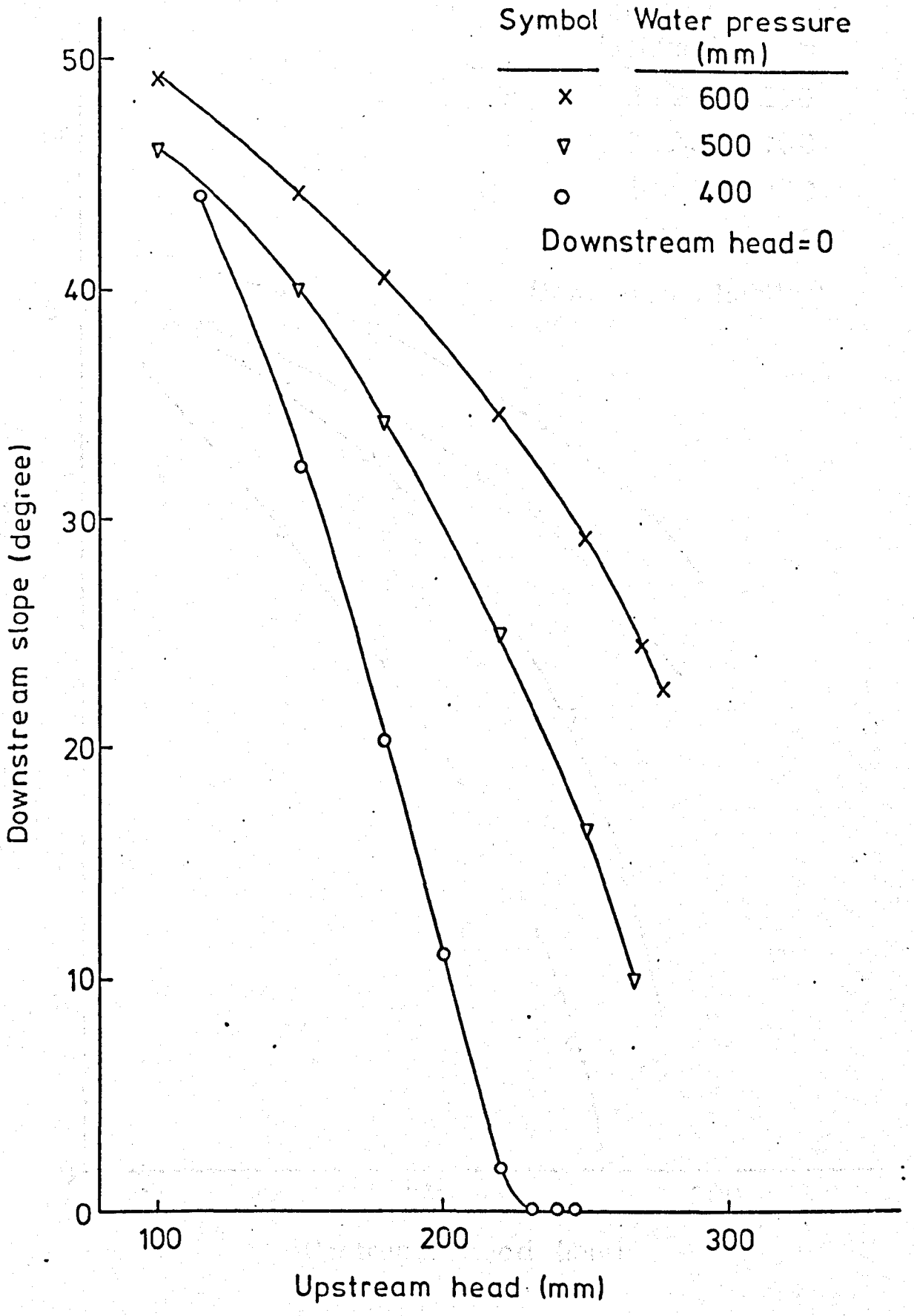

FIG. (4-21) VARIATION OF DOWNSTREAM SLOPE OF MEMBRANE WITH UPSTREAM HEAD FOR VARIOUS WATER PRESSURES

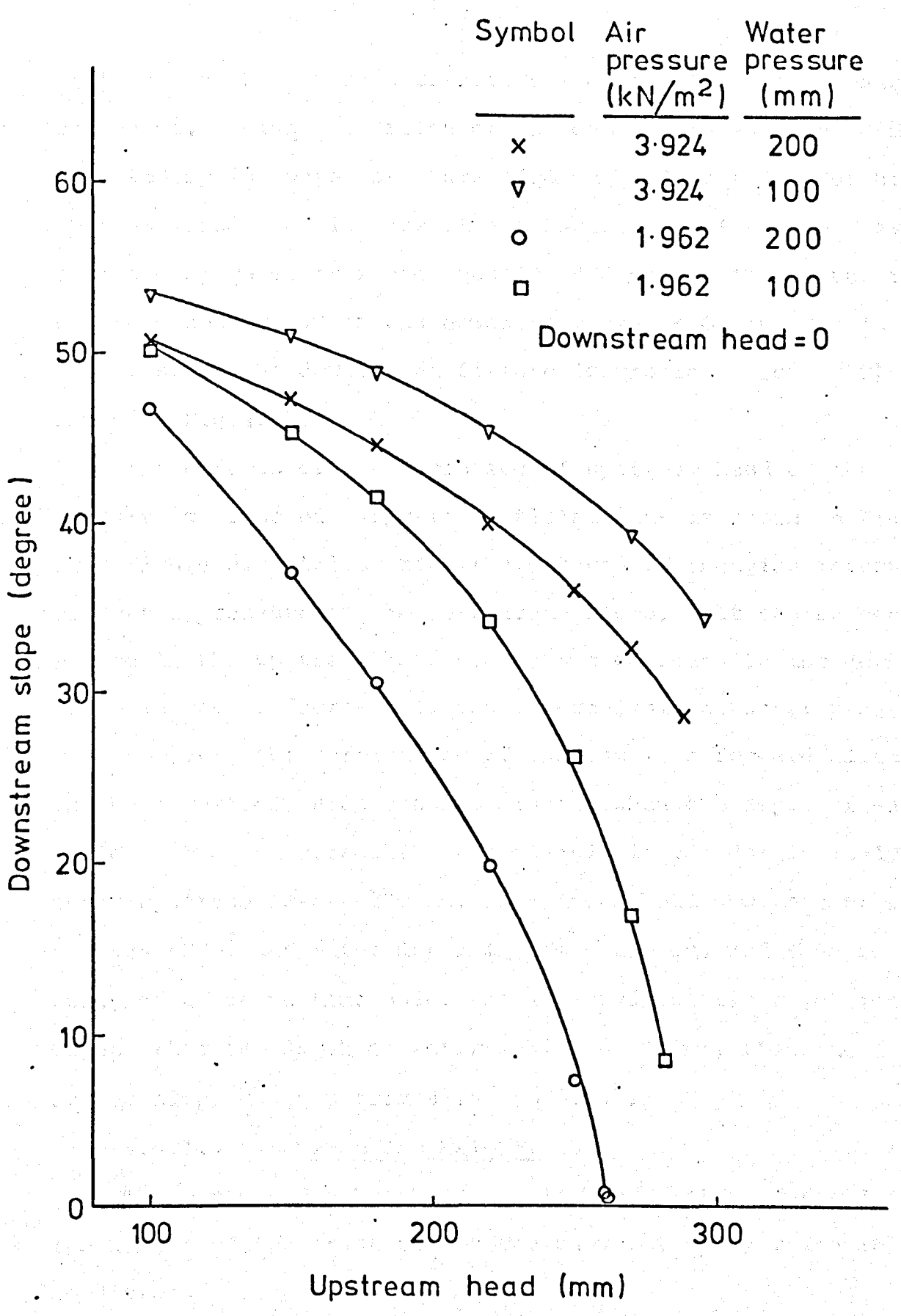

FIG. (4—22) VARIATION OF DOWNSTREAM SLOPE OF MEMBRANE WITH UPSTREAM HEAD FOR VARIOUS AIR/WATER PRESSURES

distorts in the upstream direction when the internal pressure decreases. High distortion of the dam occurs when the dam is inflated by low water pressure (400 mm) and tested under high upstream heads and low downstream heads, i.e. if the dam is inflated by water pressure equal to 400 mm and tested under upstream head = 230 mm and downstream head = 0, the dam is laid flat at the downstream fixture (downstream slope = 0) as shown in Fig.4.21.

The effects of the variation of upstream head on the downstream slope of air/water inflated dams is shown in Fig.4.22. This figure also illustrates the effects of changing internal air/water pressure on the downstream slope. It can be seen that a rise in the upstream head produces a decrease in the downstream slope as does a decrease in the internal air or water pressure.

However, the deformation of the dam in a forward direction on the downstream side becomes greater when the depth of water inside the dam increases. For example if the dam is analysed under upstream head = 200 mm, downstream head = 0, air pressure = 3.924 kN/m^2 and water depth inside = 200 mm, and then analysed a second time under the same hydrostatic conditions, except that the depth of water inside = 100 mm, then the downstream slope changes from 42.5^{o} to 47.3^{o}.

4.5.1.5 Maximum Dam Height.

The maximum dam height (Y_{max} in Fig.4.1A) is defined as the height of the crest of the dam under given hydrostatic conditions.

The rise in upstream head initially results in an increase in the maximum height of the air dam as shown in Fig.4.23.

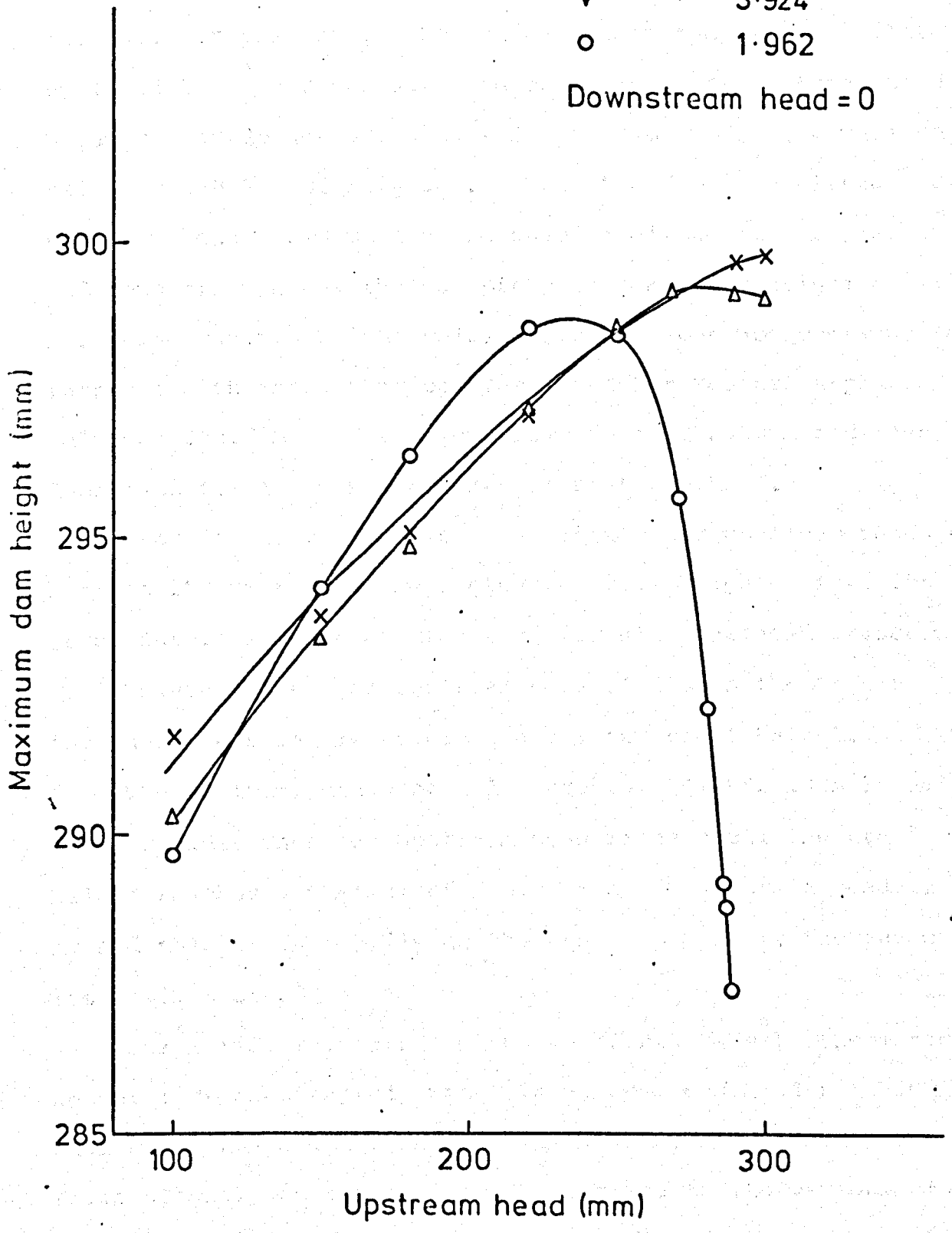

FIG.(4-23) VARIATION OF MAXIMUM DAM HEIGHT WITH UPSTREAM HEAD FOR VARIOUS AIR PRESSURES

However, the increase in maximum height may or may not continue with increasing upstream head this depending on the internal air pressure. For example when the dam is inflated by 1.962 kN/m^2 air pressure and analysed under upstream head = 250 mm and downstream head = 0, the dam produces a maximum height = 298.5 mm (Fig.4.23). When the dam is analysed under upstream head = 270 mm and the same magnitude of air pressure and downstream head, the dam produces a maximum height = 295.8 mm. The maximum height value therefore does not continue to increase with increasing upstream head but reaches a peak value of 298.7 mm under an upstream head of 230 mm and then decreases for further increases in upstream head.

From Fig.4.22 it can be seen that under upstream heads of between 150 mm and 250 mm a greater crest height exists for lower internal air pressures than for high inflated pressures.

However, above an upstream head of 250 mm the higher internal pressure always gives a greater crest height.

The maximum height of a low pressure (1.962 kN/m^2) dam rises rapidly when the upstream head rises until the crest height reaches a maximum of 298.8 mm at an upstream head of 230 mm and then falls rapidly as the upstream head is increased to its maximum of 288 mm.

For a medium internal pressure (2.924 kN/m^2), the maximum height increases rapidly with rising upstream head reaching a maximum of 299.3 mm under an upstream head of 280 mm and then falls slightly as the upstream head rises to its maximum of 299.1 mm.

For a high pressure (5.886 kN/m^2), the maximum height increases to a maximum value of 299.8 mm, this crest height occurring at an upstream head of 300.0 mm.

This means that the higher the internal pressure the higher the ultimate crest height that can be achieved and maintained for higher upstream heads reflecting the greater ability to resist deformation at higher internal pressure.

In the case of a dam inflated by water, a similar type of relationship is found between crest height and upstream head for different internal pressure and these are illustrated in Fig.4.24.

The one major difference for water inflation from air inflation is that the maximum crest height achieved always increases with increasing internal water pressure and a low internal water pressure can never achieve a crest height greater than a higher internal water pressure for the same upstream head.

In every case as upstream head increases the crest height increases until it reaches a maximum and then decreases for a continued increase in upstream head. This effect becomes less, the higher the internal pressure.

The variation of maximum height with changing upstream head and internal pressure of the air/water dam is illustrated in Fig.4.25. Again the maximum height increases rapidly with a rising upstream head in all cases reaching a peak and then falls as the upstream head rises further.

However, for a given air pressure an increase in the water pressure results in a decrease in the crest height for the same

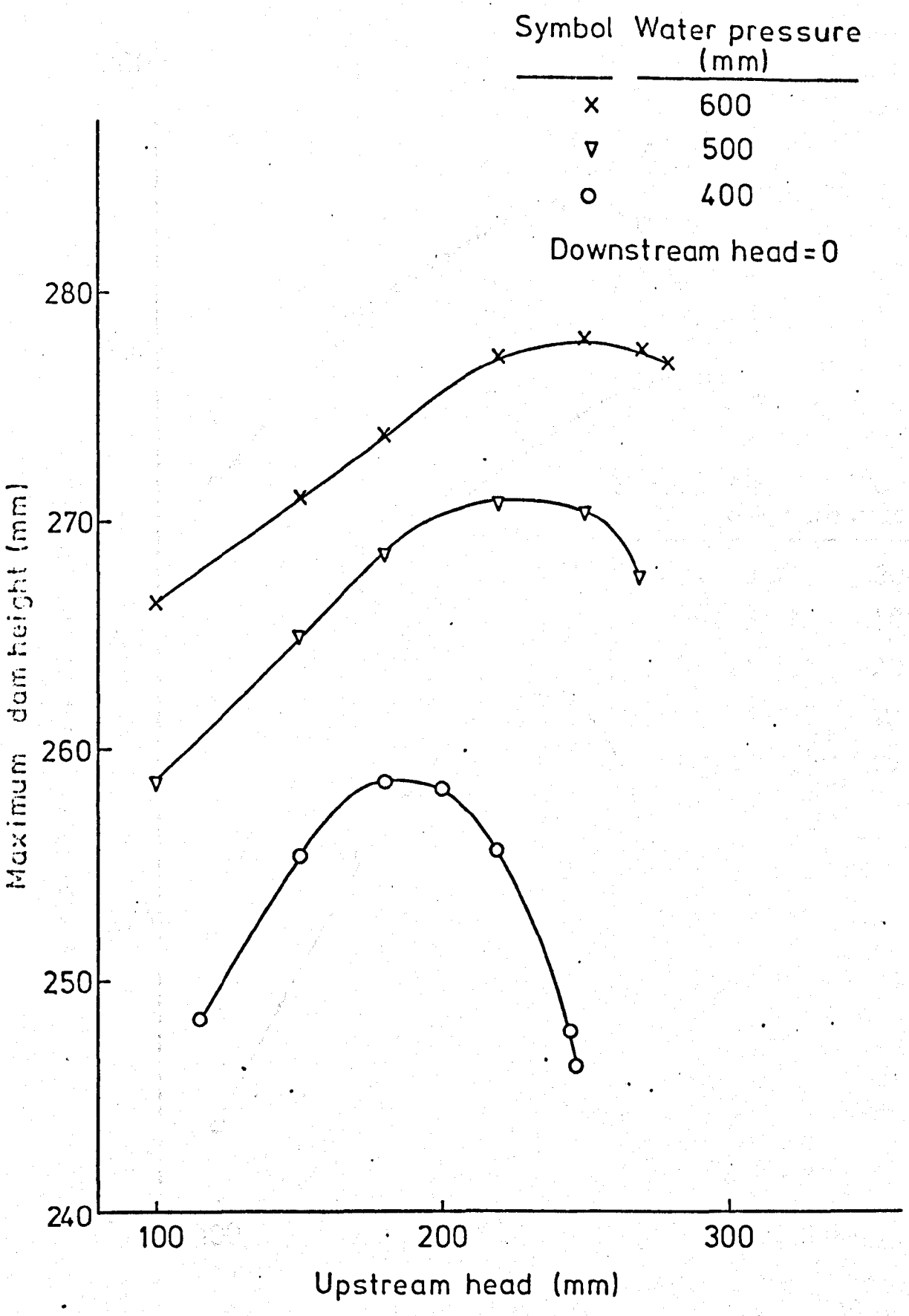

FIG.(4–24) VARIATION OF MAXIMUM DAM HEIGHT WITH UPSTREAM HEAD FOR VARIOUS WATER PRESSURES

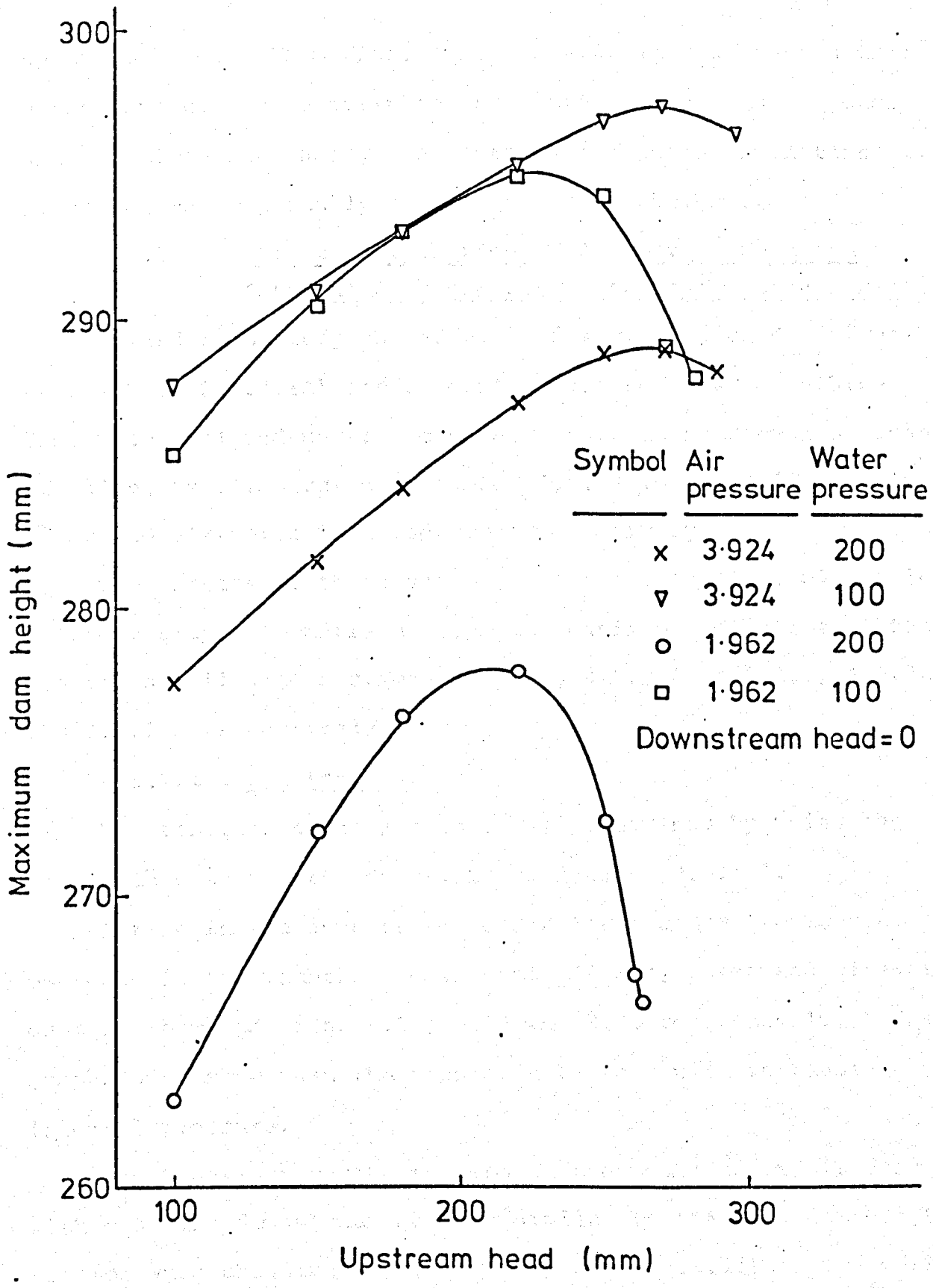

FIG. (4-25) VARIATION OF MAXIMUM DAM HEIGHT WITH UPSTREAM HEAD FOR VARIOUS AIR/WATER PRESSURES

upstream head. From Figs. 4.23 and 4.24 it can be seen that water dams cannot maintain the same crest height as air dams and therefore increasing the contribution to the inflation by adding water actually reduces the crest height.

4.5.2 Effect of Variation of Downstream Head and Internal Pressure for a Constant Upstream Head.

In order to study the effects of variation of downstream head (DH in Fig.4.1A) and internal pressure on a dam, three dams were analysed under a constant upstream head over a range of values as illustrated in tables 4.8, 4.10 and 4.12 for air, water and air/water inflated dams respectively.

The effects of these variations on the tension, elongation, upstream slope, downstream slope and maximum dam height of the dam are detailed in sections 4.5.2.1, 4.5.2.2, 4.5.2.3, 4.5.2.4, and 4.5.2.5 respectively.

4.5.2.1 Tension.

The tension in the membrane was determined by using the same method as before, described in section 4.5.1.1.

A rise in the downstream head below the dam produces a decrease in the membrane tension of all air, water and air/water dams as shown in Figs. 4.26, 4.27 and 4.28 respectively. These graphs also show that the tension decreases with increasing internal pressure.

The behaviour of the tension in the membrane of air dams with changing downstream head is similar to the behaviour of the tension when changing the upstream head (Fig.4.11). Therefore the tension in the membrane decreases whether the upstream head or downstream head increases. This applies even if both change

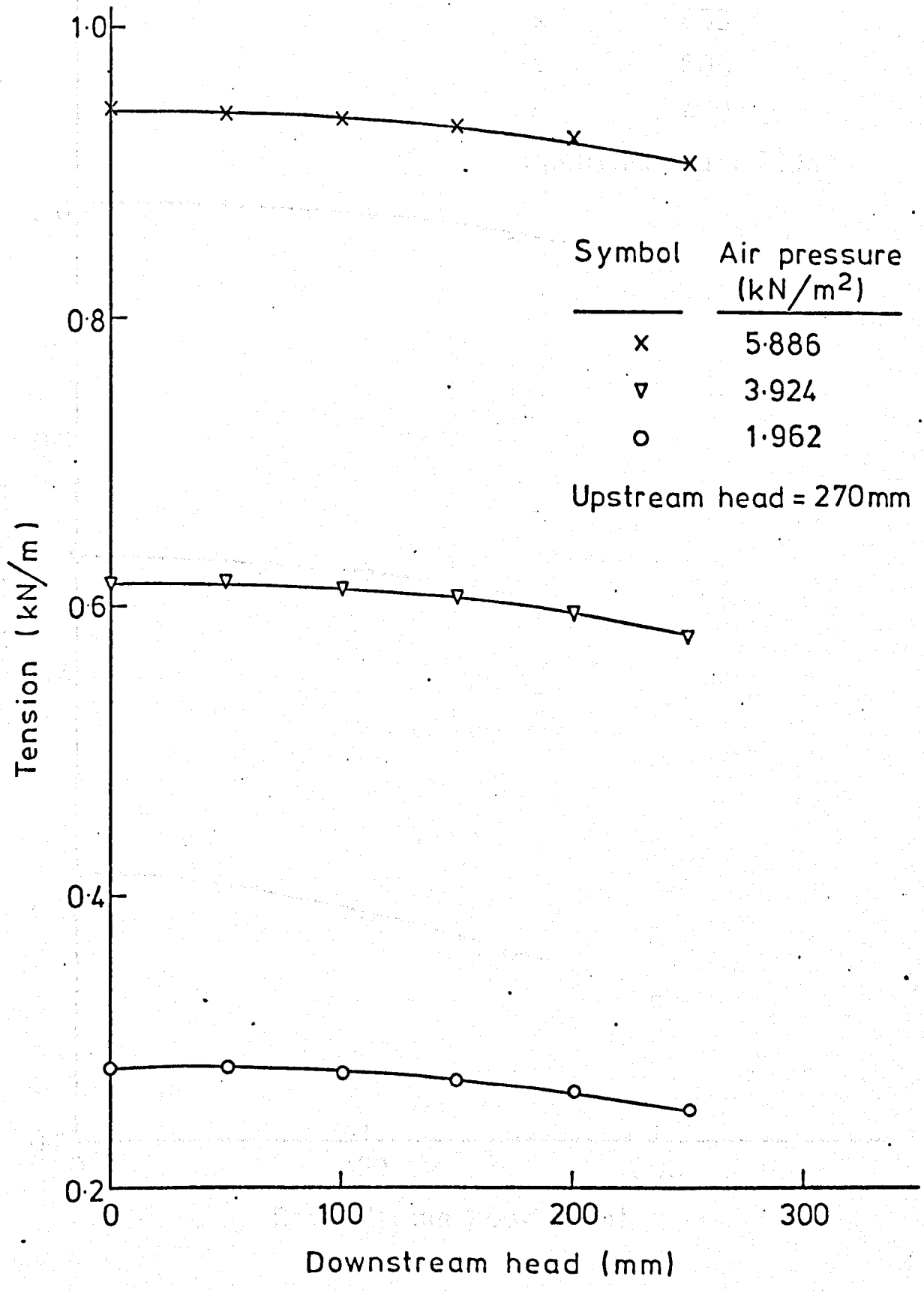

FIG. (4—26) VARIATION OF TENSION IN MEMBRANE WITH DOWNSTREAM HEAD FOR VARIOUS AIR PRESSURES

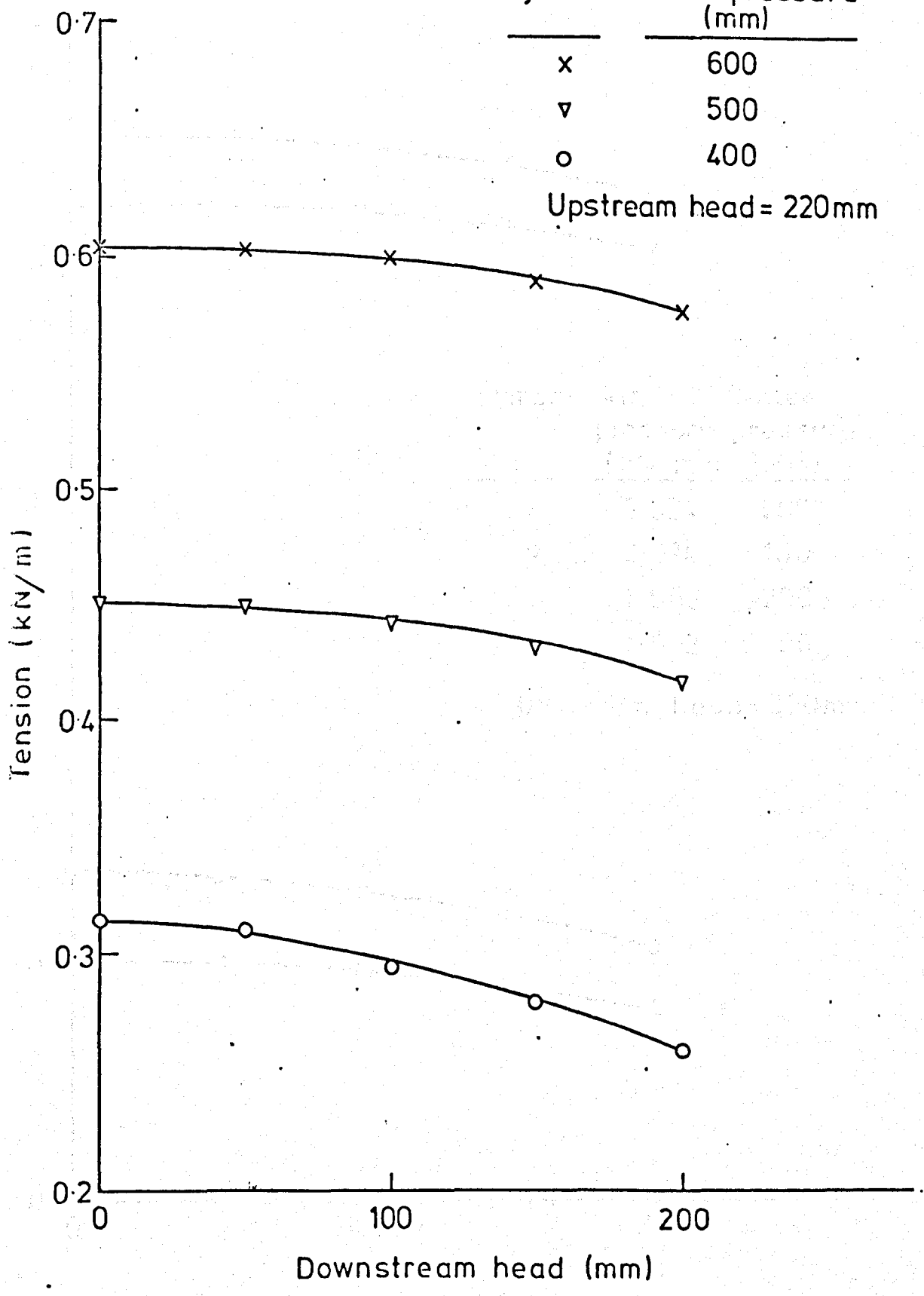

FIG. (4–27) VARIATION OF TENSION IN MEMBRANE WITH DOWNSTREAM HEAD FOR VARIOUS WATER PRESSURES

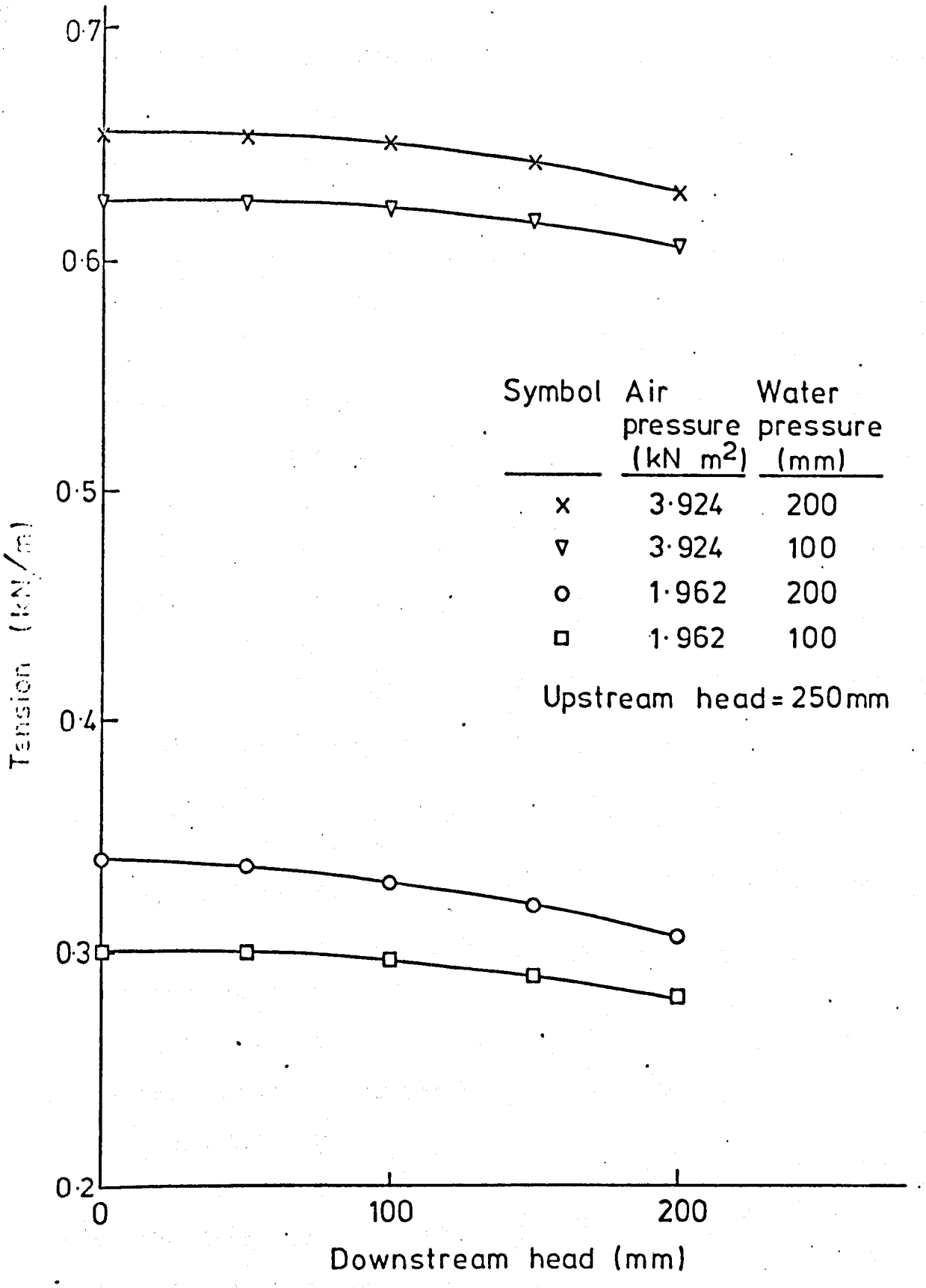

FIG. (4-28) VARIATION OF TENSION IN MEMBRANE WITH DOWNSTREAM HEAD FOR VARIOUS AIR/WATER PRESSURES

simultaneously. However, this similarity of change in tension under changing upstream head and downstream head does not occur if the dam is inflated by water (Figs. 4.12 and 4.27).

Fig.4.27 shows that the tension under an inflation to low pressures drops rapidly with rising downstream head, whereas when the upstream head rises, there is a decrease in tension which is much lower. If both heads increase simultaneously there will still be a reduction in the tension.

In the case of an air/water inflated dam, the tension decreases with rising downstream head and also decreases with decreasing internal pressure (Fig.4.28). It can be seen from Fig.4.13 that the tension decreases with rising upstream head, therefore the tension will decrease when both upstream and downstream head increase simultaneously.

4.5.2.2 Elongation.

The effects of the variation of downstream head on the elongation of air, water and air/water dams are shown in Figs. 4.29, 4.30 and 4.31 respectively. The elongation of the membrane behaves similarly to the behaviour of tension under varying upstream head and internal pressures, in that the elongation decreases with increasing downstream head and also decreases with lower internal pressures.

4.5.2.3 Upstream Slope.

A rise in the downstream head causes the dam to distort in the direction of the upstream side. This distortion produces an increase in upstream slope for all types of air, water and air/water dams as shown in Fig.4.32, 4.33 and 4.34

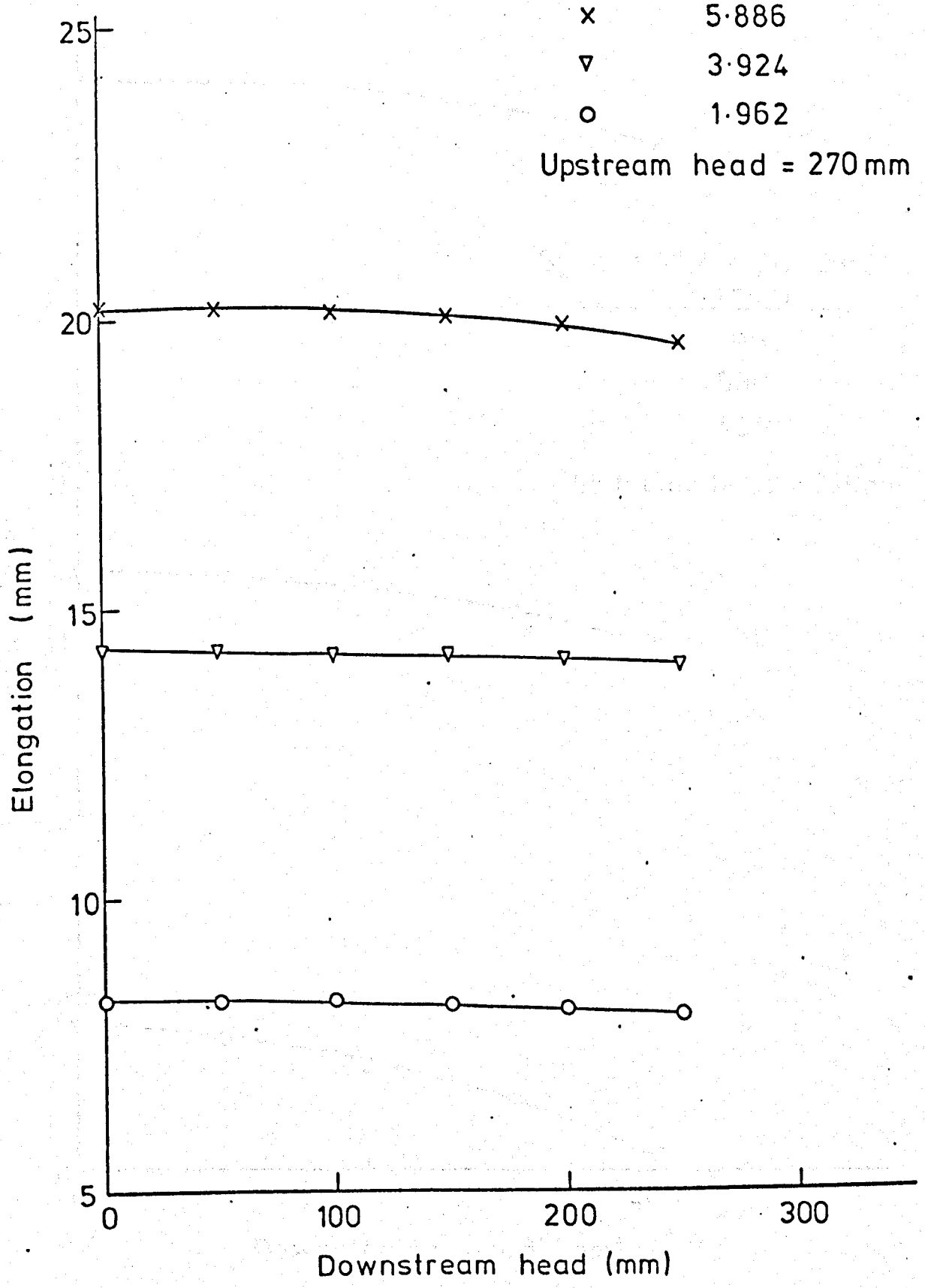

FIG. (4-29) VARIATION OF ELONGATION IN MEMBRANE WITH DOWNSTREAM HEAD FOR VARIOUS AIR PRESSURES

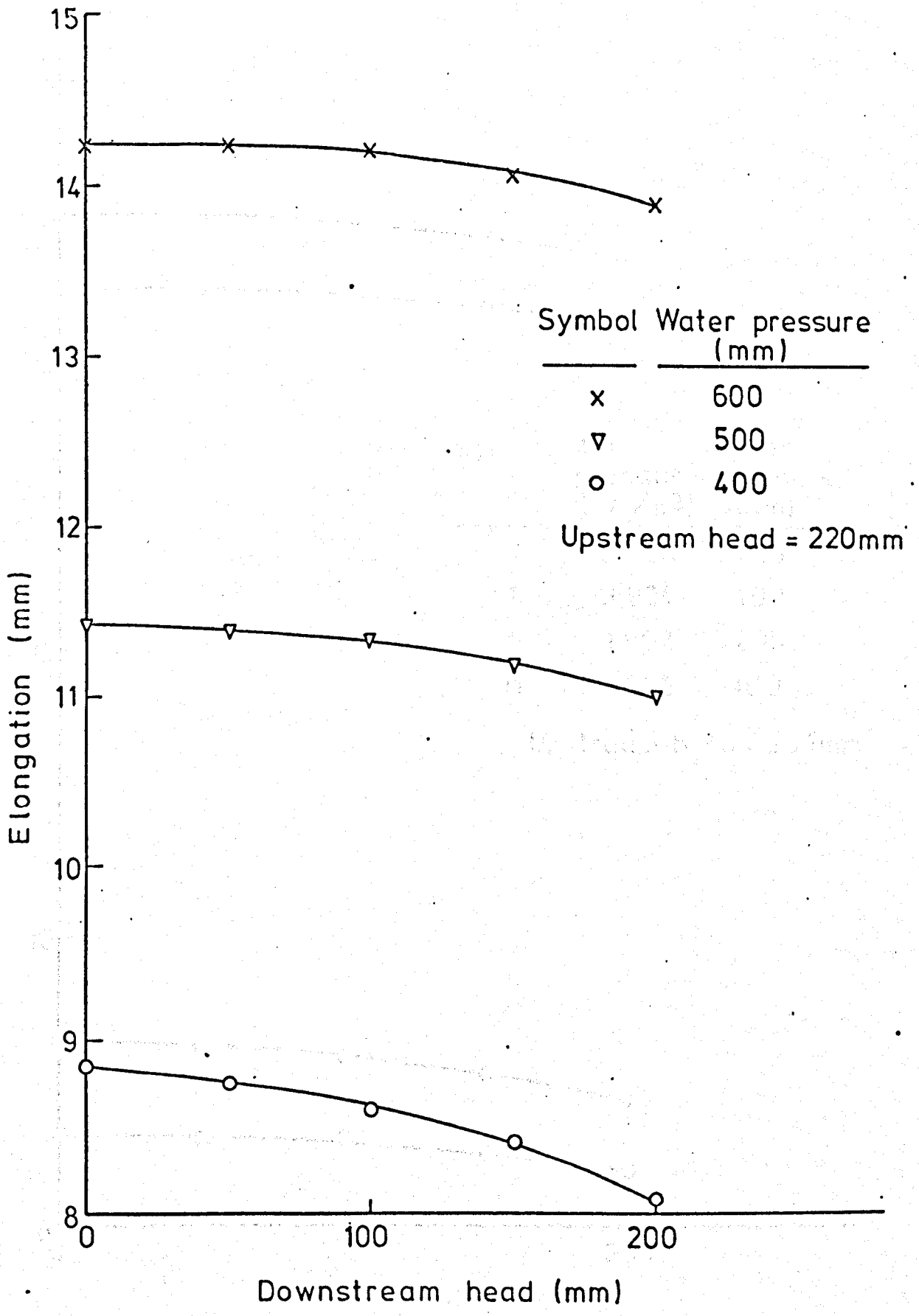

FIG. (4-30) VARIATION OF ELONGATION IN MEMBRANE WITH DOWNSTREAM HEAD FOR VARIOUS WATER PRESSURES

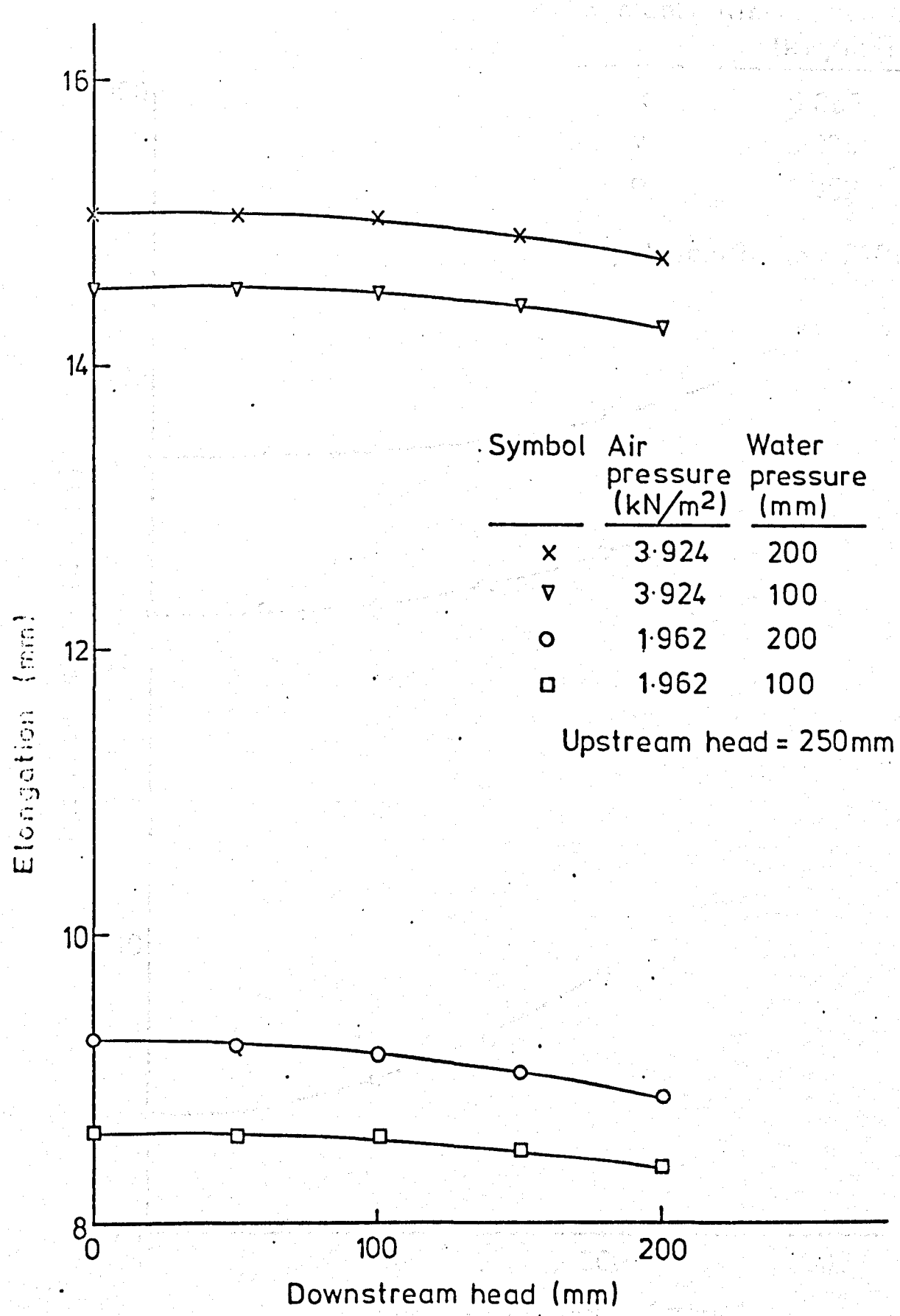

FIG. (4-31) VARIATION OF ELONGATION IN MEMBRANE WITH DOWNSTREAM HEAD FOR VARIOUS AIR/WATER PRESSURES

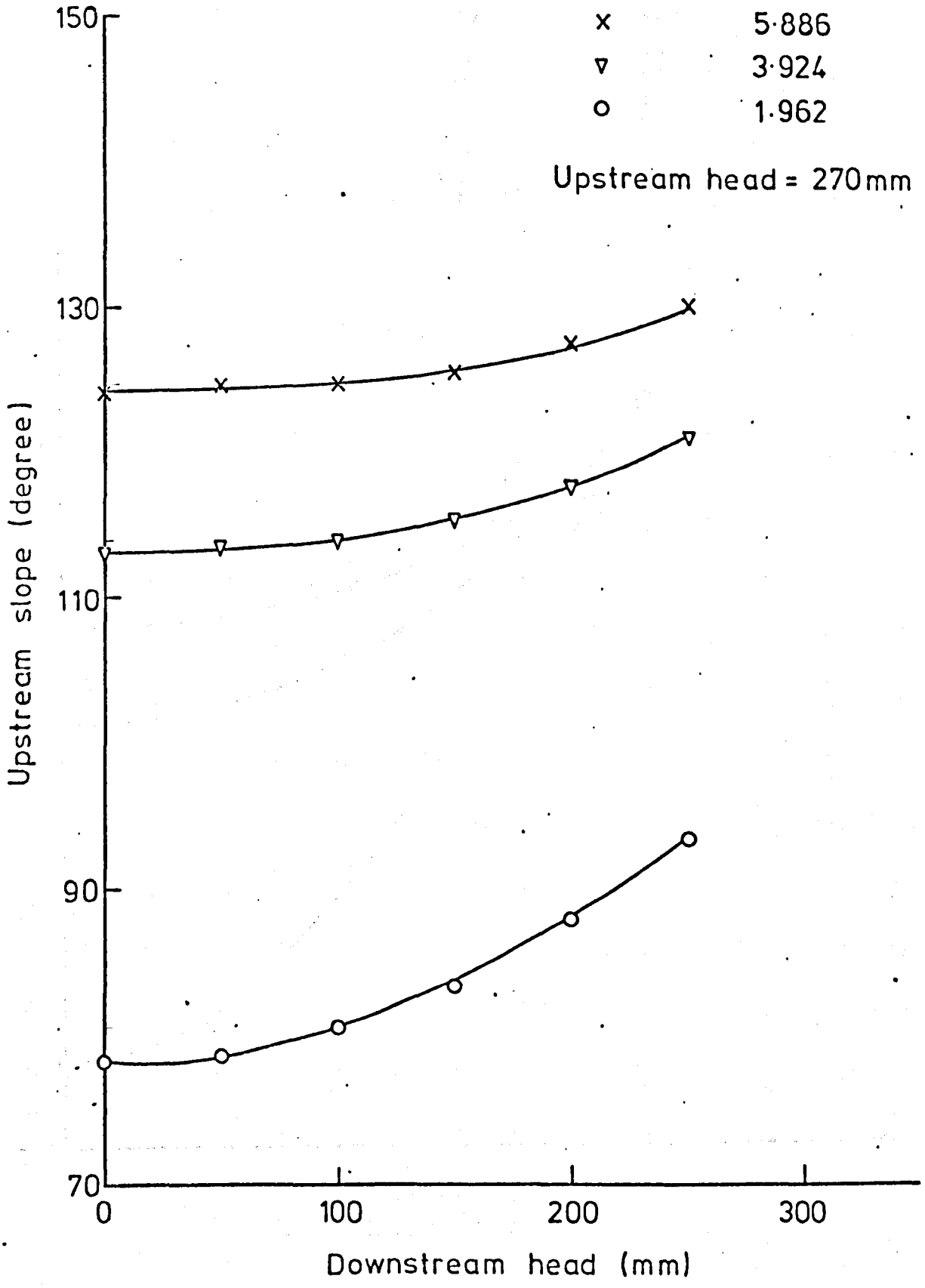

FIG. (4-32) VARIATION OF UPSTREAM SLOPE OF MEMBRANE WITH DOWNSTREAM HEAD FOR VARIOUS AIR PRESSURES

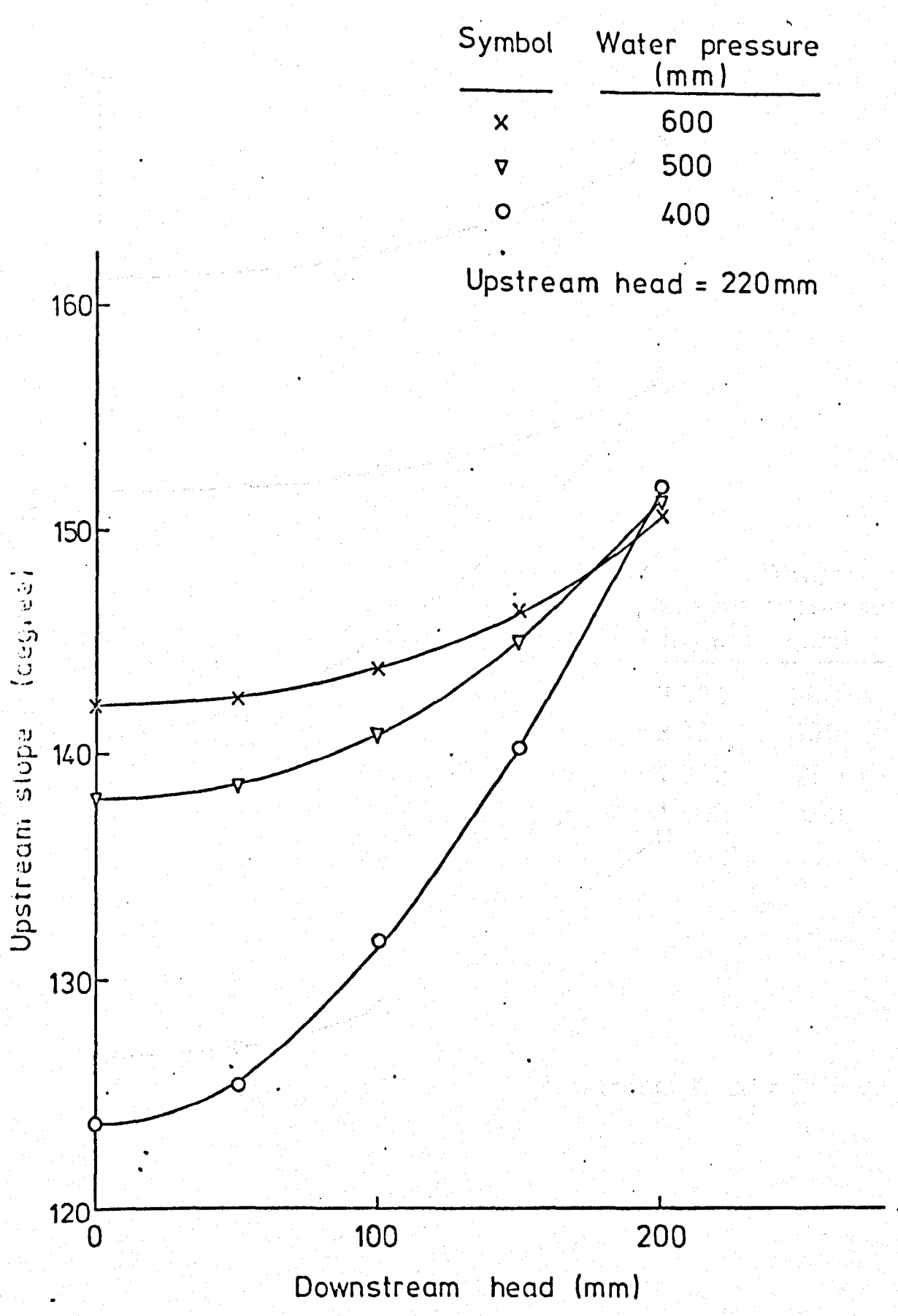

FIG. (4—33) VARIATION OF UPSTREAM SLOPE OF MEMBRANE WITH DOWNSTREAM HEAD FOR VARIOUS WATER PRESSURES

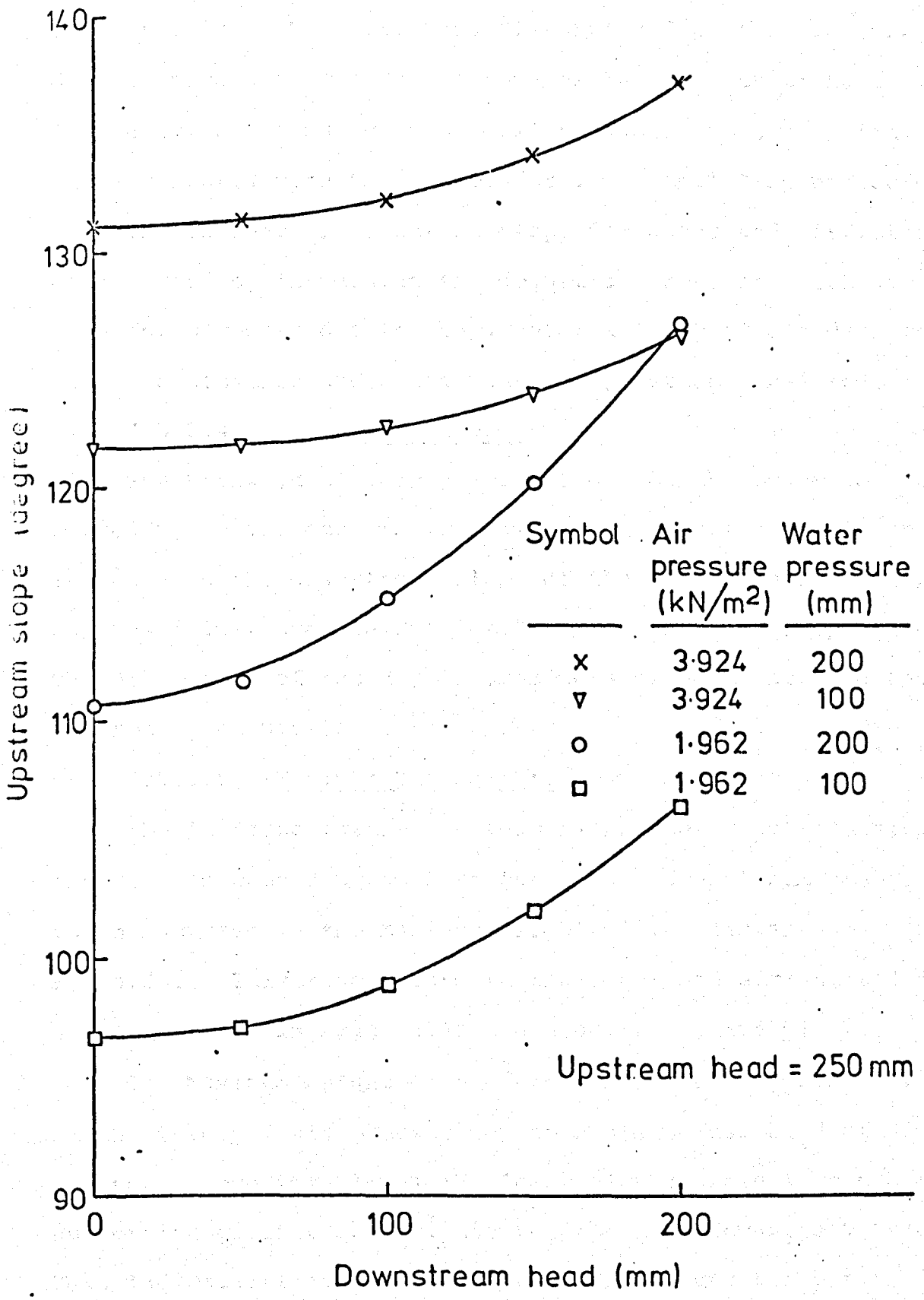

FIG. (4-34) VARIATION OF UPSTREAM SLOPE OF MEMBRANE WITH DOWNSTREAM HEAD FOR VARIOUS AIR/WATER PRESSURES

respectively. However, this distortion for high pressure dams is more difficult to achieve as the downstream head increases resulting in much smaller changes in the upstream slope compared with the effect for lower inflation pressures.

The increase in upstream slope for water and air/water dams caused by increasing the downstream head are much greater than for air dams due to the greater ability of air dams to resist distortion under the range of pressures analysed.

4.5.2.4 Downstream Slope.

The backward distortion of the dam on the upstream side caused by an increase in the downstream head results in an increase in the downstream slope of the air, water and air/water dams as illustrated in Figs. 4.35, 4.36 and 4.37 respectively. The distortion of the dam becomes more significant when the internal pressure is decreased.

4.5.2.5 Maximum Dam Height.

The increase in the upstream slope and downstream slope of the air dam caused by an increase in the downstream head results in an increase in the maximum height of the dam as shown in Fig.4.38. This also occurs in the water and air/water dams as illustrated in Figs. 4.39 and 4.40 respectively.

The maximum height of the air dam increases with an increase in the internal air pressure up to a downstream head of 95 mm. However, above this level the lower air pressure is capable of supporting greater dam heights for the same downstream head. This indicates that a low air pressure dam under a particular downstream head could support an upstream head higher than the same dam under a higher pressure as shown in Fig. 4.41. For

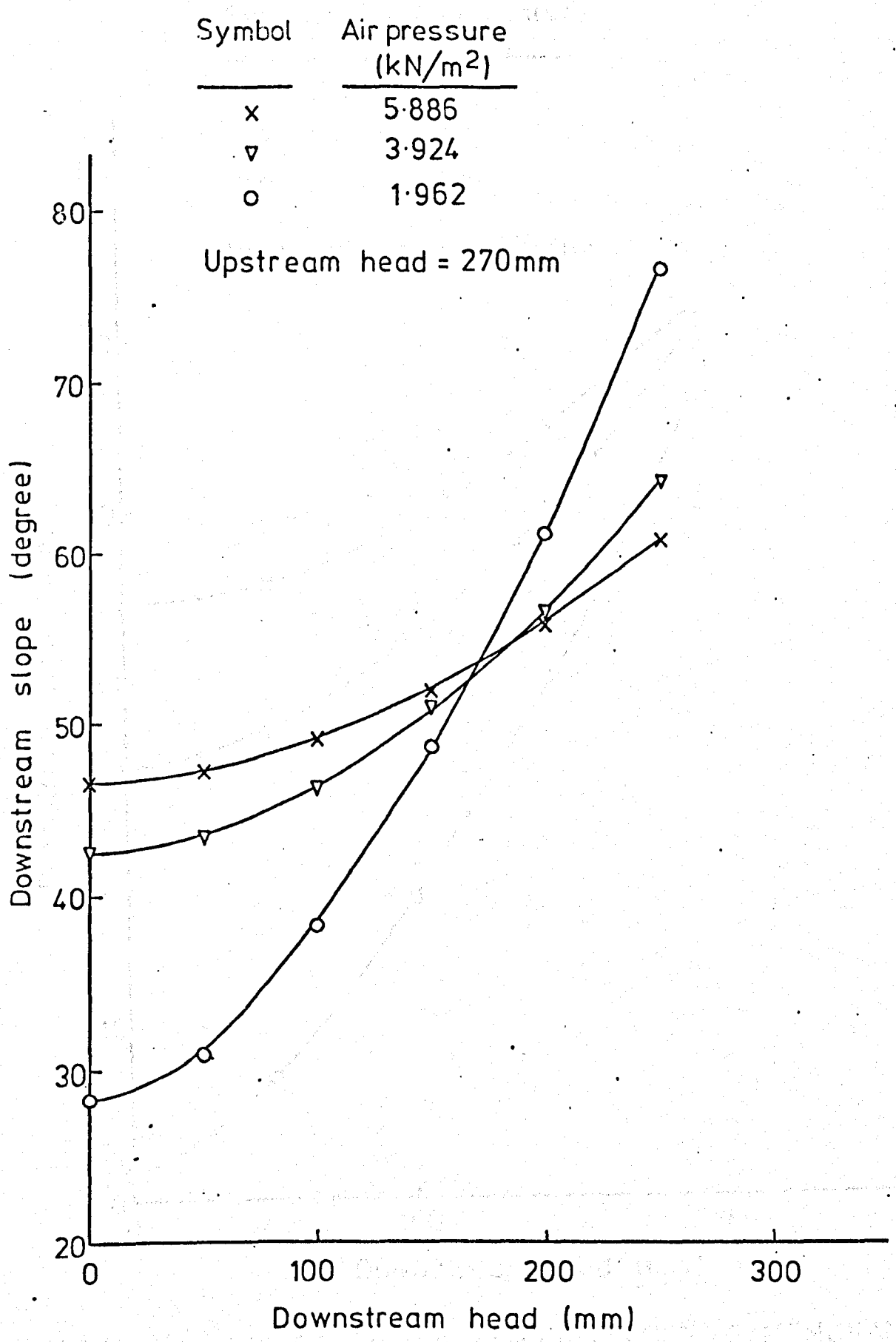

FIG. (4–35) VARIATION OF DOWNSTREAM SLOPE OF MEMBRANE WITH DOWNSTREAM HEAD FOR VARIOUS AIR PRESSURES

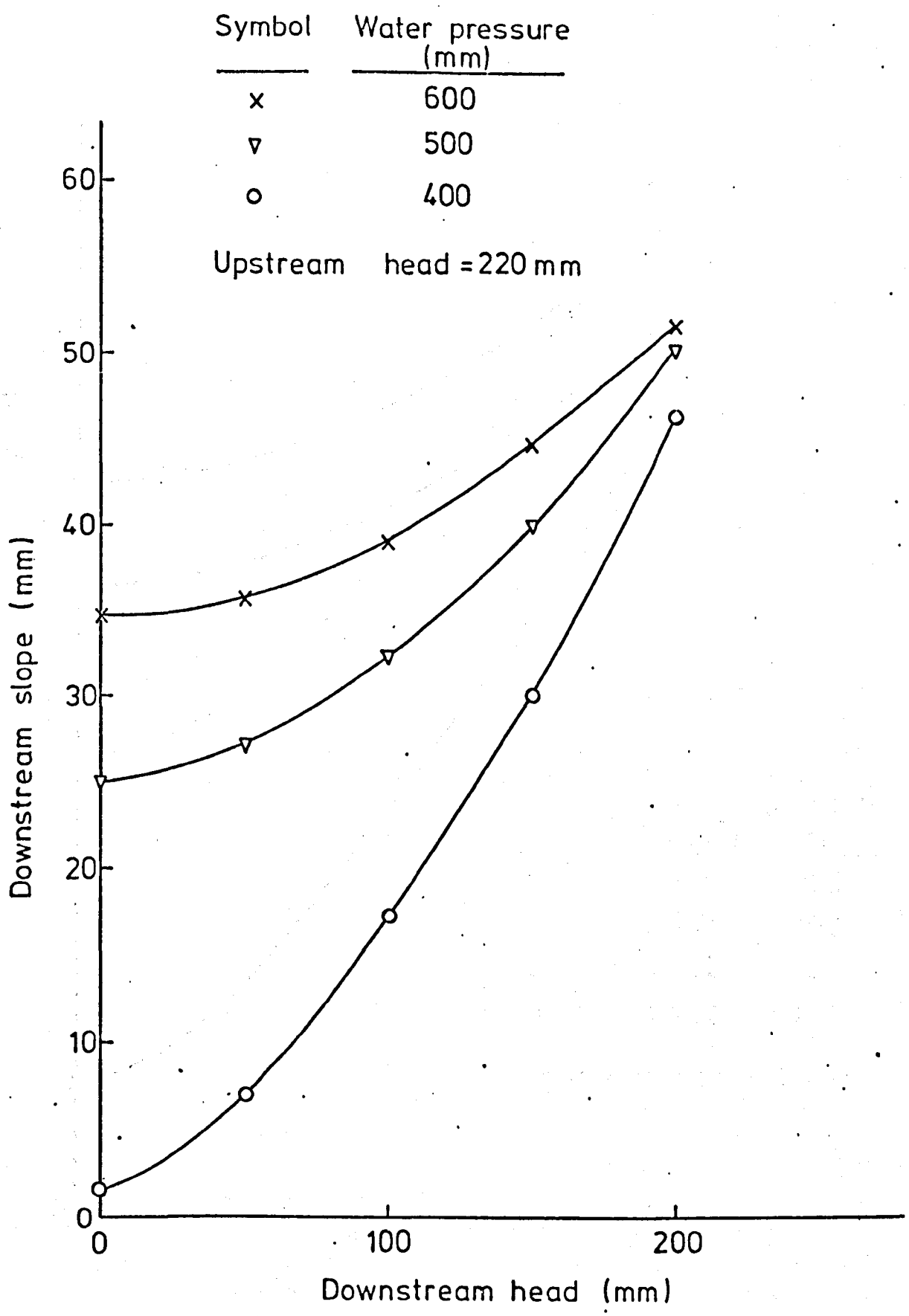

FIG. (4-36) VARIATION OF DOWNSTREAM SLOPE OF MEMBRANE WITH DOWNSTREAM HEAD FOR VARIOUS WATER PRESSURES

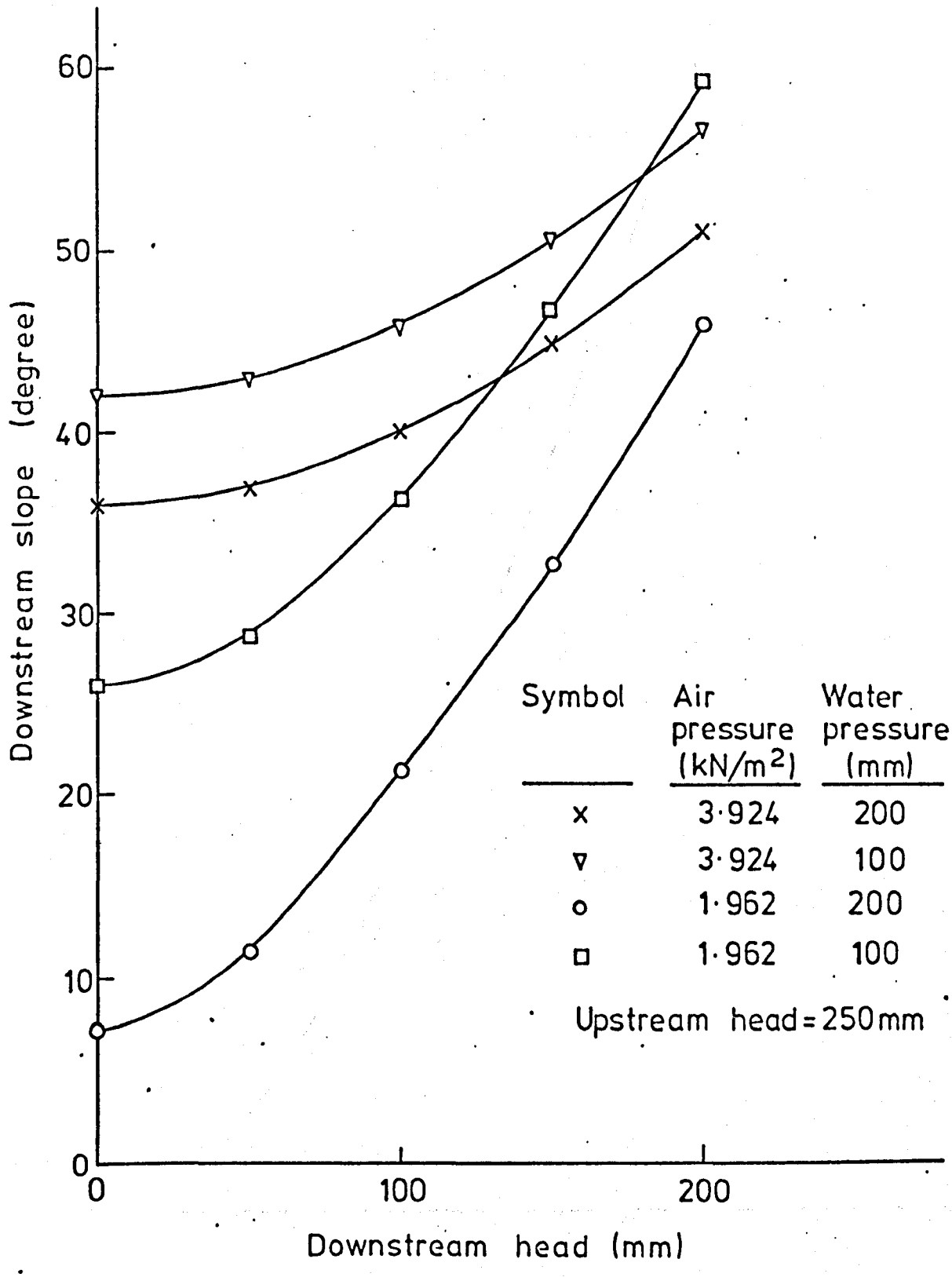

FIG. (4–37) VARIATION OF DOWNSTREAM SLOPE OF MEMBRANE WITH UPSTREAM HEAD FOR VARIOUS AIR/WATER PRESSURES

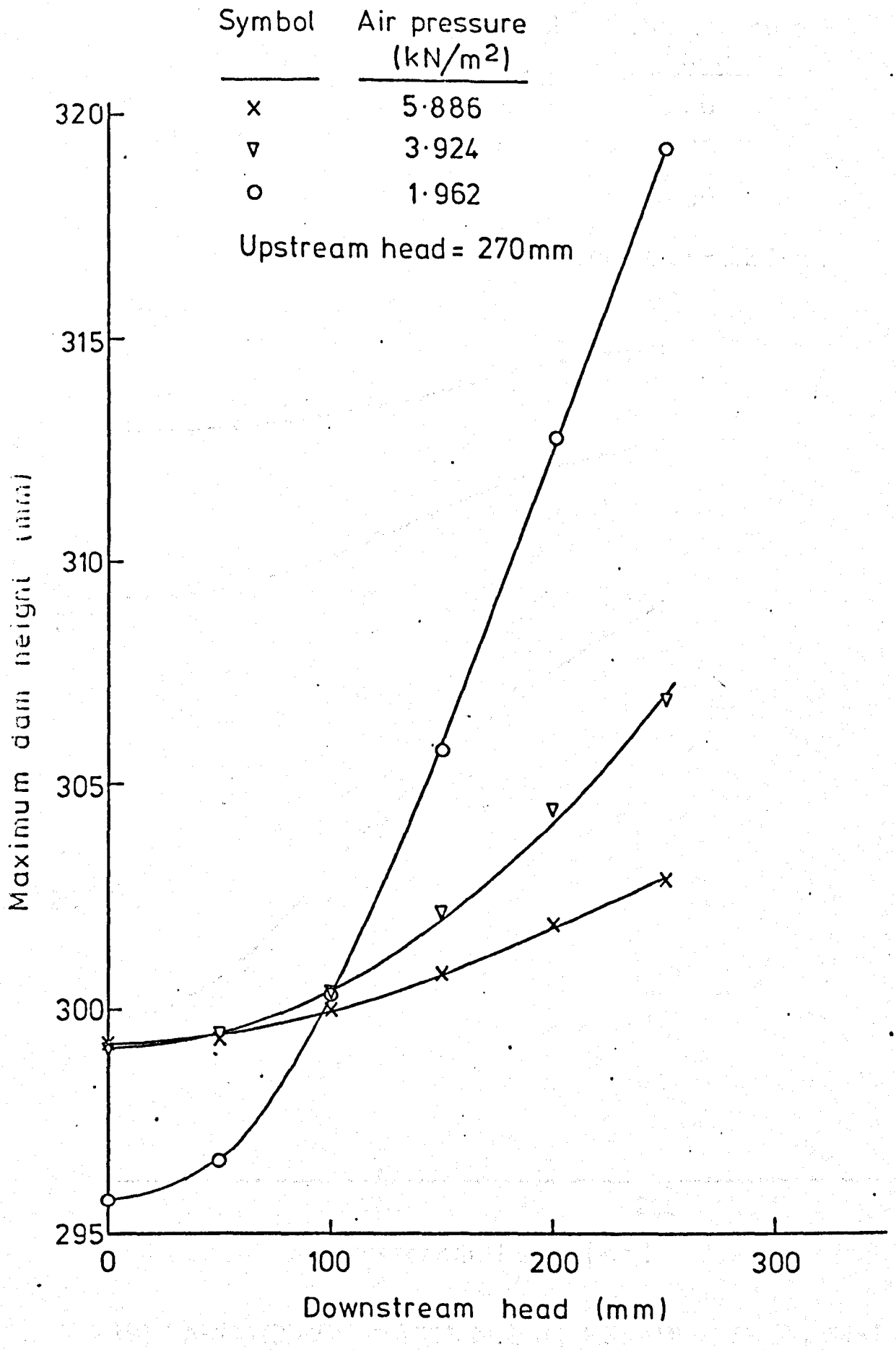

FIG. (4–38) VARIATION OF MAXIMUM DAM HEIGHT WITH DOWNSTREAM HEAD FOR VARIOUS AIR PRESSURES

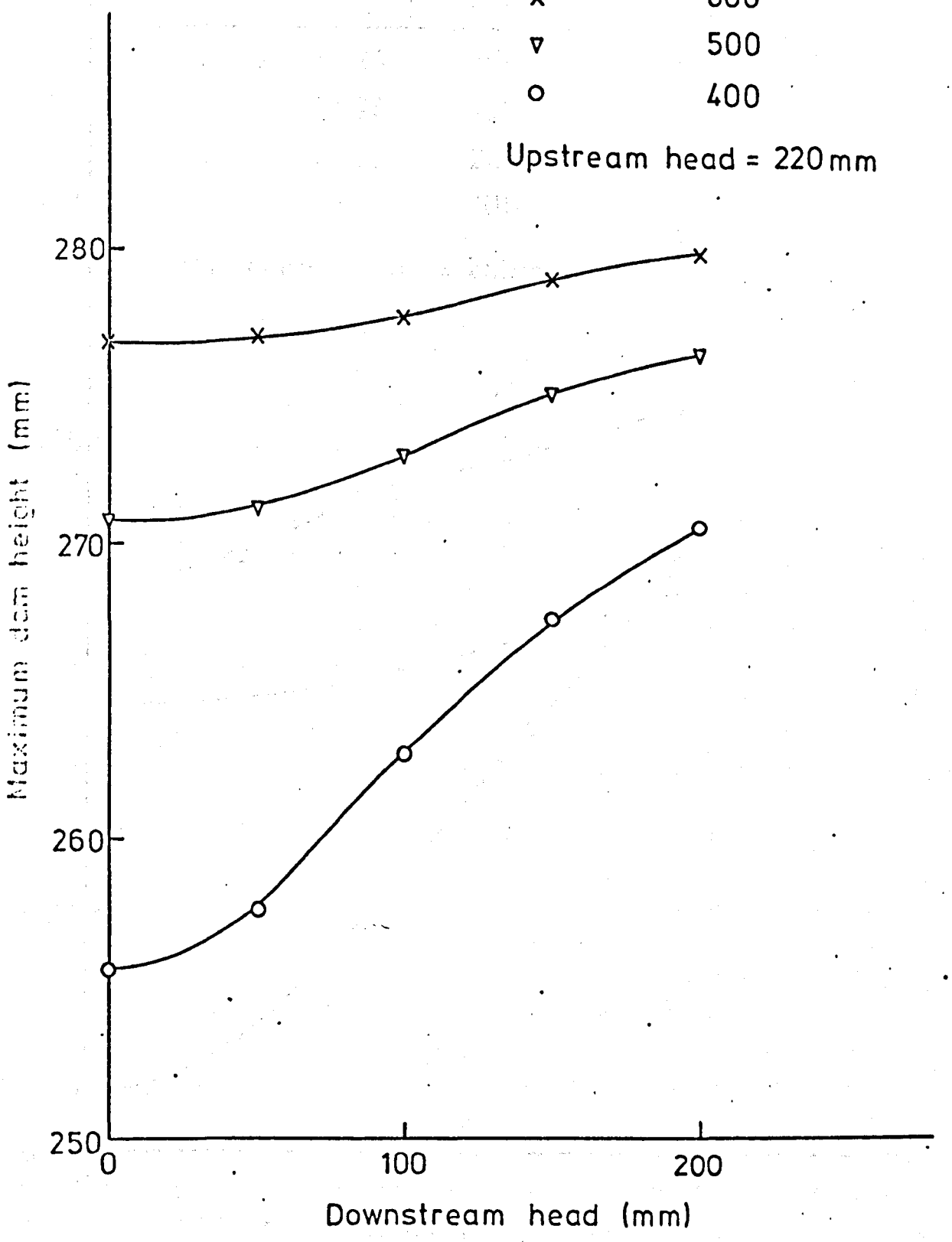

FIG. (4-39) VARIATION OF MAXIMUM DAM HEIGHT WITH DOWNSTREAM HEAD FOR VARIOUS WATER PRESSURES

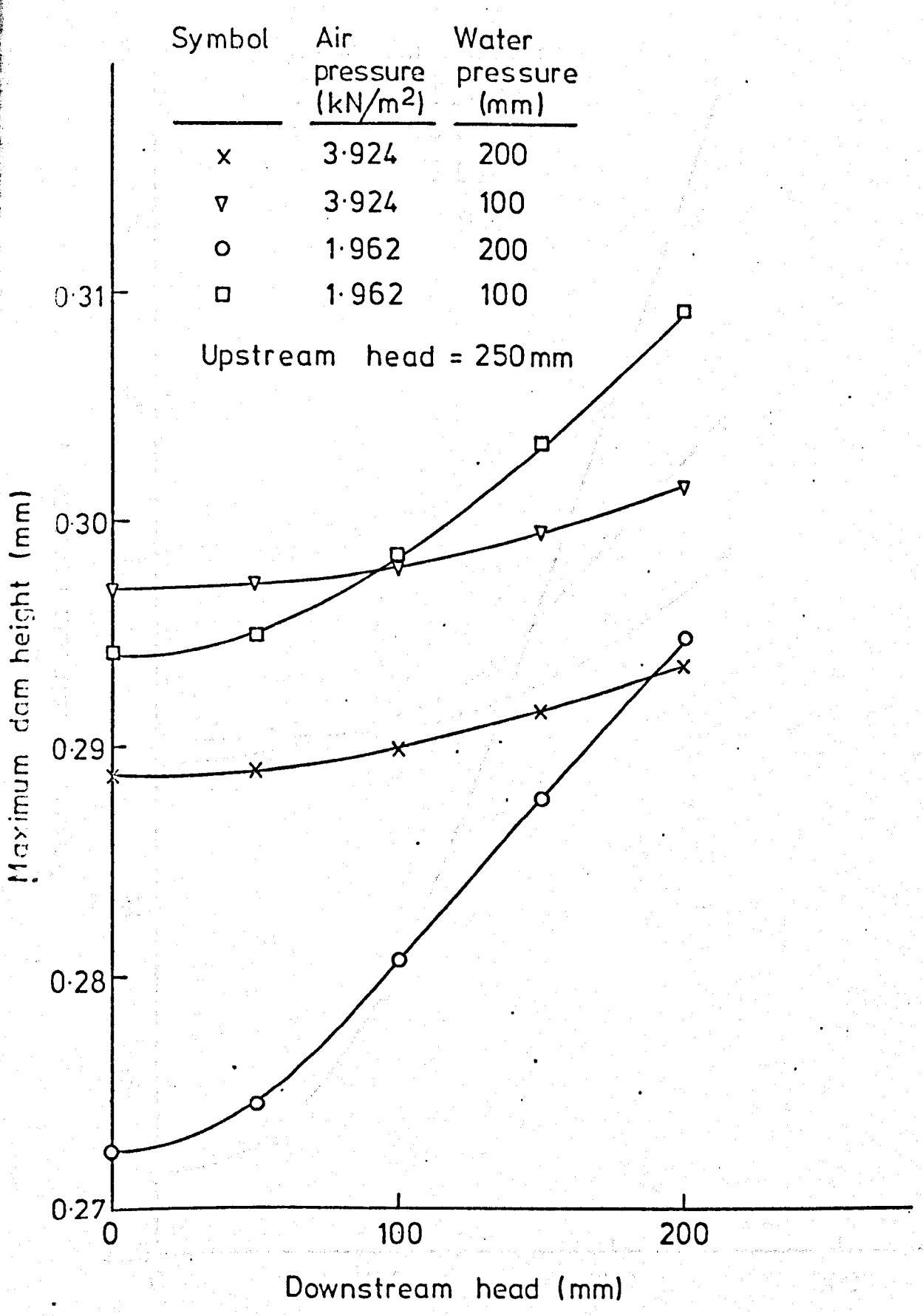

FIG. (4-40) VARIATION OF MAXIMUM DAM HEIGHT WITH DOWNSTREAM HEAD FOR VARIOUS AIR/WATER PRESSURES

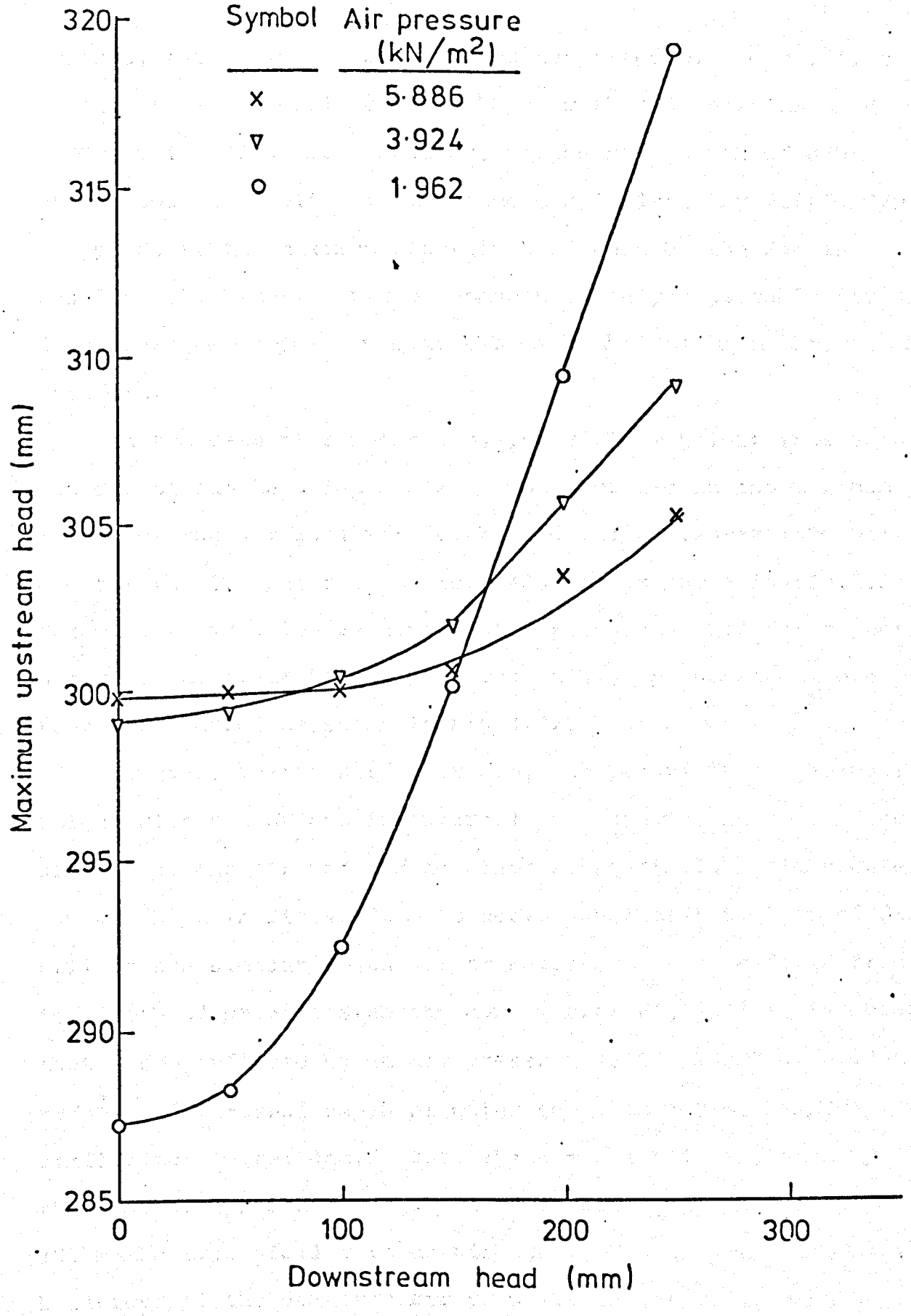

FIG (4-41) VARIATION OF MAXIMUM UPSTREAM HEAD WITH DOWNSTREAM HEAD FOR VARIOUS AIR PRESSURES

example, the maximum upstream head supported by a dam inflated by air pressure equal to 1.962 kN/m^2 with a downstream head = 200 mm is 309.5 mm. However, if the same depth of downstream head is applied to the same dam inflated by 5.886 kN/m^2 air pressure the maximum upstream head held by the dam is equal to 303.0 mm. This phenomenon is only applicable for downstream heads greater than 150 mm to 170 mm depending on air pressure.

In the case of a water dam, the maximum height increases as the downstream head increases. The increase in the maximum height of the dam is lower for high water pressures (600 mm) and greater for low water pressures (400 mm) as shown in Fig.4.39. For water dams a low internal water pressure could not support a maximum upstream head higher than a high pressure dam over the range considered as shown in Fig.4.42.

However, in the air/water dam, the behaviour of the maximum height with variations in internal pressure was in some cases similar to the air dam and in other cases similar to the water dam as shown in Fig.4.40. To decide whether this type of dam will behave similar to an air or water dam, can be found from the depth of water inside the dam. From Fig.4.43 it is noted that a dam inflated by an air pressure (1.962 kN/m^2 or 3.924 kN/m^2) and internal depth of water equal to 200 mm behaves similar to a water dam. But, the dam which is inflated by the same air pressure and depth of internal water equal to 100 mm behaves similar to an air dam. However, the transition behaviour of the dam from air to water inflated dam occurs when

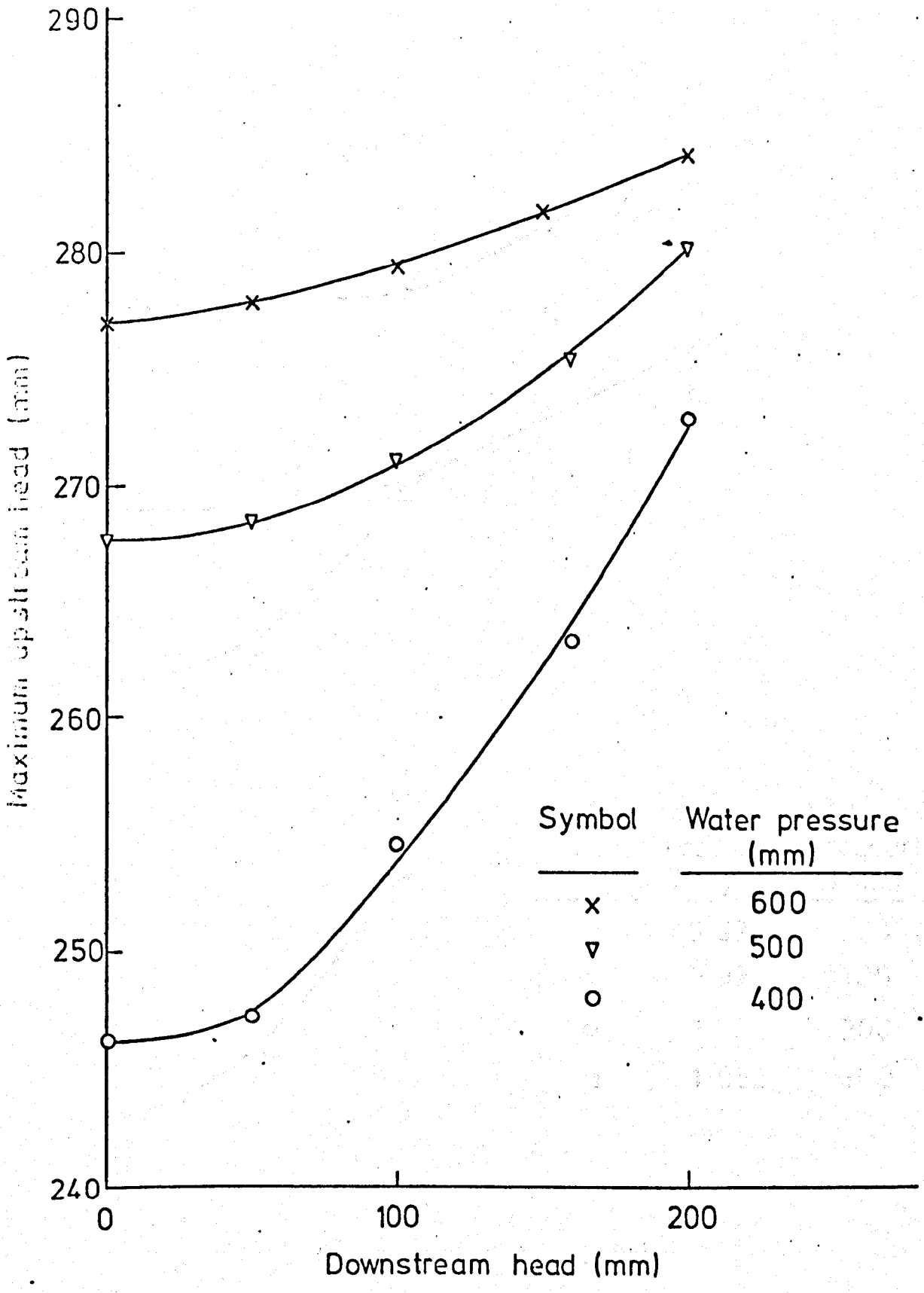

FIG. (4—42) VARIATION OF MAXIMUM UPSTREAM HEAD WITH DOWNSTREAM HEAD FOR VARIOUS WATER PRESSURES

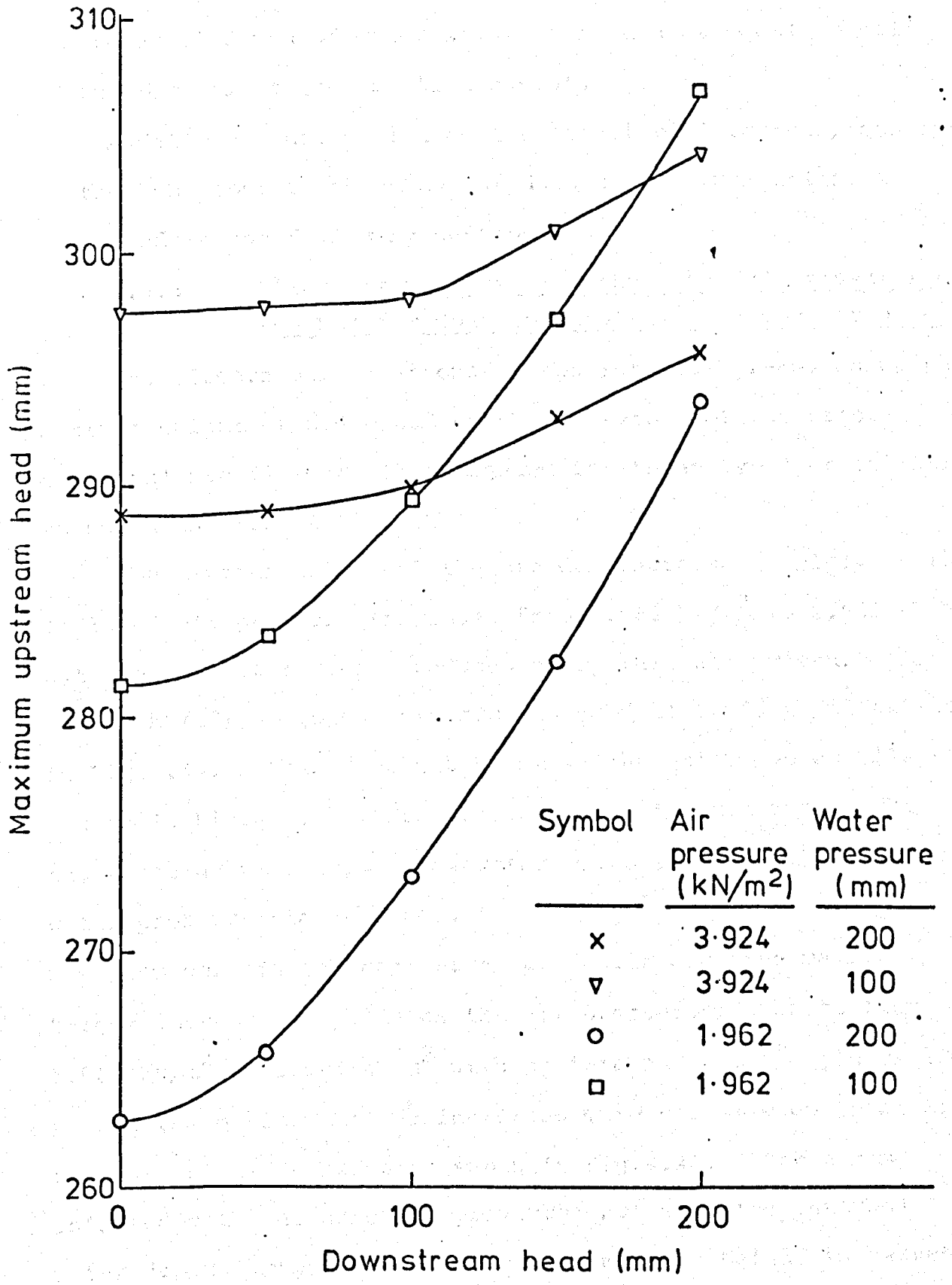

FIG. (4–43) VARIATION OF MAXIMUM UPSTREAM HEAD WITH DOWNSTREAM HEAD FOR VARIOUS AIR/WATER PRESSURES

the internal depth of water is greater than or equal to half of the dam height (see section 3.6.4).

Additional information on the effect of internal pressures on the behaviour of the shape of dams and maximum height is described in the following section.

4.5.3 Effect of Variation in the Internal Pressures on the Dam for Constant Upstream and Downstream Heads.

The effects of variations in the internal pressures on the maximum height of a dam and on the behaviour of the cross-sectional profile were investigated for three types of inflation as shown in table 4.13.

The maximum height of the air dam increases rapidly as the inflated air pressure increases from 1.962 kN/m^2 to 2.649 kN/m^2 but the rate of increase reduces above this air pressure (2.649 kN/m^2) up to the maximum analysed of 5.886 kN/m^2 as shown in Fig.4.44. This does not occur in the water dam as illustrated in Fig.4.45. It can be seen that the maximum height has a steady rise from a low water pressure (400 mm) to a high water pressure dam (600 mm).

However, in the case of an air/water dam, the maximum height increases rapidly as the air pressure increases from 1.962 kN/m^2 to 2.943 kN/m^2 with an internal water depth of 100 mm and the maximum height increases more steadily up to an air pressure of 5.886 kN/m^2 as shown in Fig.4.46. For a dam inflated with the same air pressures but with the internal water depth increased to 200 mm, the maximum height increases steadily with increasing air pressure (Fig.4.46).

No.	Air Pressure (kN/m^2)	U/S Head (mm)	D/S Head (mm)
1	1.962	270.0	0.0
2	2.256	270.0	0.0
3	2.345	270.0	0.0
4	2.649	270.0	0.0
5	2.759	270.0	0.0
6	2.943	270.0	0.0
7	3.924	270.0	0.0
8	4.905	270.0	0.0
9	5.886	270.0	0.0

(A) AIR INFLATED DAM.

No.	Air Pressure (kN/m^2)	U/S Head (mm)	D/S Head (mm)
1	400.0	220.0	0.0
2	425.0	220.0	0.0
3	450.0	220.0	0.0
4	475.0	220.0	0.0
5	500.0	220.0	0.0
6	525.0	220.0	0.0
7	550.0	220.0	0.0
8	575.0	220.0	0.0
9	600.0	220.0	0.0

(B) WATER INFLATED DAM.

No.	Air Pressure (kN/m^2)	Water Pressure (mm)	U/S Head (mm)	D/S Head (mm)
1	1.962	100.0	250.0	0.0
2	2.943	100.0	250.0	0.0
3	3.924	100.0	250.0	0.0
4	4.905	100.0	250.0	0.0
5	5.886	100.0	250.0	0.0
6	1.962	200.0	250.0	0.0
7	2.943	200.0	250.0	0.0
8	3.924	200.0	250.0	0.0
9	4.905	200.0	250.0	0.0
10	5.886	200.0	250.0	0.0

(C) AIR/WATER INFLATED DAM.

TABLE 4.13 ANALYSIS OF THREE TYPES OF INFLATION UNDER VARIOUS INTERNAL PRESSURES FOR CONSTANT UPSTREAM AND DOWNSTREAM HEADS.

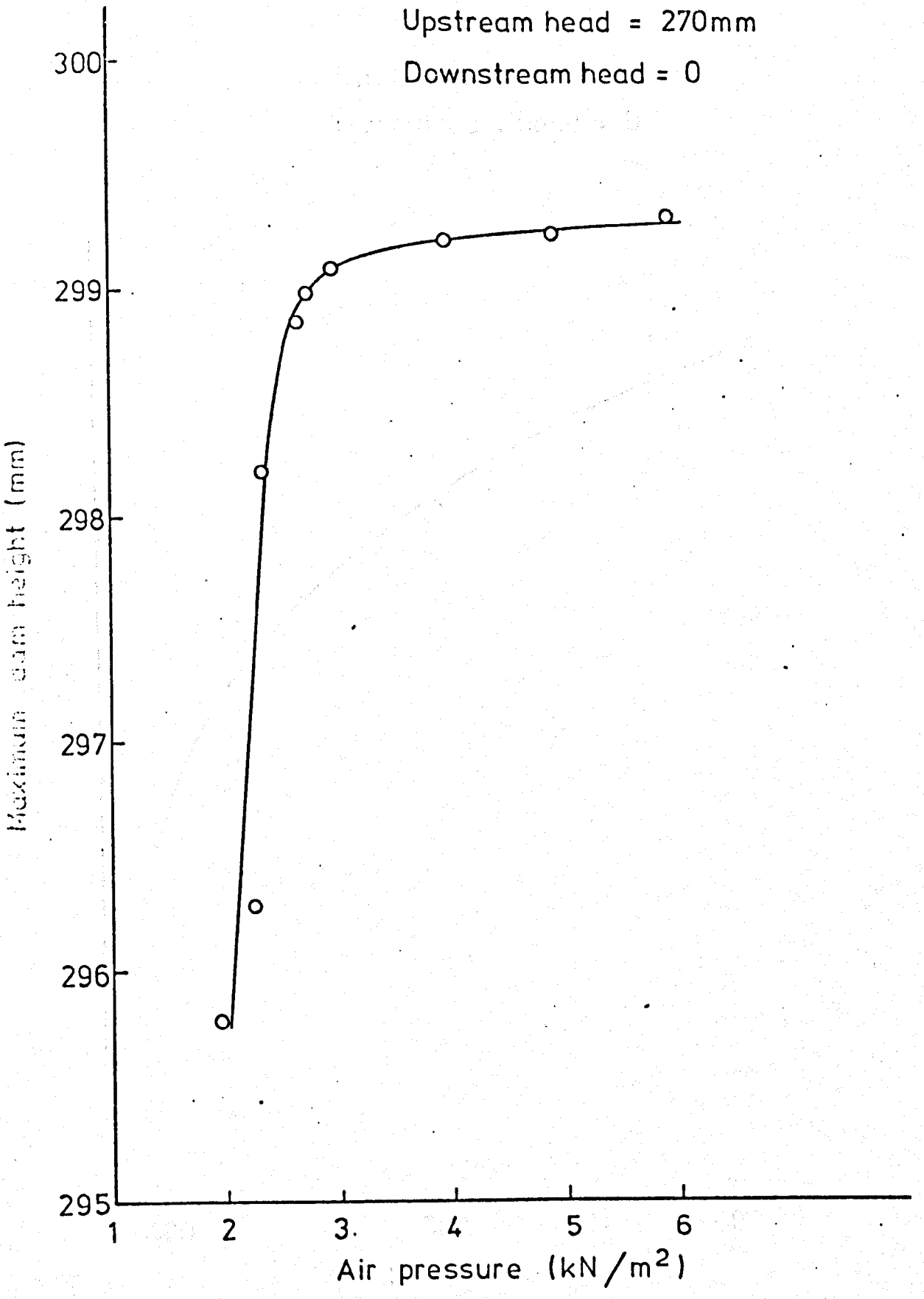

FIG. (4-44) VARIATION OF MAXIMUM DAM HEIGHT WITH AIR PRESSURE FOR CONSTANT UPSTREAM AND DOWNSTREAM HEADS

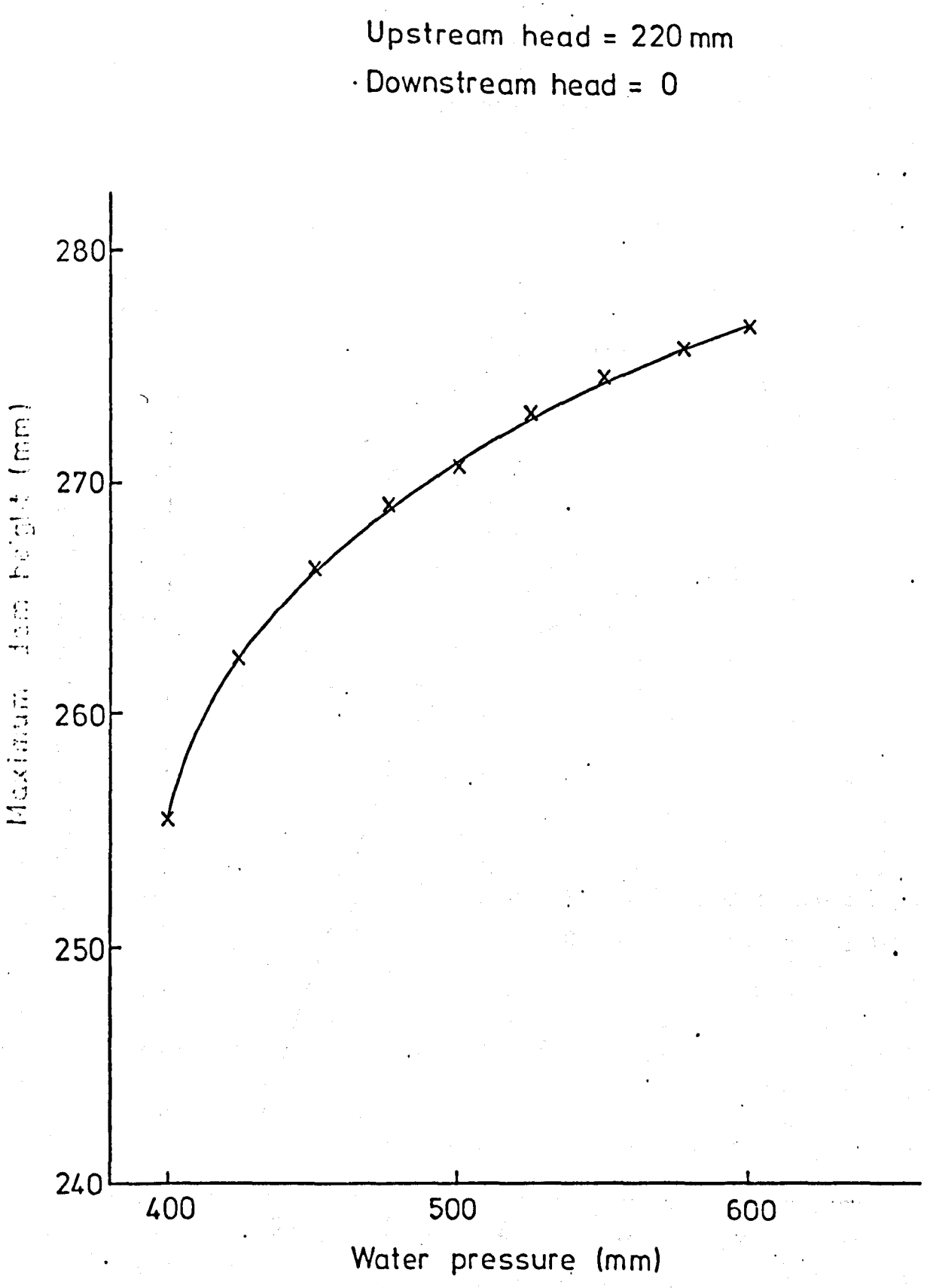

FIG. (4-45) VARIATION OF MAXIMUM DAM HEIGHT WITH WATER PRESSURE FOR CONSTANT UPSTREAM AND DOWNSTREAM HEADS

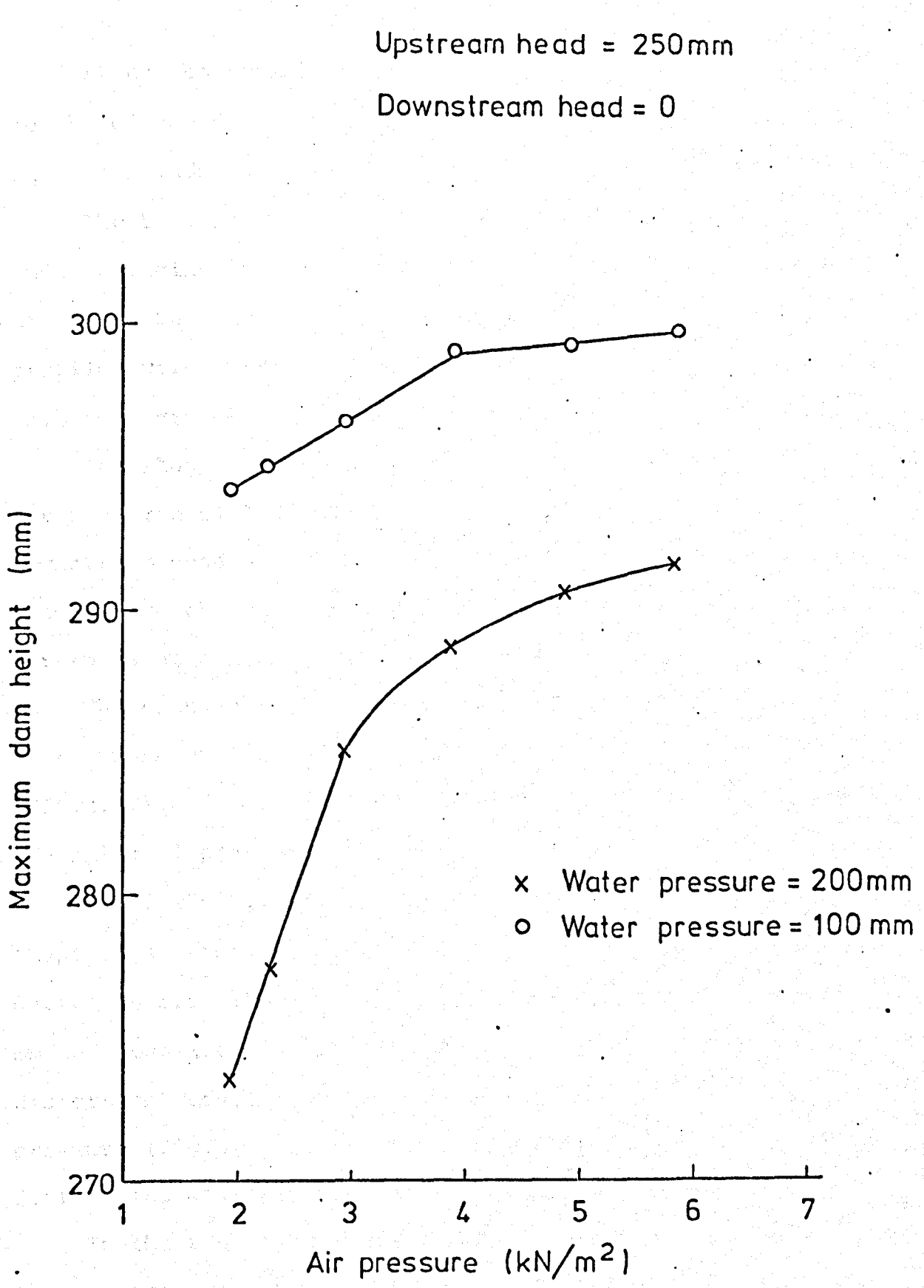

FIG. (4-46) VARIATION OF MAXIMUM DAM HEIGHT WITH AIR WATER PRESSURES FOR CONSTANT UPSTREAM AND DOWNSTREAM HEADS

It can be seen from the Fig.4.4 6 that the maximum height of the dam decreases when the internal depth of water increases under a given air pressure.

The behaviour of the cross-sectional profile of the dams under changing internal air, water and air/water pressures are shown in Figs. 4.47, 4.48 and 4.49 respectively. These profiles were obtained from an analysis of the dams with the membranes divided into 180 elements.

The shape of the dam in Fig.4.47A results from an internal air pressure of 5.886 kN/m^2 and upstream head = 270 mm and downstream head = 100 mm. Fig.4.47 B, C, D and E show the progressive change in shape for the same upstream and downstream heads as the air pressure is decreased.

The changes in shape are due to the decrease in tension in the membrane (Fig.4.26), decrease in the upstream slope (Fig.4.32) and decrease in downstream slope (Fig.4.35) when the internal pressure is decreased.

Similarly Fig. 4.45 shows the progressive change in the shape of a water inflated dam as the internal water pressure decreases from 1000 mm to 400 mm under an upstream head at 240 mm and downstream head = 100 mm. It can be seen that high distortion occurs when the dam is inflated by low water pressure (Fig.4.48E), and the phenomenon of the dam laying flat on the downstream side can be seen to develop.

In the case of the air/water dam, the dam was inflated by air pressure varying from 5.886 kN/m^2 to 1.962 kN/m^2 and the internal water depth was equal to 150 mm. Analysis took

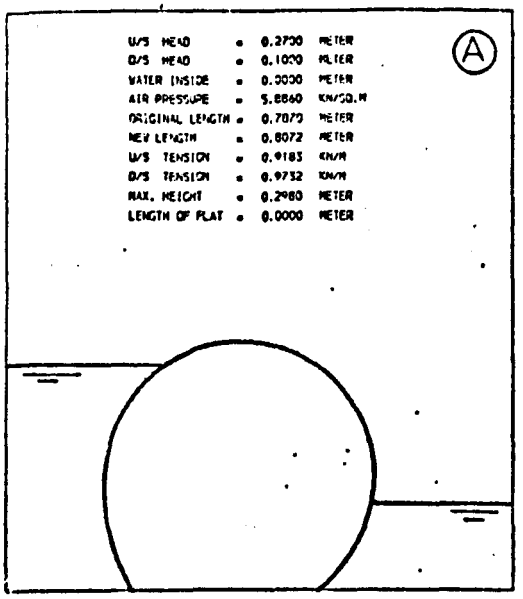

Air = 5·886 kN/m²

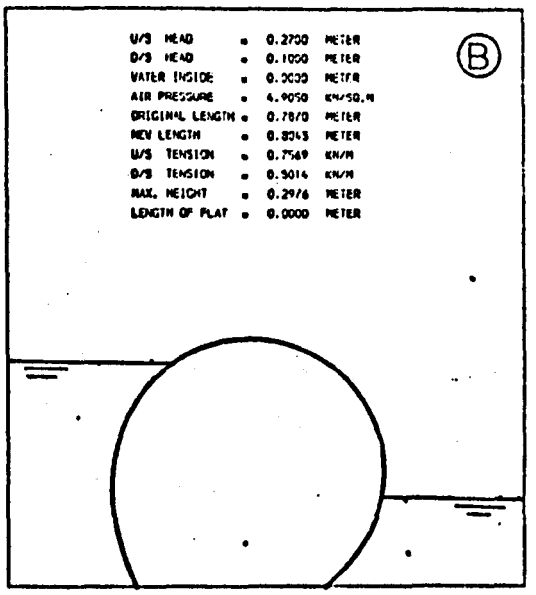

Air = 4·905 kN/m²

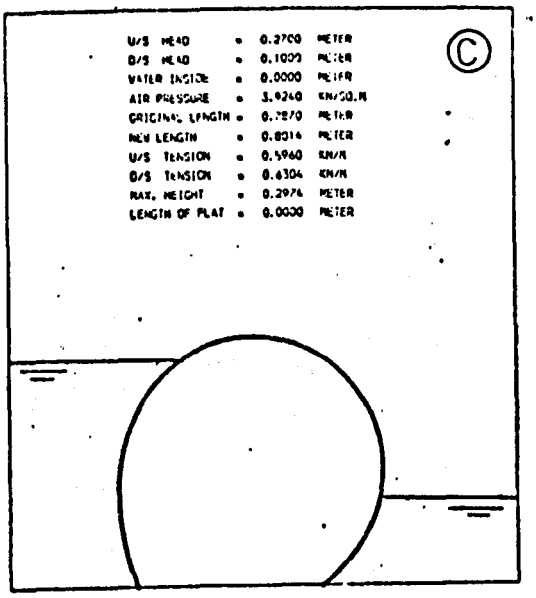

Air = 3·924 kN/m²

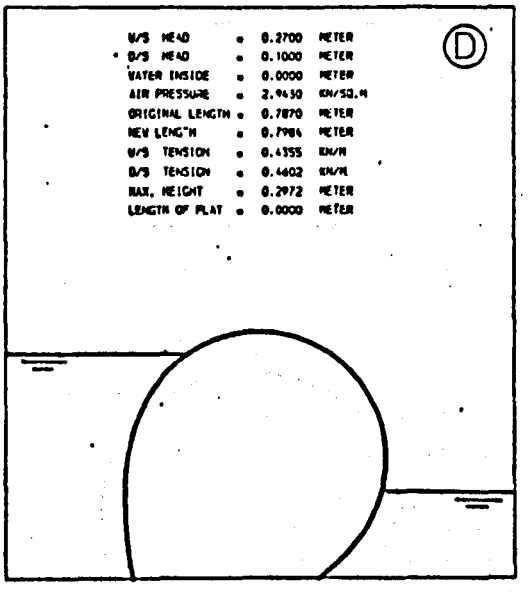

Air = 2·943 kN/m²

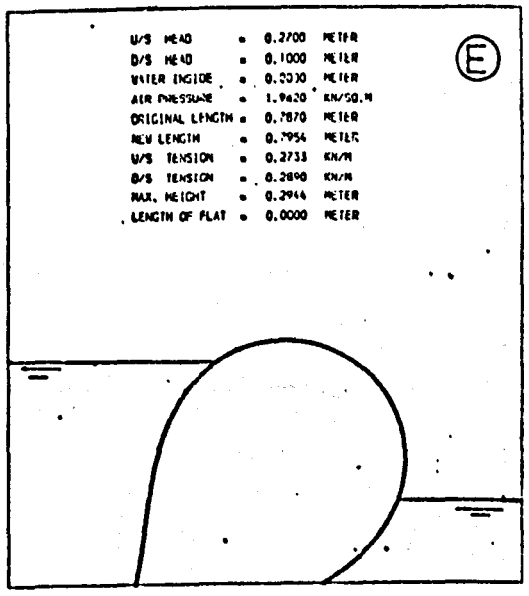

Air = 1·962 kN/m²

FIG. (4–47) TYPICAL BEHAVIOUR OF THE CROSS-SECTIONAL PROFILES OF INFLATED DAM UNDER HYDROSTATIC CONDITON FOR VARIOUS INTERNAL AIR PRESSURES

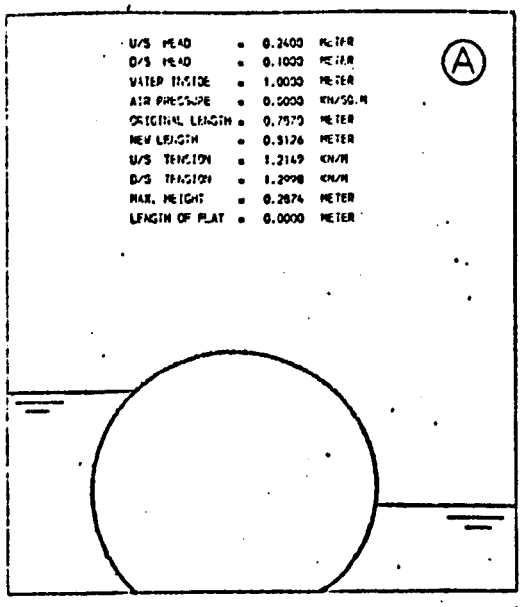

Water = 1000 mm

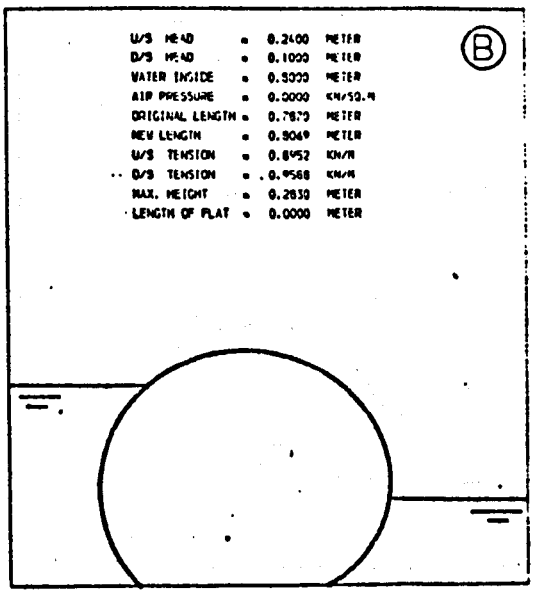

Water = 800 mm

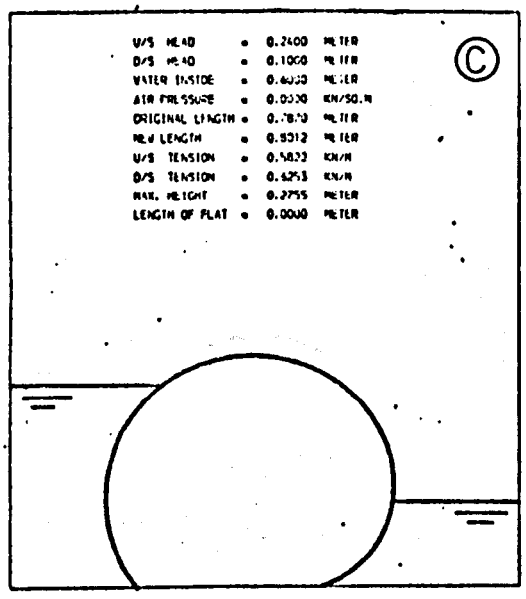

Water = 600 mm

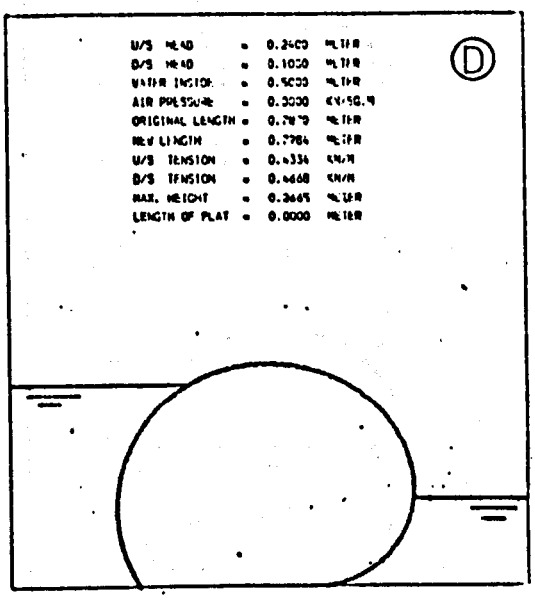

Water = 500 mm

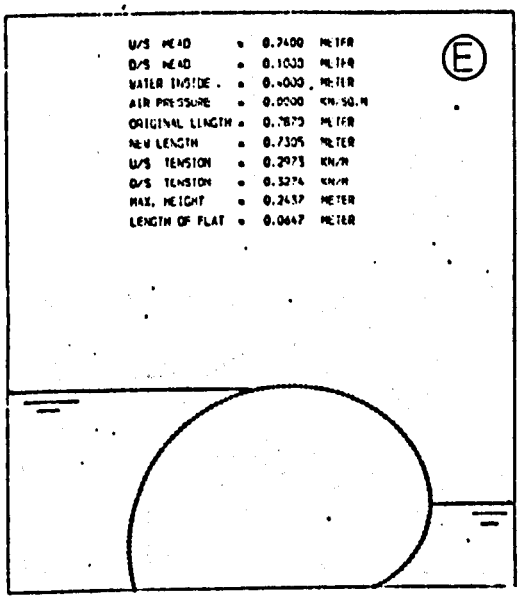

Water = 400 mm

FIG.(4-48) TYPICAL BEHAVIOUR OF CROSS-SECTIONAL PROFILES OF WATER DAMS UNDER HYDRO-STATIC CONDITIONS FOR VARIOUS INTERNAL WATER PRESSURES

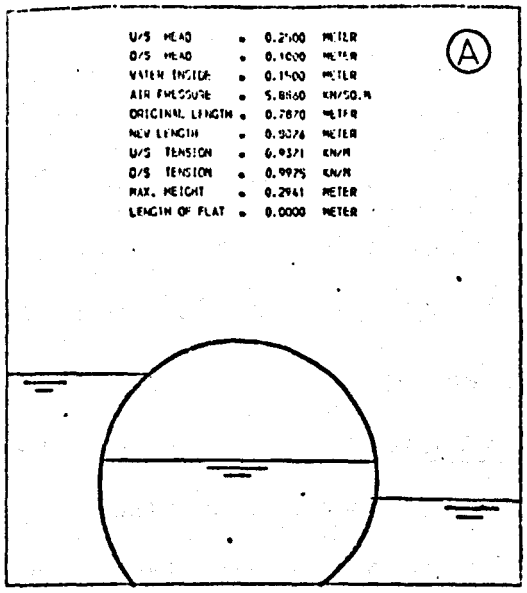

Air = 5·886 kN/m^2

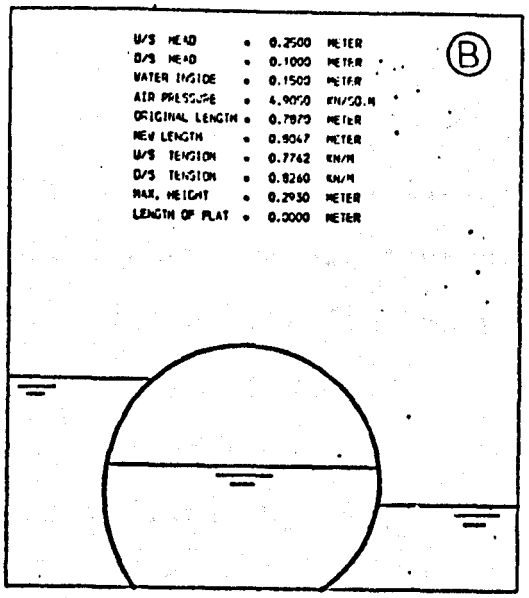

Air = 4·905 kN/m^2

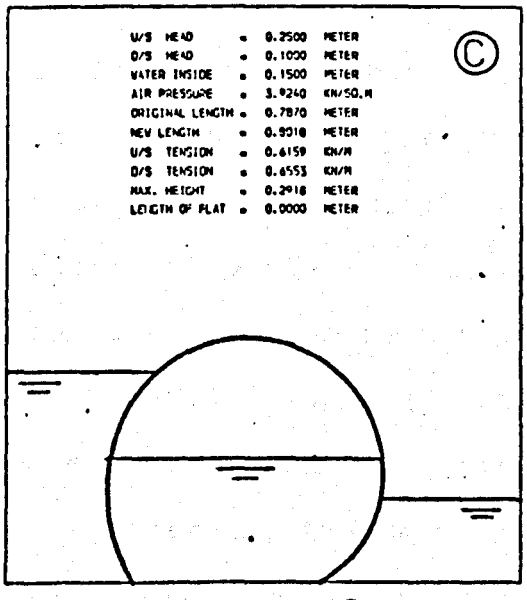

Air = 3·924 kN/m^2

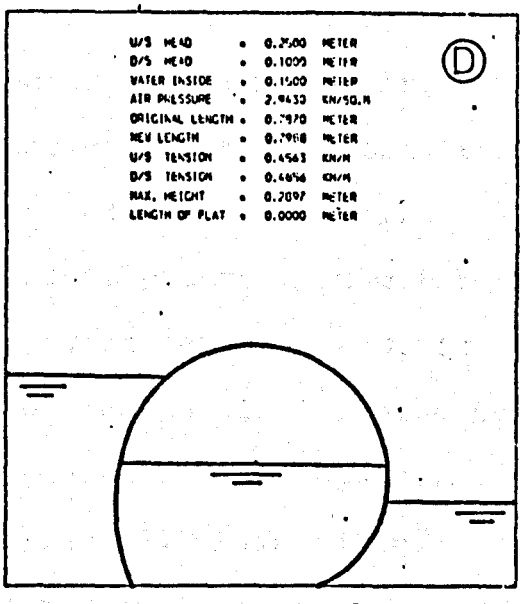

Air = 2·943 kN/m^2

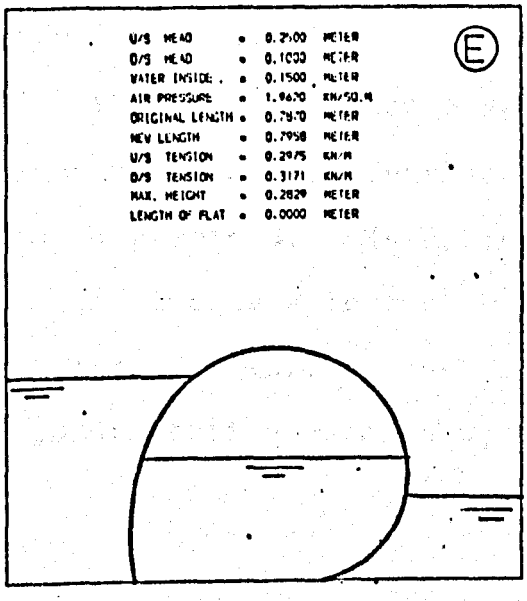

Air = 1·962 kN/m^2

Water pressure = 150 mm

FIG.(4–49) TYPICAL BEHAVIOUR OF THE CROSS-SECTIONAL PROFILE OF AIR/WATER DAMS UNDER HYDROSTATIC CONDITION FOR VARIOUS INTERNAL AIR PRESSURES

place under an upstream head = 250 mm and downstream head = 100 mm. The dam behaved at high air pressures in a similar way to the water dam (Fig.4.49A and B). When the air pressure was reduced to 3.924 kN/m^2 it was observed that the dam behaved similarly to an air pressure dam (Fig.4.49 C, D and E).

4.6 Comparison Between Air, Water and Air/Water Dams.

Comparisons were made between dams inflated by air, water and a combination of air and water in order to determine if there is any difference in the behaviour of the dams dependent on the inflation fluid. The tension in the membrane of the air dam was higher than for the water dam and the air/water dam, when analysed under the same upstream and downstream heads. For example, the tension when inflated by an air pressure of 3.924 kN/m^2 (400 mm equivalent pressure in water head) and upstream head = 200 mm and downstream head = 0, is equal to 0.633 kN/m (Fig.4.11). When the dam is inflated by 400 mm water head and analysed under the same depth upstream and downstream, the resulting tension is 0.313 kN/m (Fig. 4.12). For the equivalent air/water dam inflated by 1.962 kN/m^2 air pressure and 200 mm water head, the tension is 0.394 kN/m (Fig. 4.13).

This high tension associated with air dams means that the membrane stretches further than for the other types of inflation fluids examined, (see Figs. 4.15, 4.16 and 4.17).

An increase in the upstream head results in the dam being distorted forward on the downstream side and the magnitude of this distortion depends upon the type of inflation (air, water

or air/water). Higher distortions are associated with larger decreases in the upstream slope of a dam. For example, the upstream slope of 3.924 kN/m^2 air pressure dam decreased by 28^o when the upstream head increased from 100 mm to 240 mm (Fig.4.17). Whereas the upstream slope of a water (400 mm) dam decreased 43^o for the same head change (Fig.4.18).

For an air dam the upstream slope decreases with a decrease in air pressure. However, for the water dams a low pressure dam has an upstream slope greater than the slope for a higher pressure dam (see Fig.4.18).

This phenomenon of water dams may occur in air/water dams provided the depth of internal water in an air/water dam is greater than 150 mm, the dam will behave with respect to variation in distortion and upstream slope as a water dam (Fig. 4.19).

The variation of the downstream slope of the water dam (Fig.4.21) is greater than for the equivalent air dam (Fig. 4.20) and air/water dam (Fig.4.22). This big variation of downstream slope in the water dam can cause the dam to be laid flat (downstream slope = 0) at the downstream fixture.

The air dam has always a height of crest higher than other dams under equivalent conditions of upstream head, downstream head and internal pressure. For example, the height of crest of a 3.924 kN/m^2 air dam under an upstream head = 220 mm and downstream head = 0 is equal to 296.7 mm (Fig.4.23) and the 400 mm water dam is equal to 255.5 mm (Fig.4.24). For the air/water (1.962 kN/m^2/200 mm) dam, the height of crest is

found equal to 278 mm (Fig.4.25) when the dam is analysed under the same upstream and downstream head for both air and water dams.

However, it is possible for an air dam to have a height of crest higher under low inflation pressure than the height of crest under a high pressure. This phenomenon does not occur for water inflation but may occur for air/water dams.

The results of these observations are summarised in table 4.14 for the same dam under equivalent conditions except for the inflation fluid.

Parameters	Air	Water	Air/Water
Tension	High	Low	Medium
Elongation	High	Low	Medium
Upstream Slope (θ_1)	Low	High	Medium
Downstream Slope (θ_2)	High	Low	Medium
Maximum Height of the Dam.	High	Low	Medium

TABLE 4.14 COMPARISON BETWEEN AIR, WATER AND AIR/WATER DAMS.

A further study was carried out to determine the maximum upstream head which could be supported by air, water and air/water dams. Three dams were analysed under downstream = 0 and various internal pressures as shown in table 4.13.

It can be seen that from Figs. 4.50, 4.51 and 4.52 the maximum upstream head capable of support for the equivalent

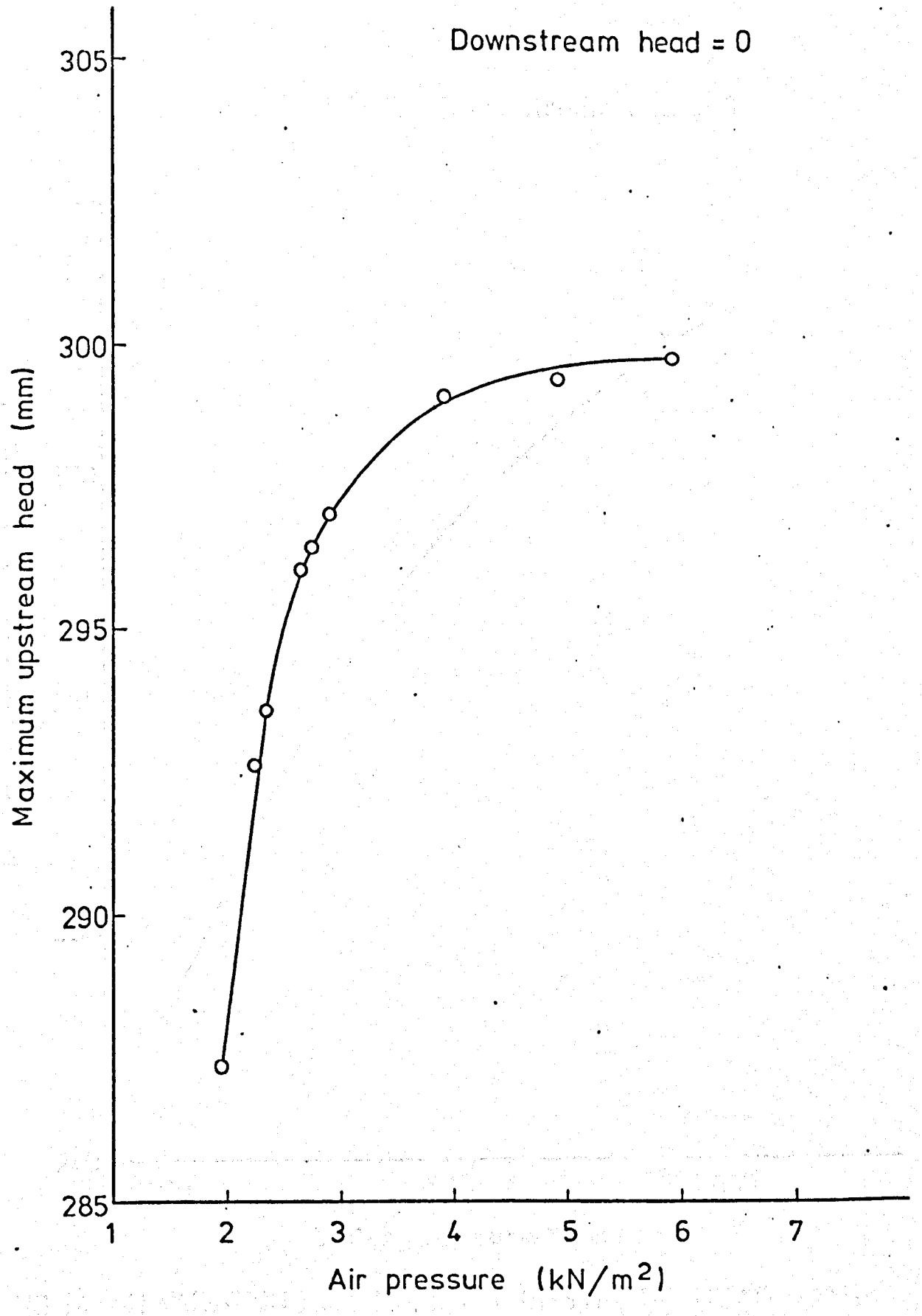

FIG. (4-50) VARIATION OF MAXIMUM UPSTREAM HEAD WITH AIR PRESSURE

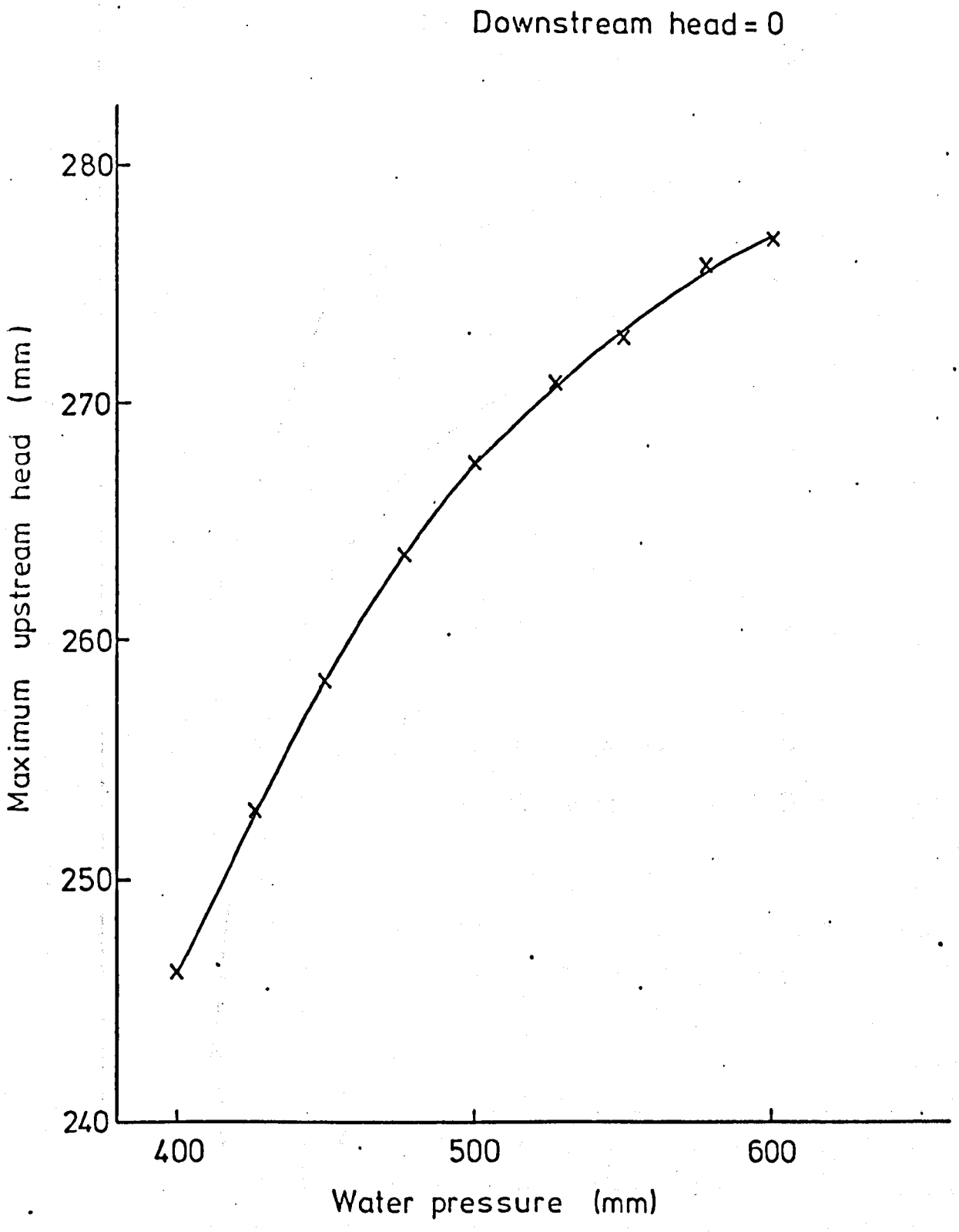

FIG. (4-51) VARIATION OF MAXIMUM UPSTREAM HEAD WITH WATER PRESSURE

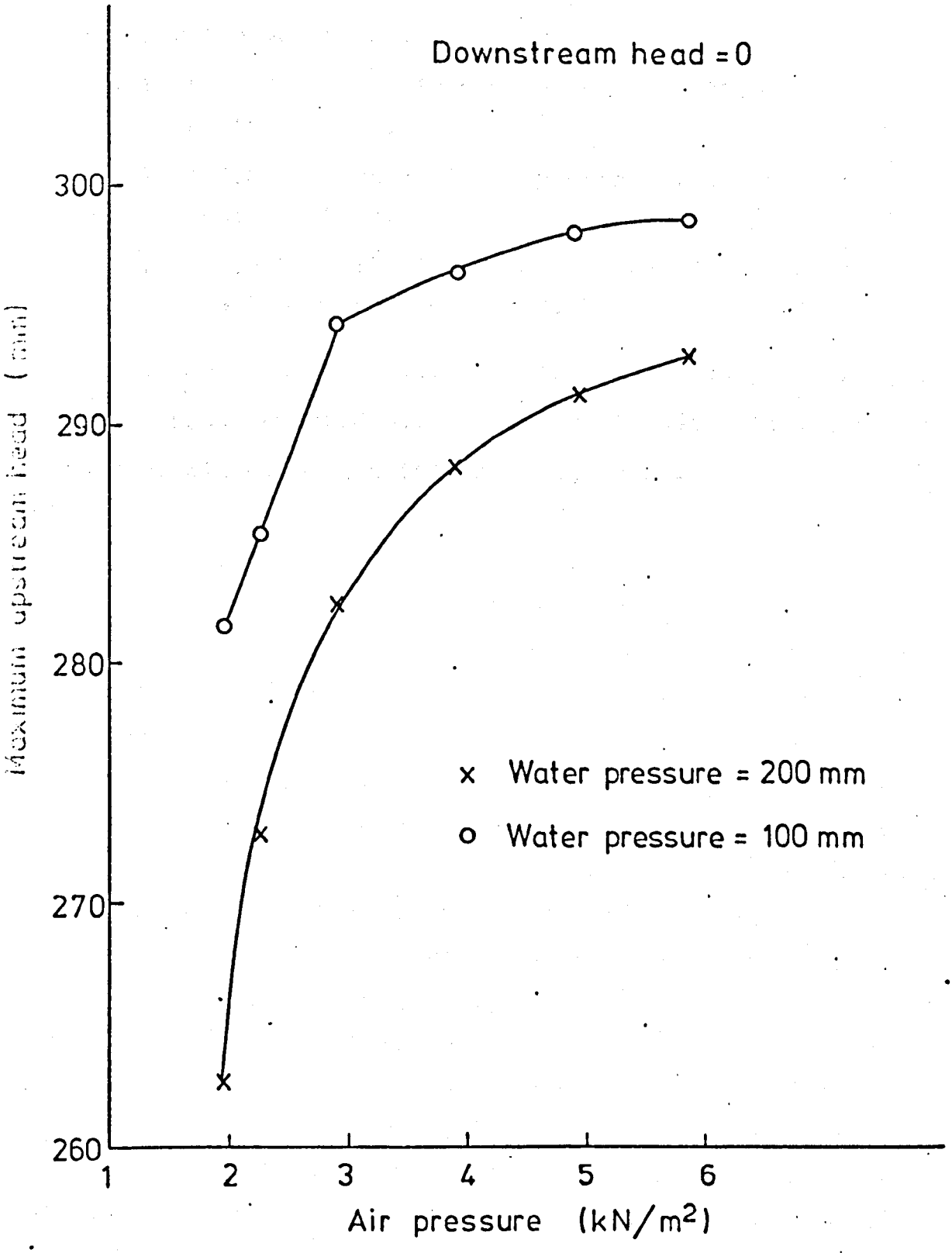

FIG. (4-52) VARIATION OF MAXIMUM UPSTREAM HEAD WITH AIR/WATER PRESSURES

internal pressure is always greatest for the air dam and lowest for the water dam. For example:

(a) A 3.924 kN/m^2 air dam supports a 299.0 mm upstream head.

(b) A 400.0 mm water dam supports a 246.0 mm upstream head.

(c) A 1.962 kN/m^2 air/200.0 mm water dam supports a 262.5 mm upstream head.

This means that an air dam will always support the greater upstream head compared with water or air/water inflation of the same dam, all other conditions being equal.

CHAPTER 5.

THE ANALYSIS OF DAMS UNDER HYDRODYNAMIC CONDITIONS.

5.1 Introduction.

The theoretical analysis of an inflatable dam under hydrodynamic (overflow) conditions is considerably more complex than for the hydrostatic state. This is because the shape of the dam alters with variations in the hydrodynamic conditions (overflow head, downstream head and internal pressure), which in themselves may be changing.

The only attempt at a theoretical solution was made by Anwar (1967)[6] in which he dealt with the mathematical analysis of air inflated dam when overflow occurs.

Baker (1964)[1], and Shepherd (1969)[2] and Clare (1972)[8] also have observed the behaviour of the inflatable dams under various hydrodynamic conditions but have made no attempt at a theoretical analysis.

This chapter deals with a theoretical analysis for hydrodynamic conditions developed by the author. The performance of the dams under variations of overflow head, downstream head, and internal pressures is also investigated.

A computer program was written to analyse the dam under these various hydrodynamic conditions and in particular to produce a plot of the shape of the cross-sectional profile and calculate the tension in the membrane.

The theoretical shapes and tensions of various dams were compared with experimental shapes and tensions obtained from laboratory tests.

5.2 Design and Construction of the Model.

The computer program (DID)(see Chapter 7) was used to design a model dam to support an upstream head of 150 mm and downstream head of 50 mm and this was then used to investigate how it performed under hydrodynamic conditions. Air was chosen to inflate the model and N.T. fabric (see section 3.3) was used for the bag.

Although designed as an air inflated dam, water and air/water inflation was also used to compare the effect on the dam performance of different inflation fluids.

The program determined the membrane length, base length, and the magnitude of air pressure for the design heads requiring the minimum amount of material. The design criteria are:-

(i) Membrane length (exclusive of base length) = 396.0 mm.

(ii) Base length = 112.5 mm.

(iii) Air pressure = 1.962 kN/m^2.

The shape of the cross-sectional profile of the dam was plotted as shown in Fig.5.1.

The model was constructed in a similar way to the hydrostatic model (see section 3.5). The bag of the model was made from a single sheet (section 3.5.1) and the end effects on the shape of the dam were reduced to a minimum (section 3.5.5).

The base of the model was made from 12.5 mm perspex and was fitted to the base of the test tank. The length of the base was 212.5 mm (112.5 mm base length of the model and 50 mm on each side of base length used for fixing the bag to the base

U/S HEAD	=	0.1500	METER
D/S HEAD	=	0.0500	METER
WATER PRESSURE	=	0.0000	METER
AIR PRESSURE	=	1.9620	KN/SQ.M
ORIGINAL LENGTH	=	0.3957	METER
NEW LENGTH	=	0.3987	METER
U/S TENSION	=	0.1305	KN/M
D/S TENSION	=	0.1658	KN/M
BASE LENGTH	=	0.1125	METER
MAX. HEGHTH	=	0.1492	METER

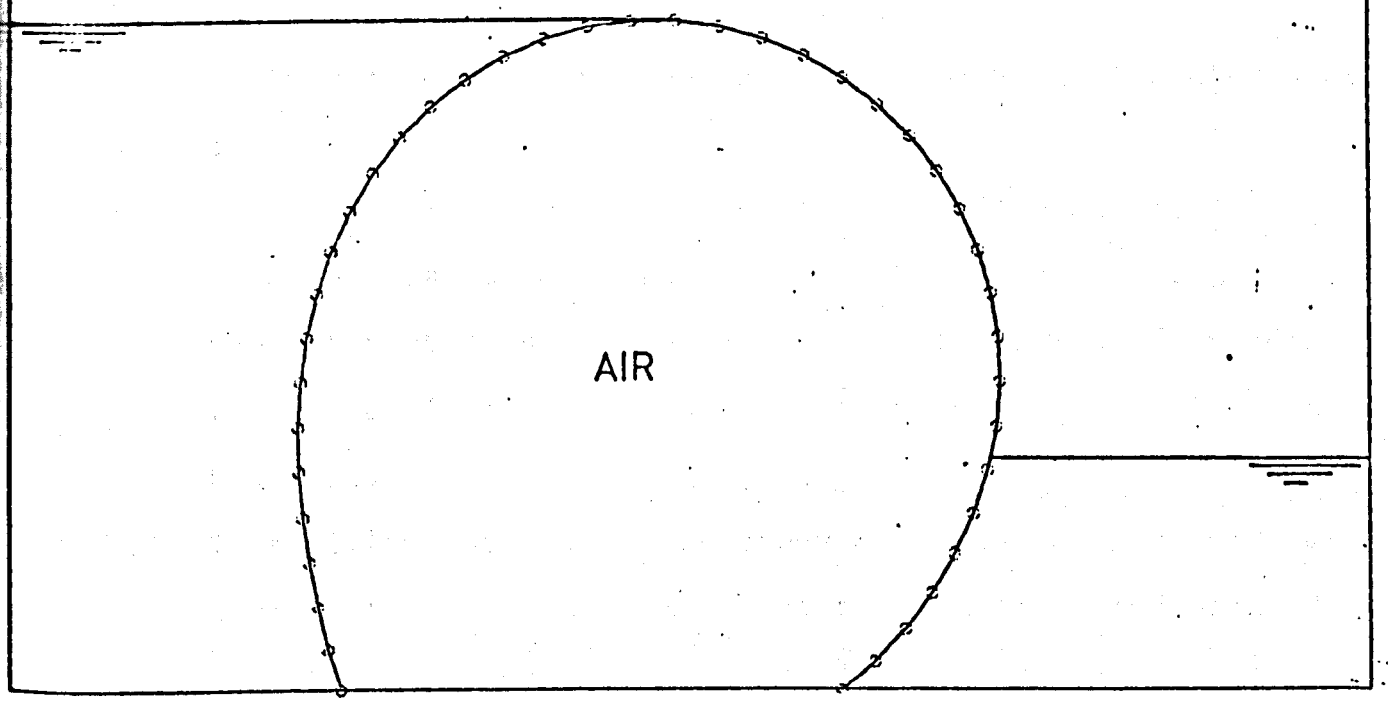

FIG. (5- 1) TYPICAL PROFILE OF AN AIR INFLATED MODEL DAM SUBJECTED TO HYDRODYNAMIC CONDITIONS USING PROGRAM (DID)

on the upstream sides of the dam). The fixing technique used was as for the hydrostatic model described in section 3.5.3.

The apparatus which was used to inflate the dam by air or water has already been described in sections 3.2.2 and 3.2.3.

A valve was fixed on the crest of the water and on the air/water bags in order to free the air in the first bag, and, to control the air pressure in the second bag.

The leaks at the ends of the model and underneath the base were controlled by using oil tape (Dinso tape).

In total six dams of the same size were constructed so that a dam could be discarded after inflation under high pressure had taken place.

5.3 Experimental Test.

Tests were carried out on the air, water and air/water dams as follows:-

(1) The dams were tested under various overflow heads, downstream heads, and internal pressures in order to measure the deformation of the cross-sectional profile of the dams. The range of head and pressure values covered is given in table 5.1.

(2) In addition, visual observations were made of the performance of the dams under extremes of high flows and both high and low pressures down to almost complete deflation and these are described in section 5.3.2.

5.3.1 Shape of the Dam.

5.3.1.1 Profile Measuring Technique.

Some difficulty was experienced in applying the previous

technique used to measure the cross-sectional profile of the dam under hydrostatic conditions (see section 3.6.1). This was due to the difficulty of observing the contact between the point of the profile gauge and the membrane surface under flowing water.

A new technique was developed by painting a 20 mm strip of high conductivity paint (Electrically conductive paint, supplied by RS Components Limited) around the outside of the membrane of the dam at the centre. A galvonometer was connected between the profile gauge and the paint strip in order to indicate when contact between the paint of the profile gauge and the membrane surface occurred. The system used is shown in Fig.5.2.

Because water is a good conductor of electricity, a half scale deflection of the galvonometer occurred as soon as the point of the gauge came into contact with the water. However, as soon as contact was made between the point of the gauge and the paint strip a full deflection of the galvonometer occurred. By using this method the co-ordinates of all points round the membrane could be measured more accurately than using the technique of visual contact.

5.3.1.2 Measurement of Shape of the Dams.

The shapes of the dams were measured under various over-flow heads, downstream heads, and internal pressures as given in table 5.1, for air, water and a combination of air and water inflation.

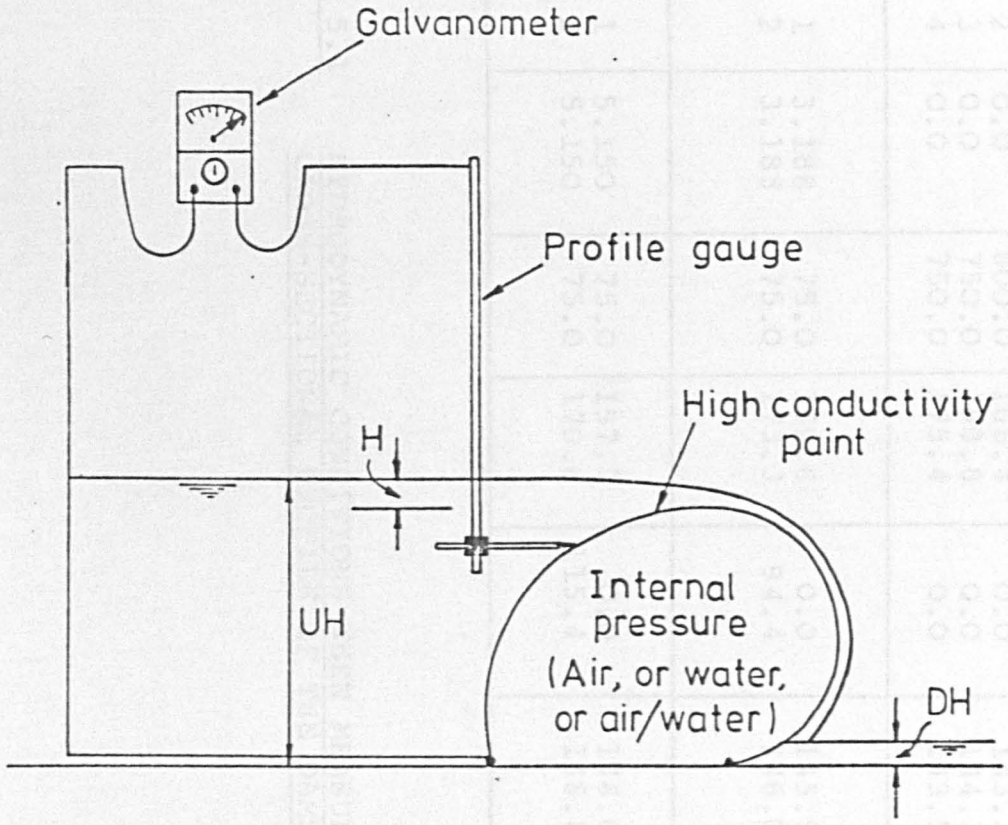

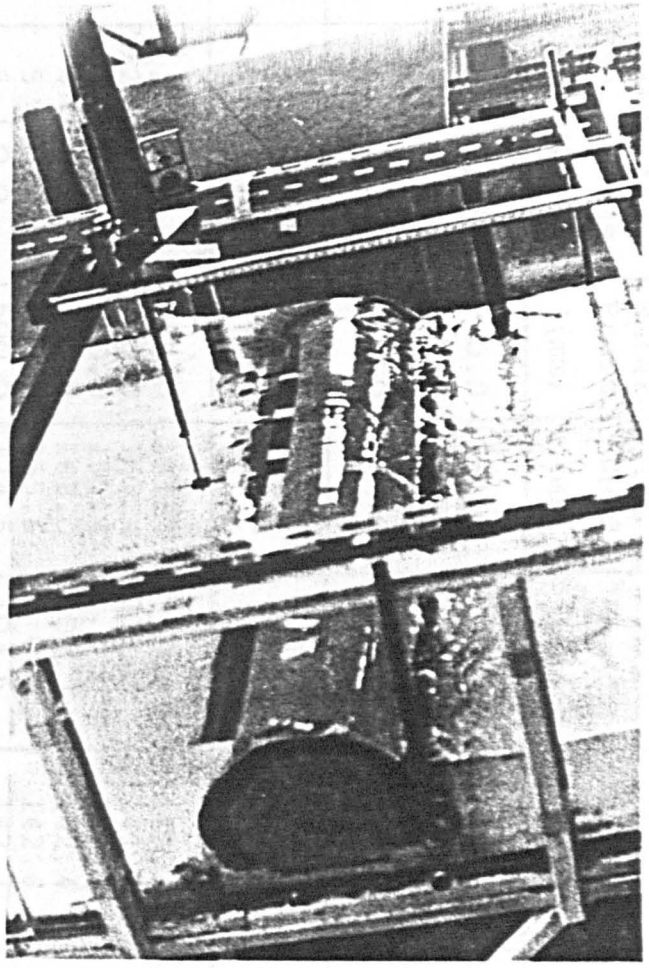

FIG. (5-2) PROFILE GAUGE

Inf. type	Model No.	Test No.	Air Press. (kN/m^2)	Water Press. (mm)	U/S Head (mm)	D/S Head (mm)	Dam Height (mm)	Overflow Head (mm)
Air Pressure	1	1	1.962	0.0	161.4	0.0	147.5	13.6
		2	1.962	0.0	178.0	0.0	145.8	32.2
		3	3.924	0.0	163.2	0.0	148.5	14.7
		4	3.924	0.0	179.0	0.0	147.7	31.3
	2	1	5.886	0.0	156.8	0.0	148.2	8.6
		2	5.886	0.0	173.9	0.0	147.6	26.3
Water Pressure	3	1	0.0	350.0	151.4	0.0	139.4	12.0
		2	0.0	350.0	163.4	112.0	141.6	21.8
		3	0.0	400.0	155.4	0.0	141.0	14.4
		4	0.0	400.0	168.0	108.3	142.4	25.6
		5	0.0	500.0	155.6	0.0	142.6	13.0
		6	0.0	500.0	174.5	103.6	142.7	31.8
	4	1	0.0	600.0	156.7	0.0	143.5	13.2
		2	0.0	600.0	168.4	0.0	143.2	25.2
		3	0.0	750.0	153.8	0.0	144.3	9.5
		4	0.0	750.0	175.4	0.0	143.5	31.9
Air/Water Pressure	5	1	3.188	75.0	159.6	0.0	145.5	14.1
		2	3.188	75.0	173.3	94.4	146.0	27.3
	6	1	5.150	75.0	157.7	0.0	146.0	11.7
		2	5.150	75.0	170.6	115.4	146.8	23.8

TABLE 5.1 HYDRODYNAMIC CONDITIONS WHEN MEASURING THE CROSS-SECTIONAL PROFILE OF THE DAMS.

The overflow head (H in Fig.5.2) was found by subtracting from the total upstream head measured with a point gauge (UH in Fig.5.2) the vertical co-ordinate of the crest of the dam measured by the profile gauge.

The computer program was used to plot the profile of the dam for the experimental co-ordinates as described in section 3.6 and typical plots are shown in Fig.5.3.

A comparison between the experimental and the theoretical shapes of the dams is described in section 5.6.

5.3.2 Behaviour of the Dams.

5.3.2.1 Air Inflated Dam.

In order to study the behaviour of air inflated dams under hydrodynamic conditions, two series of tests were carried out. The first of these tests were carried out on two dams inflated by air pressure varying from 1.962 kN/m^2 to 5.886 kN/m^2 and exposed under overflow heads varying from 9 mm to 41 mm. The downstream head was equal to zero. The first dam was used for the lower pressure and the second for the highest air pressure.

As the overflow head (H) increased this resulted in a distortion of the dam forward on the downstream side causing a reduction in the dam crest height level (Y_{max}) as illustrated in Fig.5.4. The rate of decrease in the crest height is lower for increasing overflow head at high inflation pressures compared with low inflation pressures (Fig.5.4A). For example, with the dam inflated by 5.886 kN/m^2 air pressure and tested under overflow heads 10 mm and 40 mm, the crest height fell by 0.7 mm. When the dam was inflated by 1.962 kN/m^2 and tested under the same levels of overflow head, the crest height fell by 5.9 mm.

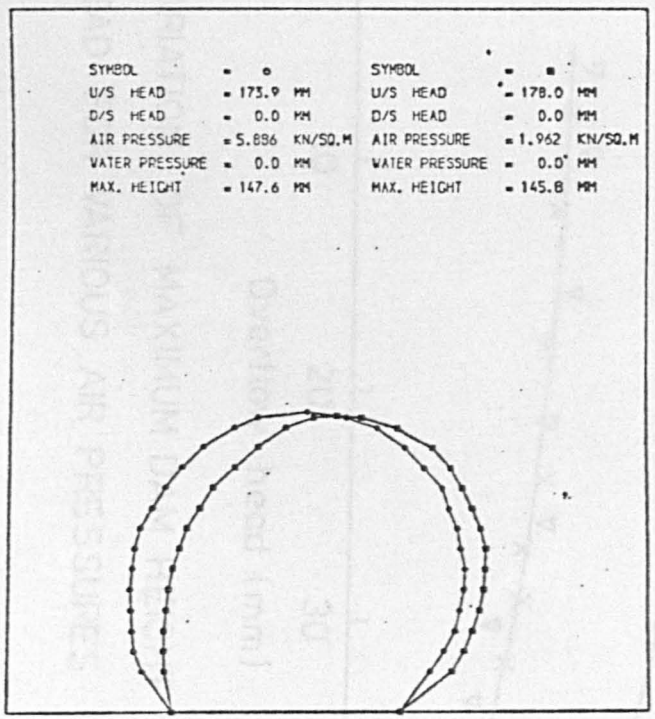

(A) Air inflated dam

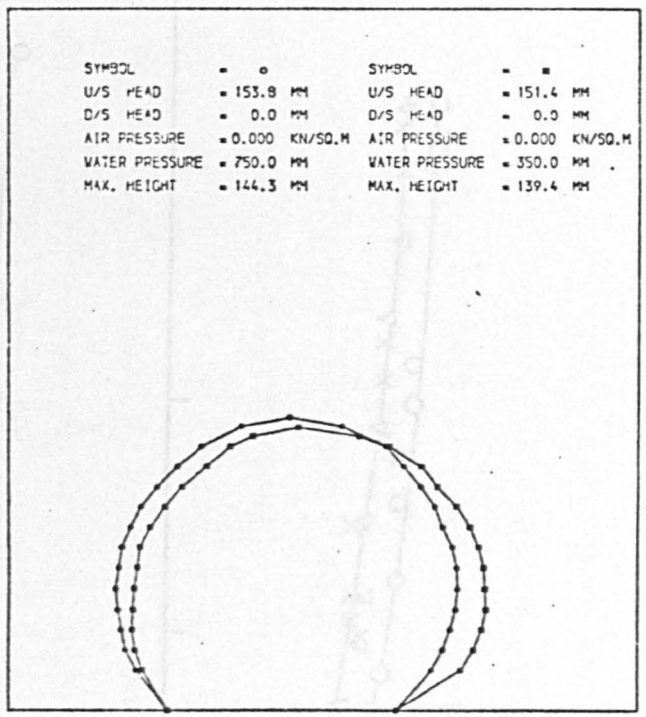

(B) Water inflated dam

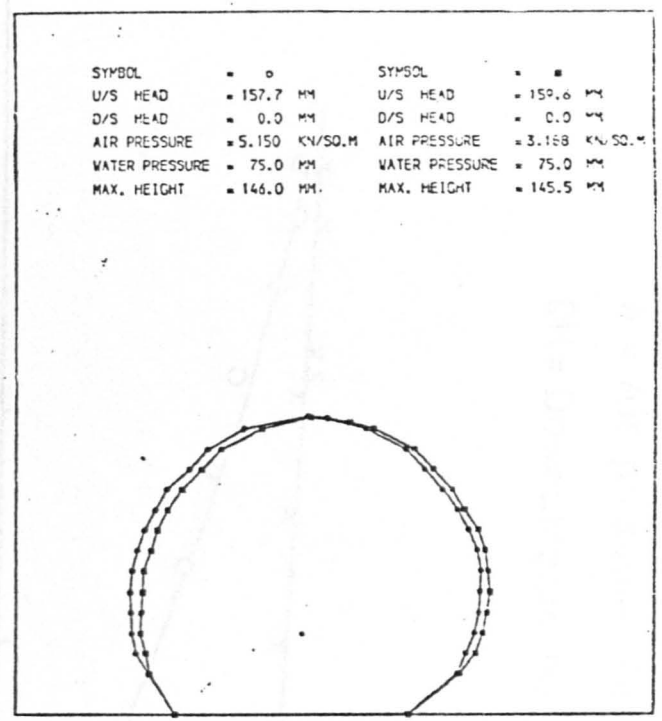

(C) Air/water inflated dam

FIG. (5 – 3) TYPICAL EXPERIMENTAL PROFILES OF INFLATABLE DAMS FOR VARIOUS AIR AND WATER PRESSURES

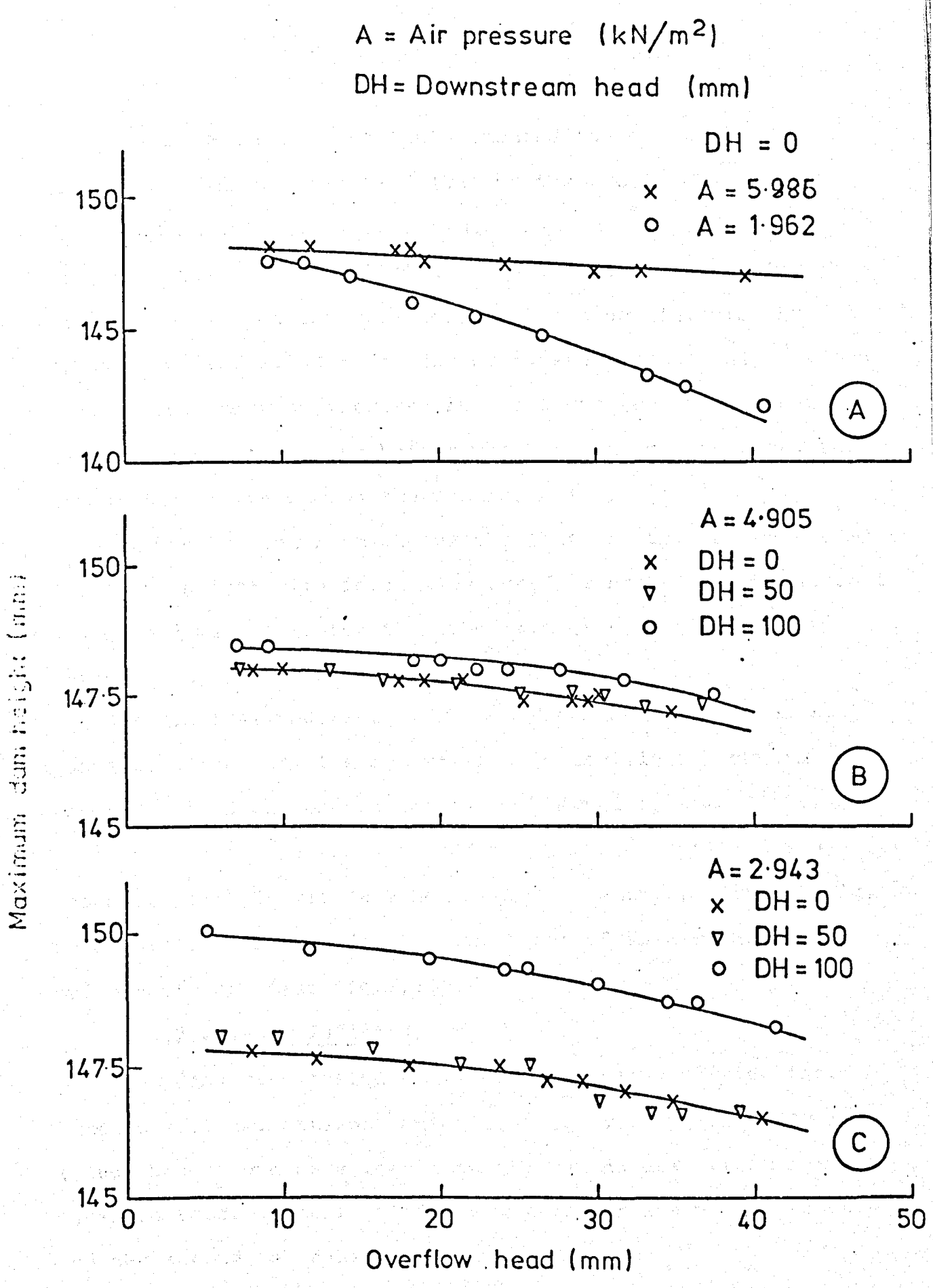

FIG.(5–4) VARIATION OF MAXIMUM DAM HEIGHT WITH OVERFLOW HEAD FOR VARIOUS AIR PRESSURES

The second series of tests studied the effects of variation of downstream head (DH) on the crest height of the dam when the internal air pressure changed.

Fig. 5.4 B and C illustrate the effect of increasing the downstream head on the crest height for a dam inflated by 4.905 kN/m^2 and 2.943 kN/m^2 air pressures respectively. Both figures show that an increase in the downstream head produces an increase in the crest height which is due to the backward distortion of the dam on the upstream side.

It can be seen from the graphs that the rate of change of the crest height with increasing overflow head for low internal pressure dams is greater than the rate of change of crest height for the high internal pressure dam.

It was observed, when the downstream head increased to above crest height, the dam started to oscillate backward and forward; this phenomenon was also observed by Anwar[29].

The changes in the shape of the dam when deflated are shown in Fig.5.5, with a V-notch at the centre occurring (Fig. 5.5C) similar to that for the deflation of an air inflated hydrostatic dam (see Fig.3.10).

5.3.2.2 Water Inflated Dam.

Two dams were tested under overflow heads varying from 5 mm to 42.5 mm, internal water pressure varying from 300 mm (water head above base level) to 750 mm and downstream head equal to zero. The first dam was used for low water pressure and the second for a high pressure.

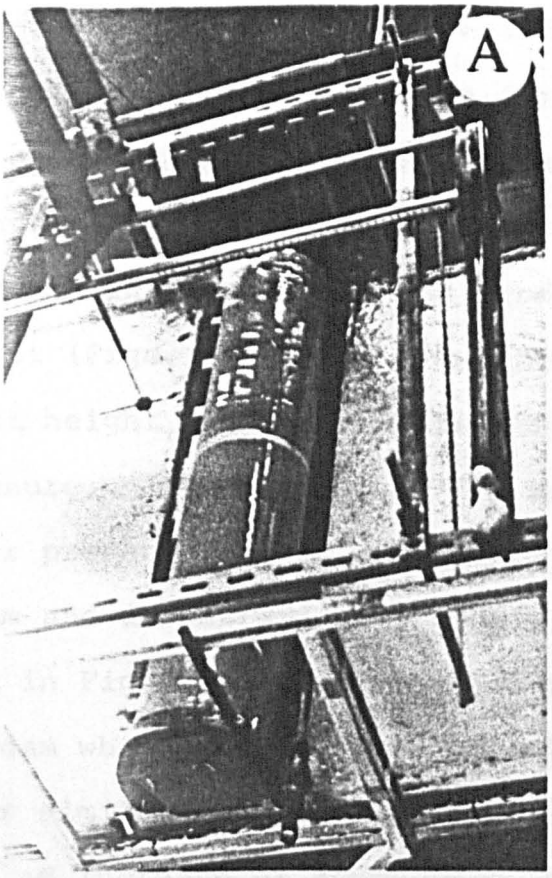

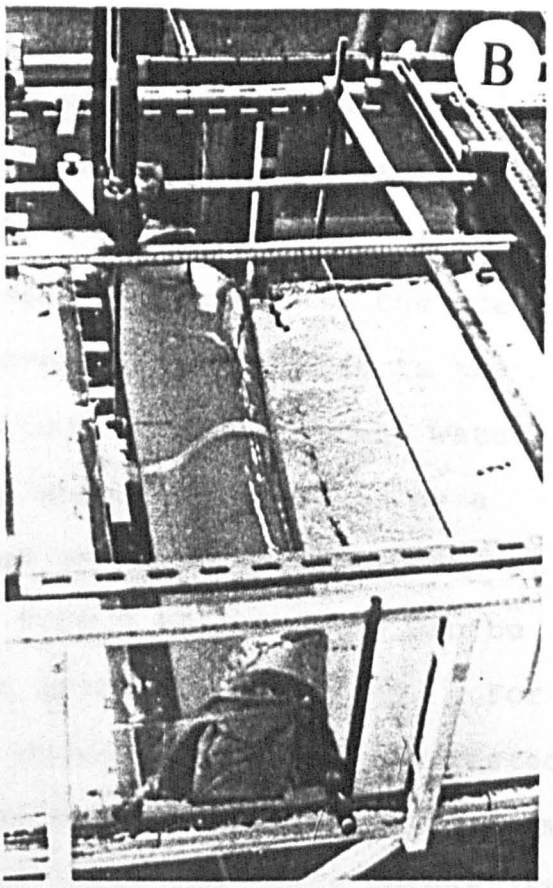

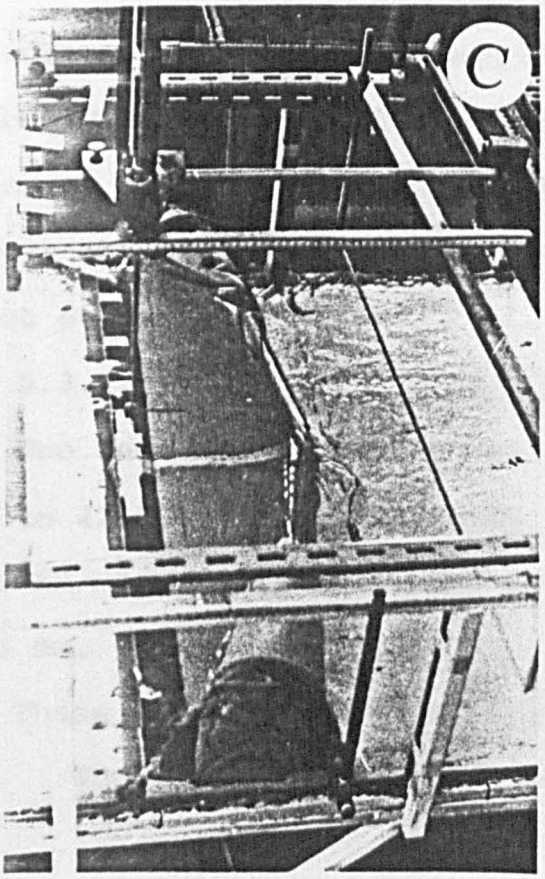

(A)
Air pressure = 5·886 kN/m^2

(B)
Air pressure = 0·981 kN/m^2

(C)
Air pressure = 0·196 kN/m^2

FIG.(5–5) BEHAVIOUR OF AIR INFLATED DAM WHEN DEFLATED (HYDRODYNAMIC)

Fig.5.6 shows that the crest height of the dam decreased when the overflow head increased and also decreased with decreasing internal pressure (Fig.5.6A). This reduction in the crest height was less for the high internal pressure dam than for the low pressure dam. It was also noted that the increase in downstream head produced an increase in the crest height (Figs. 5.6 B and C). However, this increase in the crest height depended on the magnitude of the internal water pressure. In the case of the dam which was inflated by a water pressure of 600 mm and tested under an overflow head at 20 mm and downstream head varying from 0 to 100 mm as can be seen in Fig.5.6B, the crest height increased by 0.6 mm. For the dam which was inflated by 400 mm water pressure and tested under similar conditions, the crest height increased by 1.1 mm. With an increase of downstream head above the crest height, it was observed that the dam oscillated backward and forward. The behaviour of the dam when deflated is shown in Fig. 5.7. The crest height decreased steadily until the dam was laid flat at the base of the downstream fixture without a V-notch effect occurring.

5.3.2.3 Air/Water Inflated Dam.

Two dams were tested under overflow heads varying from 5 mm to 42.5 mm and inflated by air pressures varying from 2.207 kN/m^2 to 5.15 kN/m^2 and an internal water pressure head of 75 mm.

These dams behaved similarly to the air and water pressure dams. Thus, the crest height gradually decreased when the

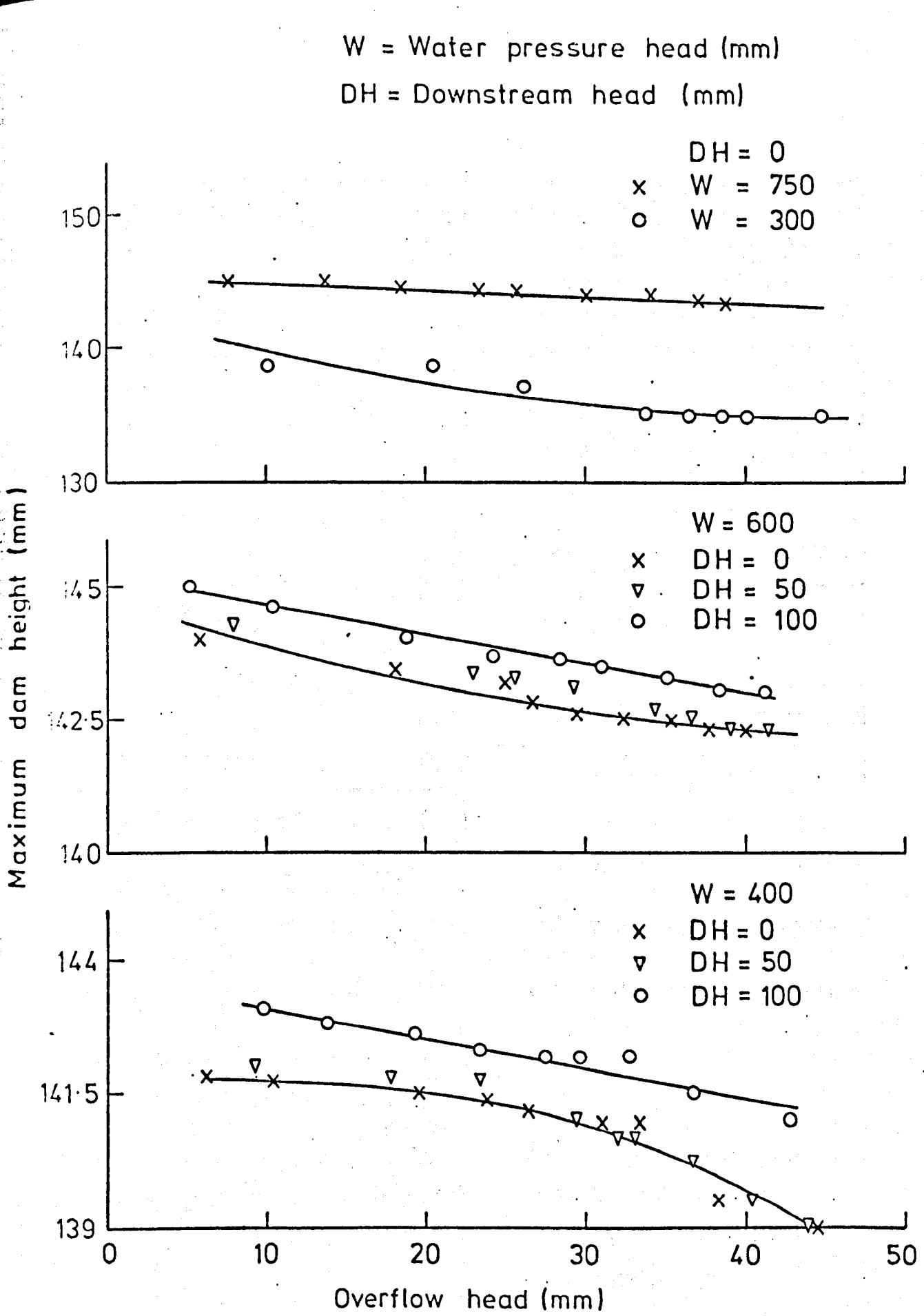

FIG.(5-6) VARIATION OF MAXIMUM DAM HEIGHT WITH OVERFLOW HEAD FOR VARIOUS WATER PRESSURES

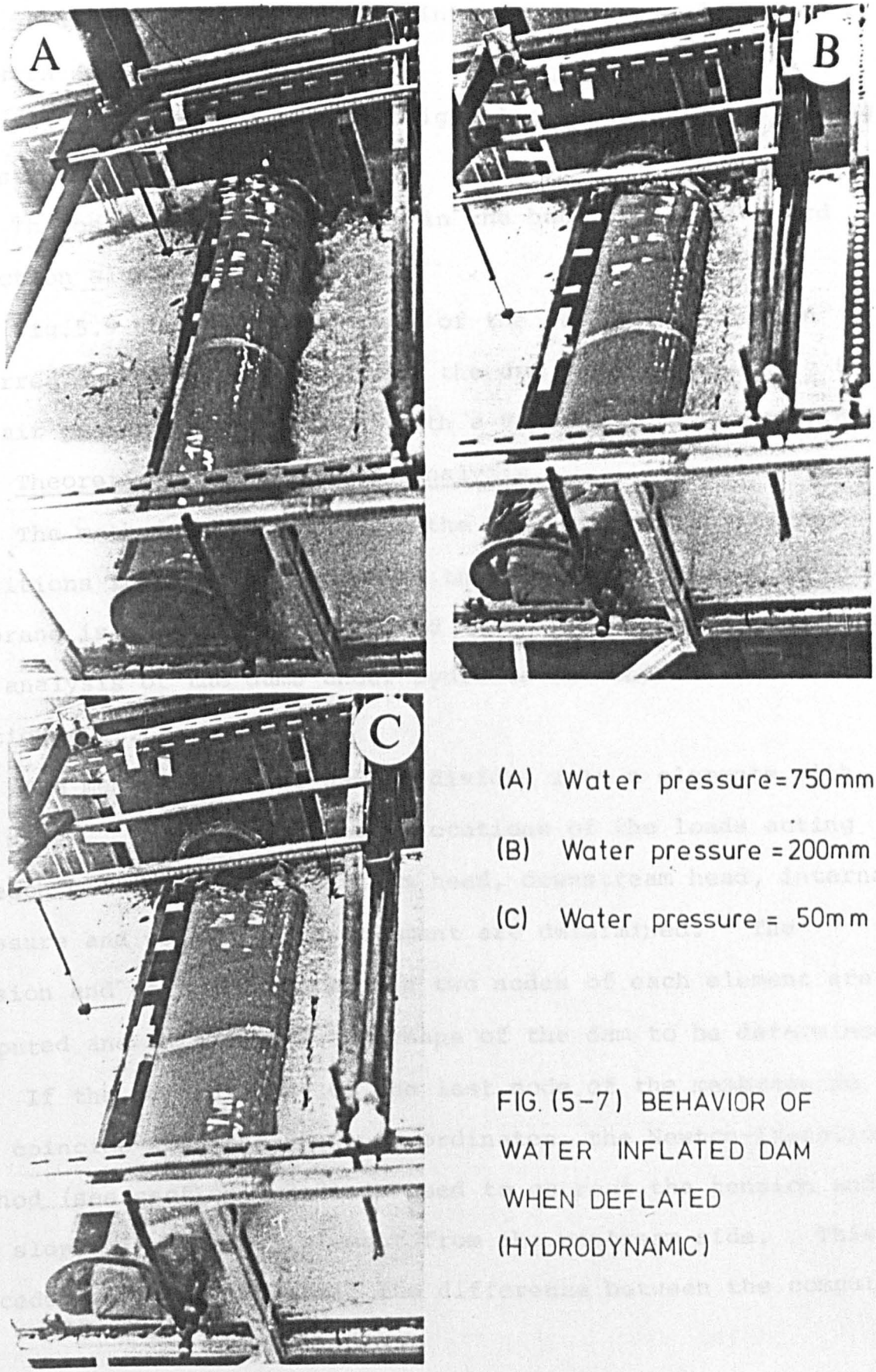

(A) Water pressure=750mm

(B) Water pressure =200mm

(C) Water pressure = 50mm

FIG. (5-7) BEHAVIOR OF WATER INFLATED DAM WHEN DEFLATED (HYDRODYNAMIC)

overflow head increased for the low internal pressure but the rate of change increased as the internal pressure decreased as illustrated in Fig.5.8A.

Fig.5.8B shows the crest height increases with increasing downstream head.

The oscillation of the dam in the backward and forward direction also occurred.

Fig.5.9 shows the behaviour of the dam when deflation occurred and Fig.5.9C shows that the dam behaved similarly to the air pressure inflated dam with a V-notch effect occurring.

5.4 Theoretical Method of Dam Analysis.

The method used to analyse the dams under hydrodynamic conditions in order to determine the shape and tension of the membrane is similar to the method which was used previously for the analysis of the dams under hydrostatic conditions (see section 4.2).

The membrane of the dam is divided into n elements with n+1 nodes. The magnitude and locations of the loads acting on each element due to upstream head, downstream head, internal pressure and weight of the element are determined. The tension and co-ordinates of the two nodes of each element are computed and this allows the shape of the dam to be determined.

If the co-ordinates of the last node of the membrane do not coincide with the known co-ordinates, the Newton-Iteration method (see section 4.2.3) is used to correct the tension and the slope of the first element from the upstream side. This procedure is repeated until the difference between the computed

A = Air pressure (kN/m²)

W = Water pressure head (mm)

DH = Downstream head (mm)

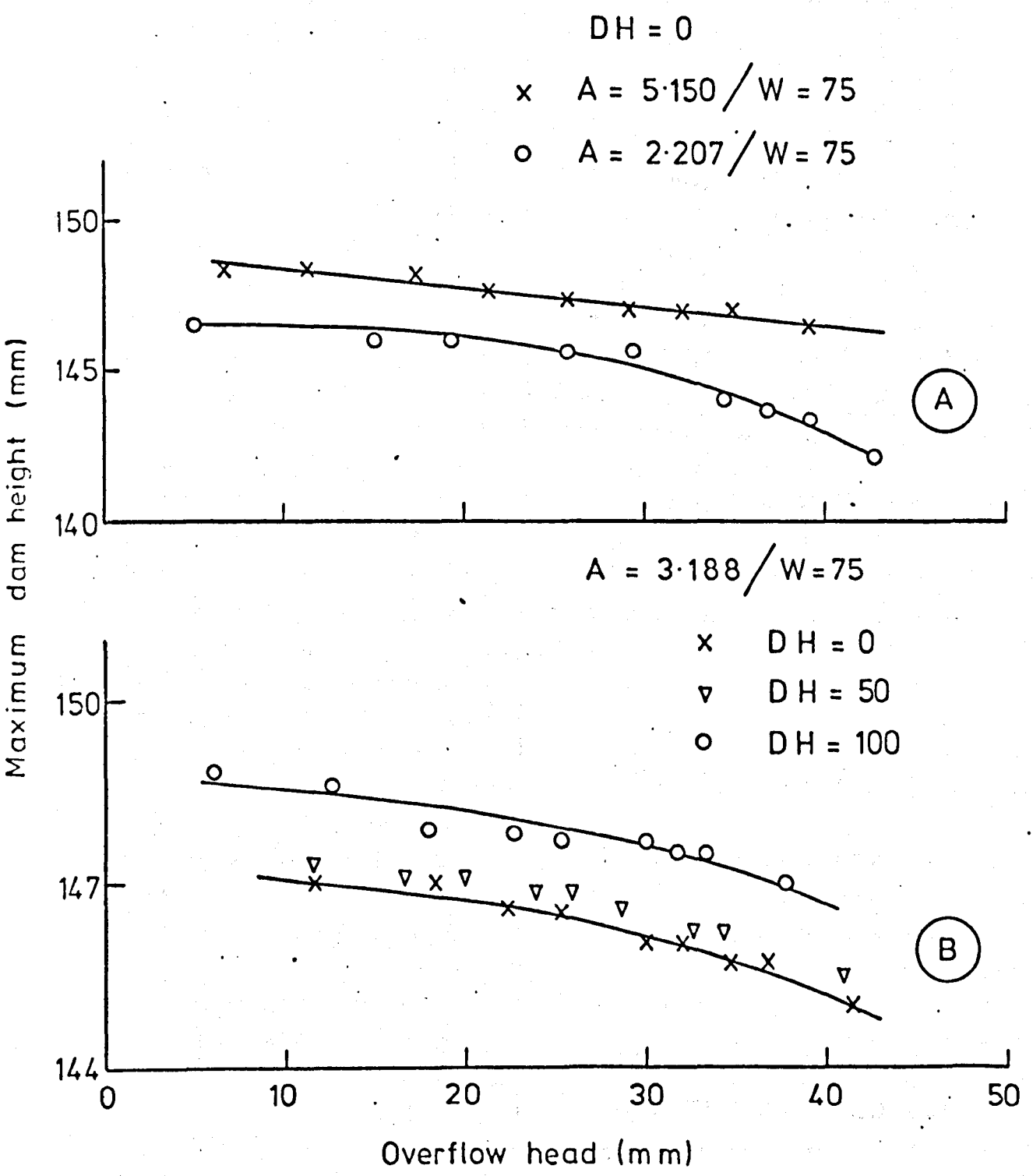

FIG. (5–8) VARIATION OF MAXIMUM DAM HEIGHT WITH OVERFLOW HEAD FOR VARIOUS AIR/WATER PRESSURES

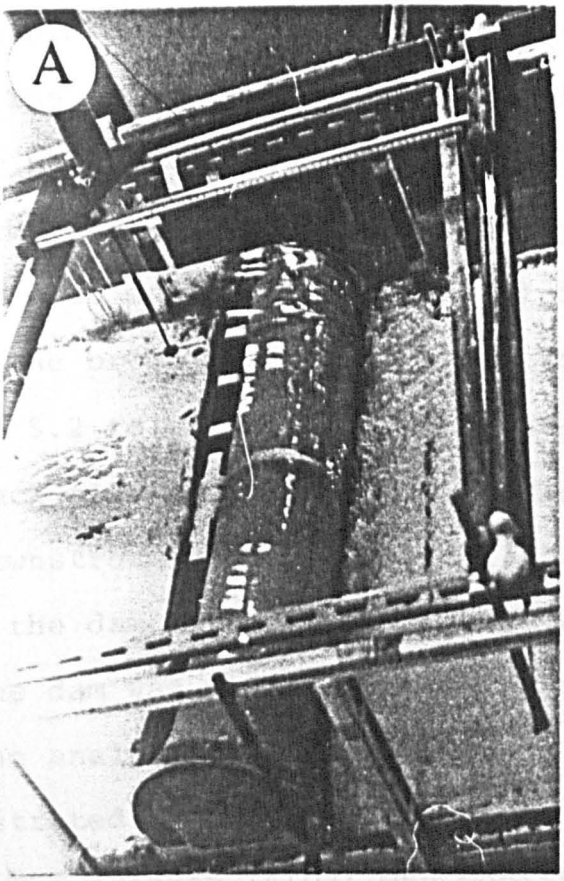

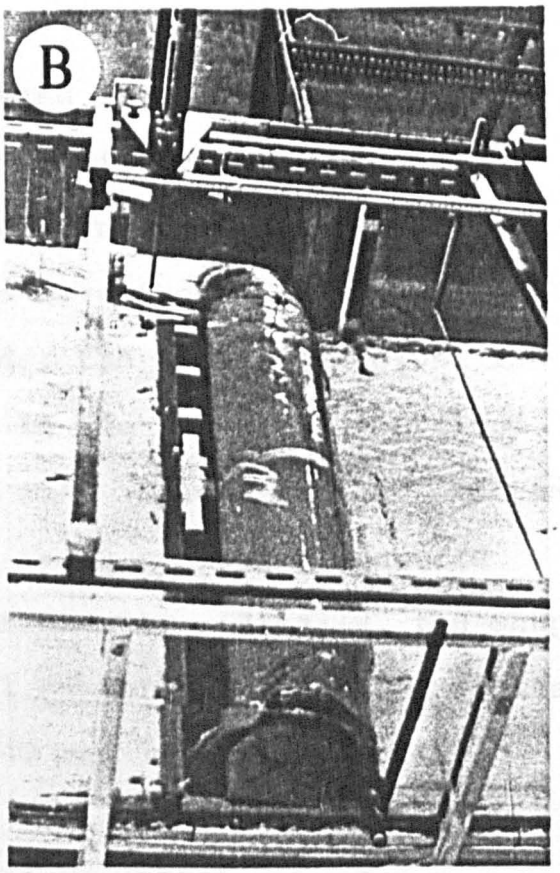

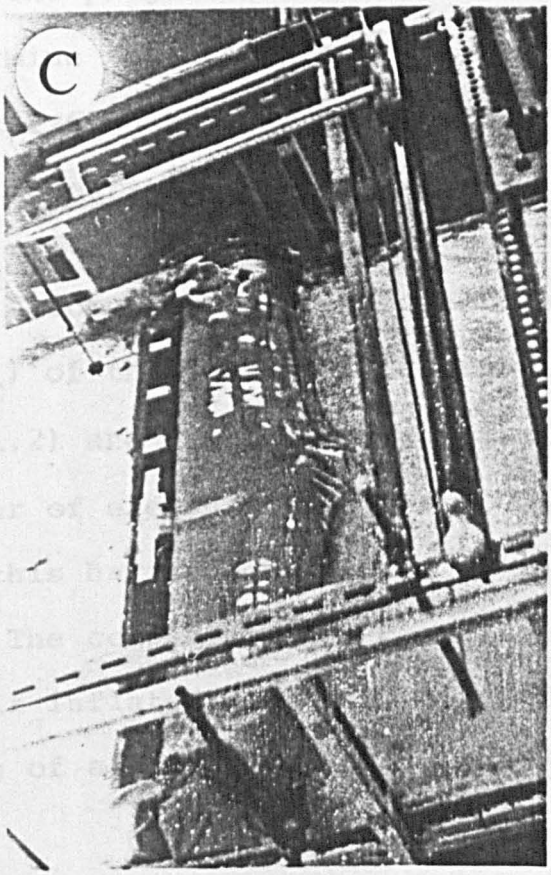

(A)
Air pressure = 5·15 kN/m^2
Water pressure = 75 mm

(B)
Combined pressure = 200 mm

(C)
Combined pressure = 60 mm

FIG.(5-9) BEHAVIOUR OF AIR/WATER INFLATED DAM WHEN DEFLATED

and known co-ordinates position of the last node is within a predetermined limit of 1 mm.

The computer program (AID1) (used for analysis of dams under hydrostatic conditions) was modified to program (AID2) in order to analyse a dam under hydrodynamic conditions. The input data of the program (AID2) is described in table 5.2.

The program analysed a dam under the conditions given in table 5.2 to calculate the tension in the membrane, the slope of each element, the length of the flat (the length of membrane at downstream side when laid flat, which sometimes occurred when the dam was inflated by low pressure). Finally, the shape of the dam was plotted. A typical example showing the results of the analysis of a dam by using 40 and 180 elements is illustrated in Fig.5.10.

The program (AID2) was modified to (AID3) in order to determine the discharge over the dam and this is described in Chapter 6.

5.5 Comparison Between Experimental and Theoretical Shapes of the Dams.

A comparison was made between the shape and crest height (Y_{max}) of the dam obtained from laboratory tests (section 5.3.1.2) and the theoretical analysis using program (AID2). The number of elements used was 40 and 180 elements and the basis for this having been justified in section 4.4.

The comparison was carried out on the results of 6 tests of air inflated dams, 10 tests of water inflated dams and 4 tests of air/water inflated dams (see table 5.1).

Card No.	Information
1	number of dams to be analysed.
2	number of elements and nodes of the membrane.
3	thickness of fabric, length of membrane and weight of fabric per unit area.
4	polynomial coefficients of the stress-strain relationship for the fabric.
5	base length, design crest height, X and Y misclose allowed, condition of analysis (static or dynamic), maximum upstream head and plot profile at maximum upstream head (see section 4.3.2.1).
6	X and Y co-ordinates of first and final node.
7	upstream head, downstream head, internal water pressure and internal air pressure.
8	X-scale and Y-scale.

TABLE 5.2 DESCRIPTION OF INPUT DATA OF PROGRAM (AID2).

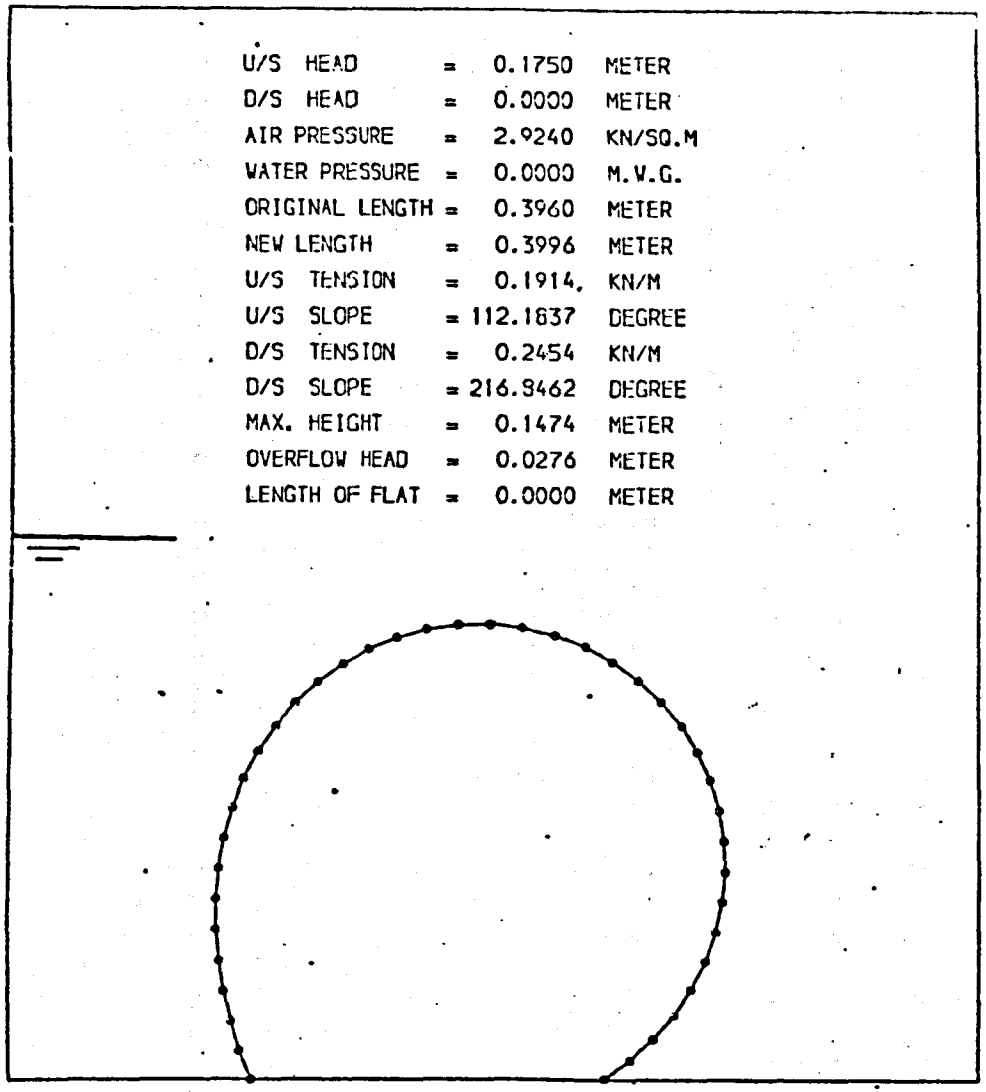

(A) 40 Elements analysis

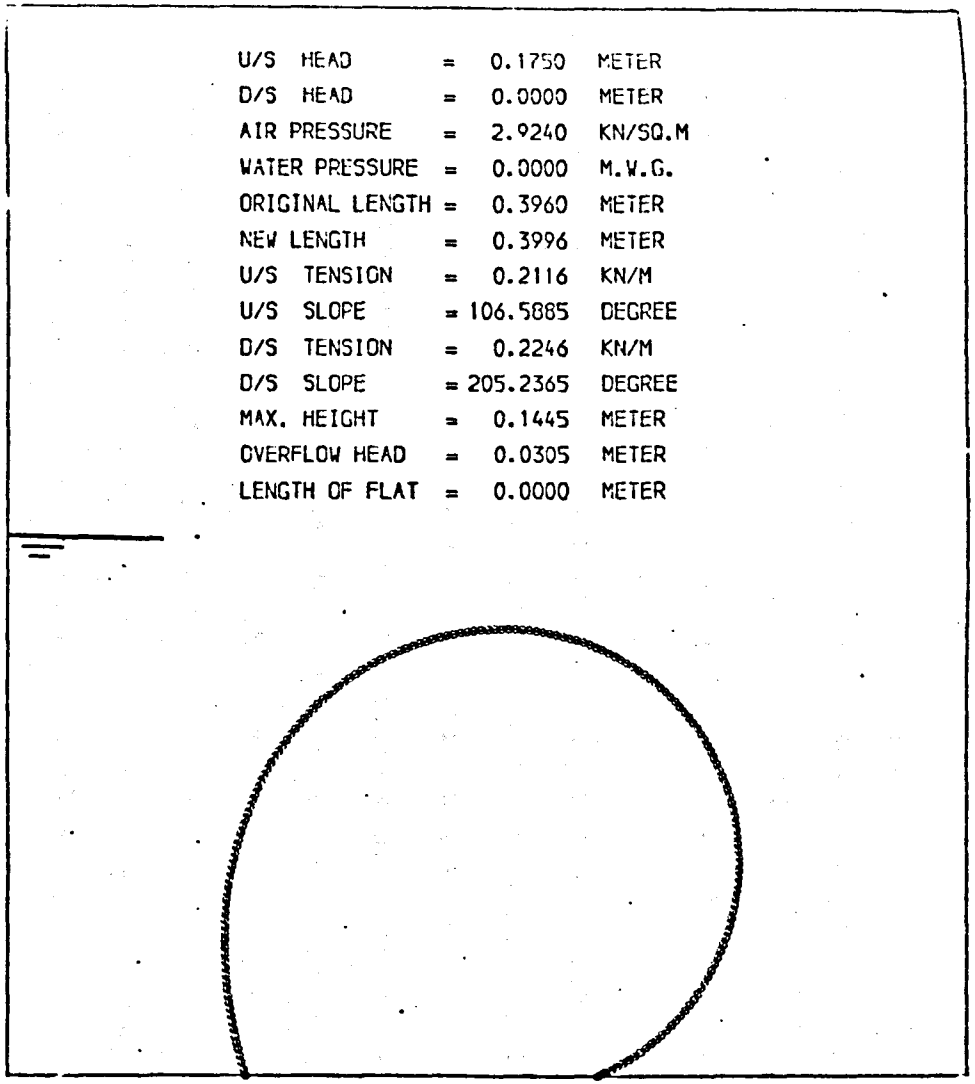

(B) 180 Elements analysis

FIG.(5-10) EXAMPLE OF OUTPUT FROM PROGRAM (AID 2) FOR ANALYSIS OF DAMS UNDER HYDRODYNAMIC CONDITIONS

Fig.5.11 illustrates an example of the comparison between the measurement shapes and the theoretical shapes of air (Fig.5.11A), water (Fig.5.11B), and, air/water (Fig.5.11C) inflated dams.

It was evident from this figure that the shape of the 180 elements dam more closely resembled the experimental shape than that predicted by the 40 element for most dams.

The results of all the comparisons are given in table 5.3. The percentage difference in shapes was calculated in a similar manner for the comparison of the dams under hydrostatic conditions (see section 4.4).

From the table 5.3 it can be seen that a higher percentage difference occurs between the theoretical and experimental shape when the dam is inflated by low pressure. This may have been due to the end effects of the dam (Fig. 4.10), as when the internal pressure was decreased and the overflow head increased the profile of the dams began to rapidly distort forward on the downstream side but the ends of the bag tried to restrain this distortion.

5.6 Effects of Operational Parameters on the Tension and the Shape of the Membrane.

The operational parameters of a dam are:

(1) Overflow head.

(2) Downstream head.

(3) Internal pressure.

The effects of the above parameters on the tension and shape of the dams were investigated by using program (AID2).

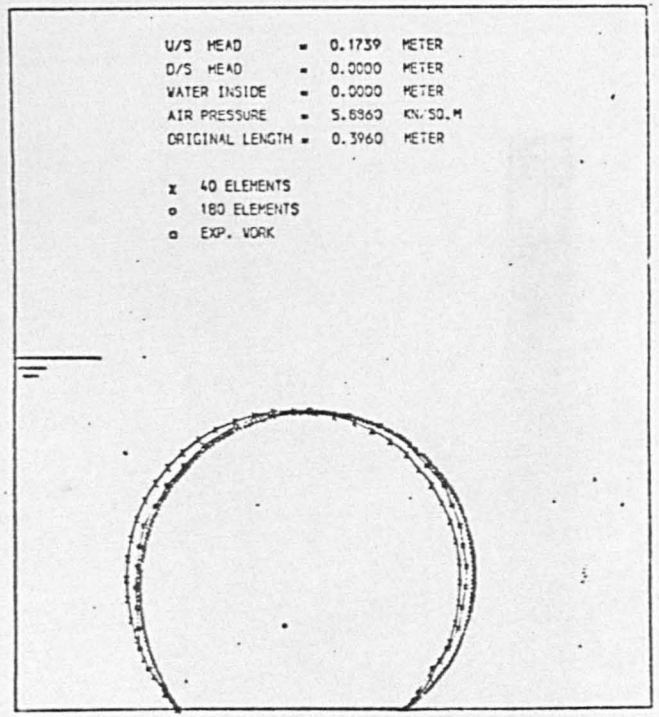

(A) Air inflated dams

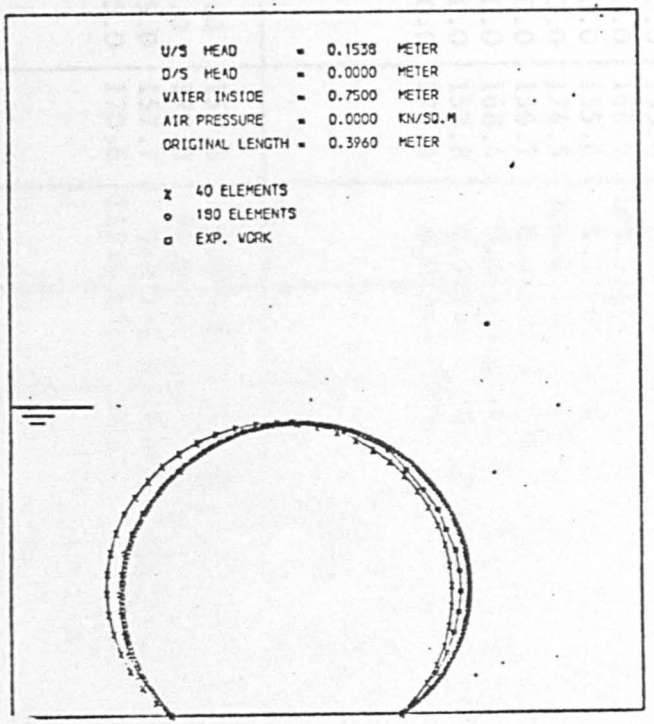

(B) Water inflated dams

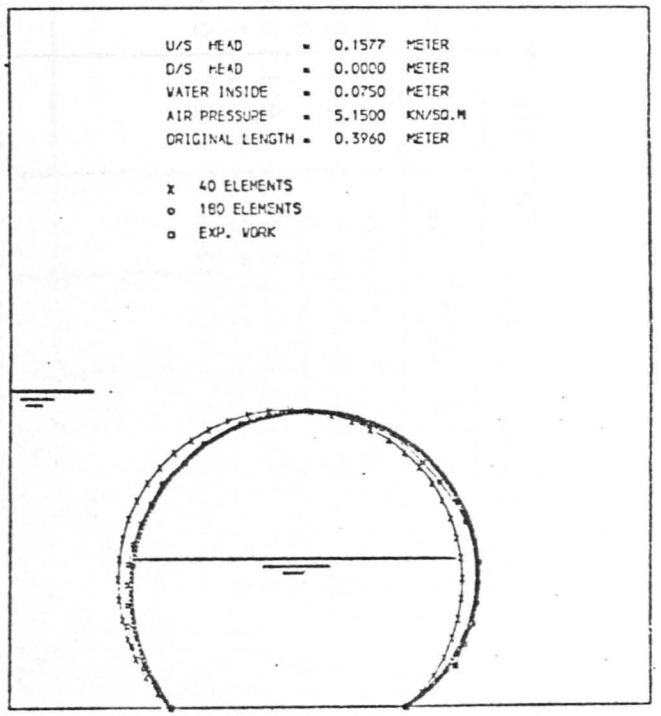

(C) Air/water inflated dams

FIG. (5-11) TYPICAL EXAMPLES OF THE COMPARISON BETWEEN EXPERIMENTAL SHAPE AND THEORETICAL (40 AND 180 ELEMENTS) SHAPE OF DAMS

Test No.	Air Press. (kN/m^2)	Water Press. (mm)	U/S Head (mm)	D/S Head (mm)	Crest Height (Y_{max}) (mm)			% Abs.Diff. in Y_{max}		% Abs.Diff. in Shape	
					Exp.	40 El.	180 El.	40 El.	180 El.	40 El.	180 El.
1	1.962	0.0	161.4	0.0	147.8	147.20	143.63	0.40	2.82	9.82	9.30
2	1.962	0.0	178.0	0.0	145.8	143.46	137.97	1.64	5.37	7.56	9.77
3	3.924	0.0	163.2	0.0	148.5	147.58	146.35	0.67	1.48	3.98	6.19
4	3.924	0.0	179.0	0.0	147.7	147.50	145.62	0.14	1.42	2.88	7.00
5	5.886	0.0	156.8	0.0	148.2	147.40	146.86	0.54	0.94	6.86	2.06
6	5.886	0.0	173.9	0.0	147.6	147.64	146.57	0.03	0.69	4.98	4.02
							Mean	0.57	2.12	6.01	6.38
1	0.0	350.0	151.4	0.0	139.4	139.90	134.75	0.36	3.33	3.20	8.80
2	0.0	350.0	163.4	112.0	141.6	143.00	141.20	0.49	0.28	4.36	1.58
3	0.0	400.0	155.4	0.0	141.0	140.99	137.42	0.0	2.55	2.16	8.01
4	0.0	400.0	168.0	108.3	142.4	143.20	141.58	0.56	0.57	6.36	9.73
5	0.0	500.0	155.6	0.0	142.6	142.58	140.63	0.01	1.38	8.48	4.52
6	0.0	500.0	174.5	103.6	142.7	143.88	142.62	0.82	0.05	8.64	2.62
7	0.0	600.0	156.7	0.0	143.5	143.44	142.48	0.04	0.69	7.09	8.95
8	0.0	600.0	168.4	0.0	143.2	143.40	141.76	0.14	1.00	7.50	6.19
9	0.0	750.0	153.8	0.0	144.3	144.18	143.60	0.08	0.48	8.07	4.06
10	0.0	750.0	175.4	0.0	143.5	144.23	142.12	0.51	0.28	7.18	4.74
							Mean	0.35	1.06	6.30	5.92
1	3.188	75.0	159.6	0.0	145.5	146.76	144.16	0.86	0.92	6.47	5.88
2	3.188	75.0	173.3	94.4	146.0	147.90	146.44	1.30	0.30	9.27	2.46
3	5.150	75.0	157.7	0.0	146.0	146.65	145.64	0.44	0.24	9.51	4.70
4	5.150	75.0	170.6	115.4	146.8	147.8	147.46	0.68	0.45	8.68	3.18
							Mean	0.82	0.48	8.48	4.05

TABLE 5.3 PERCENTAGE DIFFERENCES BETWEEN EXPERIMENTAL AND THEORETICAL CREST HEIGHT AND SHAPE OF DAMS.

The number of elements used for analysis was 40 elements (see section 4.4) and N.T. fabric used for building the dams (properties of this material were described previously in section 3.3.1).

5.6.1 Effects of Operational Parameters on the Tension in the Membrane.

The mean tension in the membrane was calculated by taking the average tension between the first and last elements.

Fig.5.12 illustrates the behaviour of the tension with increasing overflow head (H) and different internal air, water and air/water pressures. A decrease in the tension with increasing overflow head can be seen to exist for all inflation types. This reduction in tension with increasing overflow head reduces the elongation of the fabric as shown in Fig.5.13, also an increase in downstream head also decreased the tension in air, water and air/water dams as shown in Fig.5.14, and would be accompanied by a reduction in the elongation of the membrane.

A comparison between calculated and measured tensions was attempted by determining experimentally the tension in the membrane using strain gauges as described in section 5.7.

5.6.2 Effects of Operational Parameters on the Shape of the Dams.

As the overflow head increases, the profile of the dam changes resulting in a decrease in the crest height of the dam (Y_{max}) (see Figs. 5.4, 5.6 and 5.8). This is due to a reduction of the tension in the membrane of the dam (Figs.5.11

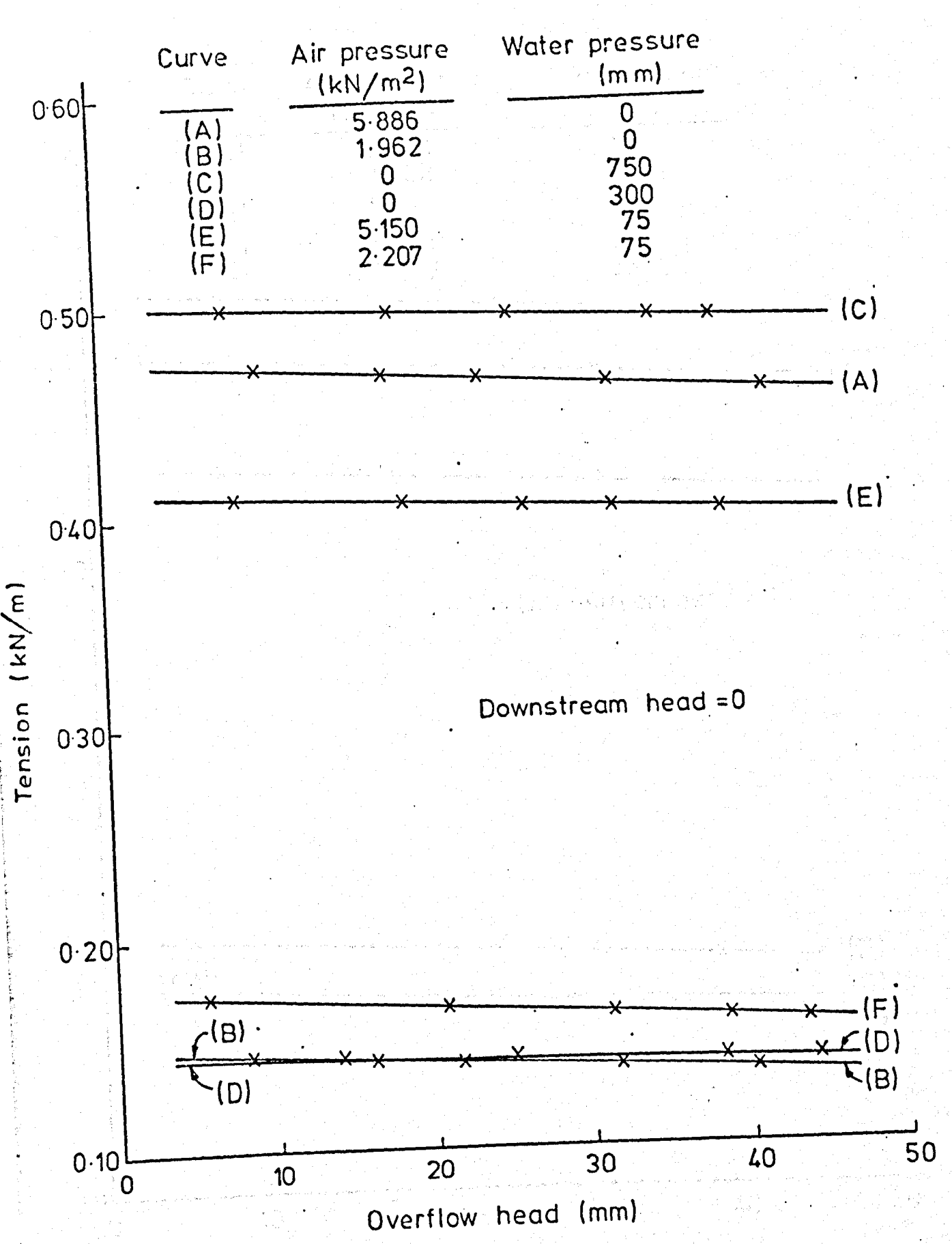

FIG. (5–12) VARIATION OF TENSION IN MEMBRANE WITH OVERFLOW HEAD FOR VARIOUS AIR, WATER AND AIR/WATER PRESSURES

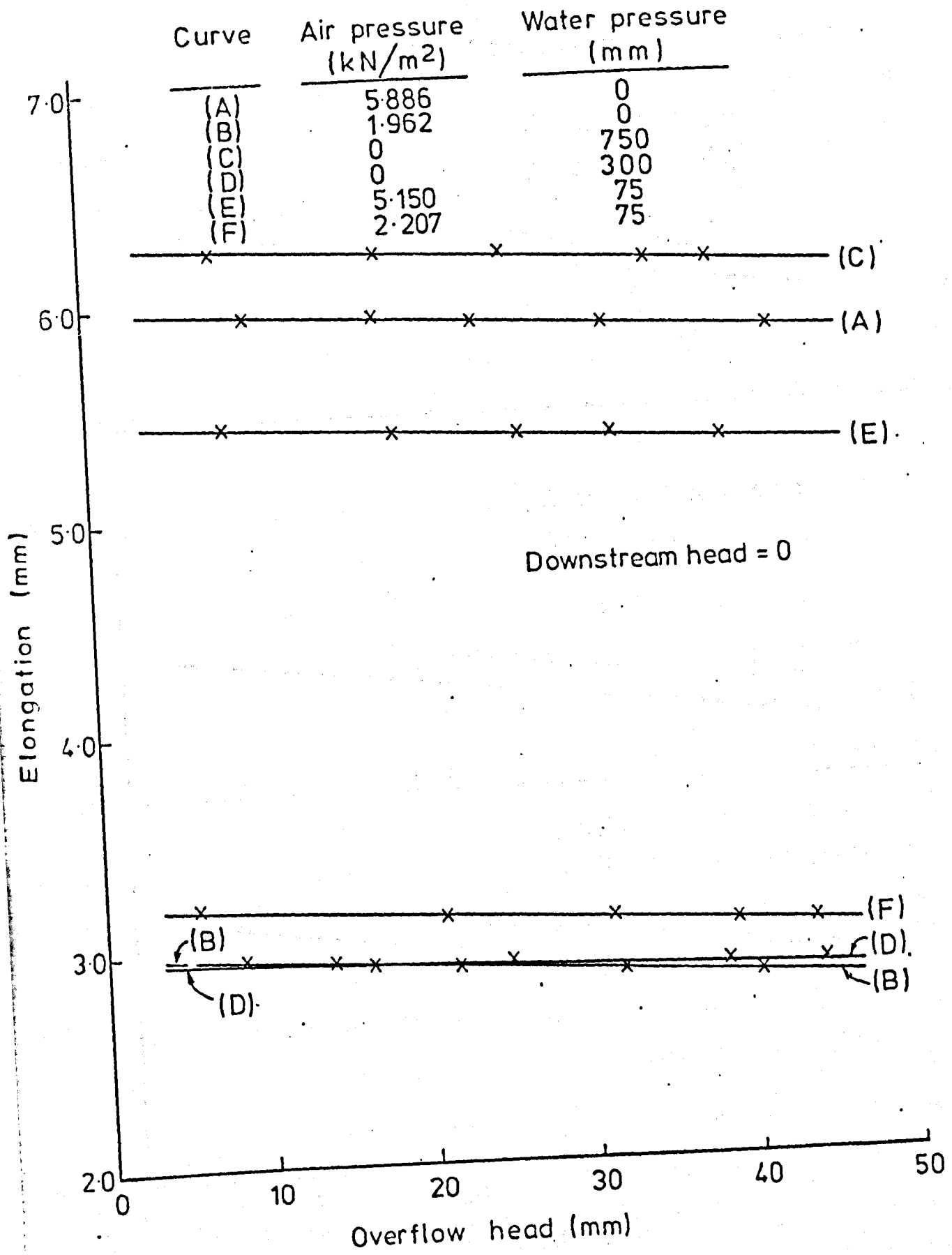

FIG. (5-13) VARIATION OF ELONGATION IN MEMBRANE WITH OVERFLOW HEAD FOR VARIOUS AIR, WATER AND AIR/WATER PRESSURES

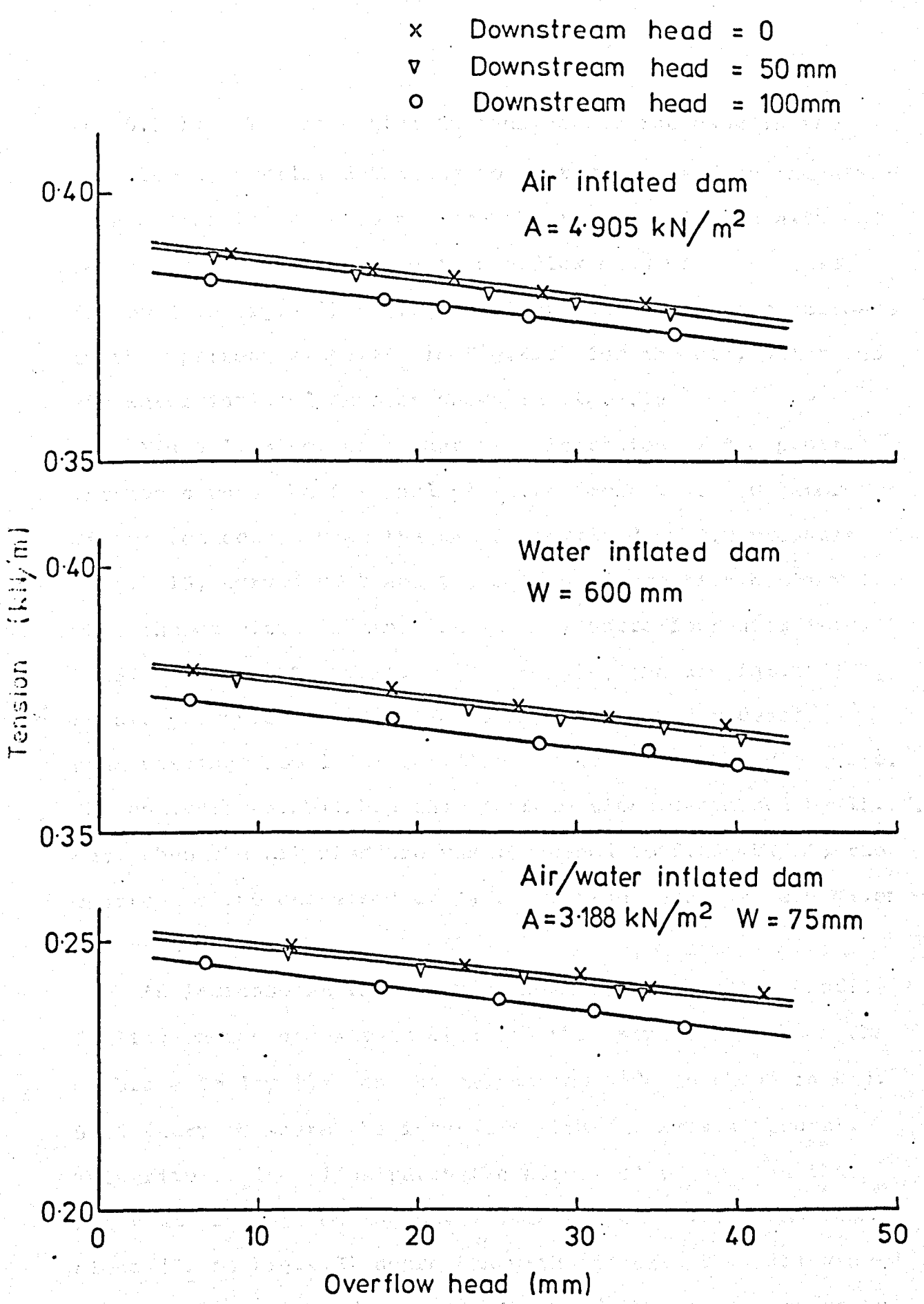

FIG. (5–14) VARIATION OF TENSION IN MEMBRANE WITH OVERFLOW HEAD FOR VARIOUS DOWNSTREAM HEADS

and 5.14). The reduction in tension and increase in the overflow head allowed the dam to distort forward on the downstream side in order to balance the increase in the external forces due to the increase in overflow head with internal forces (see Fig.4.1). This distortion results in a decrease in the upstream slope (θ_1 in Fig.4.3) for the air, water and air/water inflated dams as shown in Fig.5.15.

Fig.5.15 also shows that the distortion of the profile increases when the internal pressure decreases. Greater distortion occurs when the dam is inflated by low pressure (Fig.5.15, curves B, D and F), but the distortion becomes less when the magnitude of the internal pressure increases (Fig. 5.15, Curves A, C and E). For example, the dam inflated by an air pressure of 1.96 kN/m^2 and analysed under overflow head varying from 10 mm to 40 mm and downstream head of zero. The analysis established the upstream slope decreased by 15.8°. But, when the air pressure was increased to 5.886 kN/m^2, the upstream slope decreased by 44°. Further examples are given in table 5.4.

An increase in the overflow head results in the profile falling on the downstream side and this sometimes causes the membrane to lay flat on the downstream side as shown in Fig. 5.16 (curve D where the intersect with the x-axis occurs). This figure also illustrates the effect of changes in the internal pressure on the downstream slope. The downstream slope (θ_2 in Fig.4.2) decreases with increasing overflow head for the high inflated pressure dams and the rate of decrease

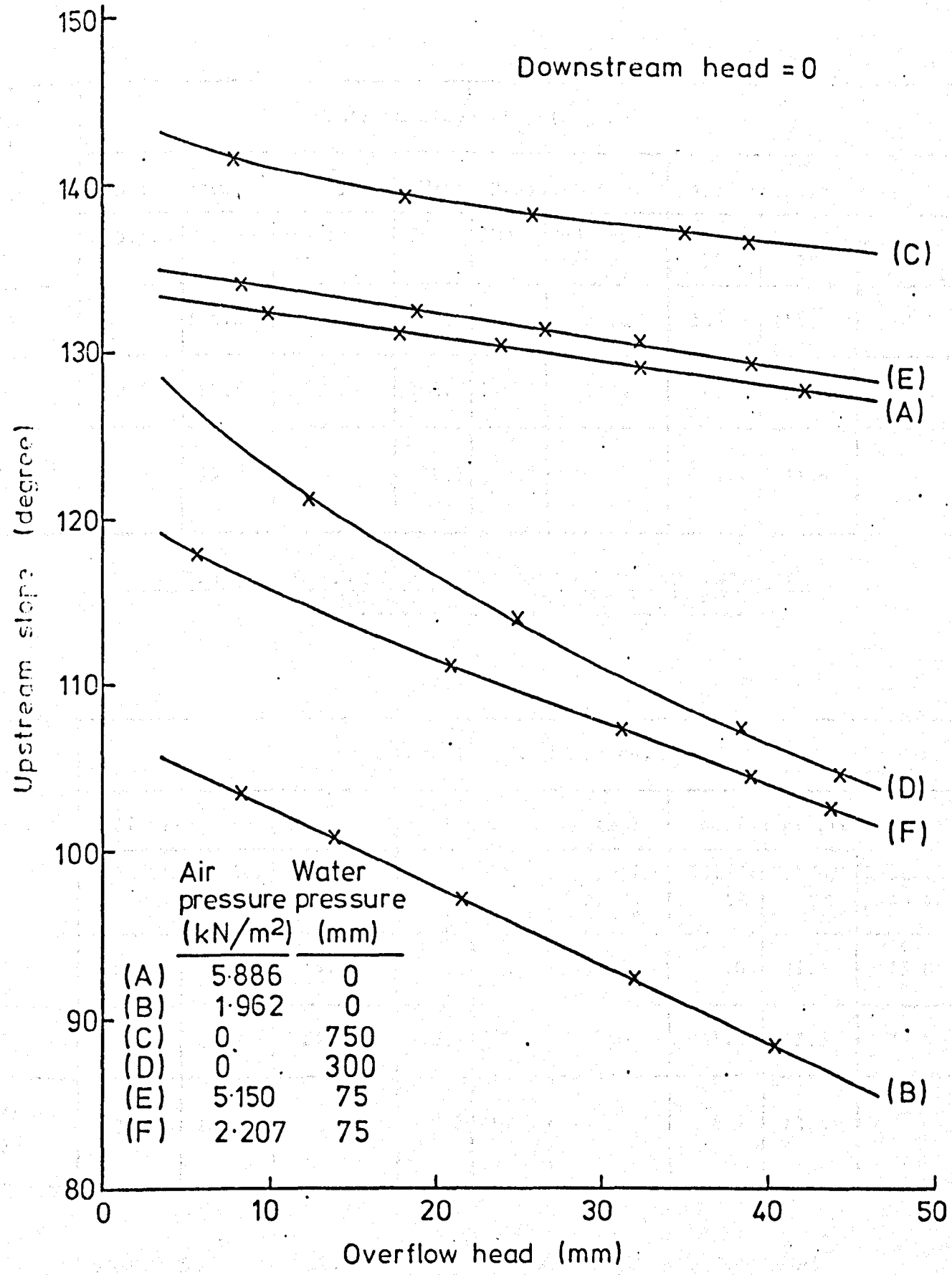

FIG. (5-15) VARIATION OF UPSTREAM SLOPE OF MEMBRANE WITH OVERFLOW HEAD FOR VARIOUS AIR, WATER AND AIR/WATER PRESSURES

Over-flow Head (mm)	Upstream Slope (θ_1) (degree)								
	Air Pressure (kN/m^2)			Water Pressure (mm)			Air/Water Pressure		
	5.886	1.962	Reduction in θ_1	750	300	Reduction in θ_1	5.150/ 75	3.188/ 75	Reduction in θ_1
10	132.4	104.0	28.4	143.0	123.0	20.0	134.0	115.6	18.4
40	128.0	88.8	39.2	126.7	116.3	10.4	129.3	104.0	25.3
duction in θ_1	4.4	15.2		16.3	6.7		4.7	11.6	

TABLE 5.4 EFFECTS OF OVERFLOW HEAD AND INTERNAL PRESSURES ON THE UPSTREAM SLOPE.

Over-flow Head (mm)	Downstream Slope (θ_2) (degree)								
	Air Pressure (kN/m^2)			Water Pressure (mm)			Air/Water Pressure		
	5.886	1.962	Reduction in θ_2	750	300	Reduction in θ_2	5.150/ 75	3.188/ 75	Reduction in θ_2
10	48.7	33.8	14.9	46.5	18.3	28.2	46.0	31.0	15.0
40	45.3	21.0	24.3	42.8	1.8	41.0	41.5	17.5	24.0
duction in θ_2	3.4	12.8		3.7	16.5		4.5	13.5	

TABLE 5.5 EFFECTS OF OVERFLOW HEAD AND INTERNAL PRESSURES ON THE DOWNSTREAM SLOPE.

becomes greater for low pressure inflated dams as shown in Fig.5.16 with examples given in table 5.5.

Tables 5.4 and 5.5 show that the water inflated dam is distorted forward more than an air and air/water inflated dam when the internal pressure is decreased. The water inflated dam is laid flat (downstream slope = 0) at the downstream side when the overflow head reaches 42.6 mm.

The effects of changes of downstream head on the upstream and downstream slopes of the dam are shown in Figs. 5.17 and 5.18 respectively. An increase in the downstream head causes the dam to distort backwards on the upstream side which results in an increase in the upstream and downstream slopes. This distortion is due to an increase in the external forces in the opposite direction to the flow which causes the reduction in the tension of the membrane (Fig.5.14) and tries to distort the dam on the upstream side. This deformation in the profile produces an increase in crest height of the dam (see Figs. 5.4 B & C, 5.6 B & C and 5.8 B).

The distortion of the cross-sectional profile of the dams under constant upstream head of 170 mm, constant downstream head of 50 mm and various internal pressures for air, water and air/water inflated dams are illustrated in Figs. 5.19, 5.20 and 5.21 respectively.

5.7 Measuring Tension in the Membrane.

The tension in the membrane of the dam was measured experimentally under overflow conditions by using nine high-elongation strain gauges (KYOWA-KFE-5.C1), distributed around

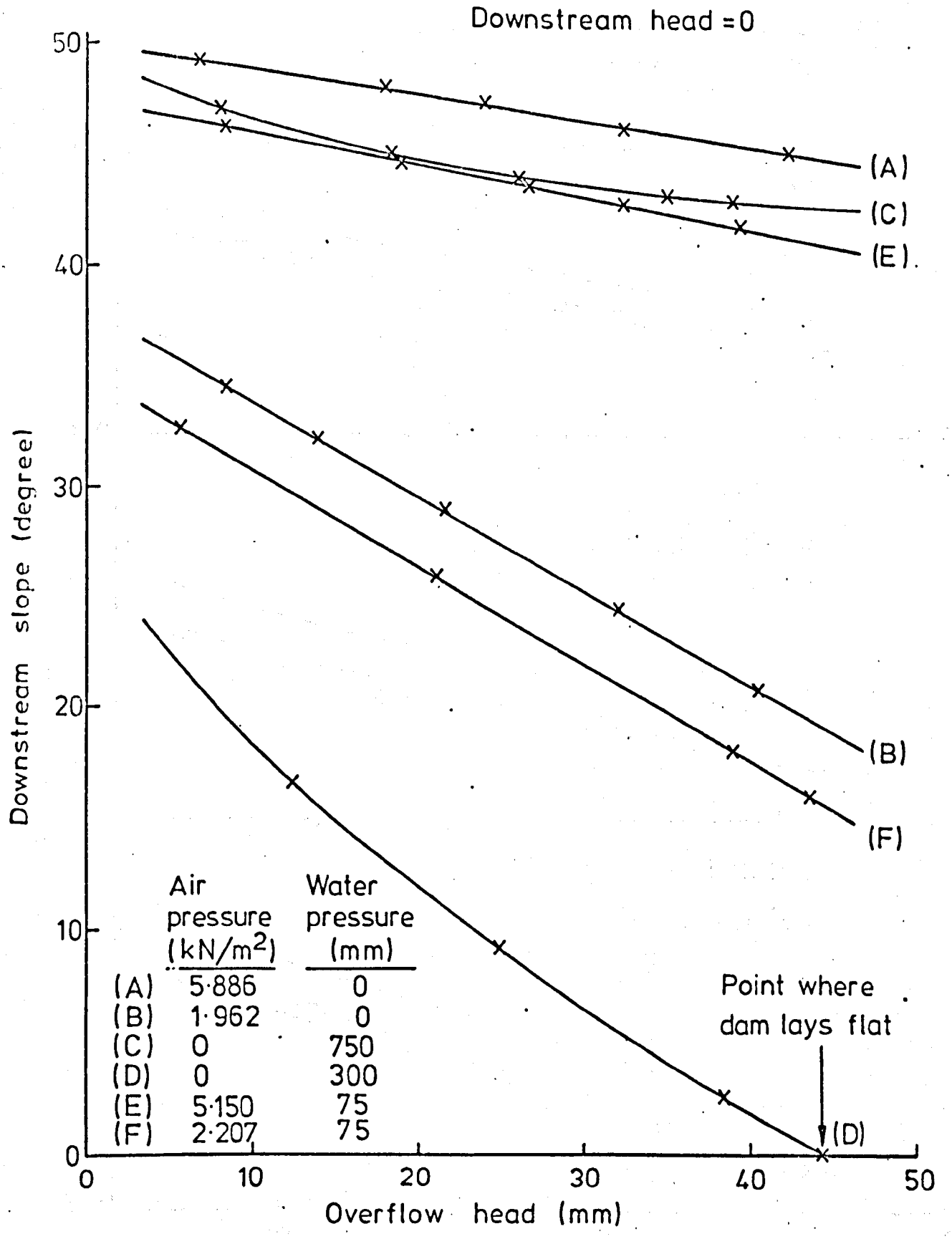

FIG. (5–16) VARIATION OF DOWNSTREAM SLOPE OF MEMBRANE WITH OVERFLOW HEAD FOR VARIOUS AIR, WATER AND AIR/WATER PRESSURES

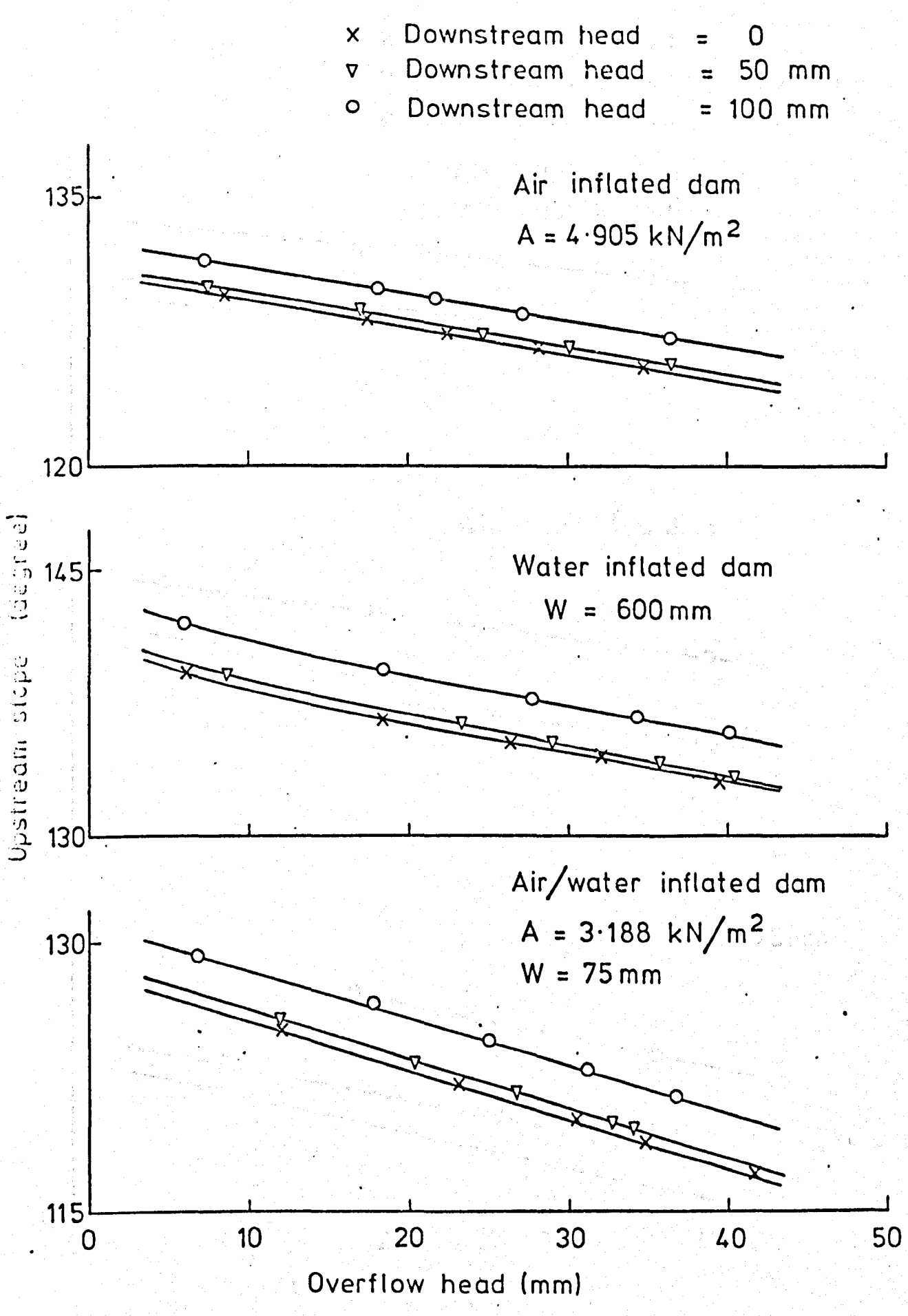

FIG. (5-17) VARIATION OF UPSTREAM SLOPE OF MEMBRANE WITH OVERFLOW HEAD FOR VARIOUS DOWNSTREAM HEADS

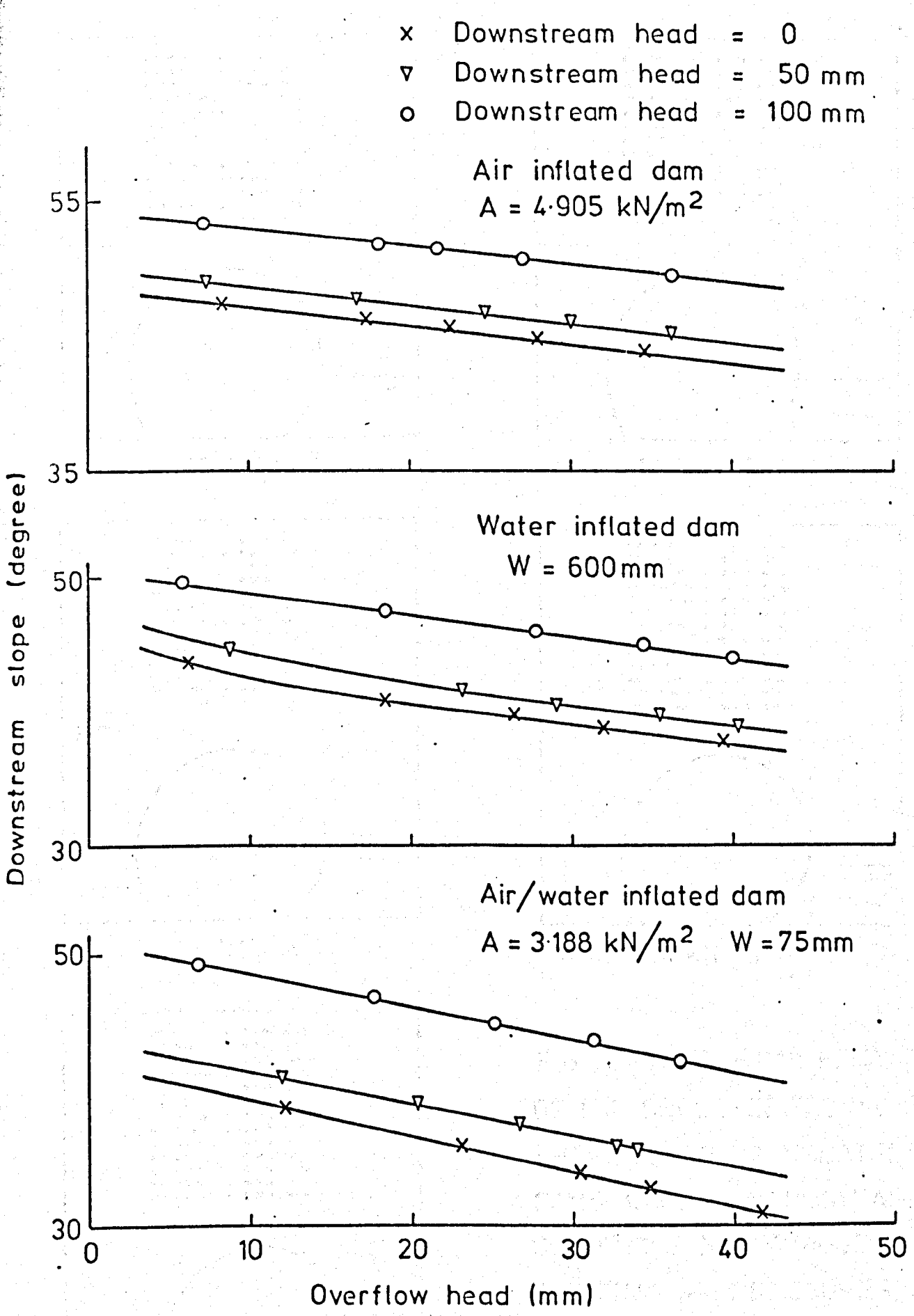

FIG. (5–18) VARIATION OF DOWNSTREAM SLOPE OF MEMBRANE WITH OVERFLOW HEAD FOR VARIOUS DOWNSTREAM HEADS

U/S HEAD	=	0.1700 METER
D/S HEAD	=	0.0500 METER
AIR PRESSURE	=	5.8860 KN/SQ.M
WATER PRESSURE	=	0.0000 M.W.G.
ORIGINAL LENGTH	=	0.3960 METER
NEW LENGTH	=	0.4019 METER
U/S TENSION	=	0.4542 KN/M
U/S SLOPE	=	124.6599 DEGREE
D/S TENSION	=	0.4824 KN/M
D/S SLOPE	=	218.3293 DEGREE
MAX. HEIGHT	=	0.1469 METER
OVERFLOW HEAD	=	0.0231 METER
LENGTH OF FLAT	=	0.0000 METER

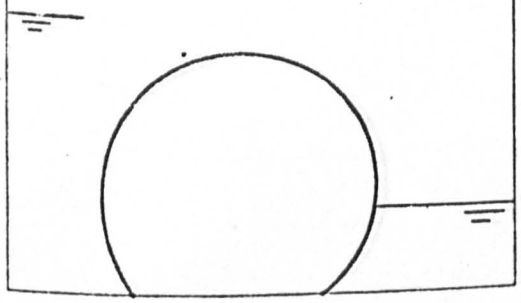

Air = 5·886 kN/m^2

U/S HEAD	=	0.1700 METER
D/S HEAD	=	0.0500 METER
AIR PRESSURE	=	4.9050 KN/SQ.M
WATER PRESSURE	=	0.0000 M.W.G.
ORIGINAL LENGTH	=	0.3960 METER
NEW LENGTH	=	0.4012 METER
U/S TENSION	=	0.3763 KN/M
U/S SLOPE	=	121.6564 DEGREE
D/S TENSION	=	0.3973 KN/M
D/S SLOPE	=	217.0448 DEGREE
MAX. HEIGHT	=	0.1468 METER
OVERFLOW HEAD	=	0.0232 METER
LENGTH OF FLAT	=	0.0000 METER

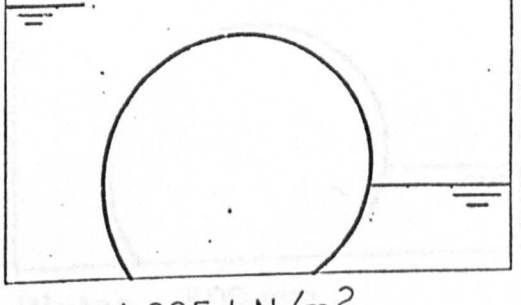

Air = 4·905 kN/m^2

U/S HEAD	=	0.1700 METER
D/S HEAD	=	0.0500 METER
AIR PRESSURE	=	3.9240 KN/SQ.M
WATER PRESSURE	=	0.0000 M.W.G.
ORIGINAL LENGTH	=	0.3960 METER
NEW LENGTH	=	0.4004 METER
U/S TENSION	=	0.2942 KN/M
U/S SLOPE	=	117.0077 DEGREE
D/S TENSION	=	0.3121 KN/M
D/S SLOPE	=	214.6627 DEGREE
MAX. HEIGHT	=	0.1464 METER
OVERFLOW HEAD	=	0.0236 METER
LENGTH OF FLAT	=	0.0000 METER

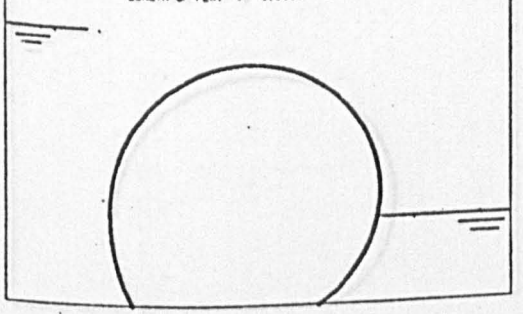

Air = 3·924 kN/m^2

U/S HEAD	=	0.1700 METER
D/S HEAD	=	0.0500 METER
AIR PRESSURE	=	2.9240 KN/SQ.M
WATER PRESSURE	=	0.0000 M.W.G.
ORIGINAL LENGTH	=	0.3960 METER
NEW LENGTH	=	0.3996 METER
U/S TENSION	=	0.2131 KN/M
U/S SLOPE	=	109.0081 DEGREE
D/S TENSION	=	0.2258 KN/M
D/S SLOPE	=	211.0593 DEGREE
MAX. HEIGHT	=	0.1459 METER
OVERFLOW HEAD	=	0.0241 METER
LENGTH OF FLAT	=	0.0000 METER

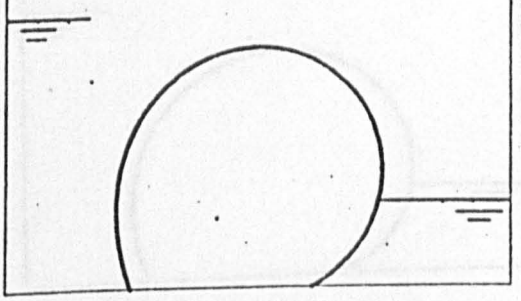

Air = 2·924 kN/m^2

U/S HEAD	=	0.1700 METER
D/S HEAD	=	0.0500 METER
AIR PRESSURE	=	1.9620 KN/SQ.M
WATER PRESSURE	=	0.0000 M.W.G.
ORIGINAL LENGTH	=	0.3960 METER
NEW LENGTH	=	0.3989 METER
U/S TENSION	=	0.1344 KN/M
U/S SLOPE	=	92.5153 DEGREE
D/S TENSION	=	0.1423 KN/M
D/S SLOPE	=	203.4668 DEGREE
MAX. HEIGHT	=	0.1434 METER
OVERFLOW HEAD	=	0.0266 METER
LENGTH OF FLAT	=	0.0000 METER

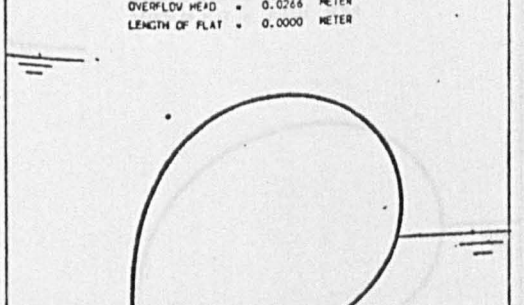

Air = 1·962 kN/m^2

FIG. (5–19) TYPICAL BEHAVIOUR OF THE CROSS-SECTIONAL PROFILES OF AIR INFLATED DAMS UNDER HYDRODYNAMIC CONDITIONS FOR VARIOUS INTERNAL AIR PRESSURES

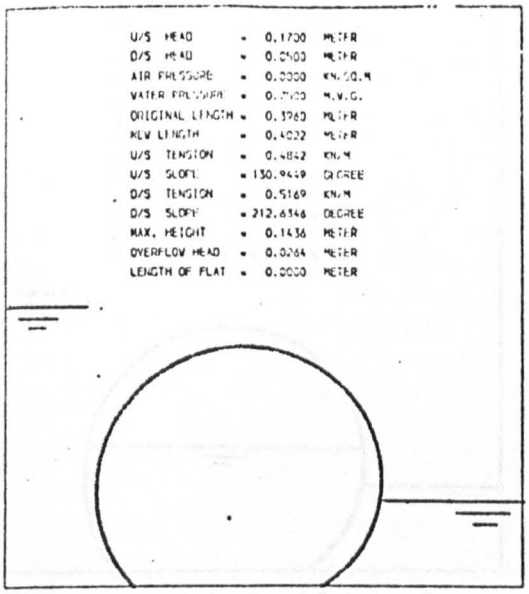

Water = 750 mm

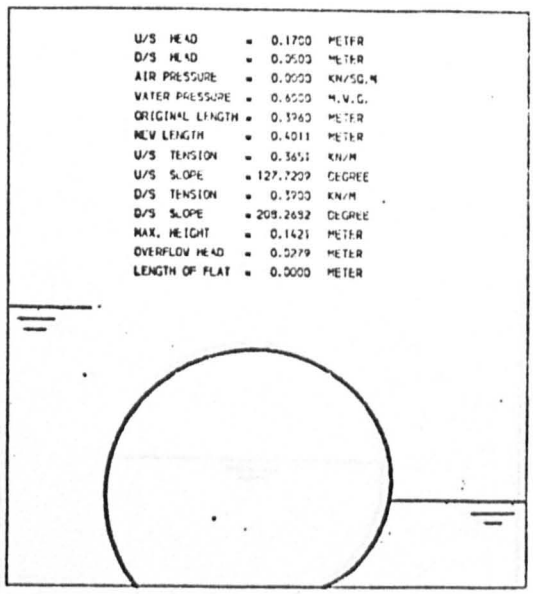

Water = 600 mm

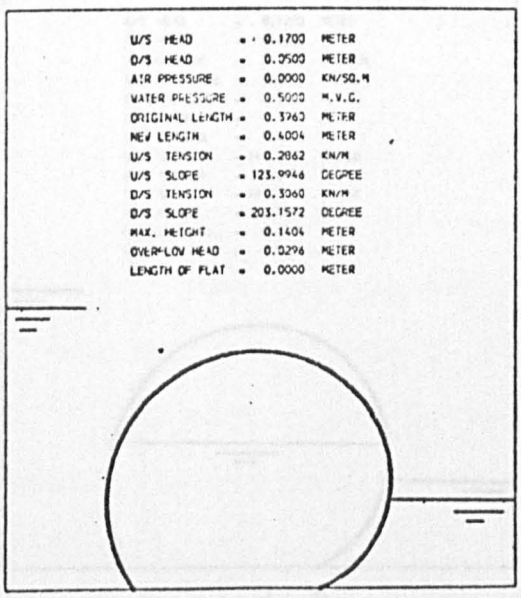

Water = 500 mm

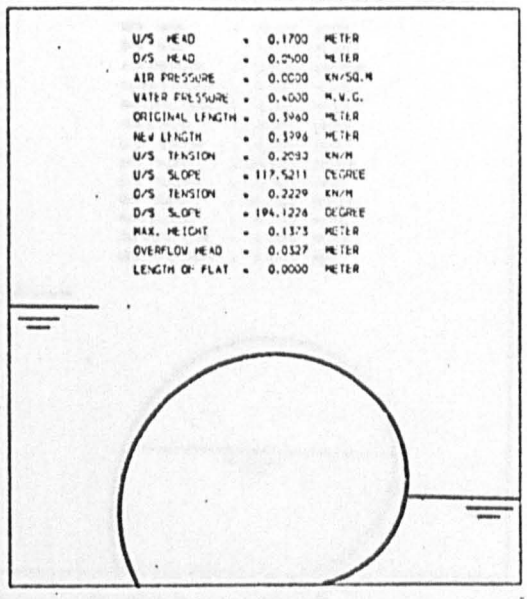

Water = 400 mm

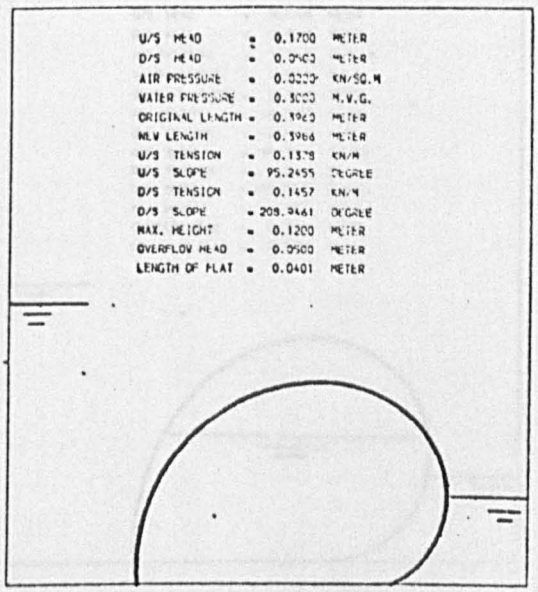

Water = 300 mm

FIG. (5–20) TYPICAL BEHAVIOUR OF THE CROSS-SECTIONAL PROFILES OF WATER INFLATED DAMS UNDER HYDRODYNAMIC CONDITIONS FOR VARIOUS INTERNAL WATER PRESSURES

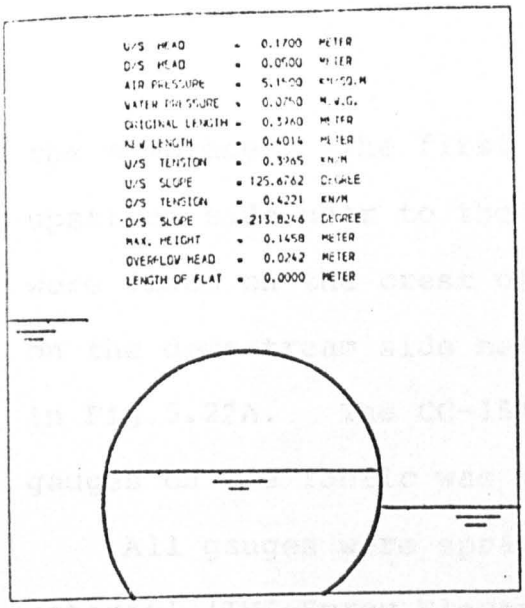

Air = 5·150 kN/m^2

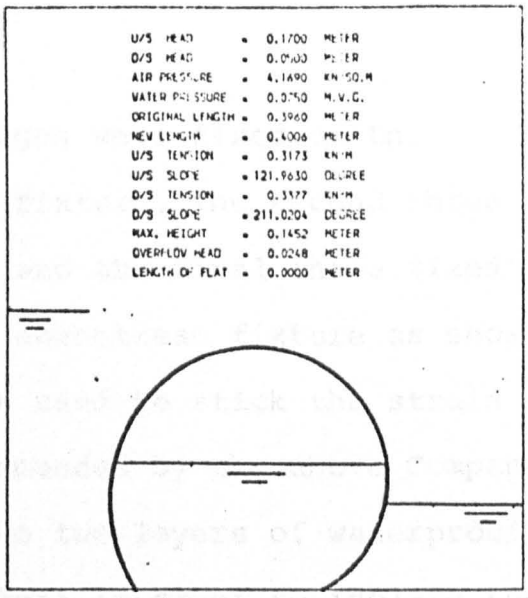

Air = 4·169 kN/m^2

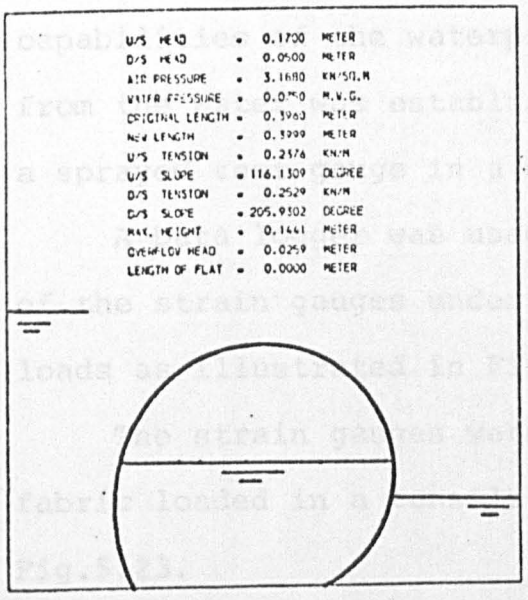

Air = 3·188 kN/m^2

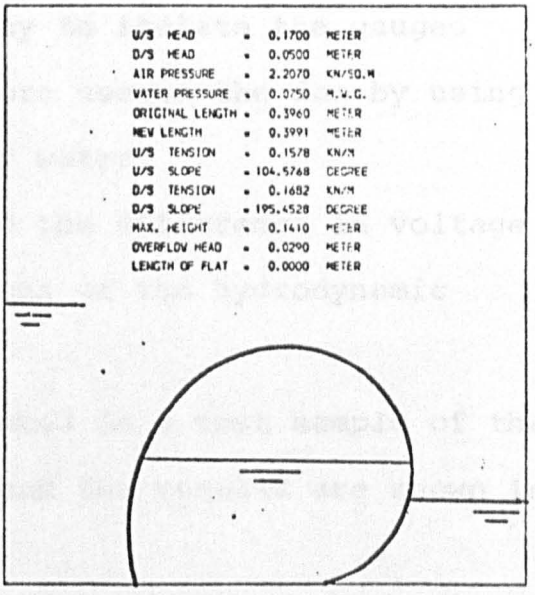

Air = 2·207 kN/m^2

Water pressure = 75mm

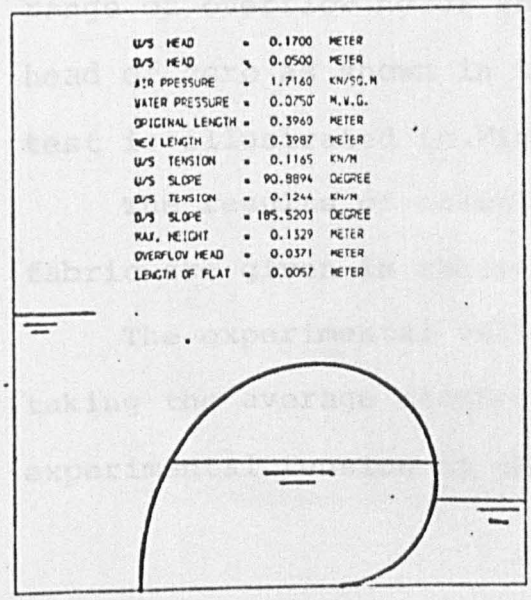

Air = 1·716 kN/m^2

FIG. (5-21) TYPICAL BEHAVIOUR OF CROSS-SECTIONAL PROFILES OF AIR/WATER INFLATED DAMS UNDER HYDRODYNAMIC CONDITION FOR VARIOUS INTERNAL AIR PRESSURES

the membrane. The first three gauges were fixed on the upstream side near to the upstream fixture, the second three were fixed on the crest of the dam and the final three fixed on the downstream side near to the downstream fixture as shown in Fig.5.22A. The CC-15A adhesive used to stick the strain gauges on the fabric was that recommended by the above Company.

All gauges were sprayed to give two layers of waterproof material (IVI-Spray Electrical Sealer) in order to isolate the wires of the gauges from water throughout the test. The capabilities of the waterproof spray to isolate the gauges from the water was established before use on the dam by using a sprayed test gauge in a beaker of water.

A Data logger was used to read the difference in voltage of the strain gauges under variations of the hydrodynamic loads as illustrated in Fig.5.22B.

The strain gauges were calibrated on a test sample of the fabric loaded in a tensile tester and the results are shown in Fig.5.23.

The dam was inflated by air pressure and tested under a range of overflow heads and internal pressures for a downstream head of zero as shown in table 5.5 and a typical dam under test is illustrated in Fig.5.22C.

The results of calculated and measured tensions in the fabric are given in table 5.6.

The experimental values of strain were calculated by taking the average readings for the nine strain gauges, and the experimental tension in the membrane was calculated from the

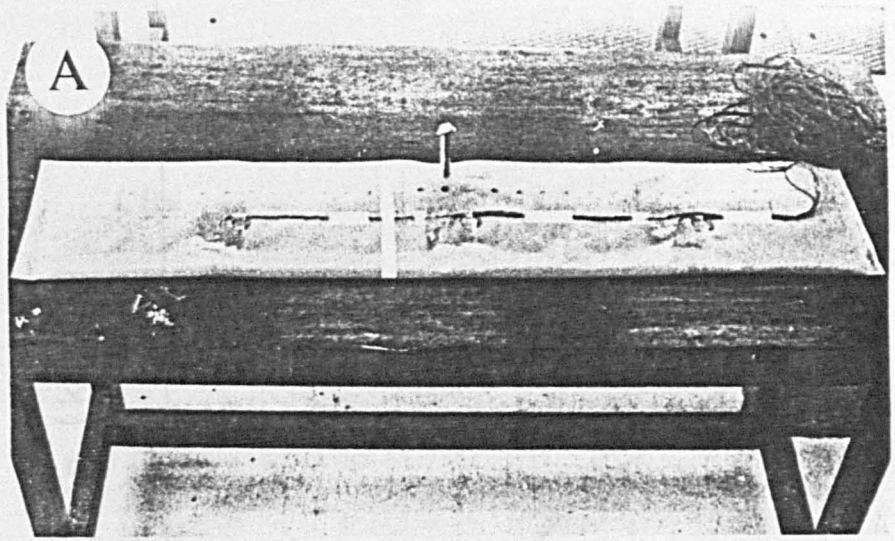

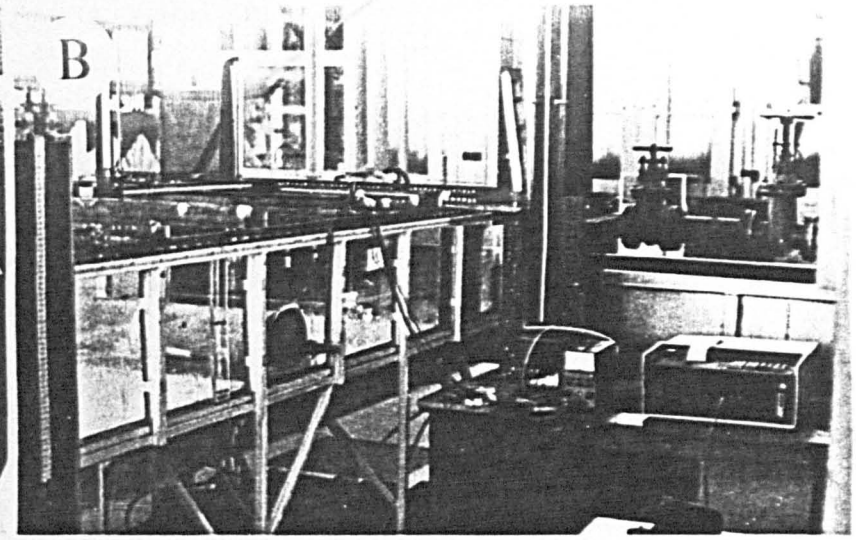

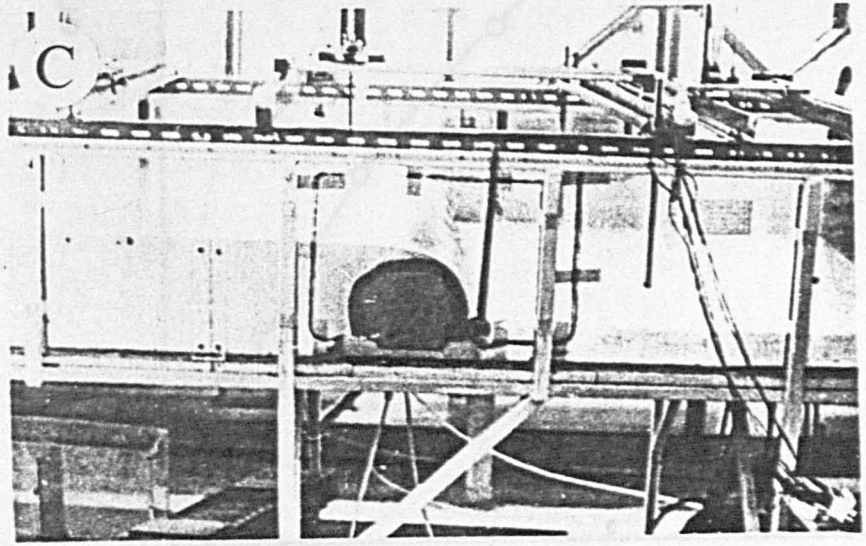

(A) Location of strain gauges on downstream side

(B) Data logger

(C) A typical dam under test

FIG. (5-22) EXPERIMENTAL MEASUREMENT OF TENSION IN THE MEMBRANE

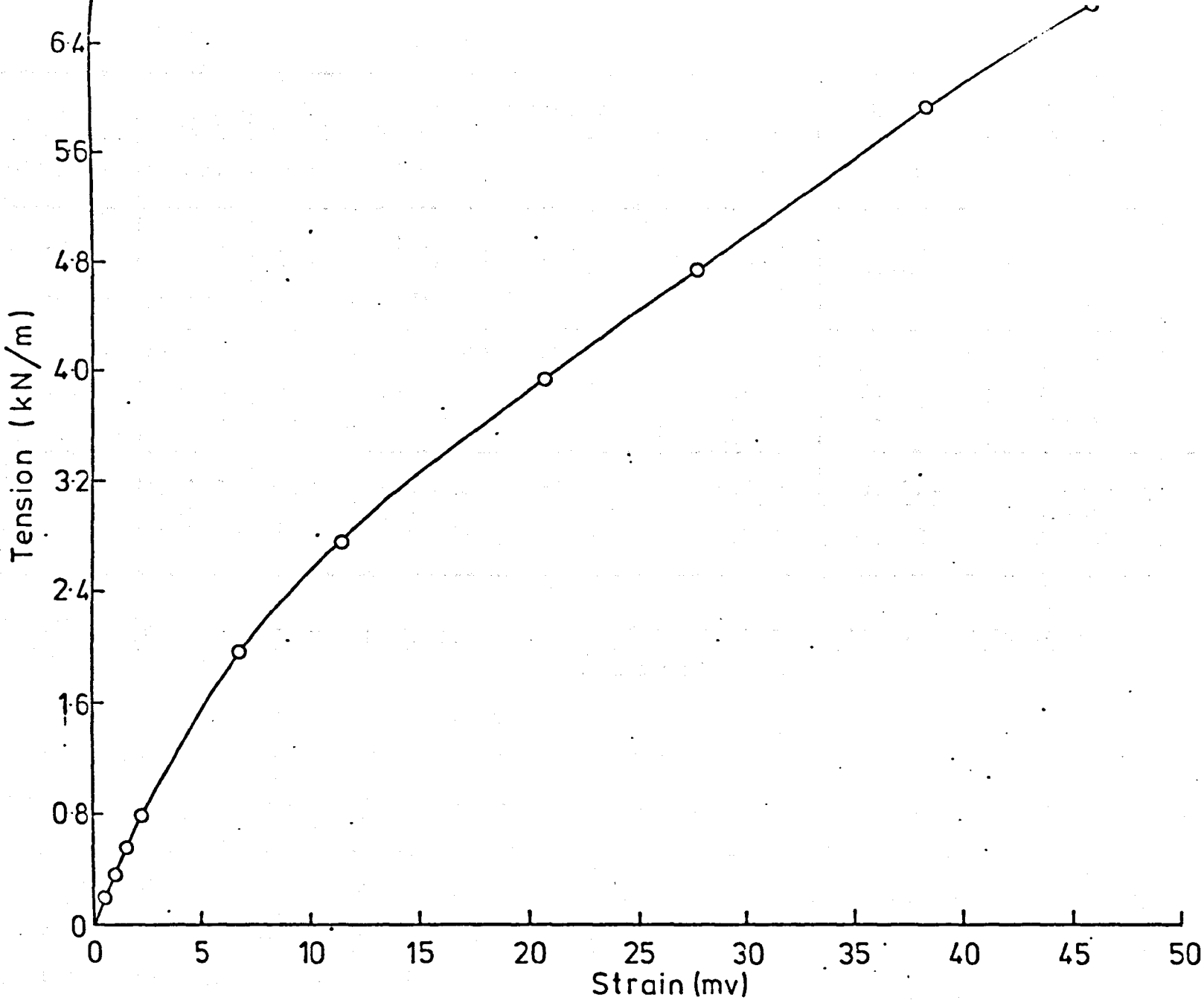

FIG. (5-23) CALIBRATION CURVE FOR THE STRAIN GAUGES

Test No.	Air Pressure (kN/m^2)	U/S Head (mm)	D/S Head (mm)	Crest Height (mm)	Overflow Head (mm)	Average Strain (mv)	Exp. Tension (kN/m)	Theor. Tension (kN/m)	% of Difference
1	1.962	161.8	0.0	146.5	15.3	0.560	0.2063	0.1442	30.1
2	1.962	171.5	0.0	145.0	26.3	0.496	0.1826	0.1407	22.9
3	1.962	179.0	0.0	143.0	36.0	0.440	0.1617	0.1371	15.2
4	3.924	163.8	0.0	147.5	16.3	0.902	0.3282	0.3054	6.9
5	3.924	173.8	0.0	147.0	26.8	0.845	0.3086	0.3017	2.2
6	3.924	181.0	0.0	146.8	34.2	0.785	0.2876	0.2989	3.9
7	5.886	162.7	0.0	148.0	14.7	1.390	0.4824	0.4672	3.1
8	5.886	168.5	0.0	147.5	21.0	1.353	0.4777	0.4661	2.4
9	5.886	176.7	0.0	147.0	29.0	1.162	0.4539	0.4630	2.0

TABLE 5.6 COMPARISON BETWEEN EXPERIMENTAL AND THEORETICAL TENSIONS IN THE FABRIC.

calibration curve shown in Fig.5.23, which was plotted by using a polynomial curve fitting method of degree 3.

The theoretical tension was calculated from an analysis of the dams under the same hydrostatic conditions by program (AID2). It can be seen from table 5.6 that the difference between the experimental and theoretical tension varied from 2 to 30 percent. The high percentage difference occurred when the dam was inflated by low air pressure (1.962 kN/m^2) and this difference may be due to the effect of the higher membrane curvature bending the strain gauge out of a flat plane, a variation in temperature and a difference in the stress-strain behaviour of the strain gauges and fabric (stress-strain relationship of the strain gauges is linear, but for the fabric it is non-linear).

However, it was felt that the exercise demonstrated that the theoretical and experimental tensions were of similar magnitude given the limitation of the equipment. A more comprehensive set of tests was not considered justified at this stage.

CHAPTER 6.

DISCHARGE COEFFICIENT FOR INFLATABLE DAMS.

6.1 Introduction.

For calculating the flow over hydraulic structures in the form of various types of weir for a known head, standard formulae can be used all incorporating a coefficient of discharge which can usually be found from standard texts[30,31]. Typically such structures have a constant shape under all conditions of both overflow head and downstream head.

The shape of an inflatable dam however changes under varying overflow head, downstream head and internal pressures. The shape also changes if the membrane length, base length and membrane material are changed. Because of this change in shape the relationship between head and discharge is more complex and variations in the coefficients of discharge are more significant than conventional structures where the coefficient in many instances is assumed constant.

Baker[1] and Clare[8] determined the coefficient of discharge (C_D) experimentally for a water inflated dam by using equation (6.1)

$$C_D = q/H^{3/2} \quad \ldots\ldots \quad (6.1)$$

where

q = discharge per unit width (cfs/ft)

H = overflow head (ft)

They both found that C_D varied from 3.0 for low flows to 4.0 for high flows. As C_D in equation 6.1 is not dimensionless then these numerical values are only applicable to the system of units used in the original work.

Both Anwar[6] and Stodulka[11] carried out an independent series of experiments on both air and water model dams and used equation (6.2) to calculate values of C_D

$$C_D = q/H\sqrt{2g.H} \quad \ldots\ldots \quad (6.2)$$

with q and H as previously defined, g = the acceleration due to gravity.

Anwar found that C_D varied from 0.35 to 0.5 and also that C_D was dependent on the ratio of H/Y_{max} (where Y_{max} is the height of the dam) with a high ratio associated with a higher C_D value.

Stodulka found that C_D varied from 0.25 to 0.45 with no indication of associating the variations with higher or lower flow rates.

Research was carried out by the Ministry of Overseas Development[16] on the value of C_D for water inflated model dams and they found that the coefficient was dependent on the ratio H_o/Y_{max} (where H_o is the internal water head above the crest level) and that the range of C_D values varied between 0.3 and 0.4.

This chapter describes a theoretical method of calculation of the coefficient of discharge and compares these values of C_D with both an experimental value of C_D and those derived by other workers. This chapter also describes the effect of variations of overflow head, downstream head and internal pressure on the value of C_D for a particular dam.

6.2 Discharge Measurement.

A rectangular channel with a rectangular sharp crested weir at the outlet was designed and connected to the outlet of the test tank (see section 3.2) to replace the galvanised channel, as shown in Fig.6.1.

The channel was made from a 1.5 mm steel sheet and was 3.0 m long, 0.6 m wide and 0.35 deep. Two baffles were fitted acorss the flow, each baffle consisting of three layers of hexagonal aluminum mesh, 16 mm thick. The baffles were placed 0.4 m apart with the upstream baffle being 1.0 m upstream of the weir plate. These baffles successfully dissipated turbulence in the flow and created more uniform conditions to assist in accurate flow measurement.

The rectangular sharp crested weir fitted at the end of the channel used for measuring the rate of flow in the system is shown in Fig.6.2. The weir plate was made from 5 mm thick brass and was designed and constructed in accordance with the British Standard B.S.3860 part 4A.

To obtain a stage-discharge relationship for the weir a volumetric calibration was carried out as described in section 6.2.1.

A piezometer was connected to the wall of the channel 0.4 m upstream of the weir crest and this was used for obtaining the depth of water above the crest.

6.2.1 Volumetric Calibration of the Weir Plate.

The standard equation for discharge over a sharp crested rectangular weir as given by[32]

$$Q = \frac{2}{3} \sqrt{2g} \cdot b \cdot C_d \cdot H_r^{3/2} \qquad \text{-----(6.3)}$$

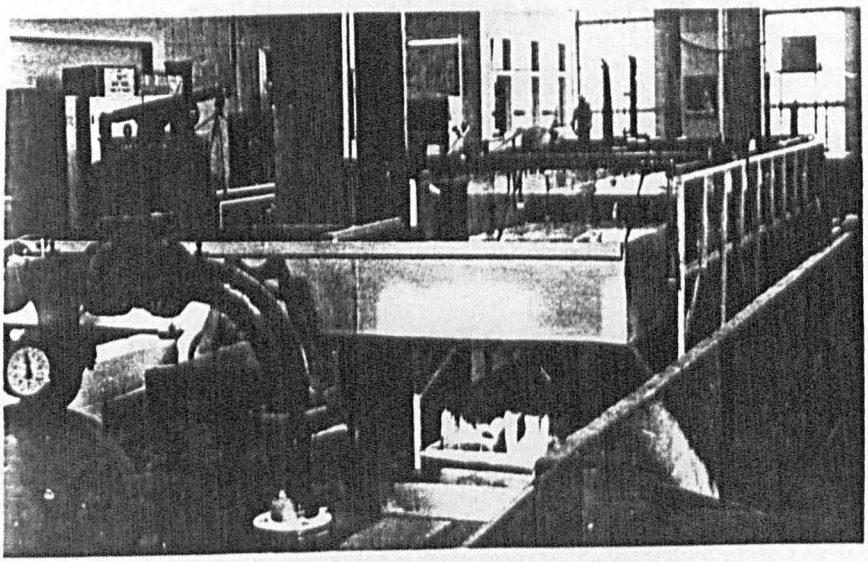

FIG. (6-1) RECTANGULAR CHANNEL

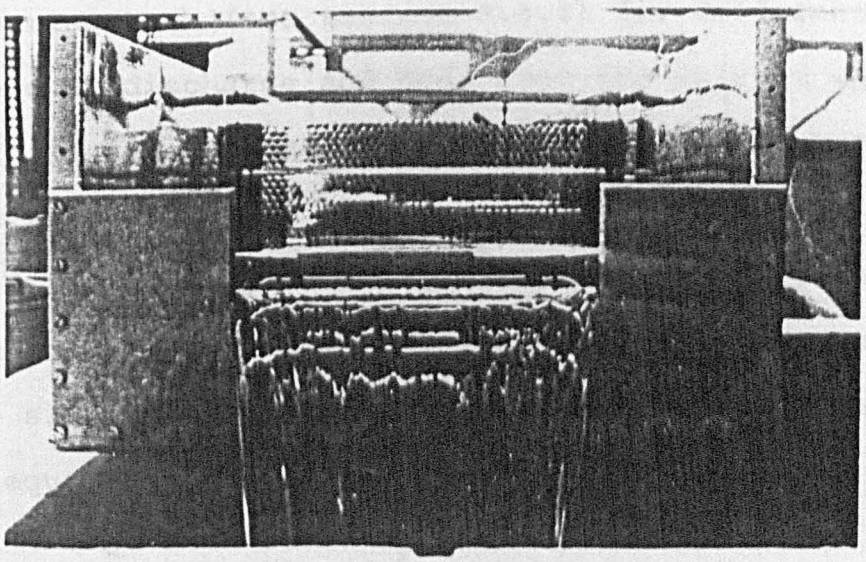

FIG. (6-2) RECTANGULAR - CRESTED WEIR

in which

Q = discharge over weir (m^3/s)

b = breadth of weir (m)

g = acceleration of gravity (m/s^2)

C_d = coefficient of discharge.

H_r = head of water above the crest level (m)

For the maximum design discharge of 18 ℓ/s and a maximum head over the weir of 95 mm with a crest height of 100 mm, the necessary breadth of the weir was evaluated as 0.32 m assuming a coefficient of discharge equal to 0.63.

By considering $\frac{2}{3}\sqrt{2g} \cdot b\ C_d$ of equation (6.3) as a coefficient K this gave a theoretical stage discharge relationship of

$$Q = 0.595\ H_r^{3/2} \quad \ldots\ldots \quad (6.4)$$

By finding the time for known volumes to accumulate in the measuring tank (see section 3.2.1) for different steady conditions of discharge and head over the weir it was possible to obtain an experimentally derived relationship between the head and the discharge.

Fig.6.3 shows a plot of $H_r^{3/2}$ against the discharge Q and from this relationship a value of K of 0.636 was found from the slope of the graph. This gave an experimentally derived equation

$$Q = 0.636\ H_r^{3/2} \quad \ldots\ldots \quad (6.5)$$

This difference in the K values in equations (6.4) and (6.5) is probably due to the estimated value of C_d in equation (6.3) together with the scale of the weir being outside the

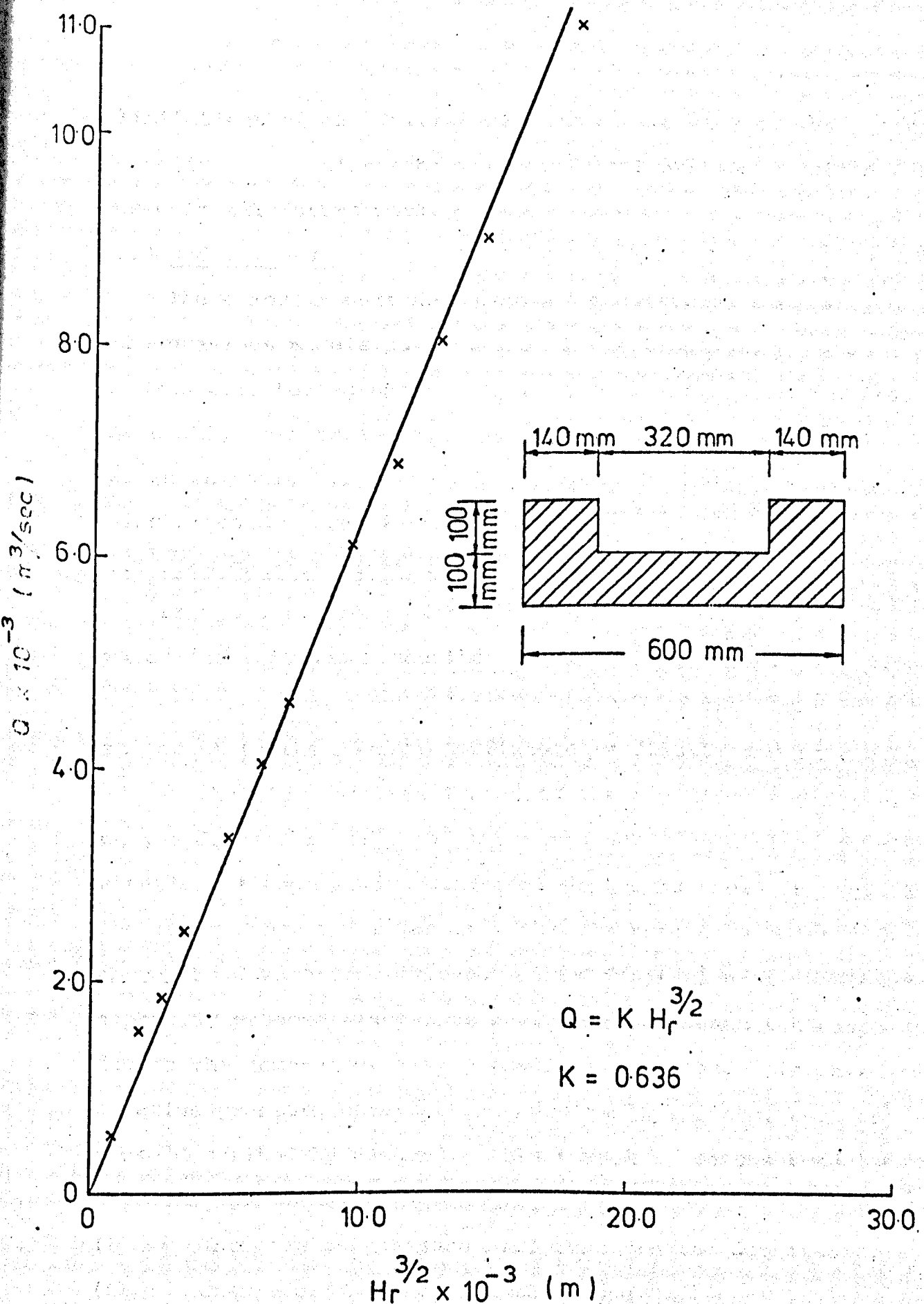

FIG. (6– 3) CALIBRATION CURVE FOR THE RECTANGULAR SHARP-CRESTED WEIR

limitations of the British Standard. In view of the difference in the K values the volumetric calibration equation was used in all future work.

6.3 Model Tests.

These models were designed and constructed similarly to the previous models as described in section 5.2. Three models were tested under different combinations of overflow head (H), downstream head (DH) and internal pressures as shown in table 6.1, with these parameters and the corresponding discharges measured in each case.

6.4 Flow Characteristics over Dams.

From observations of the flow over the air, water and air/water dams, it was noted that the lower nappe under low flows was attached continuously to the surface of the membrane from the crest to the downstream fixture as illustrated in Fig.6.4.

As the flow rate was increased the dam distorted forward on the downstream side and the nappe began to divide, forming a series of nappes with different depths as shown in Fig.6.5. The lower nappe separated from the membrane at a point just above the downstream fixture. This separation of the lower nappe may produce a negative pressure underneath the nappe due to the removal of air by the falling water. If this negative pressure occurs then undesirable effects, such as those described by Hickox[33] can result. He observed the following problems:

(i) Increase in pressure difference on the dam itself.

(ii) Change of the shape of the nappe.

Model	Overflow Head (mm)		D/S Head (mm)		Air Pressure (kN/m^2)		Water Pressure (mm)	
	Min.	Max.	Min.	Max.	Min.	Max.	Min.	Max.
Air Inflated Model	5.0	41.3	0.0	100.0	1.962	5.886	0.0	0.0
Water Inflated Model	5.6	44.5	0.0	100.0	0.0	0.0	300.0	750.0
Air/Water Inflated Model	5.0	43.5	0.0	100.0	2.207	5.150	75.0	75.0

TABLE 6.1 RANGE OF HEADS AND PRESSURES PARAMETERS FOR MODEL TESTS UNDER HYDRODYNAMIC CONDITIONS.

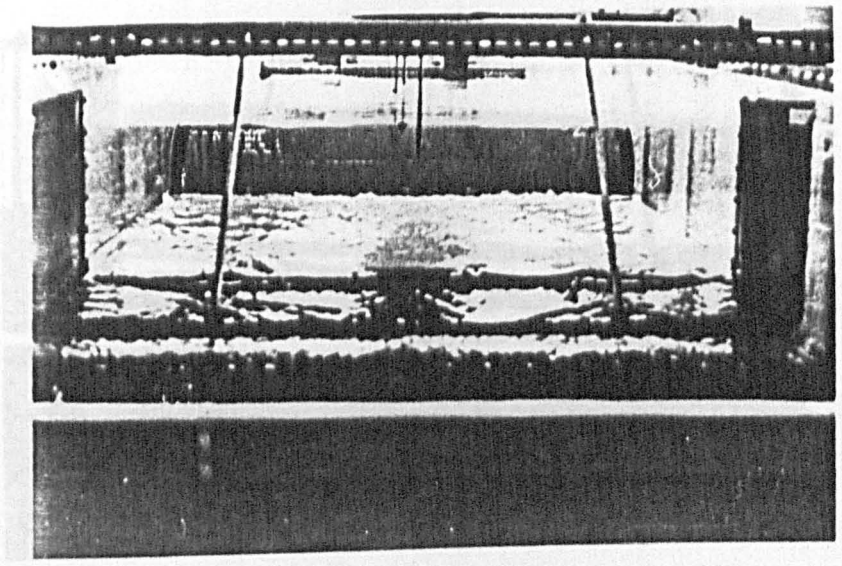

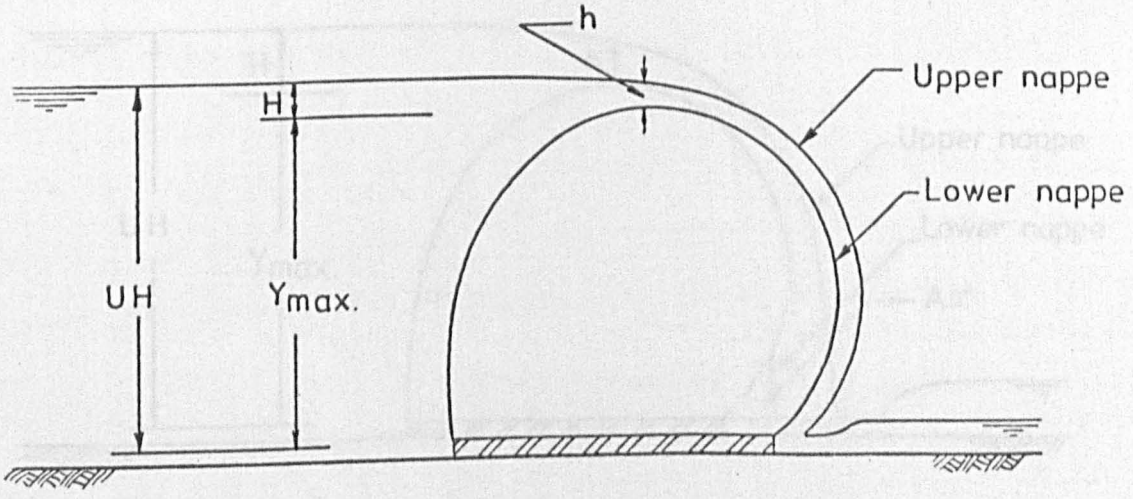

FIG. (6-4) BEHAVIOUR OF A LOW FLOW OVER THE DAM

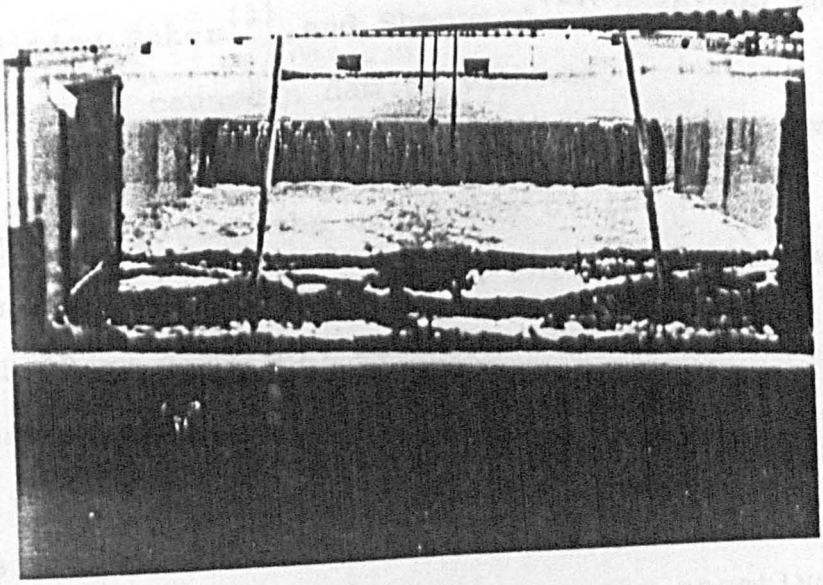

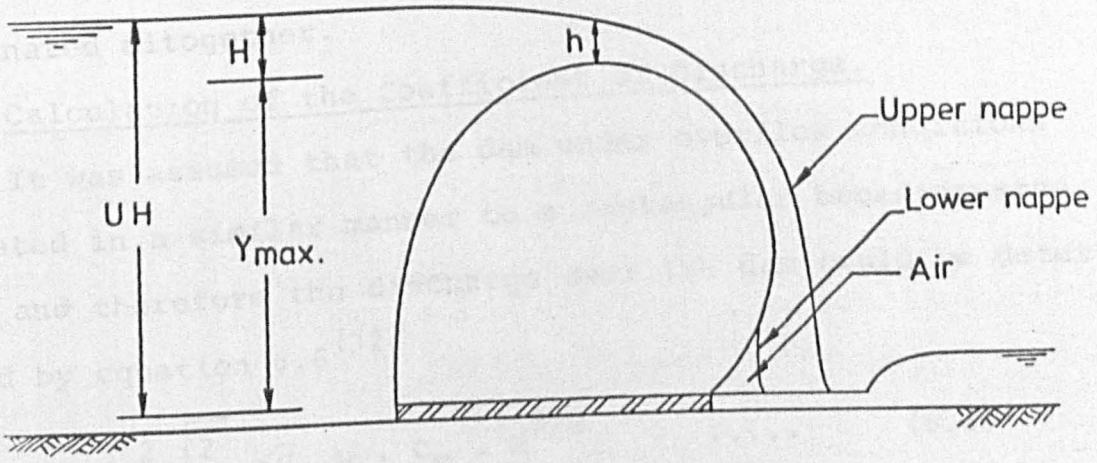

FIG.(6-5) BEHAVIOUR OF AN INTERMEDIATE FLOW OVER THE DAM

(iii) Increase in discharge over the dam.

(iv) Unstable performance of the dam.

In addition Baker[1] and Shepherd[2] observed that this negative pressure caused a dam to vibrate.

Baker reduced to a minimum the effects of a negative pressure by ventilating the underside of the nappe. This ventilation was also carried out in this study by two brass pipes, each 12 mm diameter, fitted on both sides of the dam near to the downstream fixtures as shown in Fig.6.6. The object of these pipes was to create atmospheric pressure conditions under the lower nappe.

It was observed in this study that the negative pressure area under the lower nappe was reduced as the downstream head increased and with significant increase in head could be eliminated altogether.

6.5 Calculation of the Coefficient of Discharge.

It was assumed that the dam under overflow conditions operated in a similar manner to a rectangular broad-crested weir and therefore the discharge over the dam could be determined by equation 6.6[32]

$$Q = \frac{2}{3}\sqrt{\frac{2}{3}}\ \sqrt{g}\ b \cdot C_D \cdot H^{3/2} \quad \ldots\ldots \quad (6.6)$$

in which

Q = discharge over the dam.

g = acceleration due to gravity.

b = width of the weir (normal to the direction of the flow)

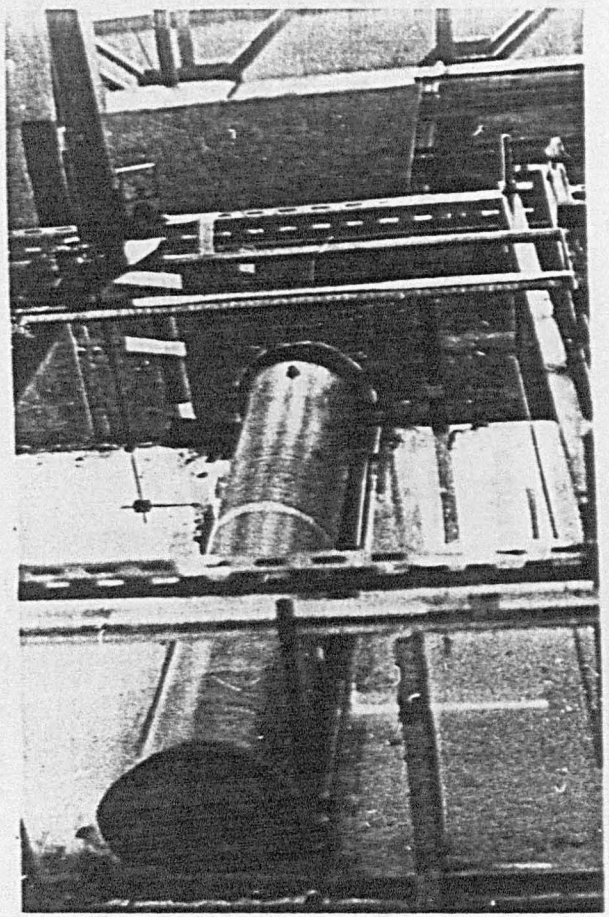

(A) Before overflow occurs

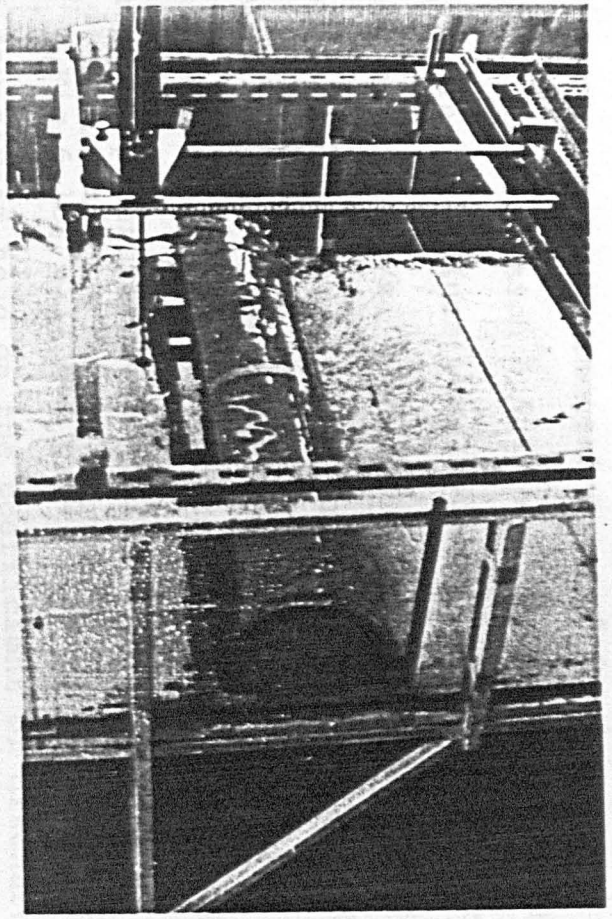

(B) Under overflow

FIG. (6-6) NATURAL VENTILATION OF THE UNDERSIDE OF THE NAPPE

C_D = coefficient of discharge.

H = overflow head.

From the experimental data of discharge and corresponding head using equation 6.6 it was possible to calculate values of C_D. The C_D values were found to vary from 0.2 to 1.10 for flow up to 18 ℓ/s, with the lower coefficients associated with lower discharges as shown in Figs. 6.7, 6.8 and 6.9 for air, water and air/water pressure dams respectively. The figures also show that the coefficient of discharge decreased as the internal pressure decreased.

Fig.6.10, 6.11 and 6.12 illustrate the effect of variation of downstream head on the coefficient of discharge with lower downstream head associated with lower coefficients of discharge.

From observations of the flow over the dams (see section 6.4), it could be expected that the discharge was dependent on the overflow head and the shape of the crest[34] (radius of curvature of the crest).

Jaegar[35] derived equation 6.7 for the flow rate of a two dimensional irrotational flow over a round-crested weir, when the radius of curvature of the flow line varied linearly with the depth of water at the crest section:

$$q = \frac{Q}{b} = \frac{1}{S-1}\sqrt{2g(H-h)} \cdot (R + Sh)^{1/S}\left[(R+Sh)^{(S-1)/S} - R^{(S-1)/S}\right] \quad \ldots\ldots \quad (6.7)$$

in which

q = rate of flow per unit width.

R = radius of curvature for surface of weir.

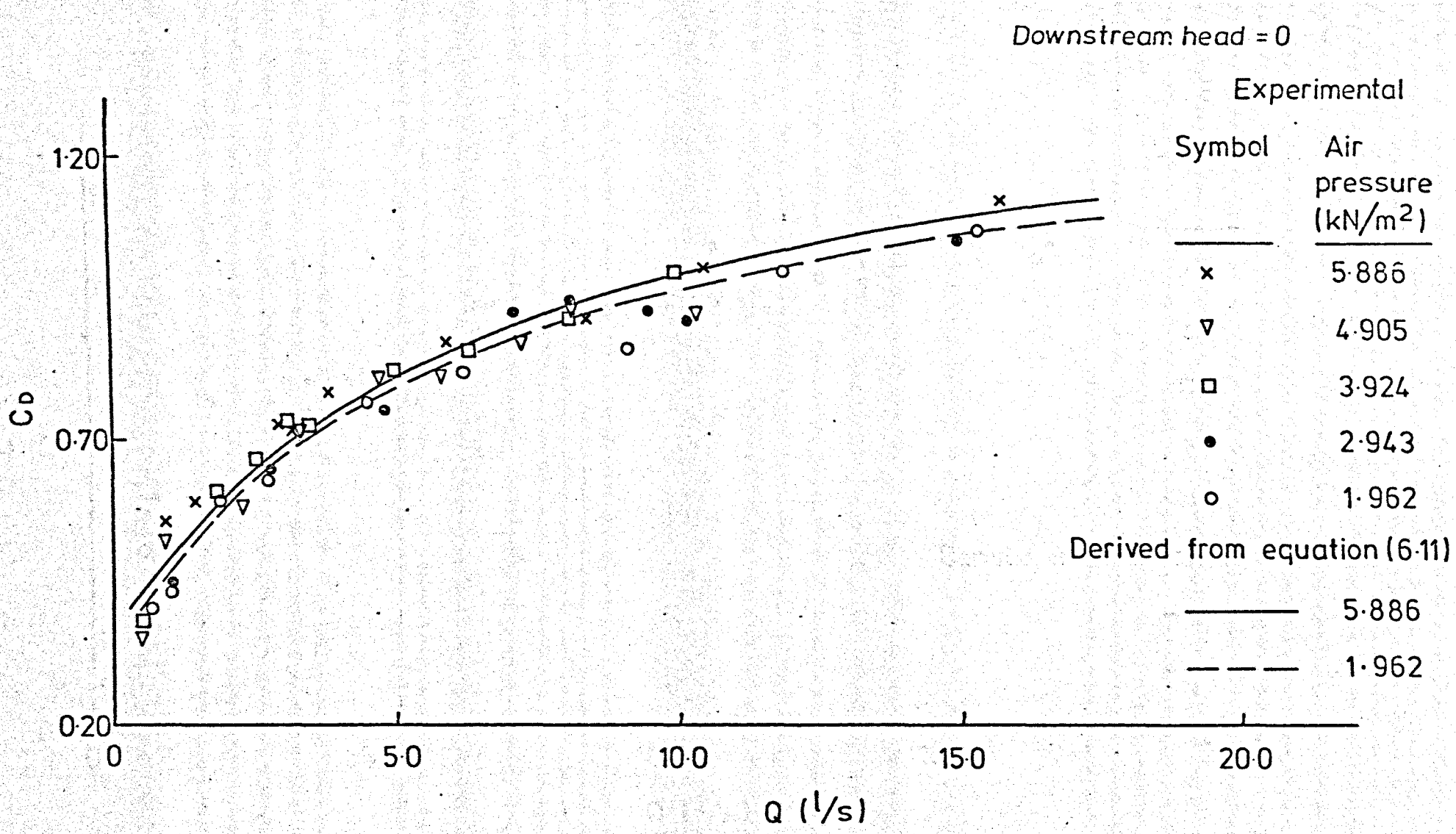

FIG.(6 – 7) VARIATION OF THE COEFFICIENT OF DISCHARGE WITH FLOW RATE FOR VARIOUS AIR PRESSURES

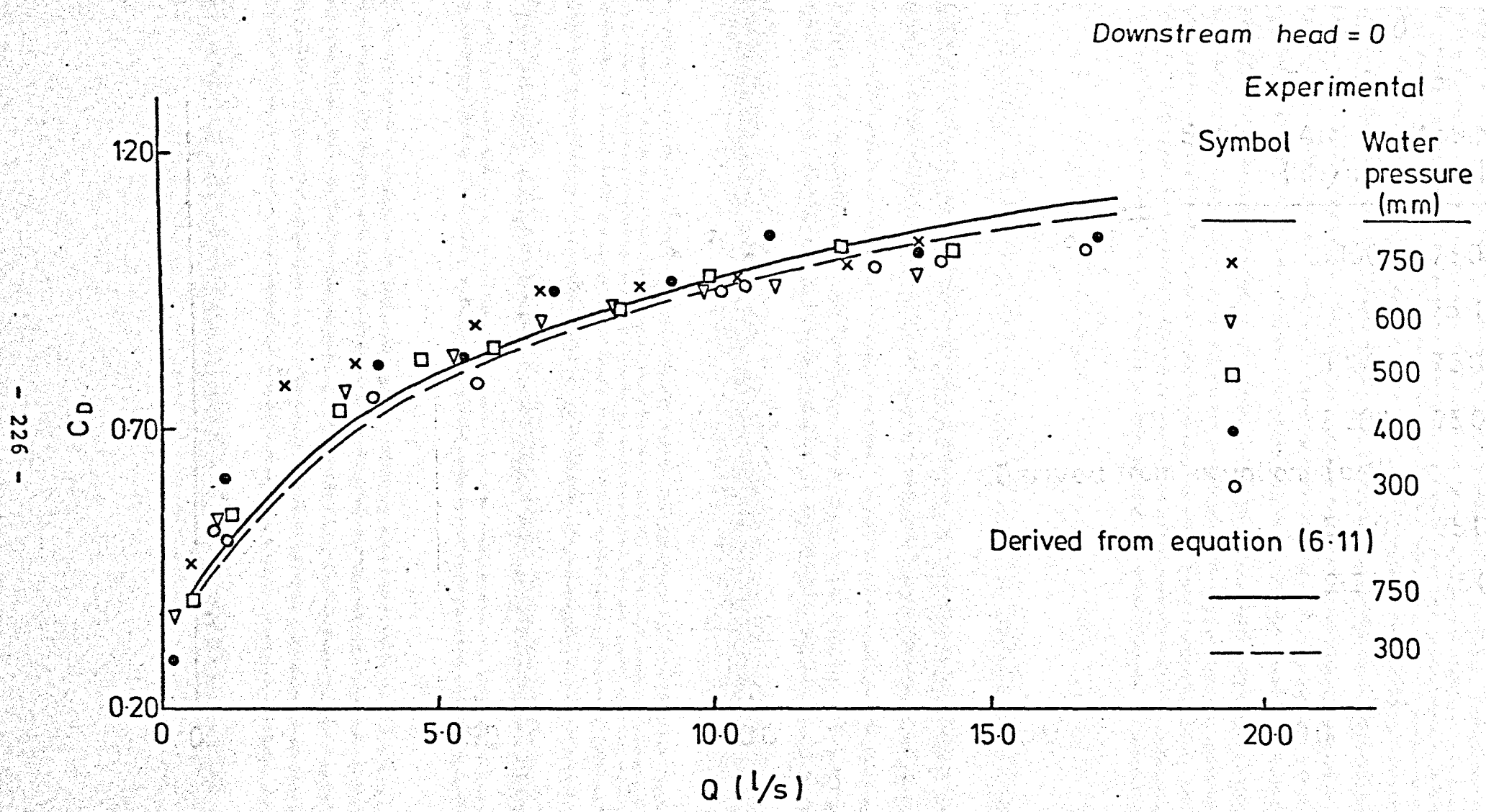

FIG. (6– 8) VARIATION OF THE COEFFICIENT OF DISCHARGE WITH FLOW RATE FOR VARIOUS WATER PRESSURES

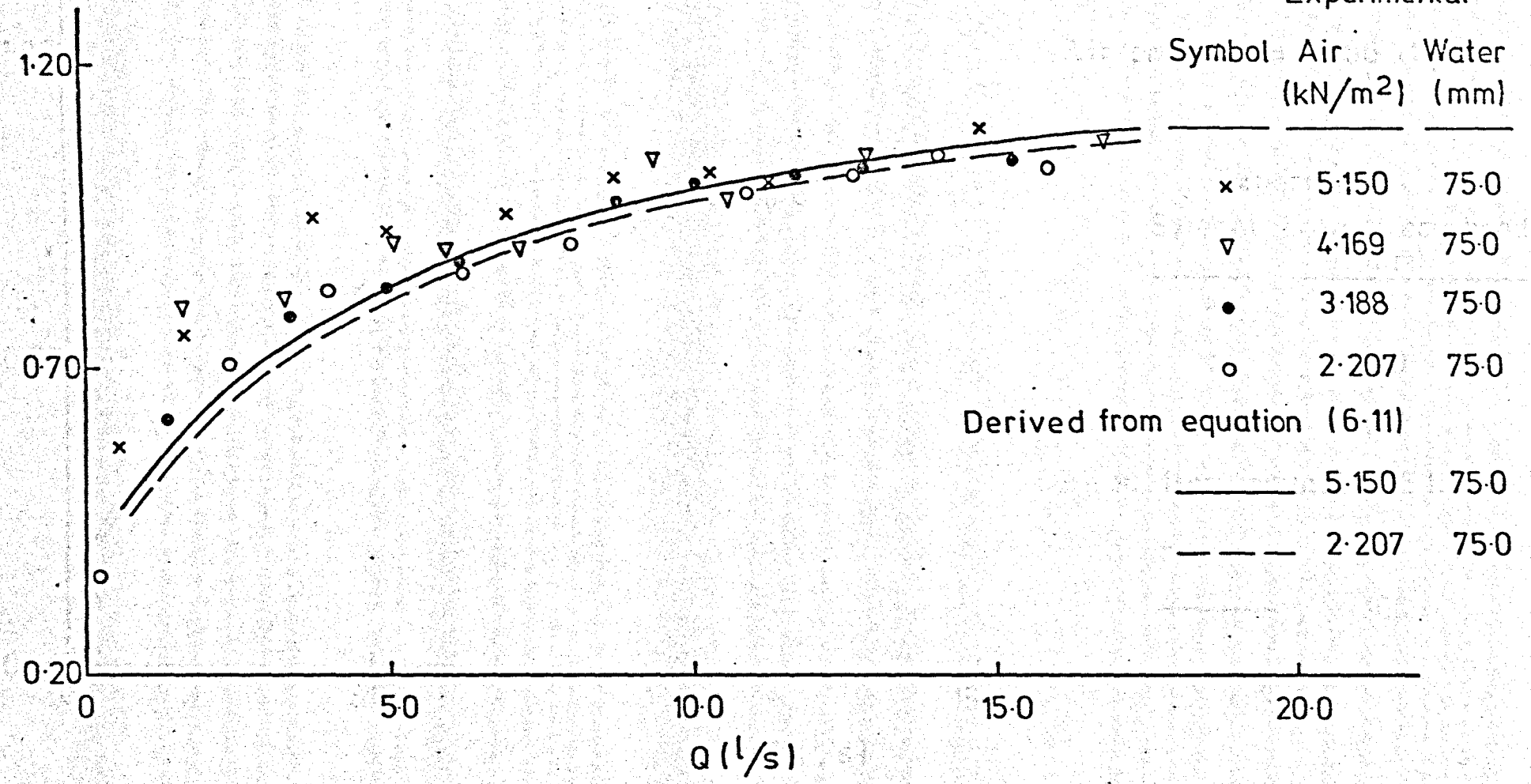

FIG. (6-9) VARIATION OF THE COEFFICIENT OF DISCHARGE WITH FLOW RATE FOR VARIOUS AIR/WATER PRESSURES

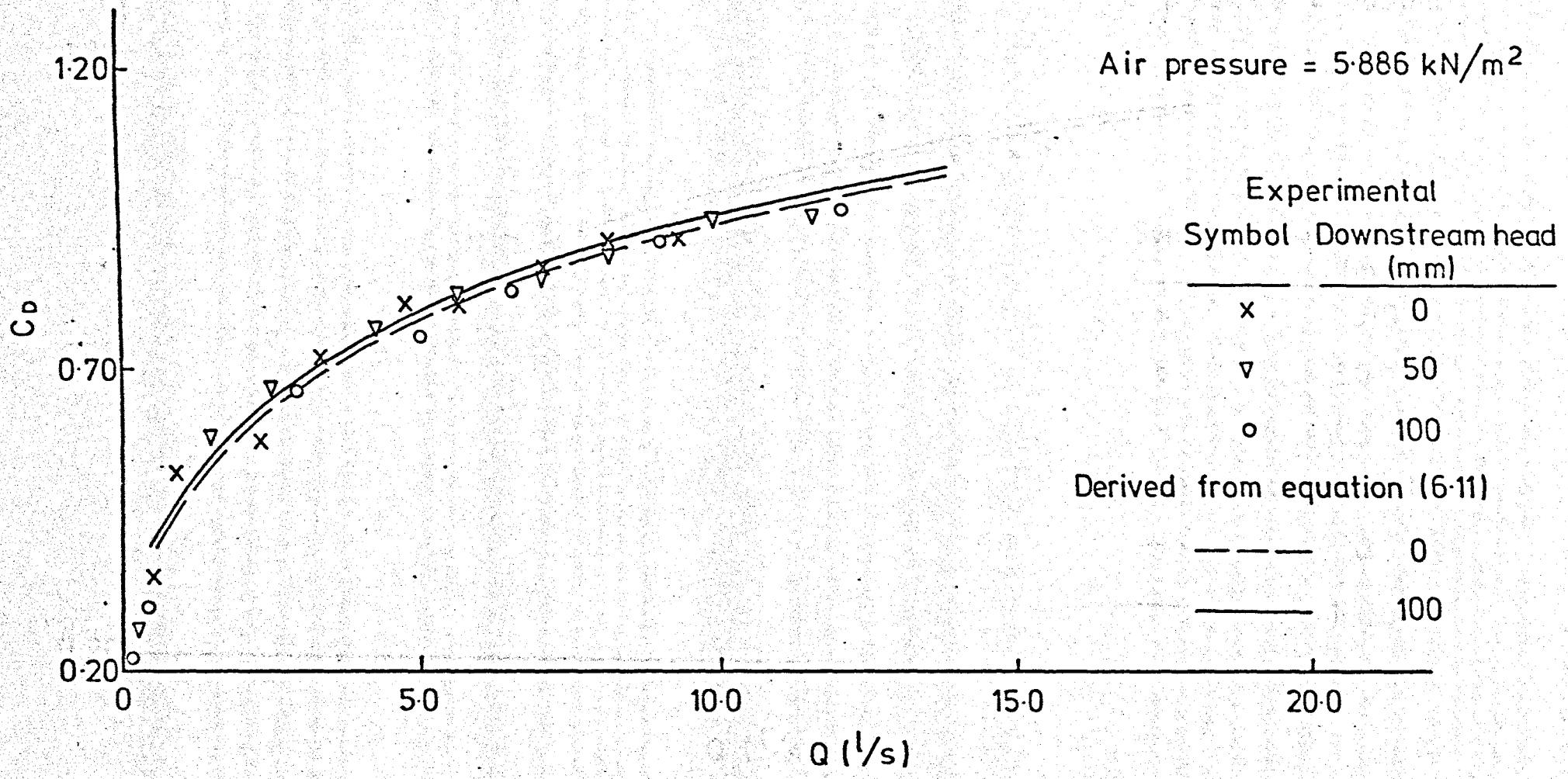

FIG. (6-10) EFFECTS OF DOWNSTREAM HEAD ON THE COEFFICIENT OF DISCHARGE FOR AN AIR INFLATED DAM

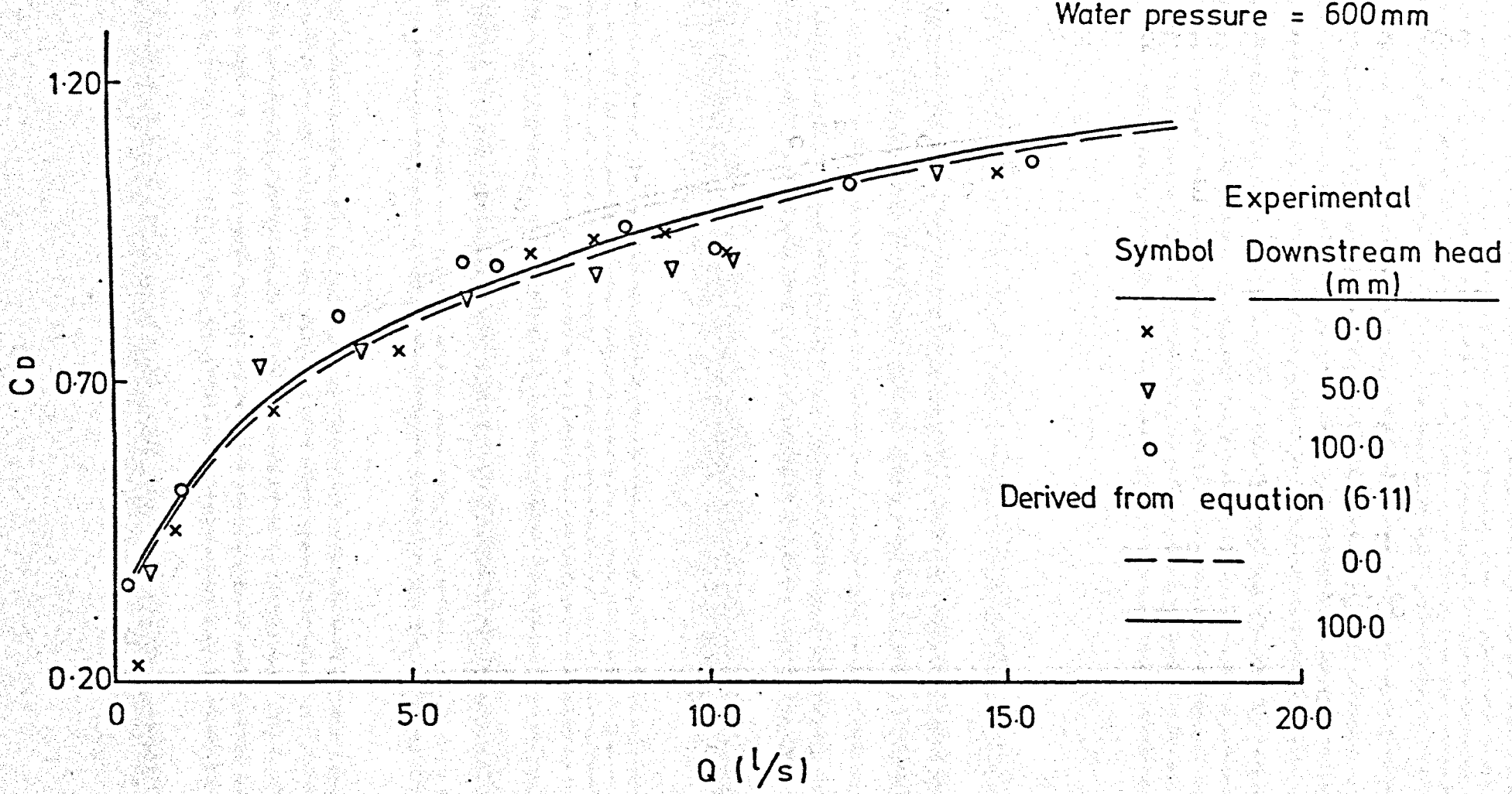

FIG. (6—11) EFFECTS OF DOWNSTREAM HEAD ON THE COEFFICIENT OF DISCHARGE FOR A WATER INFLATED DAM

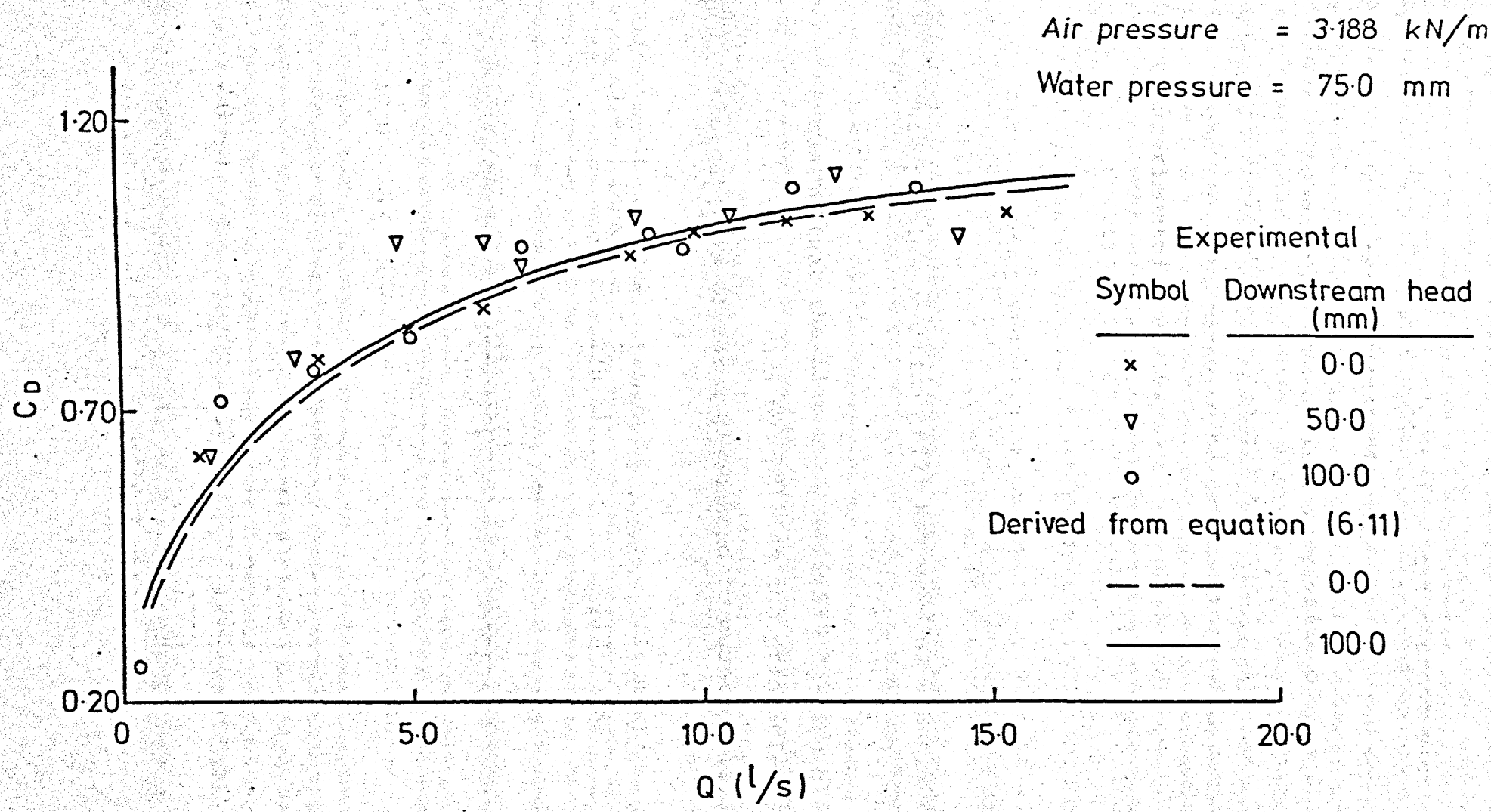

FIG. (6–12) EFFECTS OF DOWNSTREAM HEAD ON THE COEFFICIENT OF DISCHARGE FOR AN AIR/WATER INFLATED DAM

h = depth of water at the crest section.

S = a constant.

Jaegar assumed an arbitrary value of S = 2 to find the discharge for a semicircular profile weir under a particular head which he found to be satisfactory when compared with experimental results.

Equation 6.7 was used in this study to calculate the stage-discharge relationship for the inflatable dams with S=2, but when compared with experimental results it was found to be totally unsatisfactory as shown in Appendix B. To overcome this problem equation (6.7) was used as a basis for determining a general solution to find a coefficient of discharge. Assuming that the flow over the crest section was under critica flow conditions then by applying the principle of maximum discharge ($\frac{\partial Q}{\partial h} = 0$) for a given head to equation (6.7) then

$$0 = \left[(H-h)^{\frac{1}{2}} \frac{S}{R} - \frac{1+Sh/R}{2(H-h)^{\frac{1}{2}}} - (H-h)^{\frac{1}{2}} \left(\frac{(1+Sh/R)^{\frac{1}{2}}}{(R+Sh/R)} \right) + \frac{(1+Sh/R)^{1/S}}{2(H-h)^{\frac{1}{2}}} \right] \quad \ldots\ldots \quad (6.8)$$

where X = Sh/R and this can be reduced to:-

$$2(H-h) = \frac{(1+X)\left[1 - \frac{(1+X)^{1/S}}{(1+X)}\right]}{\frac{1}{R}\left[S - \frac{(1+X)^{1/S}}{(1+X)}\right]} \quad \ldots\ldots \quad (6.9)$$

Equating equations 6.6 and 6.7 gives

$$\frac{2\ C_D}{3\ \sqrt{3}} = \frac{1}{S-1}\left(1 - \frac{h}{H}\right)^{3/2}\left(\frac{R(1+X)}{(H-h)}\right)\left[1 - \frac{(1+X)^{1/S}}{(1+X)}\right] \quad \ldots (6.10)$$

and substituting (H-h) from equation 6.9 into equation 6.10 gives

$$C_D = \frac{3\sqrt{3}}{S-1}\left(1 - \frac{h}{H}\right)^{3/2}\left[S - \frac{(1+X)^{1/S}}{(1+X)}\right] \quad \ldots\ldots \quad (6.11)$$

Rao[36] applied a similar approach, but assumed that S=2 for all cases and found that this gave satisfactory results when compared with the experimental value of C_D for a semi-circular solid weir but disagreement for other hydrofoil weir shapes which he attributed to variations in the approach velocities and geometry of the weir reflected in the numerical value of S.

Having assumed that the C_D of an inflatable dam is dependent on the overflow head and the radius of curvature of the dam crest (R), then because the shape of the dam changes under varying overflow heads, downstream head and internal pressures, the value of R will change hence producing variation in the S value in equation 6.7.

Jaeger suggested that the variables affecting S would be those associated with the momentum theorem. Accepting this assumption then it can be shown that

$$S = \phi(H, R, v, \rho, \mu) \quad \ldots\ldots \quad (6.12)$$

in which

v = velocity approach.

ρ = fluid density.

μ = fluid viscosity.

Applying Rayleigh's method of dimensional analysis[37], these variables can be re-grouped as follows

$$S = C_1 (H/R)^{a_1} \left(\frac{\rho v R}{\mu}\right)^{-b_1} \quad \ldots\ldots \quad (6.13)$$

where

C_1 = dimensionless constant.

a_1, b_1 = numerical exponents.

The second variable term of equation (6.13) represents the Reynolds number for water at constant temperature and for a particular flow rate then ρ, v and μ are constants and except in extreme values of R this expression is assumed to be constant as a small change in R will have no significant effect on the Reynolds number. The changes in the value of R for a change in head is always small anyway as can be seen from Figs. 6.17 and 6.19.

Equation (6.13) can now be rewritten as:

$$S = K_1 (H/R)^{a_1} \quad \ldots\ldots \quad (6.14)$$

where K_1 is a dimensionless constant = $C_1 \left(\frac{\rho v R}{\mu}\right)^{-b_1}$

By taking logs of both sides of equation (6.14) then

$$\text{Log } S = \text{Log } K_1 + a_1 \text{ Log } (H/R) \quad \ldots\ldots \quad (6.15)$$

and equation (6.15) represents a linear relationship between log (S) and log (H/R) with a slope of a_1.

The radius of curvature (R) can be obtained from the general equation[38]

$$R = \left[\frac{1 + \left(\frac{dy}{dx}\right)^2}{\frac{d^2y}{dx^2}} \right]^{3/2} \quad \ldots\ldots \quad (6.16)$$

In addition to solving equation (6.11) it is necessary to have a numerical value of (h/H) as well as S. The relationship of overflow head (H) and the depth of water above the crest level (h) for all air, water and air/water dams was determined experimentally as shown in Fig.6.13. The equation of this linear relationship was found to be

$$h = 0.70\ H \quad \ldots\ldots \quad (6.17)$$

Hence, the value of S can be calculated from equation (6.9) and is found to vary from 1.2 to 2.1. Therefore, by plotting from experimental results of air dams, log (H/R) as basic ordinate and log(S) as vertical ordinate, a straight line was obtained from which K_1 and a_1 could be found as shown in Fig. 6.14. The equation of the straight line in Fig.6.14 was calculated by using the fitting of a linear regression equation and is given by

$$S = 2.28\ (H/R)^{0.21} \quad \ldots\ldots \quad (6.18)$$

The relationship of S and H/R for water inflated dams was plotted in Fig.6.15 and the equation of the straight line was

$$S = 2.36\ (H/R)^{0.21} \quad \ldots\ldots \quad (6.19)$$

It was evident from equations (6.18) and (6.19) that the value of a_1 for the air and water inflated dams was the same but the value of K_1 was slightly different due to the slight differences in the radius of curvature and the assumption that the Reynolds number stays constant.

Because equations (6.18) and (6.19) are almost identical it was assumed that such an expression existed (equation (6.20))

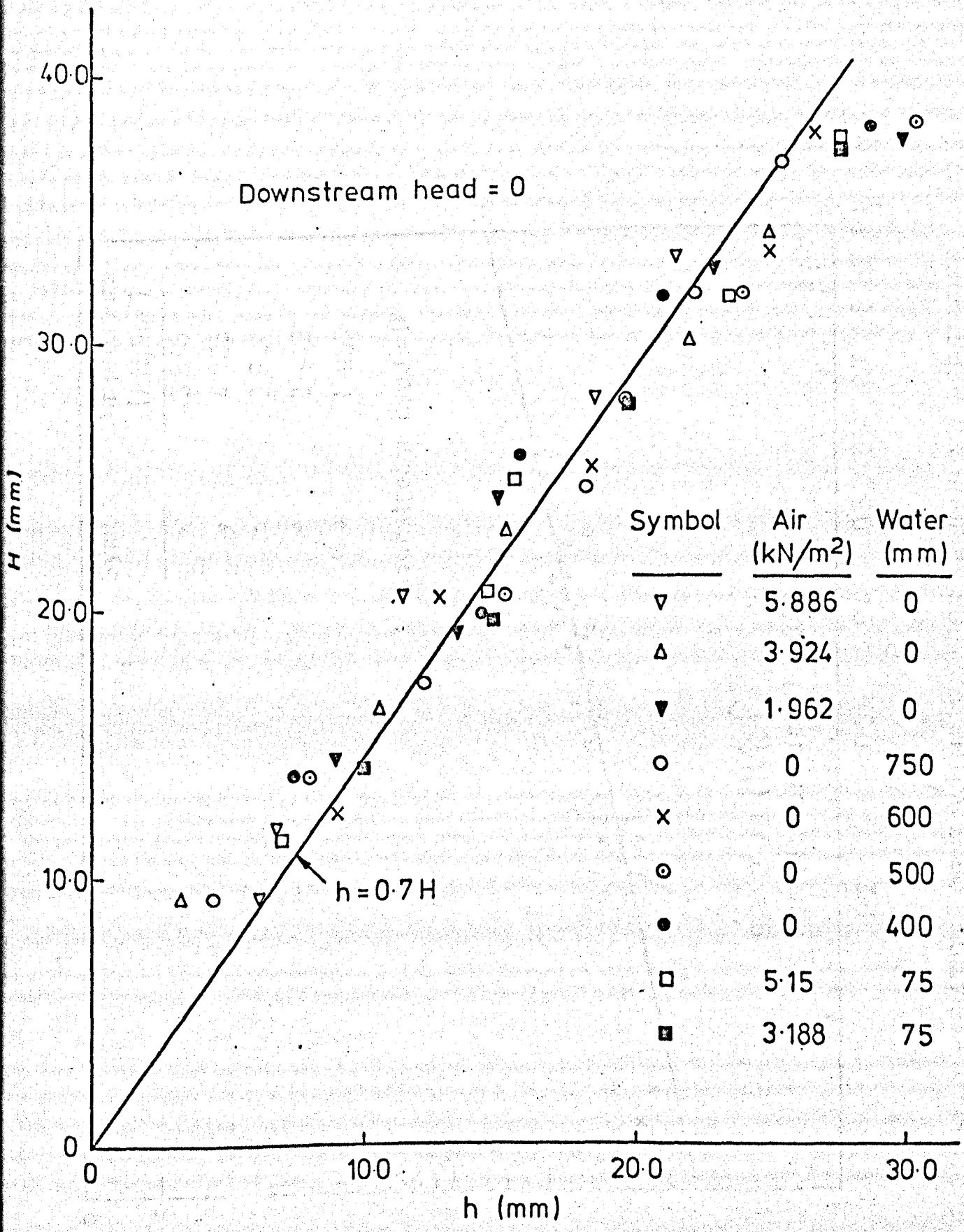

FIG. (6-13) VARIATION OF OVERFLOW HEAD, H, WITH DEPTH OF WATER ABOVE THE CREST LEVEL, h, FOR VARIOUS AIR, WATER AND AIR/WATER PRESSURES

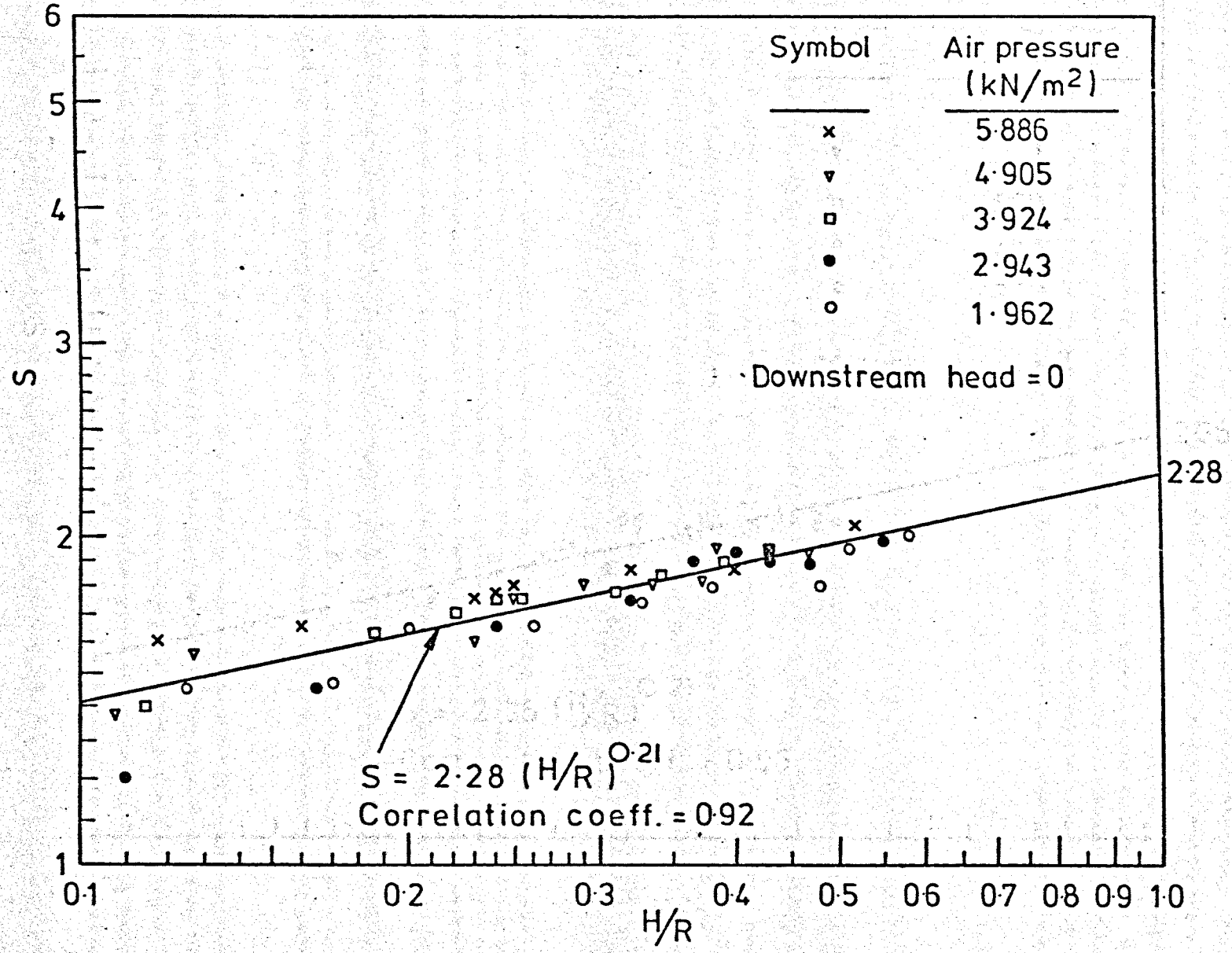

FIG. (6-14) VARIATION OF S WITH H/R FOR VARIOUS AIR PRESSURES

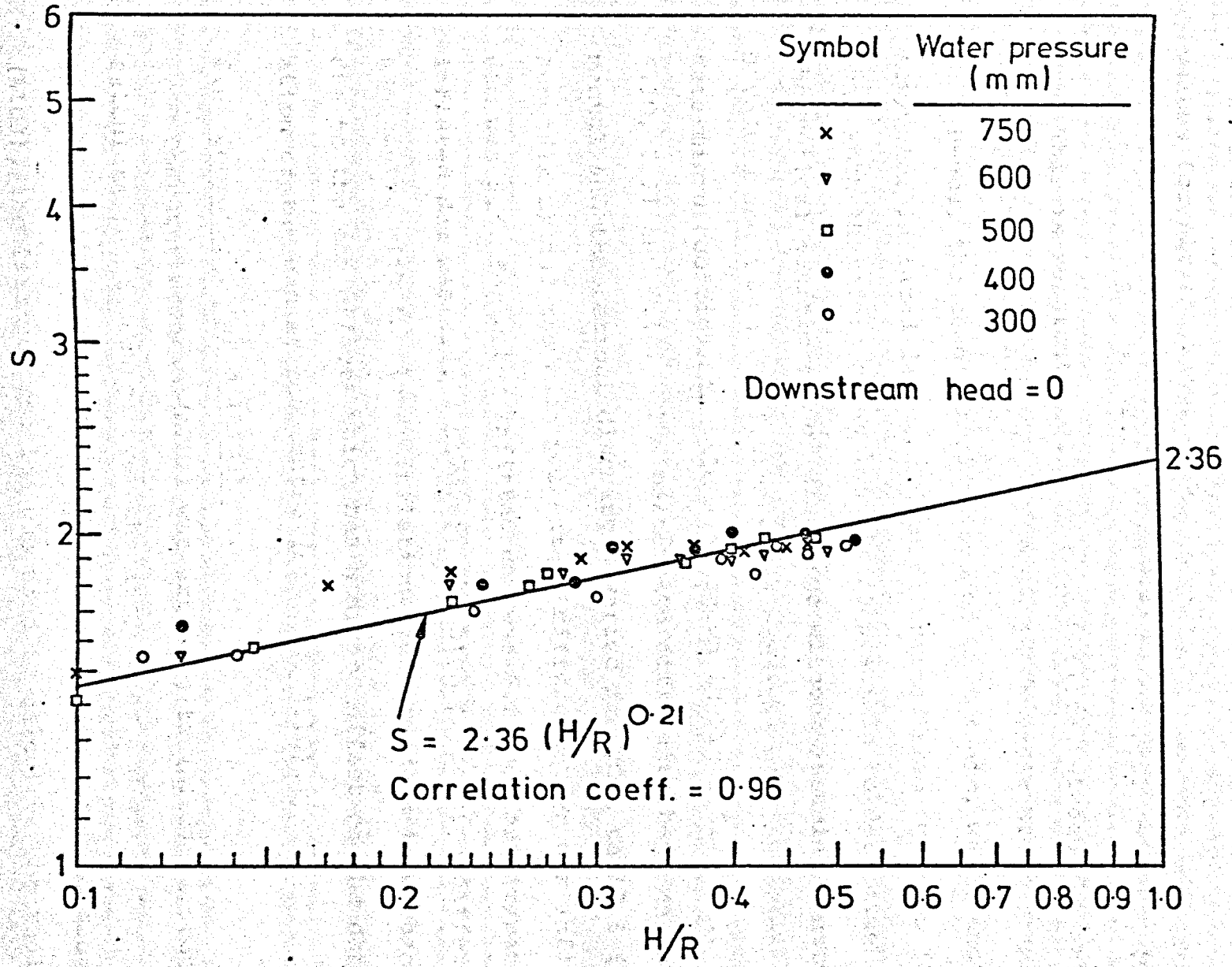

FIG. (6–15) VARIATION OF S WITH H/R FOR VARIOUS WATER PRESSURES

for air/water dams with a_1 value of 0.21 and K_1 value assumed to be equal to 2.32 this being the arithmetic mean of the values for air and water dams respectively.

$$S = 2.32\ (H/R)^{0.21} \quad \ldots\ldots \quad (6.20)$$

This is substantiated by the comparison between theoretical and experimental discharges as shown in Appendix B.

Hence, the theoretical values of C_D for air, water and air/water inflated dams could be determined from equation (6.11). This work therefore shows that it is possible to determine a theoretical coefficient of discharge without assuming constant S values and these coefficients are compared with experimentally determined coefficients values as shown in Figs. 6.7, 6.8, 6.9, 6.10, 6.11 and 6.12. The percentage difference between experimental and theoretical discharges varied from 0.2 to 17.5 (see Appendix B) and the mean percentage difference for air inflated dam was 5.4, for water inflated dam was 6.2 and for air/water inflated dam was 6.4. However, the high percentage difference associated with the lower inflation pressure dams is probably due to the end effects which has a direct effect on the deformation of the dam at the centre (see Fig. 4.10).

6.6 Computer Program (AID3).

Computer program (AID2) was extended to (AID3) in order to calculate the discharge over the air, water and air/water inflated dams. Two subroutines were connected to the program (AID3), the first subroutine was used to calculate the radius of curvature (R) of the dam crest, and the second subroutine was used for calculating the coefficient (C_D) and the discharge over the dams.

The input data of the program was similar to the input data of the program (AID2) (see table 5.2).

Examples of the output using the program (AID3) are shown in Fig.6.16. The list of the program and full details of how to use it is available in the library of the Department of Civil & Structural Engineering of the University of Sheffield.

Examples of the variation of the coefficient of discharge with flow using equation 6.11 and the program (AID3) are illustrated in Figs. 6.7, 6.8, 6.9, 6.10, 6.11 and 6.12 and also detailed in Appendix B.

The modifications to the program did not prevent its capability of use for hydrostatic conditions.

6.7 Comparison of Methods of Determining Discharges.

A comparison was carried out on the methods of deriving discharges by Clare[8], Baker[1] and the technique developed in section 6.5 using equations (6.6) and (6.11) hereafter referred to as the Alwan method, as illustrated in tables 6.2 and 6.3.

Unfortunately, both Clare and Baker did not specify the properties of the fabric which was used for building their dams and therefore the comparisons are all based on the assumption that all membranes are weightless and inextensible. However, it should be noted that the new approach can take into account material properties and the significance of this is illustrated in table 6.4.

It can be seen from tables 6.2 and 6.3 that there is a disagreement between the three methods, this probably resulting

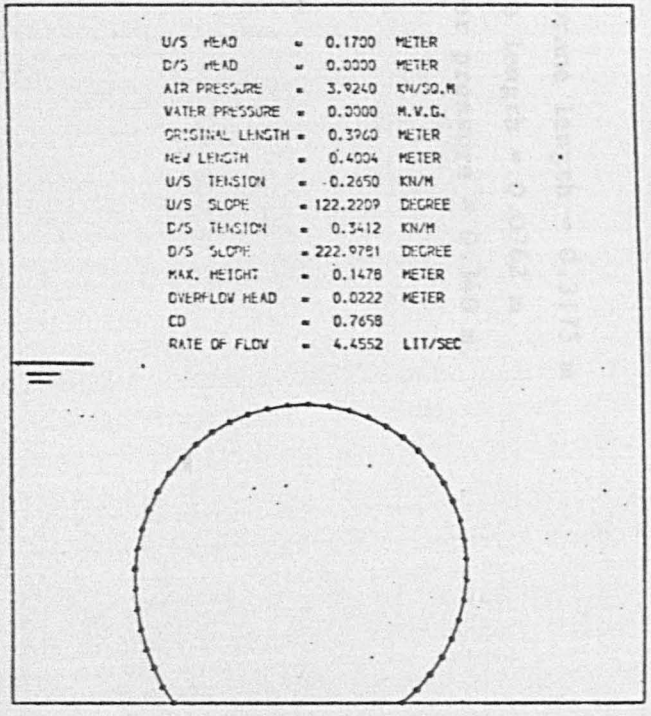

(A) Air inflated dam

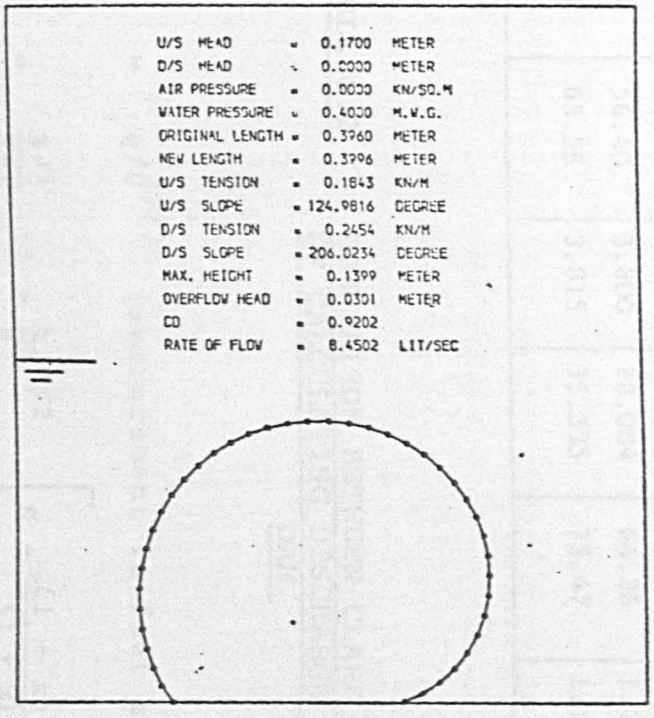

(B) Water inflated dam

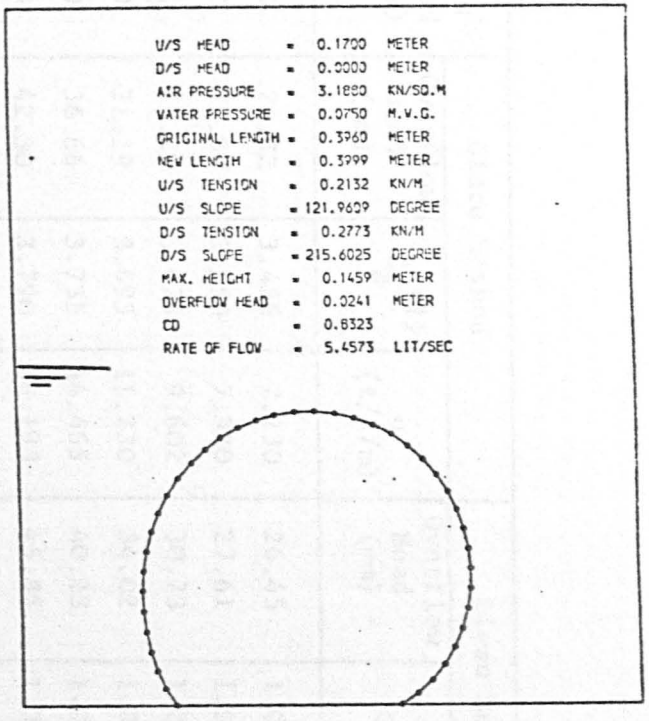

(C) Air/Water inflated dam

FIG. (6-16) TYPICAL EXAMPLES OF INFLATABLE DAMS UNDER HYDRODYNAMIC CONDITIONS BY USING PROGRAM (AID 3) AND 40 ELEMENTS

No.	U/S Head (mm)	D/S Head (mm)	Clare Method			Alwan Method			% Diff. in q
			Overflow Head (mm)	C_D (1)	q (ℓ/s/m)	Overflow Head (mm)	C_D (2)	q (ℓ/s/m)	
1	137.12	0.0	24.32	3.455	7.230	26.45	1.031	7.791	7.7
2	138.18	0.0	25.38	3.550	7.920	27.61	1.036	8.345	5.3
3	141.00	0.0	28.20	3.675	9.602	30.73	1.047	9.910	3.2
4	144.00	0.0	31.19	3.695	11.230	34.02	1.059	11.670	3.9
5	149.49	0.0	36.66	3.735	14.465	40.23	1.078	15.280	5.6
6	155.10	0.0	42.30	3.790	18.193	45.85	1.092	18.827	3.5
7	160.74	0.0	47.94	3.780	21.892	53.51	1.108	24.088	10.0
8	169.20	0.0	56.40	3.800	28.084	64.36	1.125	32.280	15.0
9	178.36	0.0	65.56	3.815	35.335	75.47	1.138	41.440	17.2
								Mean	9.0

TABLE 6.2 COMPARISON BETWEEN CLARE AND ALWAN METHODS OF CALCULATING DISCHARGE (WATER INFLATED DAM.

(1) $C_D = q/H^{3/2}$ (measurement in feet system)

(2) $$C_D = \frac{3\sqrt{3}}{S-1}\left(1 - \frac{h}{H}\right)^{3/2}\left[S - \frac{(1+x)}{(1+x)}^{1/S}\right]$$

Membrane length = 0.3175 m

Base length = 0.0762 m

Water pressure = 0.340 m.

No.	U/S Head (m)	D/S Head (m)	Baker Method			Alwan Method			% Diff. in q
			Overflow Head (m)	(1) C_D	q (ℓ/s/m)	Overflow Head (m)	(2) C_D	q (ℓ/s/m)	
1	5.478	0.896	1.733	3.073	3870	1.653	1.062	3964	2.4
2	5.837	1.344	2.005	3.294	5160	2.022	1.085	5485	6.3
3	6.110	1.612	2.234	3.500	6450	2.301	1.100	6743	4.5
4	6.375	2.106	2.455	3.647	7740	2.552	1.111	7956	2.8
5	6.633	2.463	2.670	3.750	9030	2.799	1.120	9220	2.1
6	6.889	2.823	2.882	3.823	10320	3.041	1.128	10512	1.8
7	7.148	3.271	3.054	3.901	11480	3.225	1.134	11547	0.6
								Mean	3.0

TABLE 6.3 COMPARISON BETWEEN BAKER AND ALWAN METHODS OF CALCULATING DISCHARGE (WATER INFLATED DAM).

(1) $C_D = q/H^{3/2}$ (Measurement in feet system)

(2) $$C_D = \frac{3\sqrt{3}}{S-1}\left(1 - \frac{h}{H}\right)^{3/2}\left[S - \frac{(1+x)^{1/S}}{(1+x)}\right]$$

Membrane length = 16.92 m.

Base length = 5.334 m.

Water pressure = 1.22 m above upstream level.

No.	Air Pressure (kN/m^2)	Water Pressure (mm)	U/S Head (mm)	D/S Head (mm)	Membrane (weight and extensible)				Membrane (Weightless and inextensible)				% Diff. in Q
					Y_{max} (mm)	H (mm)	C_D	Q (ℓ/s)	Y_{max} (mm)	H (mm)	C_D	Q (ℓ/s)	
1	5.886	0.0	171.7	0.0	147.60	24.10	0.792	5.21	145.46	26.24	0.836	6.25	16.6
2	4.905	0.0	164.3	50.0	147.88	16.41	0.632	2.33	145.96	18.34	0.680	2.97	21.5
3	2.943	0.0	183.0	100.0	149.65	33.35	0.989	10.58	148.27	34.73	1.014	11.53	8.2
4	0.0	75.0	162.7	0.0	144.23	18.47	0.707	3.12	142.50	20.20	0.749	3.78	17.4
5	0.0	600.0	172.4	50.0	143.30	29.10	0.916	8.02	141.37	31.03	0.952	9.14	12.2
6	0.0	400.0	175.0	100.0	142.58	32.42	0.967	9.91	141.32	33.68	0.991	10.76	7.9
7	5.150	75.0	179.0	0.0	146.38	32.52	0.970	9.94	144.36	34.64	1.009	11.43	13.0
8	3.188	75.0	180.0	50.0	146.04	33.96	1.022	10.60	144.45	35.55	1.038	12.22	13.2
9	2.207	75.0	184.7	0.0	140.89	43.81	1.160	18.69	139.34	45.36	1.182	20.07	6.8
												Mean	13.0

TABLE 6.4 EFFECTS OF WEIGHT AND EXTENSIBILITY OF MEMBRANE ON DISCHARGE.

from the assumption of the membrane being weightless and inextensible which means there is no allowance for elongation in the membrane and hence no increase in the membrane length which in turn no increase in dam height. If elongation is not considered this gives a higher overflow head and coefficient of discharge which gives a higher theoretical overflow rate as illustrated in table 6.4.

6.8 Factors Effecting the Coefficient of Discharge.

When the flow over the dam increases, the coefficient of discharge (CD) also increases (see Fig. 6.7, 6.8, 6.9, 6.10, 6.11 and 6.12). This increase in the coefficient of discharge was rapid at the lower flows but increased at a steady rate for higher flows. This can probably be attributed partly to the movement of the nappe over the dam (see section 6.4) and a broader crest to the dam developed under high overflow heads.

For a particular dam when the internal pressure was increased the coefficient of discharge was found to decrease (see Figs. 6.7,6.8 and 6.9). This effect observed in this study was also found by Anwar[6]. This can be explained by the distortion affecting the broader of the crest is attributed to a dam of low internal pressure having greater distortion than a dam of a higher internal pressure when both dams are tested under the

same overflow heads and downstream heads (see Figs. 5.14, 5.15, 5.19, 5.20 and 5.21). High distortions cause a decrease in the curvature of the dam crest which in turn causes an increase in the radius of curvature of the crest (R) as shown in Fig.6.17. This increase in R produces a decrease in the coefficient of discharge as shown in Fig.6.18. For example, if the dam was inflated by 5.886 kN/m^2 air pressure and tested under an overflow head of 20 mm and downstream head of zero, the C_D was found equal to 0.73 (Fig.6.18) and from equation (6.6) the discharge was calculated and found equal to 3.63 ℓ/s. However, when the internal pressure decreased to 1.962 kN/m^2 and the dam was tested under the same heads, the C_D was found equal to 0.7 and Q = 3.47 ℓ/s. There was of the order of 4% difference in the value of discharge when the internal pressure decreased approximately 67% (see Figs. 6.7, 6.8 and 6.9).

The increase in the downstream head causes the dam to distort backwards on the upstream side (Figs. 5.16 and 5.17) which results in an increase in the curvature of the crest and decrease in R as shown in Fig.6.19. This decrease in R produces an increase in the coefficient of discharge as shown in Fig.6.20. The increase in the C_D results in an increase in the discharge over the dam (see Figs. 6.10, 6.11 and 6.12). For example, if the dam was inflated by 600 mm water pressure and tested under overflow head of 30 mm and downstream head of zero, the C_D was found equal to 0.91 (Fig.6.20) and Q= 8.30 ℓ/s (equation 6.6). When the downstream head increased to

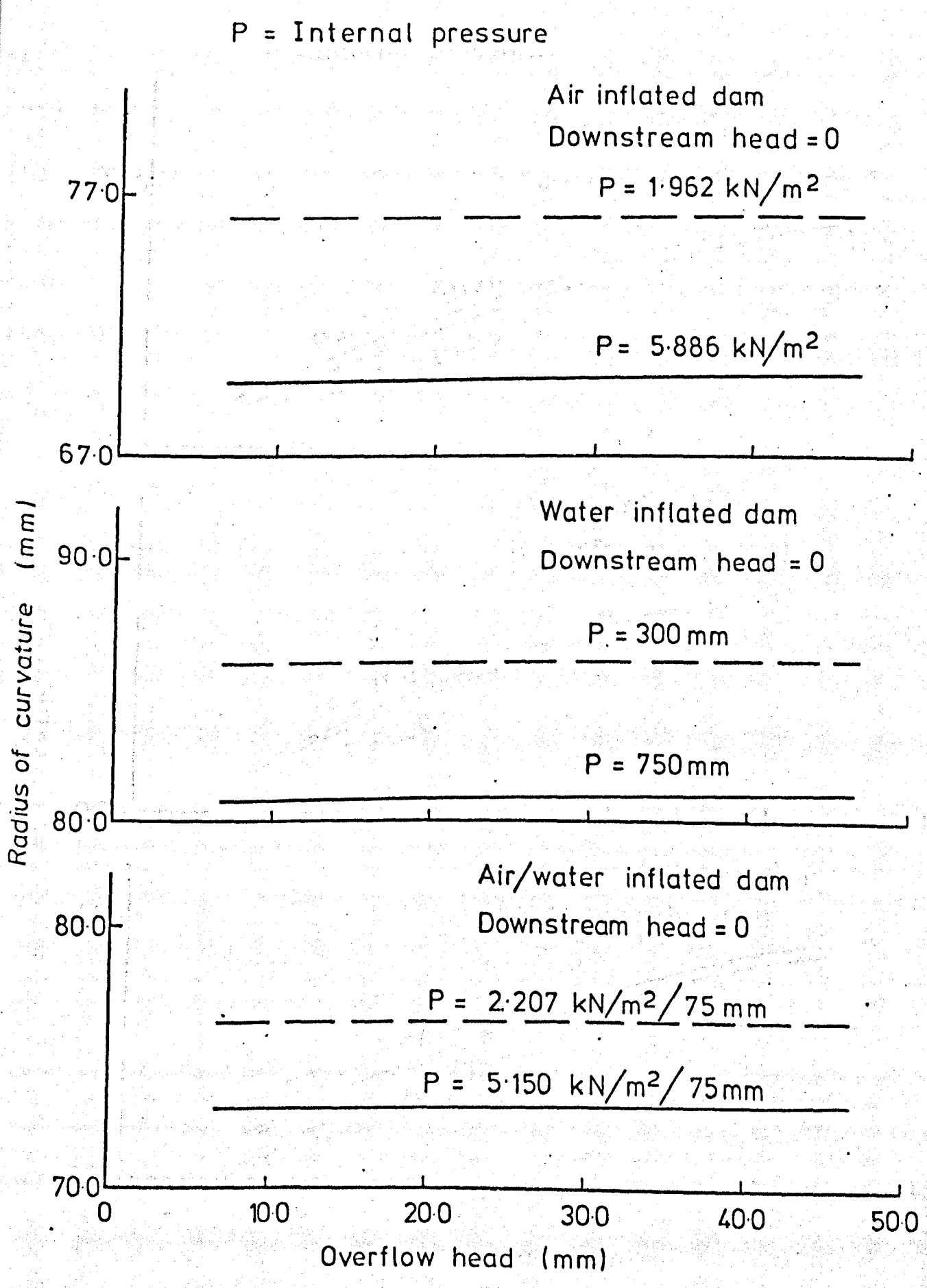

FIG. (6–17) VARIATION OF THE RADIUS OF CURVATURE OF DAM CREST WITH OVERFLOW HEAD FOR VARIOUS AIR, WATER AND AIR/WATER INFLATED DAMS

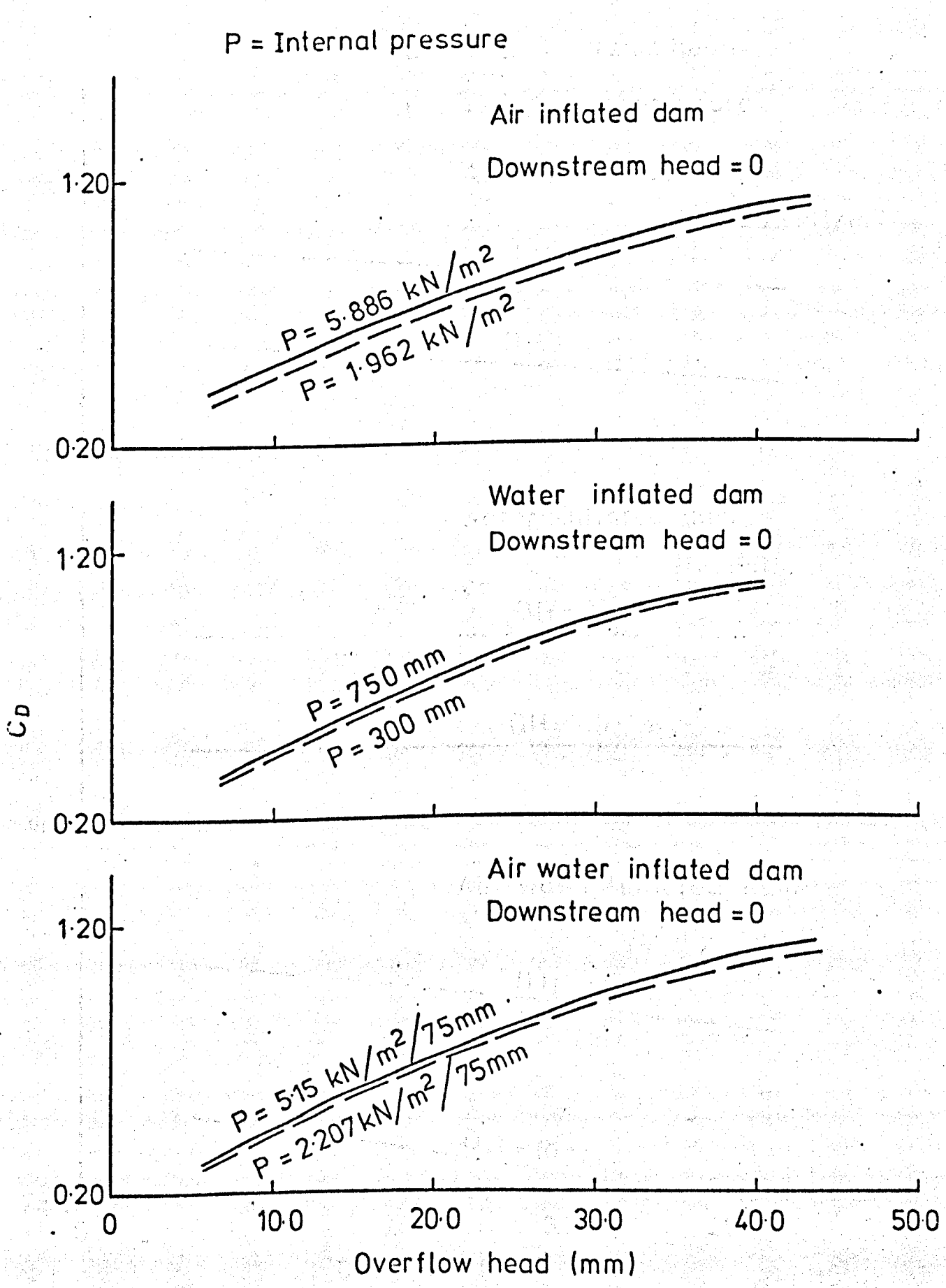

FIG. (6–18) VARIATION OF THE COEFFICIENT OF DISCHARGE WITH OVERFLOW HEAD FOR VARIOUS AIR, WATER AND AIR/WATER PRESSURES

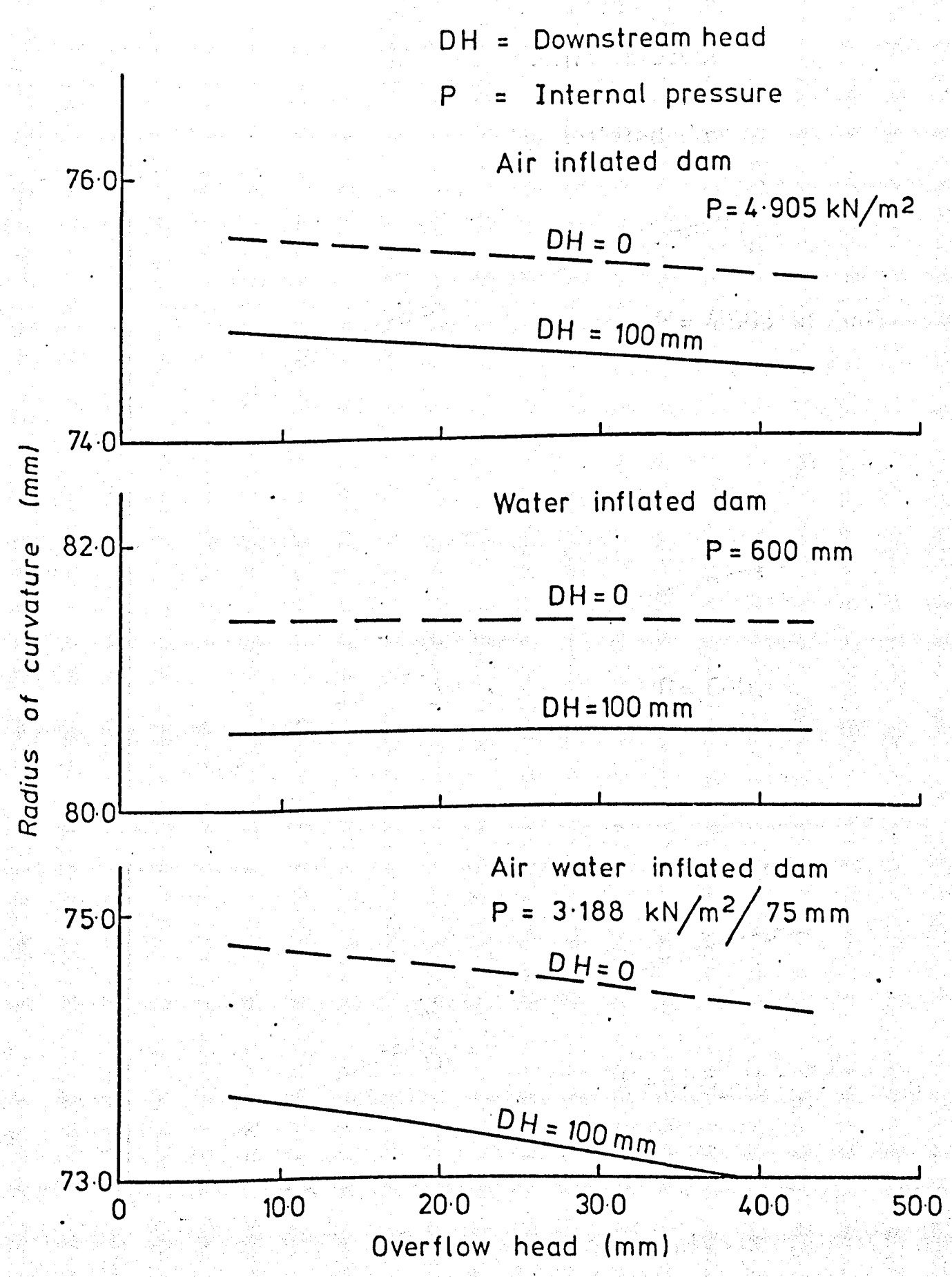

FIG. (6–19) VARIATION OF THE RADIUS OF CURVATURE OF THE DAM CREST WITH OVERFLOW HEAD FOR VARIOUS DOWNSTREAM HEADS

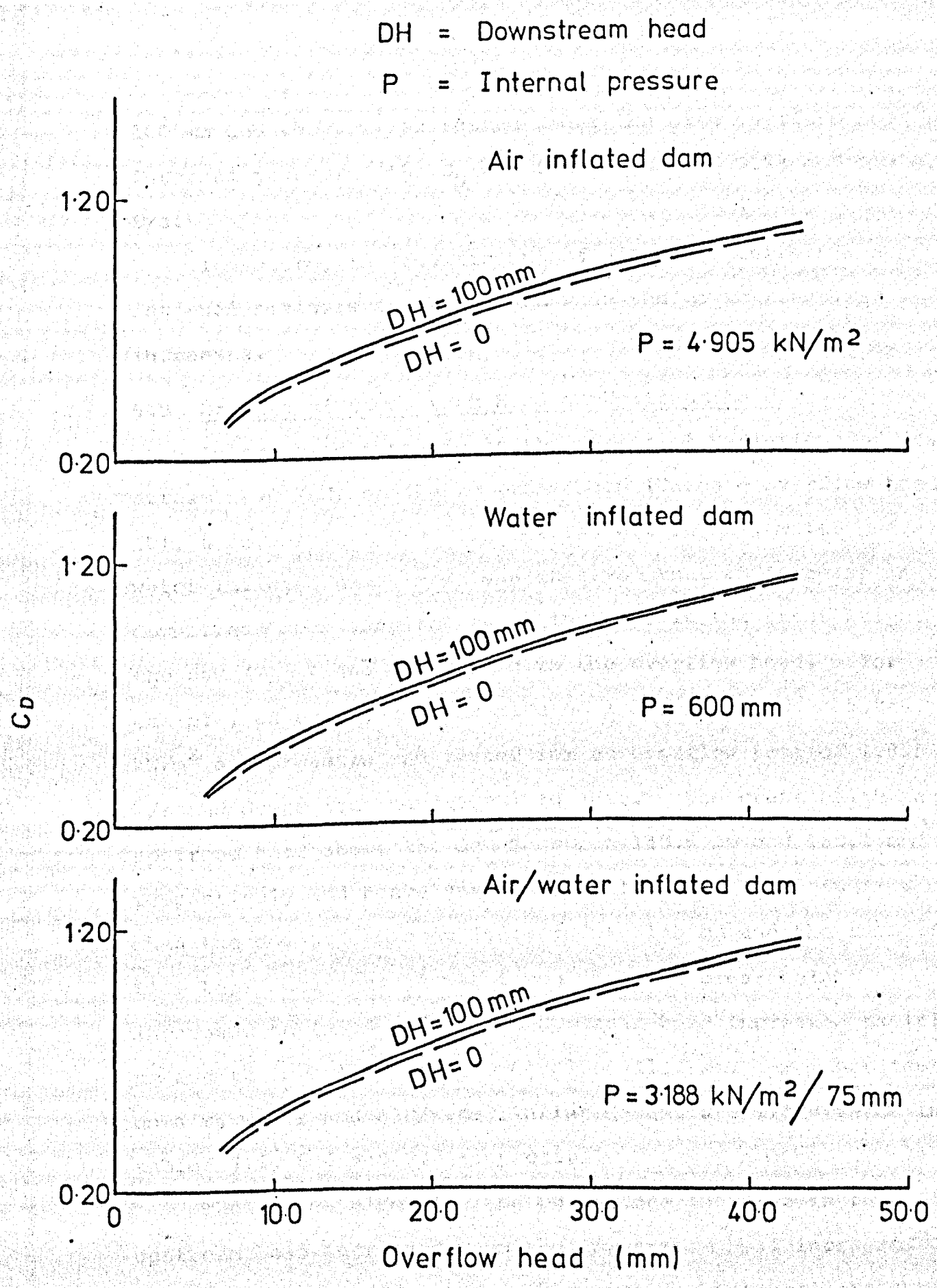

FIG.(6-20) VARIATION OF THE COEFFICIENT OF DISCHARGE WITH OVERFLOW HEAD FOR VARIOUS DOWNSTREAM HEADS

100 mm and the dam was tested under the same overflow head an internal pressure, the C_D was found equal to 0.94 and Q = 8.6 ℓ/s.

Therefore, the coefficient of discharge increases as the internal pressure increases and when the downstream head increases.

6.9 Effects of Downstream Head on Upstream Head.

In order to investigate the effect of variations of downstream head (DH) on the upstream head (UH) and overflow head (H), a series of tests were carried out on air, water and air/water inflated dams. It was observed that an increase in the downstream head resulted in an increase in the crest height of the dam (Y_{max}) and a decrease in the overflow head. For example, an experiment was made on a dam inflated to 5.886 kN/m^2 air pressure and tested for an overflow rate of 1.935 ℓ/s and downstream head equal to zero. The crest height and upstream head above the dam measured 148.5 mm and 160.1 mm respectively and hence gave an overflow head equal to 11.6 mm. When the downstream head increased to 130 mm and the rate of flow kept constant, it was found that the crest height increased to 149.6 mm and the upstream head increased to 161.0 mm and the overflow head is equal to 11.4 mm. Further tests on air, water and air/water inflated dams are illustrated in tables 6.5, 6.6 and 6.7 respectively.

The tables also show the percentage increase in the upstream head increased when the downstream head increased up to a maximum of 130 mm and with decreasing internal pressures in the three dams.

No. of Test	Air Pressure (kN/m^2)	Q (ℓ/s)	UH (mm)	DH (mm)	Y_{max} (mm)	H (mm)	% of Increase UH	% of Decrease H
1	5.886	1.935	160.1	0.0	148.5	11.6	0.559	1.724
			161.0	130.0	149.6	11.4		
2	5.886	5.088	167.9	0.0	147.8	20.1	0.655	0.500
			169.0	130.0	149.0	20.0		
3	5.886	8.203	175.0	0.0	147.6	27.4	0.286	1.481
			175.5	130.0	148.5	27.0		
						Mean	0.500	1.235
4	3.924	1.110	157.0	0.0	148.0	0.0	1.019	2.220
			158.6	130.0	149.8	8.8		
5	3.924	3.141	163.7	0.0	147.5	16.2	0.427	6.170
			164.4	130.0	149.2	15.2		
6	3.924	8.998	176.6	0.0	147.0	29.6	0.962	2.700
			178.3	130.0	149.5	28.8		
						Mean	0.802	3.696
7	1.962	1.799	161.4	0.0	147.8	13.6	1.920	8.080
			164.5	130.0	152.0	12.5		
8	1.962	5.088	169.0	0.0	146.5	22.5	1.538	3.111
			171.6	130.0	149.8	21.8		
9	1.962	11.402	180.0	0.0	143.6	36.4	2.222	3.021
			184.0	130.0	148.7	35.3		
						Mean	1.893	4.737

TABLE 6.5 EFFECT OF DOWNSTREAM HEAD ON UPSTREAM AND OVERFLOW HEADS FOR AIR INFLATED DAM.

No. of Test	Water Pressure (mm)	Q (ℓ/s)	UH (mm)	DH (mm)	Y_{max} (mm)	H (mm)	% of Increase UH	% of Decrease H
1	750.0	1.168	153.8	0.0	144.3	9.5	0.325	0.789
			154 3	130.0	145.0	9.3		
2	750.0	4.804	161.8	0.0	143.2	18.6	0.741	0.537
			163.0	130.0	144.5	18.5		
3	750.0	10.539	175.4	0.0	143.0	32.4	0.513	1.234
			176.3	130.0	144.6	31.7		
						Mean	0.526	0.853
4	600.0	2.075	155.9	0.0	142.4	13.5	1.218	1.851
			157.8	130.0	144.5	13.3		
5	600.0	7.217	168.4	0.0	142.2	26.2	0.712	0.954
			169.6	130.0	144.0	25.6		
6	600.0	14.122	175.8	0.0	142.0	33.8	0.568	0.665
			176.8	130.0	143.6	33.2		
						Mean	0.832	1.156
7	400.0	1.349	155.4	0.0	140.5	14.9	1.395	2.013
			157.6	130.0	143.0	14.6		
8	400.0	7.217	166.7	0.0	139.6	27.1	1.319	3.413
			168.9	130.0	143.7	25.2		
9	400.0	14.529	177.4	0.0	137.5	39.9	1.409	2.380
			179.9	130.0	141.5	38.4		
						Mean	1.374	2.602

TABLE 6.6 EFFECT OF DOWNSTEAM HEAD ON UPSTREAM AND OVERFLOW HEAD FOR WATER INFLATED DAM.

No. of Test	Air Pressure (kN/m^2)	Water Pressure (mm)	Q (ℓ/s)	UH (mm)	DH (mm)	Y_{max} (mm)	H (mm)	% of Increase UH	% of Decrease H
1	5.150	75.0	1.799	157.7	0.0	148.0	9.7	0.570	0.309
				158.6	130.0	149.2	9.4		
2	5.150	75.0	5.183	165.8	0.0	147.2	18.6	0.844	0.537
				167.2	130.0	148.7	18.5		
3	5.150	75.0	10.297	175.6	0.0	146.5	29.1	0.797	1.393
				177.0	130.0	148.3	28.7		
							Mean	0.737	0.746
4	3.188	75.0	2.364	159.6	0.0	147.5	12.1	1.378	1.559
				161.8	130.0	149.8	12.0		
5	3.188	75.0	4.344	164.4	0.0	147.0	17.4	1.155	1.904
				166.3	130.0	149.8	16.5		
6	3.188	75.0	10.297	175.6	0.0	146.6	29.0	1.025	3.448
				177.4	130.0	149.4	28.0		
							Mean	1.186	2.303

TABLE 6.7 EFFECT OF DOWNSTREAM HEAD ON UPSTREAM AND OVERFLOW HEADS FOR AIR/WATER INFLATED DAM.

The mean percentage increase in upstream head when the downstream head increased to 130 mm for the air inflated dam varied from 0.5 to 1.9, for water inflated dams this varied from 0.5 to 1.37 and for air/water inflated dams varied from 0.73 to 1.18. The mean percentage decrease in overflow head when the downstream head increased to 130 mm for air inflated dams varied from 1.23 to 4.73, for water inflated dams varied from 0.85 to 2.6 and for air/water inflated dams varied from 0.74 to 2.30.

The results of these observations were as expected in that the increase in the downstream head caused the dam to distort backwards on the upstream side which increased the crest height of the dam (see Figs. 5.4, 5.6 and 5.8) and this distortion increased the curvature of the crest of the dam which decreased the radius of curvature (see Fig.6.19)and resulted in an increase in C_D (see Fig. 6.20). Therefore,the overflow head decreased in order to keep the flow rate constant.

CHAPTER 7.

THE DESIGN OF AN INFLATABLE DAM.

7.1 Introduction.

The problem of the design of an inflatable dam consists of finding the membrane length, base length and internal pressure for a given upstream head, downstream head and properties of the membrane material as shown in Fig.7.1A.

Clare[8] plotted graphs for designing water inflated dams under hydrodynamic conditions, but these graphs have limited use in that:-

1. The height of the dam is assumed not to change when the hydrodynamic conditions change.
2. There is no change in the coefficient of discharge when the geometric parameters of membrane and base length change.
3. The membrane is weightless and inextensible.
4. The dam is inflated by water only.
5. The geometry of the base is assumed horizontal.
6. The downstream membrane is laid flat at the downstream fixture (downstream slope = 0).

Stodulka[11] also produced design graphs but these graphs can only be used for designing air, water and air/water inflated dams under hydrostatic conditions. However, these graphs have the same limitations of points No. 3, 5 and 6 in Clare's technique with an additional limitation of the downstream head always being equal to zero.

This chapter details a theoretical method of design for air, water and air/water inflated dams under hydrostatic conditions

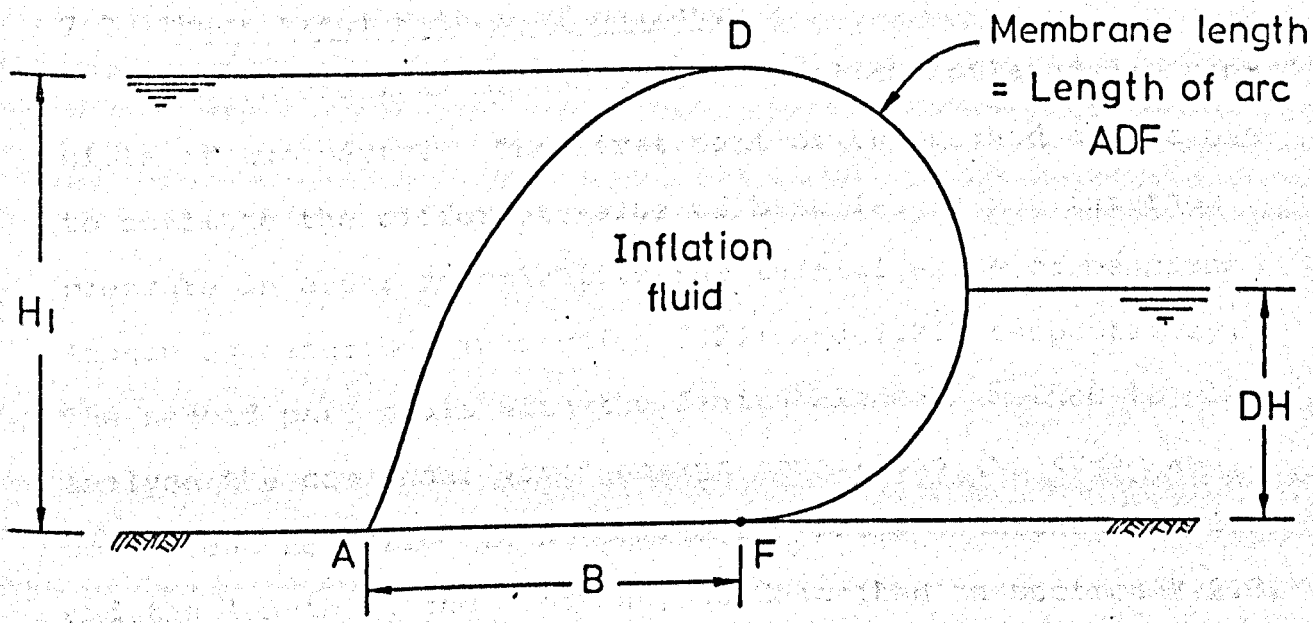

FIG.(7-1A) AN INFLATABLE DAM UNDER THE DESIGN CONDITIONS

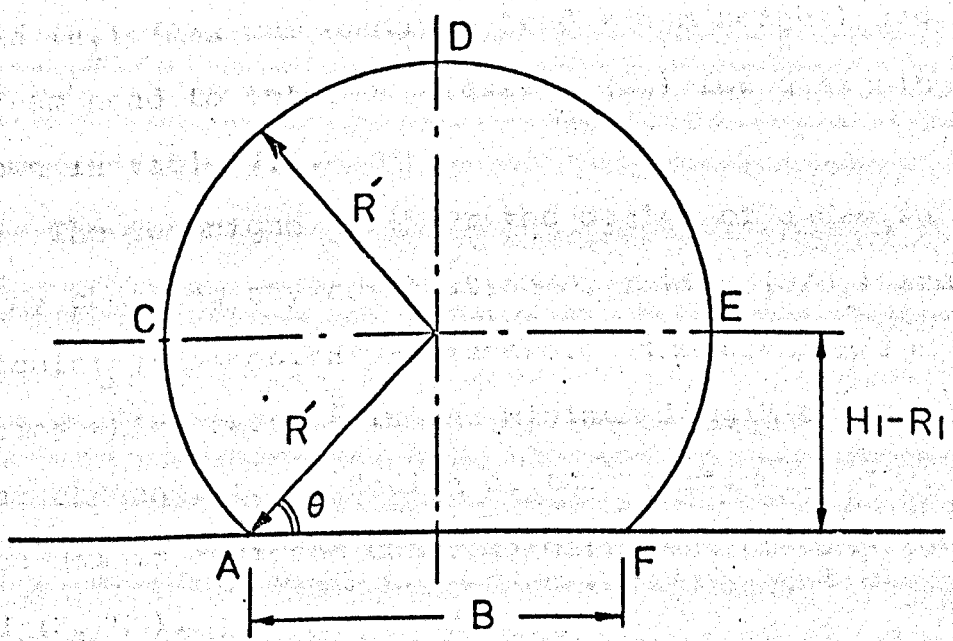

FIG.(7-1B) CALCULATION OF THE INITIAL LENGTH OF THE MEMBRANE

overcoming all the above mentioned limitations of other design methods.

7.2 Theoretical Method of Design.

The theoretical method of design of an inflated dam consists of two parts. The first part of the method allows one to estimate the different value of base length and internal pressure in order to calculate the initial value of membrane length as described in section 7.2.1 and 7.2.2 respectively. The second part deals with the finite element method to analyse the dam under given design conditions (upstream and downstream heads) and to determine the cross-sectional profile and the length of the membrane, as described in section 7.2.3.

7.2.1 Base length and Internal Pressure.

The base length and internal pressure are estimated by using different ratios of base length (B) to a maximum upstream head (H_1) (maximum upstream head = dam height) and maximum upstream head to internal pressure (H_2) for designing a dam as shown in table 7.1.

The technique used for the design of a dam in this section is by choosing any combination of ratios (B/H_1) and (H_1/H_2) to calculate the design parameters. The combination of these ratios which results in the minimum length of the membrane is that chosen for the design of that particular dam. Therefore, each dam is designed under 35 different combinations of (B/H_1) and (H_1/H_2).

No. of Trial	B/H_1	H_1/H_2
1	2.00	0.50
2	1.75	0.60
3	1.50	0.70
4	1.25	1.00
5	1.00	1.50
6	0.75	
7	0.50	

TABLE 7.1 DESIGN RATIOS OF B/H_1 AND H_1/H_2.

7.2.2 Membrane Length.

The initial membrane length of a dam can be calculated when the profile of the dam is assumed to be the arc of a circle as shown in Fig.7.1B.

The radius of the arc CDE is R' and can be calculated as

$$R' = [(H_1)^2 + (B/2)^2]/(2H_1) \quad \ldots\ldots \quad (7.1)$$

Therefore, the length of the arc CDE(L_1) is given by:

$$L_1 = \pi R' \quad \ldots\ldots \quad (7.2)$$

where π is a constant = 3.14159

The length of the arc CA (L_2) is given by

$$L_2 = \theta \cdot R'$$

where θ = angle of arc CA in radians.

$$\tan \theta = \frac{H_1 - R'}{(B/2)}$$

Then

$$\theta = \tan^{-1} [(H_1 - R')/(B/2)] \quad \ldots\ldots \quad (7.3)$$

Substituting equation (7.3) in equation (7.2) gives

$$L_2 = R' [\tan^{-1} (2 (H_1 - R')/B] \quad \ldots\ldots \quad (7.4)$$

From the geometry

The length of arc CA = the length of arc EF = L_2

Hence, the total length (TL) of the membrane ACDEF is

$$TL = L_1 + 2 L_2 \quad \ldots\ldots \quad (7.5)$$

7.2.3 Design Procedure.

The design procedure for an inflatable dam is summarized as follows:

(1) Assume a ratio between the base length and the height of the dam (see table 7.1).

(2) Assume a ratio between the upstream head and internal pressure (see table 7.1).

(3) Calculate the membrane length from section 7.2.2.

(4) Use the method of analysis of the dam under hydrostatic conditions (which is previously described in section 4.2) in order to determine the tension and the cross-sectional profile of the membrane.

(5) Compare the crest height (Y_{max}) of the dam with a given upstream head (H_1) and if the difference between these two parameters is more than $\pm$ 1 mm the following method is used to correct the value of the membrane length:-

(a) If $H_1 > Y_{max}$

Calculate the difference (D) between H_1 and Y_{max} as follows:

$$D = H_1 - Y_{max}$$

Then, the new height (H_1') of the dam becomes:

$$H_1' = H_1 + D$$

(b) If $H_1 < Y_{max}$

$$D = Y_{max} - H_1$$

and

$$H_1' = H_1 - D$$

(6) Calculate the new membrane length from 7.2.2 by using $H_1 = H_1'$

(7) Repeat the procedure from step 4 until the difference between the given upstream head and dam height is less than $\pm$ 1 mm.

(8) Repeat the procedure from step 2 with a new value of H_1/H_2 (table 7.1).

(9) Repeat the procedure from step 1 with a new value of B/H_1.

(10) Choose the condition of B/H_1 and H_1/H_2 which gave a minimum length of the membrane for the dam.

7.3 Computer Programs.

7.3.1 Computer Program (DID).

The program (DID) was written to design air, water and air/water inflated dams under hydrostatic conditions by using the theoretical method of design (which was previously described in section 7.2).

The flow chart of the program is illustrated in Fig.7.2 and a list of the program is available from the author.

The input data of the program is detailed in table 7.2. The program uses this data to calculate the cross-sectional

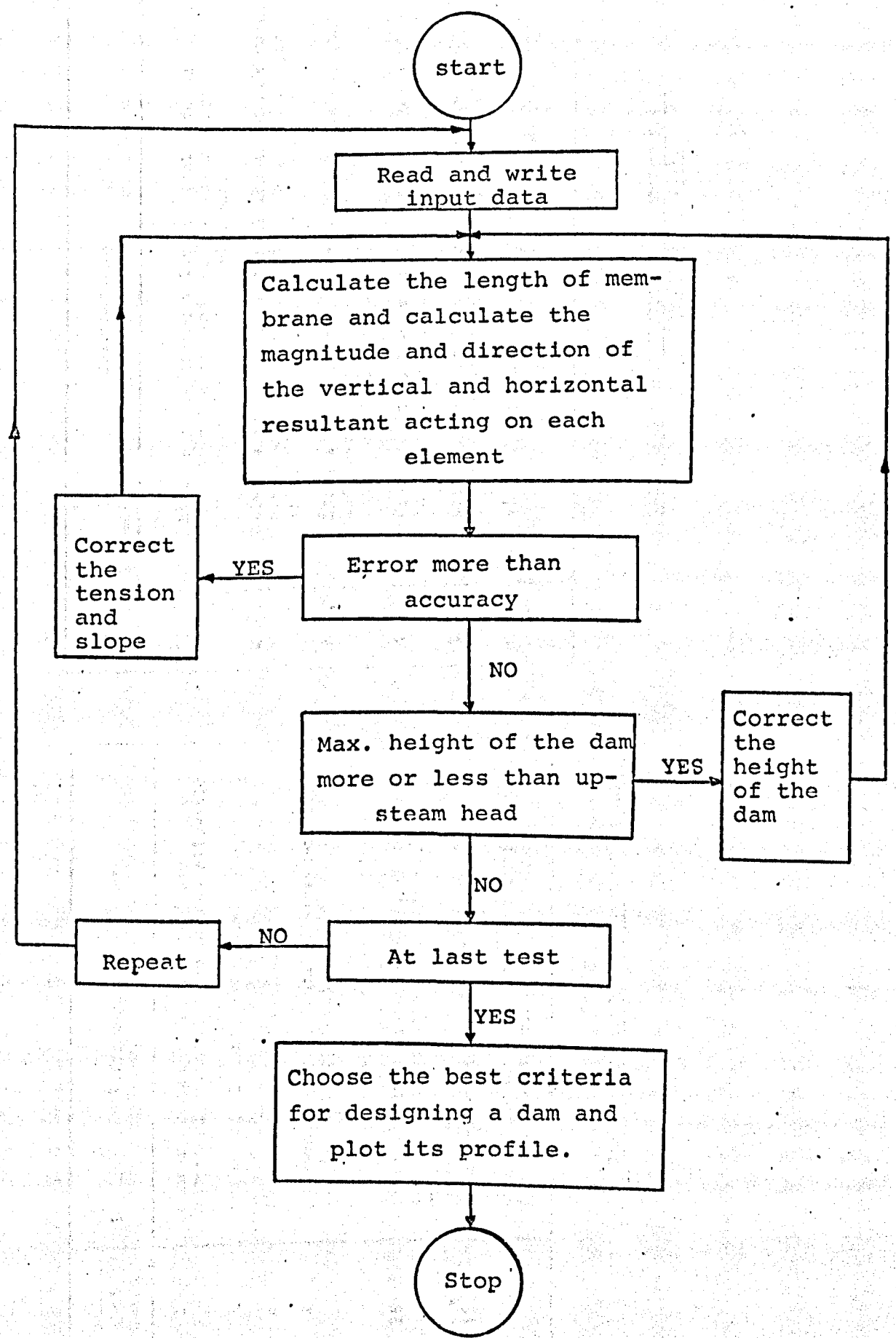

FIG. (7-2) FLOW CHART FOR COMPUTER PROGRAM (DID).

Card No.	Number of Cards	Information
1	1	number of dams to be designed and numerical value of x-y misclose allowable.
2	1	number of elements and nodes of membrane.
3	1	thickness, weight of fabric.
4	1	polynomial coefficients of stress-strain relationship of fabric.
5	1	design upstream and downstream heads.
6	35	initial values of tension and slope of the first upstream element for each condition.
7	35	values of ratios B/H_1 and H_1/H_2.
8	35	x-y co-ordinates of first and last node for each condition.

TABLE 7.2 DESCRIPTION OF INPUT DATA OF PROGRAM (DID)

No.	Information
1	Lists a table of the values of static force acting on the dam and the tension in each membrane under the 35 conditions.
2	Lists a table of the original length of membrane, stretched length, crest height and base length of the dam under 35 conditions.
3	Lists a table of the values of upstream tension and upstream slope of the first element of the dam under 35 conditions.
4	Lists a minimum membrane length, base length and internal pressure.
5	Lists a table of the x-y co-ordinates of the profile of the dam under selected condition.
6	Plot of the shape of that dam.

TABLE 7.3 DESCRIPTION OF OUTPUT DATA OF PROGRAM (DID).

profile of the dam, the tension in the membrane and the membrane length.

Under given design conditions for a dam, the program will design that dam under 35 various conditions of base length and internal pressure (see section 7.2.3) and choose the magnitude of the base length and internal pressure which gives a minimum membrane length. Then the program can plot the cross-sectional profile of the dam under selected conditions.

The output of the program is described in table 7.3, and a typical output plot is shown in Figs. 3.7 and 5.1.

7.3.2 Computer Program (DID1).

The technique of design of an inflatable dam which was used in the program (DID) required a long time in preparation of the input data and also consumed a great deal of computer time to design one dam. This resulted from using 35 various condition of base length and internal pressure for designing the dam under given upstream and downstream heads.

Therefore, a different technique of design was developed and written in a new program (DID1) in order to:-

1. Reduce time on the computer.
2. Facilitate the input date of the program.
3. Use the program for design of a dam with limited base length (see Figs. 7.9 and 7.10).

Two subroutines were connected to (DID1), the first subroutine was used to calculate the base length (see section 7.3.2.1) and initial minimum length of membrane; the second subroutine was used to calculate the initial value of tension and slope at the first element (see section 4.2.2).

The design technique used in the program (DID1) for determining the design parameters is described in section 7.3.2.1, 7.3.2.2 and 7.3.2.3. The input/output data of the program is described in section 7.3.2.4.

A list of the program (DID1) is available from the Department of Civil & Structural Engineering of the University of Sheffield.

7.3.2.1 Base and Membrane Lengths.

The procedure to calculate the base and membrane length is as follows:

(1) Assume a ratio of base length (B) to upstream head (H_1) equal to 0.6[8] and calculate the membrane length from section 7.2.2.

(2) Increase the ratio (B/H_1) by 0.1 and re-calculate the membrane length. This procedure continues until the ratio of B/H_1 reaches 2.0[11].

(3) Choose the ratio of B/H_1 which gives the minimum length of the membrane.

From this procedure, the ratio of B/H_1 can be calculated to give a minimum length for different height of dams as shown in Fig.7.3.

7.3.2.2 Calculating Internal Pressure.

The internal pressure depends on the allowable tension in the fabric and can be calculated from equation (7.5) when the cross-sectional profile of the dam is assumed to be the arc of a circle:[10]

$$P = AT/R \quad \ldots\ldots \quad (7.5)$$

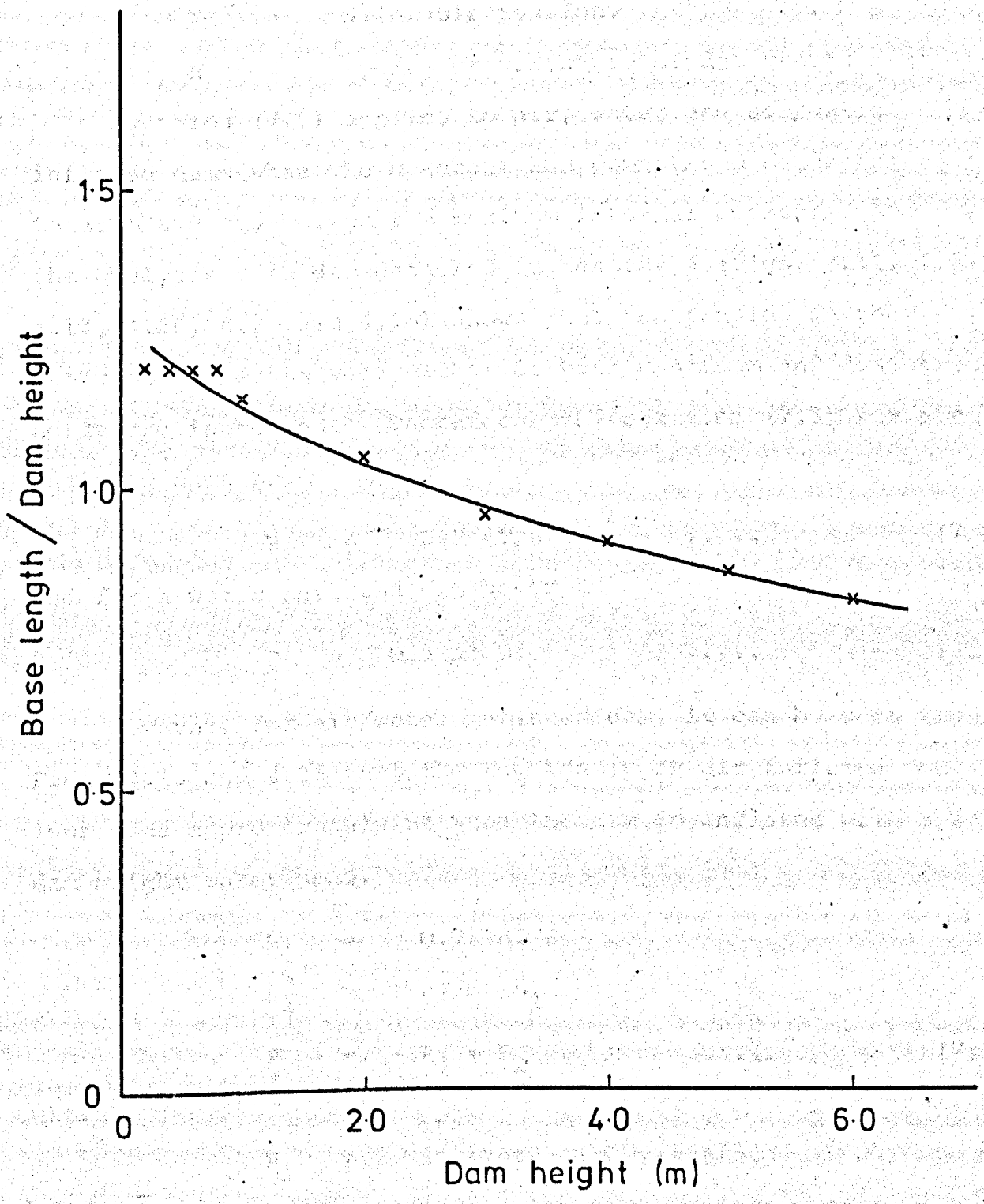

FIG.(7–3) VARIATION OF DAM HEIGHT WITH RATIO OF BASE LENGTH / DAM HEIGHT

where

P = internal pressure.

AT = allowable tension.

R = radius of curvature of dam crest.

Equation (7.5) applies to air, water and air/water inflated dams when the upstream and downstream heads are equal to zero and thus gives the maximum internal pressure. However, the analysis of a dam detailed in chapter 4 (Figs. 4.11, 4.12, 4.13, 4.26, 4.27 and 4.28) shows that the tension in the membrane decreases when either or both upstream and downstream heads are increased. Therefore, the equation (7.5) for air inflated dams becomes:

$$P = 0.8\ AT/R \quad \ldots\ldots \quad (7.6)$$

and for a water inflated dam becomes:

$$P = 0.9\ AT/R \quad \ldots\ldots \quad (7.7)$$

However, for air/water inflated dam, it can be seen from Figs. 4.13 and 4.28 that the tension in an air inflated dam increases approximately 5% when the dam is inflated with a 2/3 dam height water head. Then

$$P_1 = 0.75\ AT/R$$

$$P_2 = \rho g\ m'\ H_1$$

$$P = P_1 + P_2 \quad \ldots\ldots \quad (7.8)$$

where

P_1 = internal air pressure.

P_2 = internal water pressure.

ρg = unit weight of water.

m' = ratio of internal water head to upstream head.

P = total internal pressure.

7.3.2.3 Procedure of Design.

The procedure of design used in the program (DID1) is summarised as follows:

1. From section 7.3.2.1 the base length of an inflatable dam is determined and therefore the initial length of the membrane is found (see section 7.2.2).
2. The internal pressure can be calculated from using equation (7.6) for air inflated dam, equation (7.7) for water dam and equation (7.8) for inflating the dam by a combination of air and water. Fig. 7.4 illustrates the effects of variation of allowable tension on the internal pressure.
3. The actual membrane length of the dam is calculated as described in section 7.2.3 step 4, 5, 6 and 7. Fig. 7.5 shows the effects of variation of allowable tension on the actual membrane length.

7.3.2.4 Input/Output Data.

The input data of the program (DID1) consists of nine cards as described in table 7.4.

The base length parameter in card No. 7 gives a numerical value of the base length if the designer is limited by this condition (see section 7.4, example 4 and 5). Without this limitation of base length the numerical value is zero and the program selects a suitable base length for the dam. The ratio of air/water parameter in the same card is used only when the dam is inflated by air/water pressure.

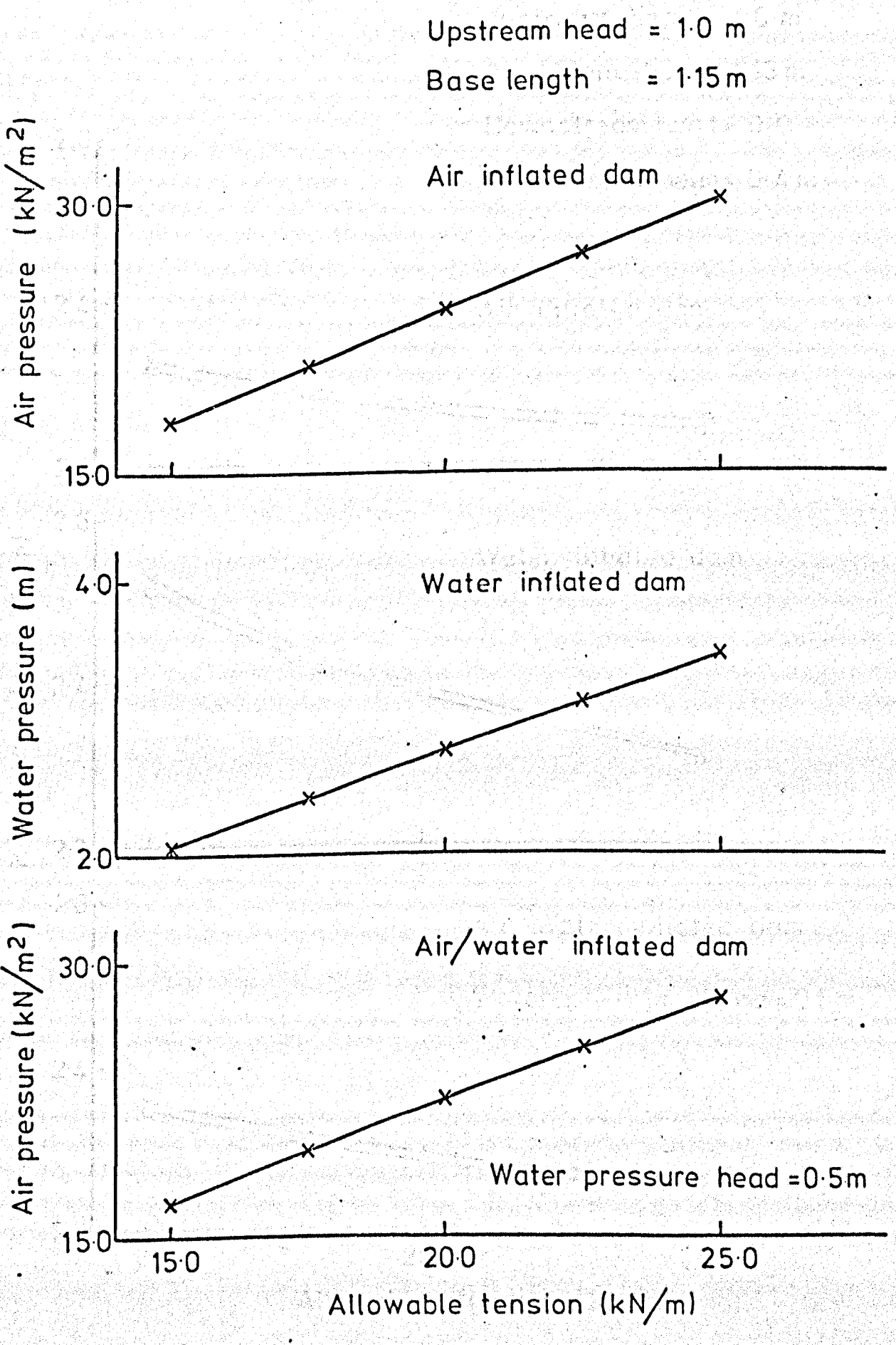

FIG.(7-4) VARIATION OF ALLOWABLE TENSION IN MEMBRANE WITH INTERNAL PRESSURES

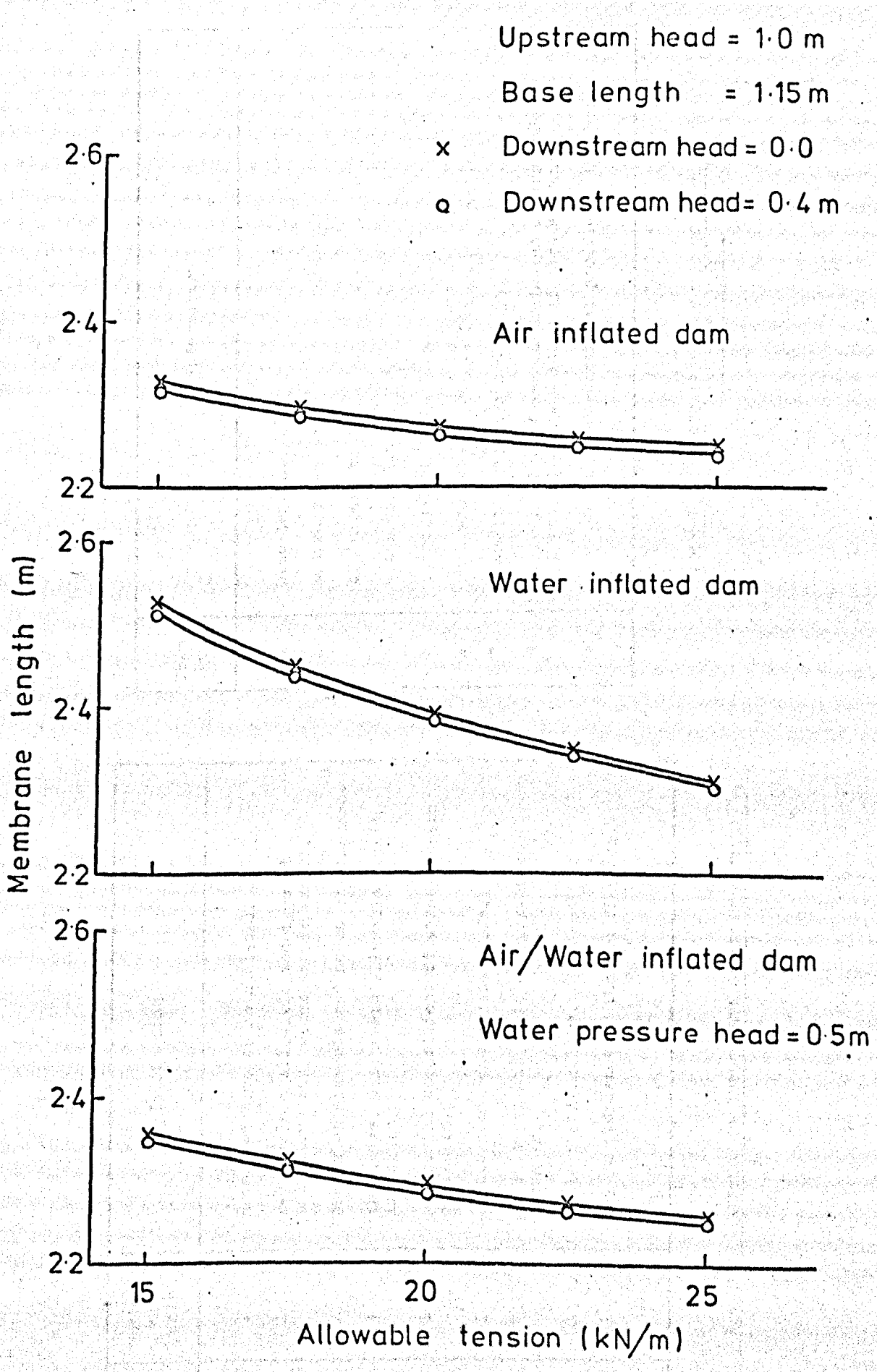

FIG. (7-5) VARIATION OF ALLOWABLE TENSION IN MEMBRANE WITH MEMBRANE LENGTH

Card No.	Number of Cards	Information
1	1	number of dams to be analysed.
2	1	x-y misclose allowable and type of inflation (air, water or air/water).
3	1	number of elements and nodes of membrane.
4	1	thickness, weight and allowable tension in fabric.
5	1	polynomial coefficient of stress-strain of fabric.
6	1	upstream and downstream heads.
7	1	base length and ratio of air/water pressure.
8	1	scale x and scale y.
9	1	x-y co-ordinates of the two fixtures.

TABLE 7.4 DESCRIPTION OF INPUT DATA OF PROGRAM (DID1).

Item No.	Information
1	base length.
2	membrane length.
3	air pressure.
4	water pressure.
5	crest height of the dam.
6	upstream tension and slope.
7	downstream tension and slope.
8	lists a table of x-y co-ordinates of the nodes and the tension and slope of each element.
9	plot of the cross-sectional profile of the dam.

TABLE 7.5 DESCRIPTION OF OUTPUT DATA OF PROGRAM (DID1).

Given the numerical value of the x-y co-ordinates of the two fixtures if limited by a known base length but without known base length, the values of x and y co-ordinates are equal to zero.

The output of the program is described in table 7.5 and examples of a typical output plot are illustrated in section 7.4.

7.4 Examples of Design of an inflatable Dam.

All examples of dams illustrated in this section were designed by program (DID1) using 40 elements and N.T. fabric (see section 3.3.1).

Example 1:

The design of an air inflated dam under upstream head of 1.0 m and downstream head equal to zero with an allowable tension in the membrane of 15 kN/m, is shown in Fig. 7.6.

Example 2:

The design of a water inflated dam under the same heads of upstream and downstream and allowable tension in the membrane as in example 1 are shown in Fig.7.7.

Example 3:

The design of an air/water inflated dam under the same upstream and downstream heads and allowable tension in the membrane as in example 1 and m'= 0.5 as shown in Fig. 7.8.

Example 4:

The design of an air, water and air/water dam with an upward slope of base length of 1.02 m under upstream head of 1.2 m and downstream head of 0.4 m and an allowable tension of 25 kN/m, is shown in Fig. 7.9.

U/S HEAD	=	1.0000	METER
D/S HEAD	=	0.0000	METER
ALLOWABLE TENSION	=	15.0000	KN/M
AIR PRESSURE	=	18.0366	KN/SQ.M
WATER PRESSURE	=	0.0000	M.WG
ORIGINAL LENGTH	=	2.3275	METER
NEW LENGTH	=	2.7399	METER
U/S TENSION	=	10.1089	KN/M
D/S TENSION	=	12.2919	KN/M
BASE LENGTH	=	1.1500	METER
MAX. HEIGHT	=	1.0009	METER

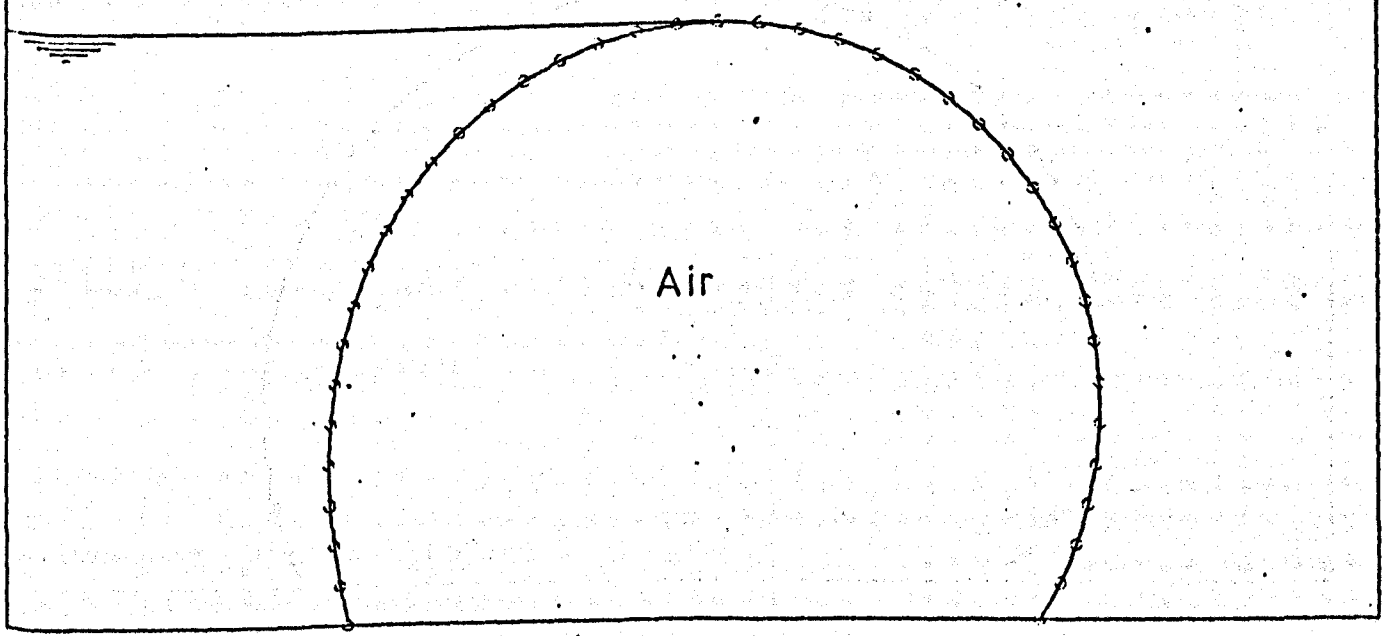

FIG. (7-6) THE DESIGN OF AN AIR INFLATED DAM

U/S HEAD	=	1.0000	METER
D/S HEAD	=	0.0000	METER
ALLOWABLE TENSION	=	15.0000	KN/M
AIR PRESSURE	=	0.0000	KN/SQ.M
WATER PRESSURE	=	2.0684	M.WG
ORIGINAL LENGTH	=	2.5256	METER
NEW LENGTH	=	2.8338	METER
U/S TENSION	=	6.9785	KN/M
D/S TENSION	=	8.9900	KN/M
BASE LENGTH	=	1.1500	METER
MAX. HEIGHT	=	1.0004	METER

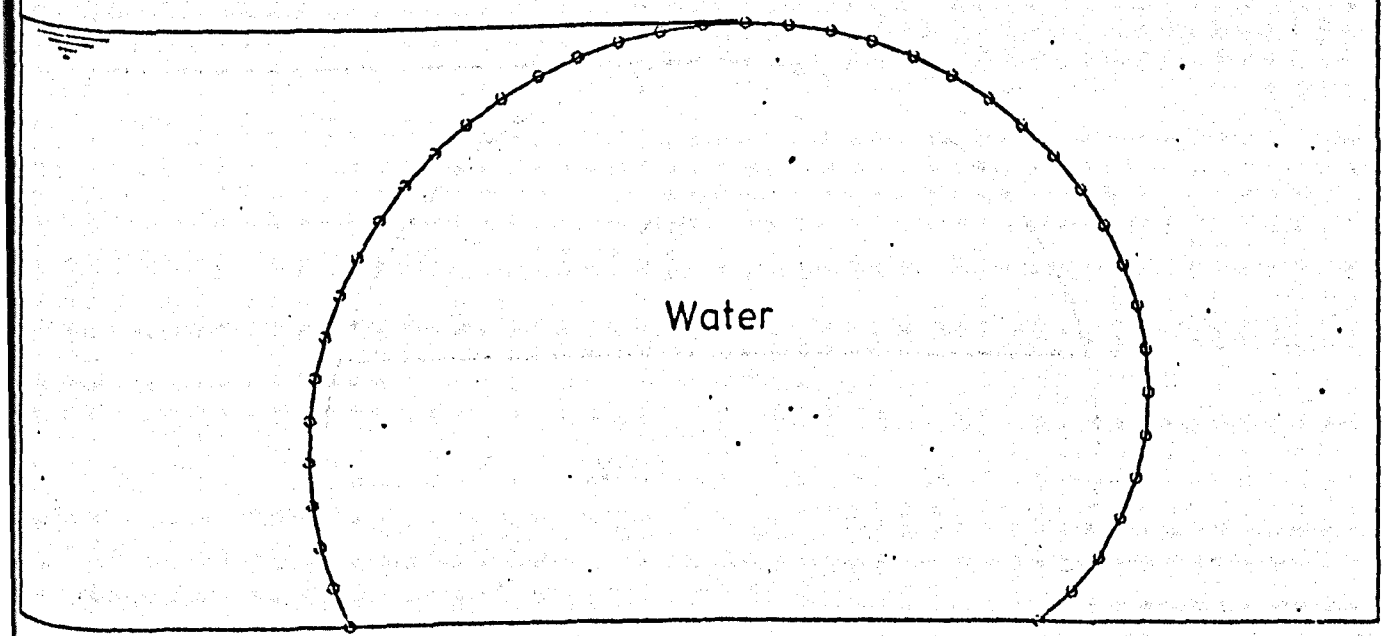

FIG.(7-7) THE DESIGN OF A WATER INFLATED DAM

U/S HEAD	=	1.0000	METER
D/S HEAD	=	0.0000	METER
ALLOWABLE TENSION	=	15.0000	KN/M
AIR PRESSURE	=	16.9093	KN/SQ.M
WATER PRESSURE	=	0.5000	M.WG
ORIGINAL LENGTH	=	2.3541	METER
NEW LENGTH	=	2.7592	METER
U/S TENSION	=	9.5625	KN/M
D/S TENSION	=	11.7836	KN/M
BASE LENGTH	=	1.1500	METER
MAX. HEIGHT	=	1.0008	METER

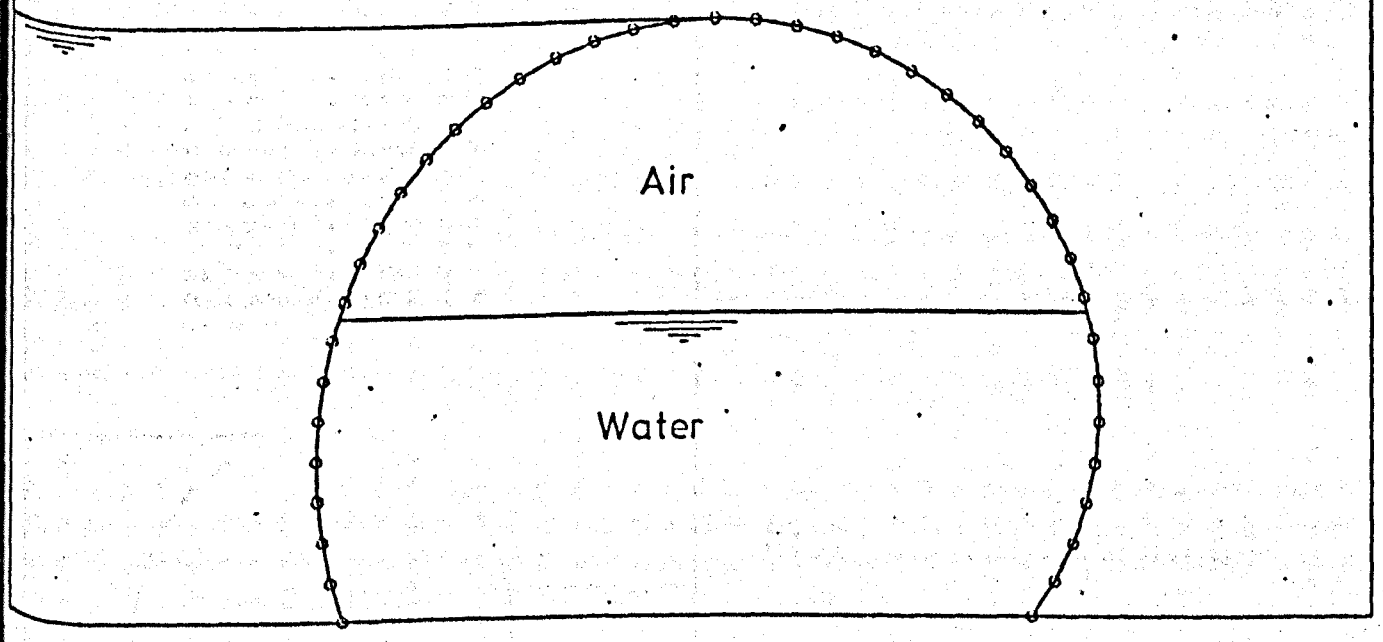

FIG.(7-8) THE DESIGN OF AN AIR/WATER INFLATED DAM

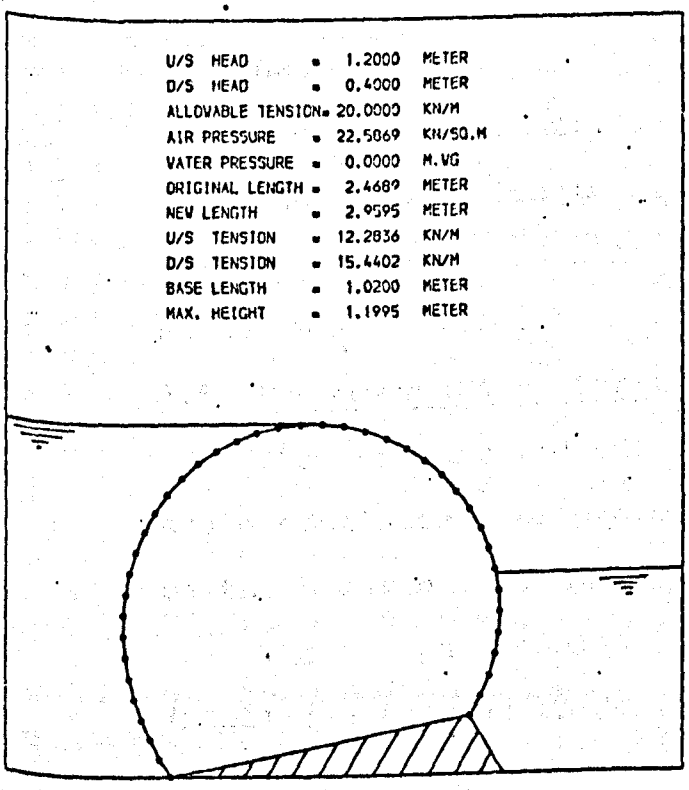

Air inflated dam

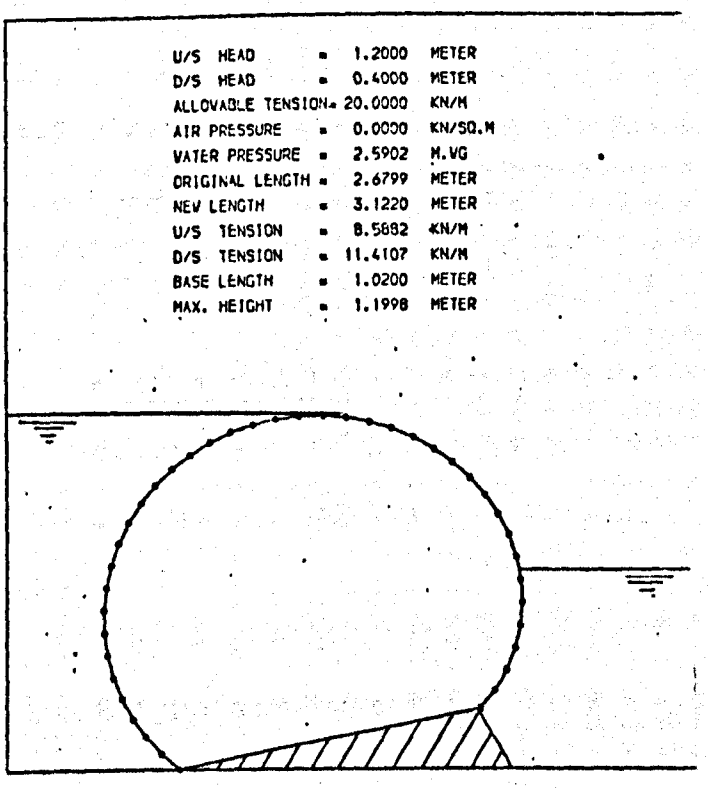

Water inflated dam

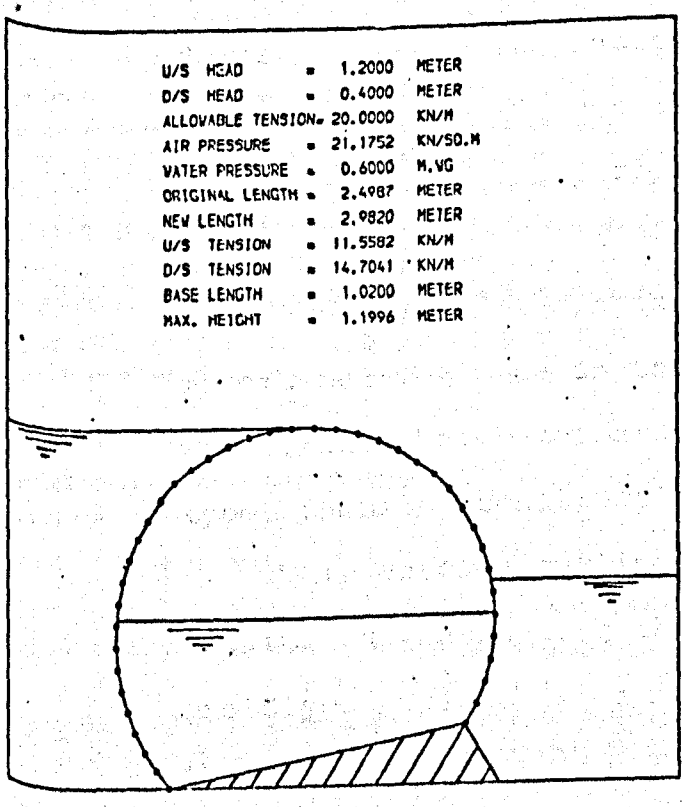

Air/water inflated dam

FIG.(7-9) THE DESIGN OF INFLATABLE DAMS WITH INCLINED BASES IN THE UPWARD DIRECTION

Example 5:

The design of air, water and air/water dams with an downward of base length of 1.20 m under the same upstream and downstream heads and allowable tension as in example 4, and shown in Fig. 7.10.

7.5 Recommendations for the Design of a Model Inflatable Dam.

The work carried out by the author was not based on scale model tests of prototype inflatable dams, but was tests on the behaviour of small inflatable dams.

The design technique which is represented in the program (DID1) can be used to design a prototype air, water and air/water inflated dam under hydrostatic conditions. From the design parameters of membrane length, base length and inflation pressure, the performance of such a dam can be theoretically analysed under different combinations of upstream head, downstream head and internal pressure by using program (AID3). This means that the construction of a prototype dam can be carried out and its performance anticipated without resorting to a model study.

However, if it is decided to study the effects of parameters not included in this theoretical approach, for example waves, snow, high temperature and high overflow on the prototype, then the construction of a model is necessary.

This section outlines the criteria that should be adopted in considering the relationship between a model and prototype inflatable dams. Any model should be similar to the prototype in three ways:

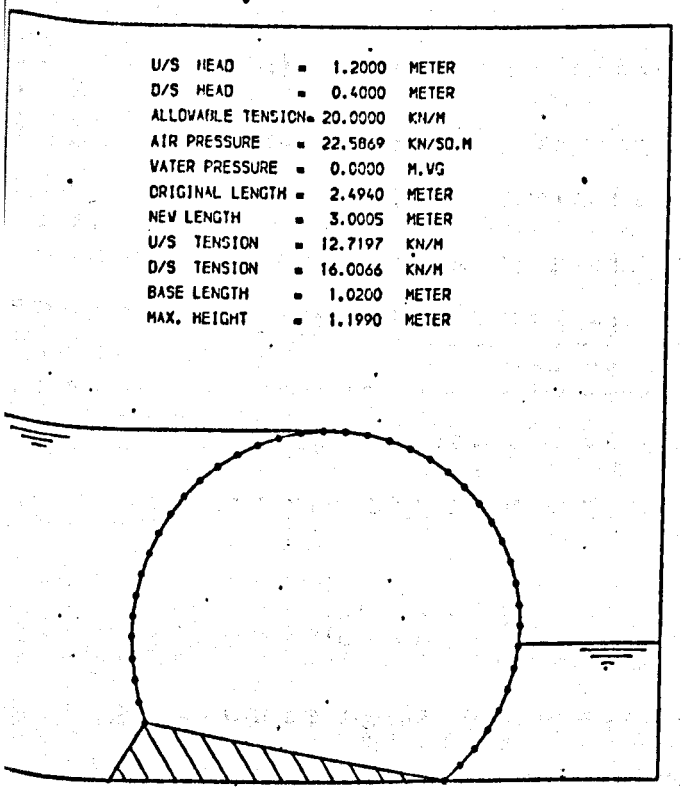

Air inflated dam

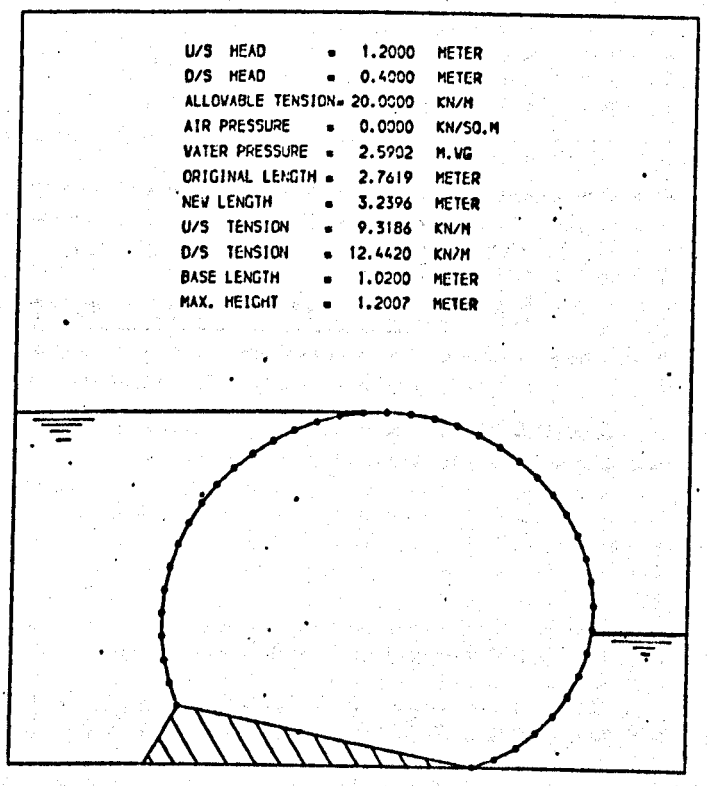

Water inflated dam

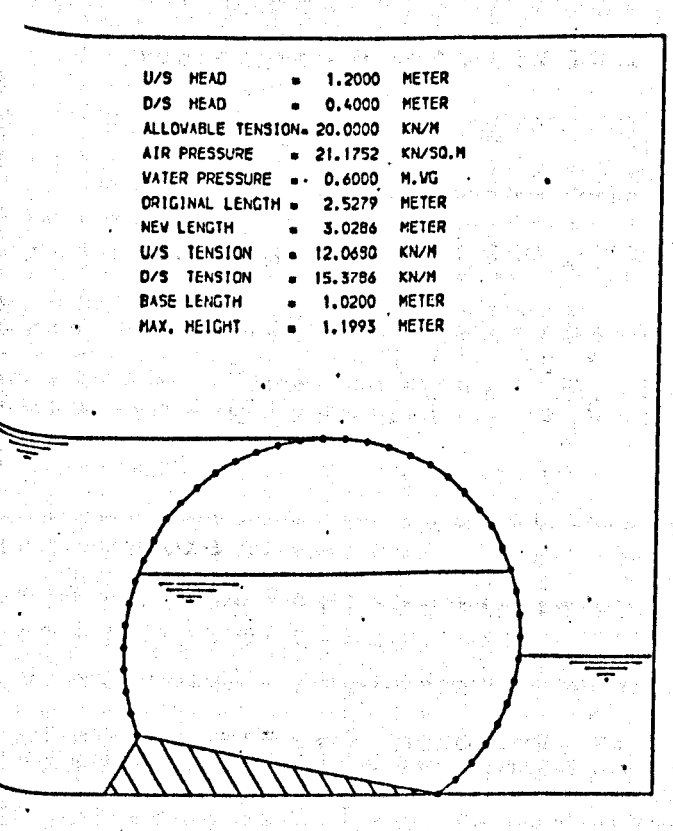

Air/water inflated dam

FIG.(7-10) THE DESIGN OF INFLATABLE DAMS WITH INCLINED BASES IN THE DOWNWARD DIRECTION

(a) Geometric similarity.

(b) Kinematic similarity.

(c) Dynamic similarity.

These three kinds of similarity are described in Appendix C.

7.5.1 Model Design to Test Under Hydrostatic Conditions.

In this test, the geometric similarity between the model and its prototype is required

$$\frac{L_m}{L_p} = L_r$$

Where L_r is the scale ratio and subscripts m and p refer to the model and prototype respectively.

Rouse[31] observed that a conventional overflow structure with scale ratio (L_r) between 1:30 and 1:60 gave a minimum effect of distorted resistance of the model and the results are transferable with few reservations.

In the case of an inflatable dam, the material of the membrane of the model must have similar properties to the material used for the prototype dam. Therefore

$$\frac{S_{1m}}{S_{1p}} = \frac{\frac{T_m'}{A_m'}}{\frac{T_p'}{A_p'}} = \frac{T_m'}{T_p'} \cdot \frac{A_p'}{A_m'} = \frac{T_m'}{T_p'} \cdot \frac{1}{L_r^2} \quad \ldots\ldots \quad (7.10)$$

where

S_1 = ultimate stress of the membrane material.

T' = ultimate tension of the membrane material.

A' = cross-sectional area of membrane material.

In order to calculate the relationship of the inflation pressure between the model and its prototype, it is necessary to assume both the model and prototype cross-sectional profiles form the arc of a circle. Therefore

$$\frac{P_m}{P_p} = \frac{\frac{T_m'}{R_m}}{\frac{T_p'}{R_p}} = \frac{T_m'}{T_p'} \cdot \frac{R_p}{R_m} = \frac{T_m'}{T_p'} \cdot \frac{1}{L_r} \quad \ldots\ldots \quad (7.11)$$

where P is the magnitude of internal pressure and R is the radius of curvature of the dam crest.

7.5.2 Model Design to Test Under Hydrodynamic Conditions.

A model which is designed to be tested under hydrodynamic conditions must satisfy the three kinds of similarity (see Appendix C). To satisfy the geometric similarity of the model to the prototype then one can follow the same approach described in section 7.5.1

The second similarity which is kinematic similarity is the similarity of motion (see Appendix C). Therefore

$$\frac{Q'_m}{Q'_p} = \frac{V_m A_m}{V_p A_p}$$

$$Q'_r = V_r \cdot A_r \quad \ldots\ldots \quad (7.12)$$

where

Q' = maximum discharge.

V = velocity approach.

A = cross-section area of the channel.

The third similarity is dynamic similarity. This similarity of forces acting on the surface due to inertia forces,

gravity forces, pressure forces, viscous forces, elastic forces and surface tension forces. In the case of an inflatable dam, the gravity forces is predominant and one can neglect the other forces (see Appendix C) when applying dynamic similarity to both the model and its prototype. Then

$$F_G = Ma' \quad \ldots\ldots \quad (7.13)$$

$$\frac{(F_G)_m}{(F_G)_p} = \frac{(Ma')_m}{(Ma')_p}$$

$$\frac{(\rho g\, L^3)_m}{(\rho g\, L^3)_p} = \frac{(\rho\, L^2\, V^2)_m}{(\rho\, L^2\, V^2)_p}$$

$$\frac{V_m^{\,2}}{g_m\, L_m} = \frac{V_p^{\,2}}{g_p\, L_p}$$

$$\frac{V_r}{\sqrt{g_r \cdot L_r}} = 1 \quad \ldots\ldots \quad (7.14)$$

where

F_G = gravity force.

M = mass.

a' = acceleration.

ρ = density of the fluid.

g = acceleration due to gravity.

Substitute V_r from equation (7.14) into equation (7.12) to yield:

$$Q_r' = L_r^{\,2} \sqrt{g_r}\ \sqrt{L_r} \quad \ldots\ldots \quad (7.15)$$

The value of g_r is unity, therefore

$$Q_r' = L_r^{\,5/2} \quad \ldots\ldots \quad (7.16)$$

Then, from equation (7.16) it is possible to calculate the corresponding discharge of the model.

CHAPTER 8.

CONCLUSION AND RECOMMENDATIONS FOR FUTURE WORK.

8.1 Conclusion.

The inflatable dam concept has been shown to be suitable for a large number of hydraulic applications. The ability of such a structure to fold flat on its foundations when not required for use and to rise into its working position when required, offer many advantages over a conventional water control structure. The object of this investigation was to obtain a design technique for a dam and to study the behaviour and performance of that dam under both hydrostatic and hydrodynamic conditions and this has been achieved.

Models were constructed and tested under hydrostatic and hydrodynamic conditions. The maximum height and shape of the model dam were measured and compared with the theoretical maximum height and shape obtained from a theoretical analysis based on a finite element approach. The comparison showed that the average difference between experimental and theoretical maximum height and shape for all dams under hydrostatic conditions were less than 1% and 5% respectively which was a considerable improvement on the previous testing. The comparison also showed that the average difference in maximum height and shape under hydrodynamic conditions is less than 1.5% and 6.5% respectively. It was concluded that when the number of elements for analysis is increased it is possible to obtain a minimal difference in the shape of the dam.

Computer programs were written for the analysis and design of air, water and air/water inflated dams based on the method of analysis (Chapter 4) and design technique method (Chapter 7) developed in this project. These programs can be used to design and study the behaviour and performance of the dam under a range of applications, such as[12]:-

1) Diversion structure.
2) Check structures for flow control.
3) Flashboard replacement.
4) Lock system.
5) Sluice gate.
6) Salinity barriers.
7) Tidal barriers.
8) Raising height of existing spillways.
9) Raising height of water reservoirs by adding to top of existing gate.
10) Control gates for water treatment plants.
11) Control gate for sewage plants.
12) Replacement of steel gate on concrete structure.
13) Replacement of low concrete dam to 7.5 m in height.
14) Barrier for beach erosion.

A new technique for deriving the flow rate over an air, water and air/water inflated dam has been developed. This lead to a new application of a dam as a device for discharge measurement.

However, the main conclusions of the behaviour and performance of an inflatable dam which resulted from this research under both hydrostatic and hydrodynamic conditions are as follows:-

a) The dam became rigid when inflated by high pressure and had insignificant deformation in shape when the upstream, downstream and overflow heads changed.

b) For air and air/water inflated dams, the V-notch effect occurred when the dams deflated under hydrostatic and hydrodynamic conditions.

c) The tension in the membrane decreased when the upstream and overflow heads increased and increased when the internal pressure increased.

d) The increase in the downstream head resulted in a decrease in the membrane tension and an increase in the crest height of the dam which enabled the dam to store a maximum quantity of water.

e) Under hydrostatic conditions the crest height increased when the upstream head increased up to certain upstream depth. It then began to decrease when the upstream head increased further. However for the hydrodynamic case the crest height decreased when the overflow head increased.

f) The air inflated dam had a crest height greater than for both water and air/water inflated dams. Therefore, this dam can support an upstream head higher than any of the other dams. However, the tension in the membrane of the air dam is higher than other inflatable dams which gave an increased elongation in the membrane and this may cause a reduction in the dam life which is expected to be approximately 20 years.

g) The dam can be used as a device to control and measure an overflow rate and the theoretical formula derived can be

used to calculate the coefficient of discharge under different combinations of overflow head, downstream head and internal air, water and air/water pressures.

h) The dam is not suitable for high overflow head because vibration will occur and also could not be used as a submerged weir due to the dam oscillating fowards and backwards when the downstream head reaches the crest height.

i) The coefficient of discharge changed significantly when the overflow head, type and magnitude of internal pressure and downstream head changed.

j) The weight and extensibility of the fabric have significant effects on the behaviour and performance of the dam which influence the rate of flow over the dam.

k) A change in the downstream head resulted in a 1% change in the upstream head and 2% change in the overflow head over all dams and the latter percent increased to 5% when the dams were inflated by low pressures.

8.2 Recommendations for Future Work.

1) To study the effects of varying hydrostatic and hydrodynamic pressure on the fabric over long periods.

2) To study the effects of different types of fabric on the behaviour and performance of the dam.

3) To study the effects of high temperature on the behaviour and performance of the dam under hydrostatic and hydrodynamic conditions.

4) To develop the computer program (DID1) by estimating the depth of overflow when the vibration occurs.

5) To study the effects of membrane and base length on the behaviour and performance under hydrostatic and hydrodynamic conditions.

6) To study the behaviour and performance of the dam when fixed at the base from one point.

7) To test additional models of different sizes to investigate the behaviour and performance of the dam under hydrostatic and hydrodynamic conditions to observe any scale effect.

8) To consider the possibility of using other fluids to inflate the membrane of a dam.

APPENDIX A.

Effect of Temperature on Inflation Fluid.

Temperature (^{o}C)	Density (kg/m^3)	
	Air	Water
4.4	1.274	1000.0
10.0	1.248	1000.0
15.6	1.222	1000.0
21.1	1.202	1000.0
26.7	1.176	995.0

TABLE A. EFFECT OF TEMPERATURE ON DENSITY OF AIR AND WATER.

It can be seen from the above table, that the density of air changes about 8% when the temperature changes from 4.4^{o}C to 26.7^{o} C. However, this change in density has insignificant effect (less than 0.3%) on the absolute air pressure. The absolute pressure can be calculated from the equation below

$$P = \rho R T$$

where

P = absolute air pressure (N/m^2)

ρ = density (kg/m^3)

R = a constant = 287.1

T = absolute temperature in degree Kelvin (273 + ^{o}C).

For water, the density changes 0.5% when the temperature changes from 4.4^{o}C to 26.7^{o}C and this results in a water

pressure change of 0.5%. The water pressure is calculated from

$$P_1 = \rho g\, h$$

where

P_1 = water pressure (N/m^2).

ρg = unit weight of water (N/m^3)

h = head of water (m)

Therefore, both air and water pressure have insignificant changes when the temperature changes throughout the range shown in table A which covers the range of temperature within a laboratory.

No.	Air (kN/m^2)	U/S Head (mm)	D/S Head (mm)	Q (exp.) (ℓ/s)	Crest Height (mm)	Overflow Head (mm)	S = 2 Q (ℓ/s)	% Diff. (Abs.)	Q* (ℓ/s)	% Diff. (Abs.)
1	5.886	165.5	0.0	2.980	147.61	17.89	3.219	8.0	2.787	6.4
2	5.886	171.7	0.0	5.869	147.60	24.10	5.839	0.5	5.406	7.8
3	5.886	180.0	0.0	10.539	147.59	32.41	10.624	0.8	9.807	6.9
4	5.886	190.0	0.0	16.781	147.55	42.45	18.479	10.1	16.681	0.6
5	4.905	165.4	0.0	2.364	147.72	17.68	3.209	35.7	2.632	11.3
6	4.905	169.9	0.0	4.711	147.72	22.18	5.016	6.4	4.403	6.5
7	4.905	175.8	0.0	7.325	147.65	28.15	7.198	1.7	7.177	2.0
8	4.905	181.9	0.0	10.418	147.56	24.34	10.747	3.1	10.885	4.4
9	4.905	164.3	50.0	2.514	147.88	16.41	2.760	9.7	2.334	7.1
10	4.905	172.5	50.0	5.770	147.86	24.64	6.161	6.7	5.487	4.9
11	4.905	177.8	50.0	8.315	147.85	29.95	8.137	2.1	8.219	1.2
12	4.905	184.0	50.0	11.778	147.80	36.10	11.967	1.6	12.068	2.4
13	4.905	166.5	100.0	2.900	148.57	17.93	3.149	8.5	2.826	1.5
14	4.905	170.4	100.0	4.711	148.56	21.84	4.769	1.2	4.272	9.3
15	4.905	175.6	100.0	6.688	148.54	27.06	7.306	9.2	6.651	0.5
16	4.905	184.8	100.0	12.287	148.50	36.30	13.301	8.2	12.145	1.2
17	3.924	164.0	0.0	2.514	147.87	16.13	2.487	1.0	2.461	2.0
18	3.924	166.2	0.0	3.304	147.80	18.40	3.180	3.7	3.133	5.1
19	3.924	172.7	0.0	6.274	147.72	24.98	5.814	7.3	6.126	2.3
20	3.924	179.0	0.0	10.057	147.56	31.44	7.695	23.4	9.816	2.4
21	2.943	165.5	0.0	2.743	147.85	17.65	2.648	3.4	2.785	1.0
22	2.943	173.9	0.0	7.110	147.31	26.59	4.773	32.8	6.561	7.7
23	2.943	178.5	0.0	9.347	146.96	31.54	6.325	32.3	9.330	0.2
24	2.943	187.0	0.0	15.071	146.06	40.94	6.221	58.7	17.818	18.2
25	2.943	163.5	50.0	2.514	148.40	15.10	1.971	21.5	2.100	16.4
26	2.943	173.2	50.0	6.071	148.08	25.12	3.062	49.5	5.404	11.0
27	2.943	180.0	50.0	9.581	147.51	32.40	7.870	17.8	9.934	3.6
28	2.943	185.5	50.0	14.122	147.46	38.04	6.549	53.6	13.663	3.2
29	2.943	168.7	100.0	3.812	149.91	18.79	3.333	12.5	3.158	17.1
30	2.943	175.0	100.0	6.480	149.80	25.20	4.824	25.5	5.871	9.4
31	2.943	183.0	100.0	10.297	149.65	33.35	8.600	16.5	10.578	2.7
32	2.943	189.5	100.0	15.622	149.40	40.10	8.710	44.2	15.410	1.3
33	1.962	161.4	0.0	1.866	147.31	14.09	1.865	0.0	1.766	5.3
34	1.962	167.9	0.0	4.526	146.19	21.71	6.574	45.2	4.402	2.7
35	1.962	176.5	0.0	9.230	144.36	32.14	11.882	28.7	9.901	7.2
36	1.962	182.8	0.0	15.483	142.58	40.22	19.247	24.3	15.624	0.9
							% Diff Mean (Abs)	17.3		5.4

TABLE B.1 COMPARISON BETWEEN EXPERIMENTAL AND THEORETICAL DISCHARGE OVER AIR INFLATED DAM.

*$S = 2.28\ (H/R)^{0.21}$

No.	Water (mm)	U/S Head (mm)	D/S Head (mm)	Q (exp.) (ℓ/s)	Crest Height (mm)	Overflow Head (mm)	S = 2 Q (ℓ/s)	Diff. (Abs.)	Q*	% Diff. (Abs.)
1	750.0	162.7	0.0	3.555	144.23	18.47	3.565	0.3	3.217	9.5
2	750.0	170.0	0.0	6.898	143.82	26.18	6.985	1.3	6.425	6.8
3	750.0	178.0	0.0	10.539	143.80	34.20	11.289	7.1	10.814	2.6
4	750.0	182.5	0.0	13.854	143.75	38.75	14.606	5.4	14.272	3.0
5	600.0	161.5	0.0	3.304	143.21	18.29	3.320	0.5	3.082	6.7
6	600.0	169.5	0.0	6.898	143.18	26.32	6.778	1.7	6.509	5.6
7	600.0	175.0	0.0	9.937	143.13	31.87	10.017	0.8	9.591	3.5
8	600.0	182.3	0.0	13.854	143.08	39.22	13.928	0.5	14.624	5.5
9	600.0	166.5	50.0	5.279	143.38	23.12	5.123	3.0	5.051	4.3
10	600.0	172.4	50.0	8.655	143.30	29.10	8.274	4.4	8.023	7.3
11	600.0	179.0	50.0	11.778	143.26	35.74	12.637	7.3	12.055	2.3
12	600.0	183.7	50.0	15.208	143.21	40.49	14.764	2.9	15.593	2.5
13	600.0	162.6	100.0	3.471	144.39	18.21	3.586	3.3	3.167	8.7
14	600.0	171.9	100.0	7.650	144.34	27.56	7.481	2.2	7.157	6.4
15	600.0	178.5	100.0	11.905	144.30	34.10	11.553	2.9	11.099	6.7
16	600.0	184.4	100.0	15.208	144.23	40.17	16.002	5.2	15.354	1.0
17	500.0	160.4	0.0	3.222	142.42	17.98	3.241	0.5	2.983	7.4
18	500.0	167.3	0.0	6.071	142.29	25.29	5.763	5.0	5.804	4.4
19	500.0	174.4	0.0	10.057	142.09	32.31	9.697	3.6	9.822	2.3
20	500.0	181.5	0.0	14.391	141.82	39.68	13.045	9.3	14.918	3.6
21	400.0	147.7	0.0	0.224	140.89	6.81	0.322	43.7	0.250	11.6
22	400.0	161.2	0.0	3.987	140.28	20.92	3.741	6.1	3.981	0.2
23	400.0	167.4	0.0	7.110	139.95	27.45	6.538	8.0	6.980	1.8
24	400.0	174.2	0.0	11.153	139.26	34.94	8.674	22.2	11.440	2.5
25	400.0	151.5	50.0	0.997	141.73	9.77	1.038	4.1	0.908	8.9
26	400.0	165.0	50.0	5.869	140.66	24.34	5.117	12.8	5.464	6.9
27	400.0	172.6	50.0	10.539	139.77	32.83	8.400	20.2	10.108	4.1
28	400.0	176.9	50.0	13.063	139.76	37.14	9.902	24.2	12.986	0.6
29	400.0	162.0	100.0	3.987	142.86	19.14	3.418	14.2	3.639	8.7
30	400.0	169.4	100.0	6.898	142.68	26.72	6.468	6.2	6.665	3.3
31	400.0	175.0	100.0	10.539	142.58	32.42	9.639	8.5	9.914	5.9
32	400.0	183.7	100.0	15.345	141.78	41.92	14.101	8.1	16.739	9.0
33	300.0	148.7	0.0	0.942	136.47	12.23	1.137	20.7	1.050	11.5
34	300.0	158.8	0.0	3.899	133.71	25.09	3.350	14.0	4.457	14.3
35	300.0	168.7	0.0	10.297	130.21	38.49	17.410	69.0	12.047	17.0
36	300.0	172.7	0.0	13.063	128.25	44.45	18.296	40.0	15.279	17.0
							Mean	10.8		6.2

TABLE B.2 COMPARISON BETWEEN EXPERIMENTAL AND THEORETICAL DISCHARGE OVER WATER INFLATED DAM.

*$S = 2.36\ (H/R)^{0.21}$

No.	Air (kN/m^2)	Water (mm)	U/S Head (mm)	D/S Head (mm)	Q (exp.) (ℓ/s)	Crest Height (mm)	Overflow Head (mm)	S = 2 Q (ℓ/s)	% Diff. (Abs.)	Q* (ℓ/s)	% Diff. (Abs.)
1	5.150	75.0	165.0	0.0	3.812	146.42	19.08	3.630	4.7	3.512	7.8
2	5.150	75.0	173.0	0.0	7.004	146.41	26.59	6.972	0.5	6.812	2.7
3	5.150	75.0	179.0	0.0	10.418	146.38	32.52	10.687	2.6	9.981	4.2
4	5.150	75.0	185.4	0.0	14.797	146.29	39.11	13.872	6.2	14.488	2.1
5	4.169	75.0	168.7	0.0	5.183	146.42	22.28	4.608	11.0	4.610	11.0
6	4.169	75.0	174.0	0.0	7.217	146.34	27.66	7.026	2.6	7.159	0.8
7	4.169	75.0	180.0	0.0	10.783	146.04	33.96	10.597	1.7	10.987	1.9
8	4.169	75.0	188.5	0.0	17.172	145.99	42.51	14.687	14.5	17.339	1.0
9	3.188	75.0	169.1	0.0	4.992	145.98	23.12	4.283	14.2	5.021	0.6
10	3.188	75.0	176.0	0.0	8.883	145.57	30.43	7.712	13.2	8.848	0.4
11	3.188	75.0	180.2	0.0	11.652	145.34	34.86	7.947	32.0	11.685	0.3
12	3.188	75.0	186.6	0.0	15.483	144.77	41.83	10.589	31.6	16.922	9.3
13	3.188	75.0	167.0	50.0	4.898	146.50	20.50	3.835	21.7	4.302	12.1
14	3.188	75.0	173.0	50.0	7.110	146.28	26.72	5.868	17.5	6.784	4.5
15	3.188	75.0	178.8	50.0	10.661	145.98	32.82	8.914	16.3	10.349	3.0
16	3.188	75.0	180.0	50.0	14.661	145.91	34.09	9.636	34.2	12.186	16.8
17	3.188	75.0	166.0	100.0	3.304	148.27	17.73	2.973	10.0	2.964	10.0
18	3.188	75.0	173.2	100.0	7.004	148.27	25.04	5.846	16.5	6.481	7.5
19	3.188	75.0	179.0	100.0	9.699	147.91	31.09	7.488	22.8	9.339	3.7
20	3.188	75.0	184.6	100.0	13.854	147.81	36.79	10.652	23.1	13.170	5.0
21	2.207	75.0	165.5	0.0	3.987	144.37	21.13	2.555	36.0	4.213	5.6
22	2.207	75.0	174.8	0.0	8.091	143.23	31.57	8.580	6.0	9.009	11.3
23	2.207	75.0	180.5	0.0	12.802	141.53	38.97	15.645	22.2	14.762	15.3
24	2.207	75.0	184.7	0.0	15.900	140.89	43.81	24.485	52.7	18.694	17.5
								Mean	18.0		6.4

TABLE B.3 COMPARISON BETWEEN EXPERIMENTAL AND THEORETICAL DISCHARGE OVER AIR/WATER INFLATED DAM.

*$S = 2.32\ (H/R)^{0.21}$

APPENDIX C.

Model Similitude.

Small-scale models are used extensively to study complex flow phenomena which could not readily be solved by theoretical analysis alone. True models have all the significant characteristics of the prototype reproduced to scale (geometrically similar) and satisfy design restrictions (kinematic and dynamic similitude).

(i) Geometric Similarity.

Geometric similarity is the similarity of shape. All parts of a model must have exactly the same geometric shape as the corresponding parts of its prototype. Therefore, the ratio of corresponding dimensions in model and prototype are equal. Such ratio may be written

$$\frac{L_m}{L_p} = L_r \quad \ldots\ldots \quad (1)$$

$$\frac{A_m}{A_p} = \frac{L_m^2}{L_p^2} = L_r^2 \quad \ldots\ldots \quad (2)$$

where L_r is defined as scale ratio, subscript m, p refer to model and prototype respectively, L is the length and A is the cross-sectional area.

(ii) Kinematic Similarity.

Kinematic similarity is similarity of motion. To satisfy kinematic similarity, both the model and its prototype must have the paths of homologous moving particles geometrically similar and the ratio of velocities of homologous particles are equal. Therefore

$$\frac{Q'_m}{Q'_p} = \frac{V_m A_m}{V_p A_p}$$

$$Q'_r = V_r A_r \quad \cdots\cdots \quad (3)$$

where Q' = rate of flow.

V = velocity approach.

A = cross-sectional area of the path.

(iii) Dynamic Similarity.

Dynamic similarity is the similarity of forces. The model is said to be dynamically similar to its prototype if the ratios of all forces acting on corresponding fluid particles or corresponding boundary surface in the model and prototype are the same.

The condition required for complete similitude is developed from Newton's second law of motion:-

$$\frac{(\Sigma F)_m}{(\Sigma F)_p} = \frac{(Ma')_m}{(Ma')_p} \quad \cdots\cdots \quad (4)$$

The term Ma' is the inertia force of the particle and ΣF is the resultant of all forces acting on the particle. The forces that may exist in a fluid flow are:

1. Pressure force (F_P).
2. Gravity force (F_G).
3. Viscous force (F_V).
4. Elastic force (F_E).
5. Surface tension force (F_T).

Therefore, the resultant force ΣF is the vectorial sum of its component force:

$$\Sigma F = F_P \leftrightarrow F_G \leftrightarrow F_V \leftrightarrow F_E \leftrightarrow F_T = Ma'$$

for complete dynamic similarity between the model and prototype requires in addition that

$$\frac{(Ma')_m}{(Ma')_p} = \frac{(\Sigma F)_m}{(\Sigma F)_p} = \frac{(F_P \leftrightarrow F_G \leftrightarrow F_V \leftrightarrow F_E \leftrightarrow F_T)_m}{(F_P \leftrightarrow F_G \leftrightarrow F_V \leftrightarrow F_E \leftrightarrow F_T)_p}$$

Rouse[31] observed, at least 90% of hydraulic model studies the forces connected with surface tension and elastic compression are relatively small and can be neglected. For all practical purposes, therefore, a particular state of fluid motion can usually be simulated in a model by considering that either gravity forces or viscous forces predominate.

Problems in open-channel flow involving overflow and underflow structures (i.e. spillways, diversion dams, sluiceways and drops), it is customary to preserve complete geometric similarity, and model heads are adjusted to the values required from equating the ratio of gravitational forces to that of inertial forces and neglecting the other forces:-

$$\frac{(F_G)_m}{(F_G)_p} = \frac{(Ma')_m}{(Ma')_p} \quad \cdots\cdots \quad (6)$$

These are the criteria that need to be adopted in considering the relationship between a model and prototype inflatable dam.

REFERENCES

(1) Baker, P.J. — "Further model tests on a proposed flexible fabric dam for the Mangla dam project, Pakistan." The British Hydromechanics Research Association, RR 827, Part II, Nov.1964.

(2) Shepherd, E.M., Hodgens, V.T. — "The Fabridam extension on Koombooloomba Dam of Tully Falls hydro-electric power project." Journ. Inst. Eng. Aust., Vol.41, Jan.-Feb., 1969, pp. 1-7.

(3) Binnie, G.M., Thomas, A.R., Gwyther, J.R. — "Inflatable weir used during constructic of Mangla Dam." Proc. Inst. Civ. Eng., Vol.54, Nov. 1974 pp. 625-639.

(4) Connor, L.J. — "Fabridam - Their application on flood mitigation projects in New South Wales." Journ. Aust. Nat. Committee on Large Dams, Vol.29, 1969, pp.56-65.

(5) O'Neill, B. — "Balloon bursts foil German engineer's stop-gap plans." N.C.E., 14 Sept., 1978, pp.24-26.

(6) Anwar, H.O. — "Inflatable dams." Proc. A.S.C.E., Vol.93, No. HY3, May, 1967, pp. 99-115.

(7) Harrison, H.B. — "The analysis and behaviour of inflatabl membrane dam under static load." Proc. Inst. Civ. Eng., Vol.45, April,197 pp.661-676.

(8) Clare, H.J. — "Design of fabric dams." Ph.D. thesis, Univ. of Liverpool, Oct.19

(9) Binnie, A.M. — "The theory of flexible dam inflated by water pressure." Journ. of Hydraulic Research, Vol.11, No 1973.

(10) Parbery, R.D. — "A continuous method of analysis for the inflatable dam." Proc. Inst. Civ. Eng., part 2, Vol.61, Dec. 1976, pp.725-736.

(11) Stodulka, A.M. — "The design and analysis of inflatable dams." M.Sc. Thesis, Univ. of Sydney, Aust., Sept., 1973.

(12) Fabridam — "General report." Firestone Tire & Rubber Company, No. 654-064-29, April 23, 1964.

(13) Construction News — "Inflatable barrage save low country water table." Construction News, Oct. 15, 1970, pp.18.

(14) Water and Waste Treatment — "Dutch collapsible rubber dam." Water and Waste Treatment, Sept.-Oct., 1969, pp.281.

(15) Gunnerson, R.A. — "Inflatable dam regulates river level." Civil Engineering - ASCE, Feb. 1976, pp.83.

(16) Research Funded by Ministry of Overseas Development — "Inflatable dams for irrigation schemes." Journ. of Hydraulic Research, 1974, pp.47-49.

(17) Anwar, H.O. — "Inflatable dam for irrigation projects." International Water Resources Assoc., New Delhi, Vol.5, Dec. 1975, pp.317-321.

(18) NRDC News — "Portable dam preserves Bournemouth water supplies." John Hudson (Birmingham) Ltd., 20 July, 1976.

(19) Iberston, N.M. — "Collapsible dam aids Los Angeles water supply." Journ. Civ. Eng., Sept. 1960, pp.42-44.

(20) Pao, R.H.F. — "Fluid Mechanics." John Wiley and Sons,Inc., New York,1961.

(21) John Hudson (Birmingham) Ltd. — "Take up your dam and walk." The Consulting Engineers, June, 1975, pp.51.

(22) Fish, D.C.E. — "Personal correspondence." John Hudson (Birmingham) Ltd., Dorset, England.

(23) Harrison, H.B. — "Suspension cable movement analysis." The Inst. of Engrs. Aust., Civ.Eng. Trans., April 1970, pp.72-78.

(24) Harrison, H.B. — "Computer Methods in Structural Analysis." Prentice Hall, Inc., 1973.

(25) Parbery, R.C. "Factors affecting the membrane dam inflated by air pressure." Proc. Inst. Civ. Eng., Part 2, vol. 65, Sept. 1978, pp.645-654.

(26) Harrison, H.B. "The analysis and behaviour of inflatable membrane dams under static loading (Discussion)." Proc.Inst.Civ.Eng., Vol.48, Jan.1971, pp.131-139.

(27) Gunnerson, R.A. "Personal correspondence." Public Service Company of Colorado, Denver, Colorado.

(28) Whittaker, E. Robinson, G. "The Calculus of Observations." Blackie & Son Ltd., London, 1946.

(29) Anwar, H.O. "Inflatable Dams (Closure)." Journ. A.S.C.E., HY6, Nov. 1968, pp.1521-1523.

(30) Chow, V.T. "Open Channel Hydraulics." McGraw-Hill, New York, 1959.

(31) Rouse, H. "Engineering Hydraulics." John Wiley & Sons, New York, 1950.

(32) Lewitt, E.H. "Hydraulics and Fluid Mechanics." Pitman & Sons, Ltd., London, 1961.

(33) Hickox, G.H. "Areation of spillways." Proc. A.S.C.E., Vol.109, Dec., 1942, pp.537-556.

(34) Ali, K.H.M. "Flow over rounded spillways." Proc. A.S.C.E., Vol.98, HY2, Feb. 1972, pp.365-381.

(35) Jaeger, C. "Engineering Fluid Mechanics." Blackie & Sons, Ltd., London, 1961.

(36) Rao, N.S.L., Rao, M.V.J. "Characteristics of hydrofoil weirs." Proc. A.S.C.E., Vol.99, HY2, Feb. 1973, pp.259-283.

(37) Langhaar, H.L. "Dimensional Analysis and Theory of Models." John Wiley & Sons, Inc., New York,1951.

(38) Bajpai, A.C., Mustoe, L.R., Walker, D. "Engineering Mathematics." John Wiley & Sons, England, 1978.